

*Eng
Office*

CALIFORNIA INSTITUTE OF TECHNOLOGY

ELECTRON TUBE AND MICROWAVE LABORATORY

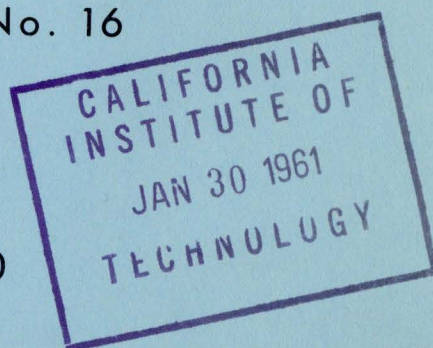
THEORY OF THE VALENCE BAND ENERGY LEVEL STRUCTURES OF GERMANIUM AND SILICON IN AN EXTERNAL MAGNETIC FIELD

by

Viktor Evtuhov

Technical Report No. 16

October 1960



A REPORT ON RESEARCH CONDUCTED UNDER
CONTRACT WITH THE OFFICE OF NAVAL RESEARCH

THEORY OF THE VALENCE BAND
ENERGY LEVEL STRUCTURES OF GERMANIUM AND SILICON
IN AN EXTERNAL MAGNETIC FIELD

by
Viktor Evtuhov

Technical Report No. 16
CALIFORNIA INSTITUTE OF TECHNOLOGY
Pasadena, California

A Technical Report to the Office of Naval Research
Contract Nonr 220(13)

October 1960

ABSTRACT

The problem of the valence band structure of Ge and Si in the presence of an external magnetic field is considered from a quantum mechanical point of view. The analysis is carried out using first and second order perturbation theory. The approach is, in principle, similar to that of W. Shockley and E. O. Kane, but is modified in some important essentials to include the effects of the magnetic field. The analytical results obtained are somewhat more general than those of J. M. Luttinger but reduce to the latter if certain approximations are introduced. Numerical calculations of the Landau energy levels are carried out for certain special cases, of which the most important are the following:

1. Magnetic field \mathcal{H} in the [001] direction, $k_H = 0$; nonspherical symmetry character of energy bands and the coupling of V_1 and V_2 bands to the V_3 band included.
2. Magnetic field \mathcal{H} in the [001] direction, $k_H \neq 0$; nonspherical symmetry character of energy bands included, decoupling of V_1 and V_2 bands from the V_3 band assumed.

In addition, a set of algebraic equations is derived whose solution should yield the valence band Landau levels for the cases of the magnetic field in the [101] and the [111] directions. However, no numerical calculations are performed for these cases.

The results of the calculations indicate the presence of some interesting transitions between the Landau levels of Ge and Si, as well as the possible presence of other interesting effects which may be observable. Certain of these seem to offer potential millimeter-wave applications possibilities, some of which are discussed.

TABLE OF CONTENTS

I.	Introduction	1
1.1	Some Important Features of the Energy Band Structures of Ge, Si, and InSb	1
1.2	Semiconductor Crystal in a Magnetic Field--Previous Investigations	9
II.	Valence Band Structure of Diamond-Type Semiconductors Near $k = 0$. Analytical Formulation of the Problem	16
2.1	Perturbation Theory Approach to the Problem of Band Structure in the Absence of an External Magnetic Field	16
2.2	Valence Band Structure in the Presence of an External Magnetic Field	26
III.	Landau Level Structure of Ge and Si at $k_H = 0$. \mathcal{H} in [001] Direction	50
3.1	Reduction of the Problem to an Algebraic One	50
3.2	Numerical Constants Characterizing the Valence Bands of Ge and Si	60
3.3	Numerical Results for Ge	65
3.4	Numerical Results for Si	74
IV.	Valence Band Landau Levels as Functions of k_H for \mathcal{H} in the [001] Direction	88
4.1	Check on the Validity of an Approximation Involving the decoupling of the V_1 and V_2 Bands from the V_3 Band	88
4.2	Landau Levels as Functions of k_H in the Valence Band of Ge	102
4.3	Landau Levels as Functions of k_H in the Valence Band of Si	124
V.	Valence Band Landau Level Structure of Ge and Si for \mathcal{H} in the [101] and the [111] Directions	134
5.1	Magnetic Field in the [101] Direction	135
5.2	Magnetic Field in the [111] Direction	148
VI.	Some Possible Practical Applications of Landau Levels in Ge and Si	155

Appendix 1.	Simultaneous Diagonalization of Two Perturbation Hamiltonians	168
Appendix 2.	Electron in a Homogeneous Magnetic Field	171
Appendix 3.	Numerical Results: Energy Levels in Ge at $k_H = 0$ as Functions of \mathcal{H} ; \mathcal{H} in [001] Direction	174
Appendix 4.	Numerical Results: Energy Levels in Si at $k_H = 0$ as Functions of \mathcal{H} ; \mathcal{H} in [001] Direction	182
Appendix 5.	Numerical Results: Energy Levels in Ge and Si at $k_H = 0$; \mathcal{H} in [001] Direction	190
Appendix 6.	Numerical Results: Energy Levels in Ge as Functions of k_H , $\delta = 0$	193
Appendix 7.	Numerical Results: Energy Levels in Ge as Functions of k_H , $\delta \neq 0$	197
Appendix 8.	Numerical Results: Energy Levels in Si as Functions of k_H , $\delta \neq 0$	202
	REFERENCES	207

I. INTRODUCTION

The purpose of the work described here is to extend the available calculations of the effect of an external magnetic field on the energy band structures of the diamond type semiconductors Ge and Si (1,2,3). The problem is particularly interesting in connection with the phenomena of interband magnetoabsorption (4,5) and cyclotron resonance of both positive and negative effective mass carriers (6,7,8,9) as well as in connection with the possibilities of utilization of these phenomena in devices operating in the millimeter and submillimeter wave frequency range (8,9,10,11).

The following is a brief summary of some of the most important features of the energy band structures of Ge and Si as well as of InSb which, although not the subject of the present work, may turn out to be of considerable interest from the point of view of applications.

1.1 Some Important Features of the Energy Band Structures of Ge, Si, and InSb

Since germanium lattice is of a face-centered cubic type, its reciprocal lattice is of the body-centered cubic type with the first Brillouin zone as shown in Figure 1.1. It is easy to see that in the majority of cases where Bloch function solution to the Schrodinger equation is used, one needs to consider only the first Brillouin zone. Consider a certain wave vector \vec{k}' and a vector \vec{k} lying in the first Brillouin zone. One may then write $\vec{k}' = \vec{k} + \vec{K}$ where \vec{K} is an appropriately chosen translation vector in the reciprocal lattice space, (i.e., $\vec{K} = n_1 \vec{b}_1 + n_2 \vec{b}_2 + n_3 \vec{b}_3$, where \vec{b}_i 's are reciprocal lattice basis vectors and n 's are integers.) One thus has for the Bloch wave functions:

$$\begin{aligned}\psi_{\vec{k}'} &= e^{i\vec{k}' \cdot \vec{r}} u_{\vec{k}'}(\vec{r}) = e^{i\vec{k} \cdot \vec{r}} u_{\vec{k}}(\vec{r}) e^{i\vec{K} \cdot \vec{r}} \\ &= e^{i\vec{k} \cdot \vec{r}} u_{\vec{k}}(\vec{r}) = \psi_{\vec{k}}\end{aligned}\quad (1.1.1)$$

since $e^{i\vec{K} \cdot \vec{r}}$ has the periodicity of the lattice. Thus it is seen that any problem can be solved by considering only the first Brillouin zone as long as the wave functions and energy surfaces are taken to be multivalued functions of \vec{k} (12,13).

The problem of determining the energy band structure for a material is essentially the problem of determining the dependence of allowed energy levels on the wave vector \vec{k} in the first Brillouin zone. In general, this dependence will obey certain symmetries associated with the lattice, but will not be isotropic. It is not generally possible to solve the complete energy band problem analytically but in conjunction with data from magnetoresistance, cyclotron resonance, and other experiments, an approximate solution can be obtained. A plot of E versus k for two directions in the Brillouin zone of Ge is given in Figure 1.2 (14). The important features to be observed are the following: 1) The lowest point in the conduction band (band edge) occurs at a point $\frac{\vec{k}a}{2\pi} = (\frac{1}{2} \frac{1}{2} \frac{1}{2})$, where a is the lattice constant, and seven other equivalent points, and belongs to the L_1 band; 2) At $k = 0$ there is a distinct minimum in the conduction band; 3) The Γ_2 band is approximately parabolic (and isotropic) for small k ; 4) The valence band edge is four-fold degenerate (including "spin" degeneracy); 5) The valence band has a maximum at $k = 0$; 6) V_1 and V_2 bands are approximately parabolic near $k = 0$ (but are not isotropic); 7) There is another

valence band, the V_3 band, which is depressed relative to the V_1 and V_2 bands by spin-orbit coupling by an amount $\Delta = 0.29$ ev. (15). This band is also approximately parabolic near $k = 0$; 8) The separation between the band edges $\epsilon_G = .66$ ev. (14); 9) The separation between the valence band and the conduction band at $k = 0$ is $\epsilon(000) = 0.88$ ev. according to reference 15, and 0.84 ev. according to reference 14.

As was mentioned previously, $E(\bar{k})$ is not generally isotropic. The anisotropy of V_1 and V_2 near $k = 0$ has been quantitatively determined by combining the results of degenerate perturbation theory with cyclotron resonance data by Dresselhaus, Kip and Kittel (6), and Zeiger, Dexter, and Lax (7). The resulting expression for $E(k)$ correct to second order in k is given by

$$E(\bar{k}) = Ak^2 \mp \left[B^2 k^4 + C^2 (k_x^2 k_y^2 + k_y^2 k_z^2 + k_z^2 k_x^2) \right]^{1/2} \quad (1.1.2)$$

where $A \approx -13.0 \frac{\hbar^2}{2m}$ (see reference 6)

$$|B| \approx 8.9 \frac{\hbar^2}{2m}$$

$$|C| \approx 10.3 \frac{\hbar^2}{2m}$$

The plus sign corresponds to the light holes (V_2) and the minus sign to heavy holes (V_1). The general shape of the constant energy contours for both heavy and light holes is shown in Figure 1.3, where $k_z = 0$.

The conduction band minimum at $\frac{\bar{k}a}{2\pi} = (\frac{1}{2} \frac{1}{2} \frac{1}{2})$ is also anisotropic. Here the three-dimensional constant energy contours appear to be ellipsoids with their major axes along the $\langle 111 \rangle$ directions. The effective masses m_ℓ and m_t corresponding to the major and minor axes of the

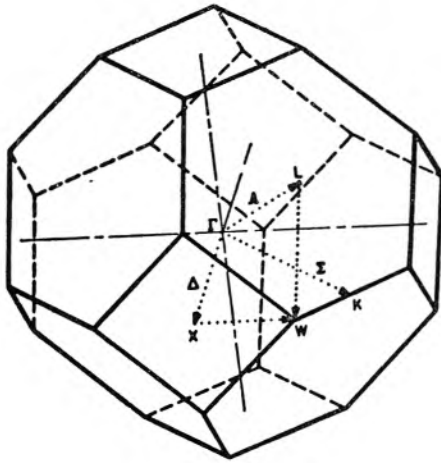


Fig. 1.1 First Brillouin Zone for Crystals Having Face-Centered Cubic Lattice. (After F. Herman, Ref. 39)

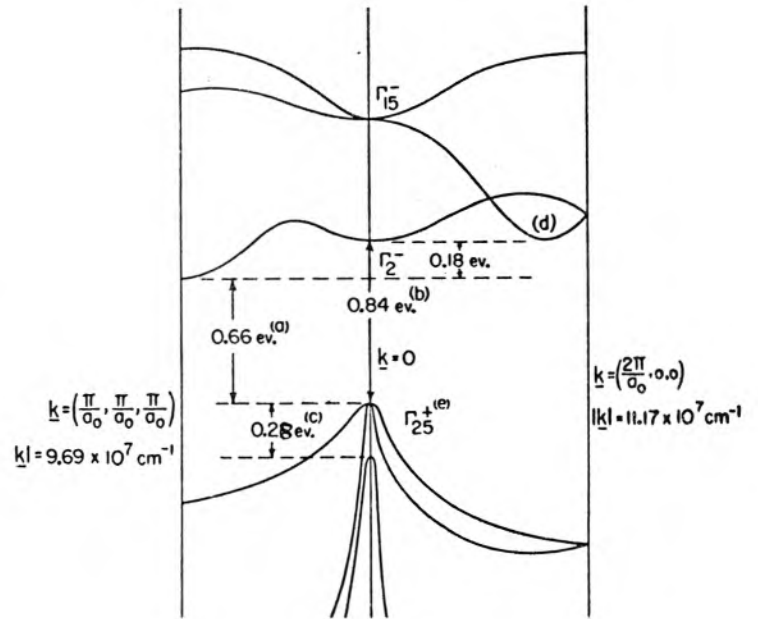


Fig. 1.2 Energy as a Function of Reduced Wave Vector for [100] and [111] Directions in Ge (After H. Brooks Ref. 14)

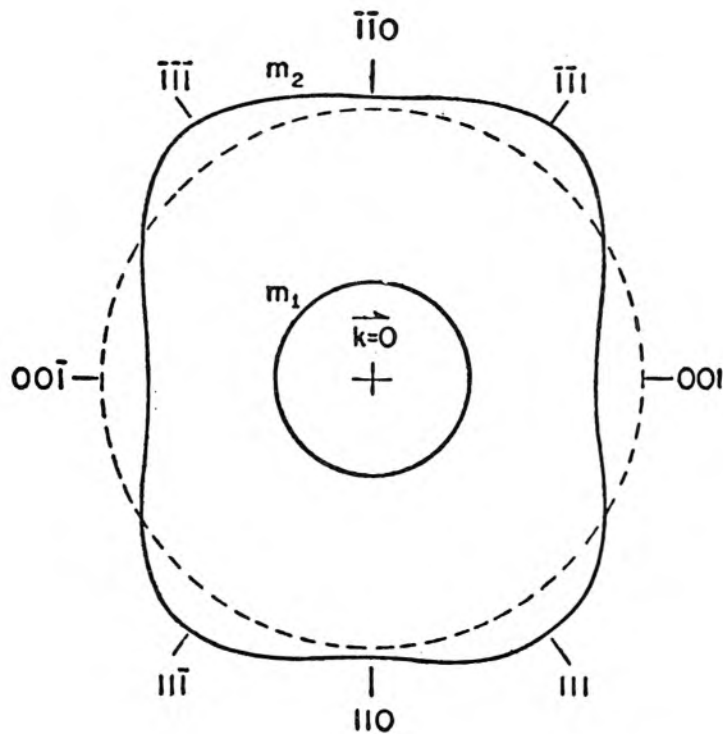


Fig. 1.3 Valence Band Constant Energy Contours in the $[110]$ plane in Ge (After Dexter, Zeiger and Lax, Ref. 7)

ellipsoids have been measured by cyclotron resonance techniques as

$$m_{\ell} = 1.58 m \quad (6) \qquad m_t = 0.082 m \quad (6)$$

The effective mass in the Γ_2 conduction band at $k = 0$ has been estimated to be $m_{\Gamma_2} = 0.034 m \quad (6)$

$$0.04 m \quad (16)$$

$$0.036 m \quad (17)$$

and is isotropic for small k .

The nonparabolic effects in Ge near the center of the Brillouin zone have been investigated by E. O. Kane (15) with the help of degenerate perturbation theory. The results are shown in Figures 1.4, 1.5, 1.6 for [100], [111], and [110] directions respectively. It will be noted that the nonparabolic effects in the V_2 band set in at approximately 0.1 ev. relative to the band edge.

Si has the same lattice as Ge and its band structure is qualitatively very similar to that of Ge. The $E(k)$ curves for [111] and [100] directions are given in Figure 1.7 (14). One should note the following: 1) the conduction band edge occurs at $\frac{\bar{k}a}{2\pi} = (\frac{1}{2}, 0, 0)$ and five other equivalent points, and belongs to Δ_1 band. 2) The valence band edge occurs at $k = 0$ and is fourfold degenerate. 3) V_1 and V_2 bands are parabolic for only very small k and are not isotropic. 4) The V_3 band is depressed relative to the V_1 and V_2 bands by only .04 ev. (6). 5) The separation between the band edges is $\epsilon_G = 1.08$ ev. (14). 6) The separation between the valence band and the conduction band at $k = 0$ is $\epsilon(000) = 2.58$ ev. (14).

As in the case of Ge, the V_1 and V_2 bands are anisotropic with the

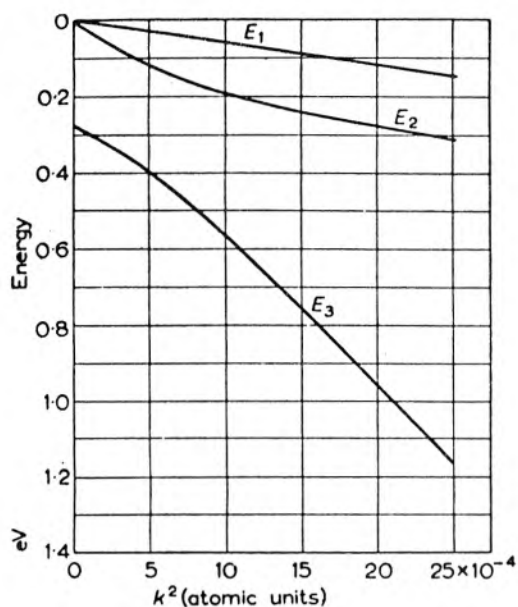


Fig. 1.4 Energy vs. k^2 for [100] Direction in the Valence Band of Ge (After E. O. Kane, Ref. 15)

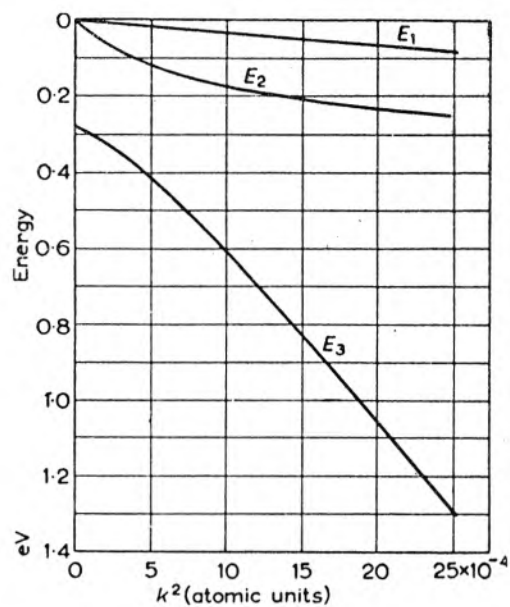


Fig. 1.5 Energy vs. k^2 for [111] Direction in the Valence Band of Ge (After E. O. Kane, Ref. 15)

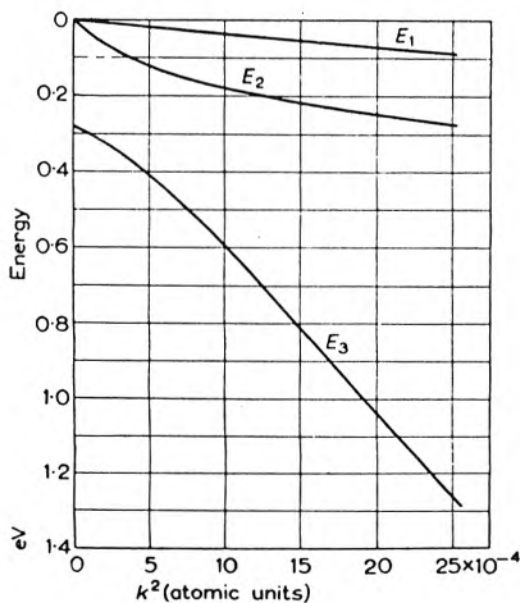


Fig. 1.6 Energy vs. k^2 for [110] Direction in the Valence Band of Ge (After E. O. Kane, Ref. 15)

energy contours still given by equation 1.1.2 but with A,B,C, given by

$$A \approx -4.1 \quad \hbar^2/2m \quad (6)$$

$$|B| \approx 1.6 \quad \hbar^2/2m \quad (6)$$

$$|C| \approx 3.3 \quad \hbar^2/2m \quad (6)$$

Thus the anisotropy in Si is greater than that in Ge. Expression 1.1.2 is not as good an approximation for Si as it is for Ge due to small spin-orbit splitting in the case of Si.

The constant energy contours near the conduction band edge in Si are again ellipsoids but with their major axes along the $\langle 100 \rangle$ direction. The longitudinal and transverse effective masses are

$$m_{\ell} = 0.97 m \quad (6) \quad m_t = 0.19 m \quad (6) .$$

According to H. Krömer (18) the Si conduction band near $k = 0$ has probably the curvature corresponding to negative effective mass which could have significant consequences as far as applications are concerned. This, however, has apparently not been conclusively established.

The results of Kane's (15) calculations on the nonparabolic effects in Si near $k = 0$ are shown in Figures 1.8 and 1.9. In this case the nonparabolic effects appear at energies as low as .015 ev. This is due to the proximity of the V_3 band to the V_1 and V_2 bands.

The band structure of InSb, which has the zinc blende structure and therefore the Brillouin zone of Figure 1.1, is shown in Figure 1.10 for $[100]$ and $[111]$ directions. Most of the qualitative differences between the band structures of InSb and Ge and Si arise from the fact that

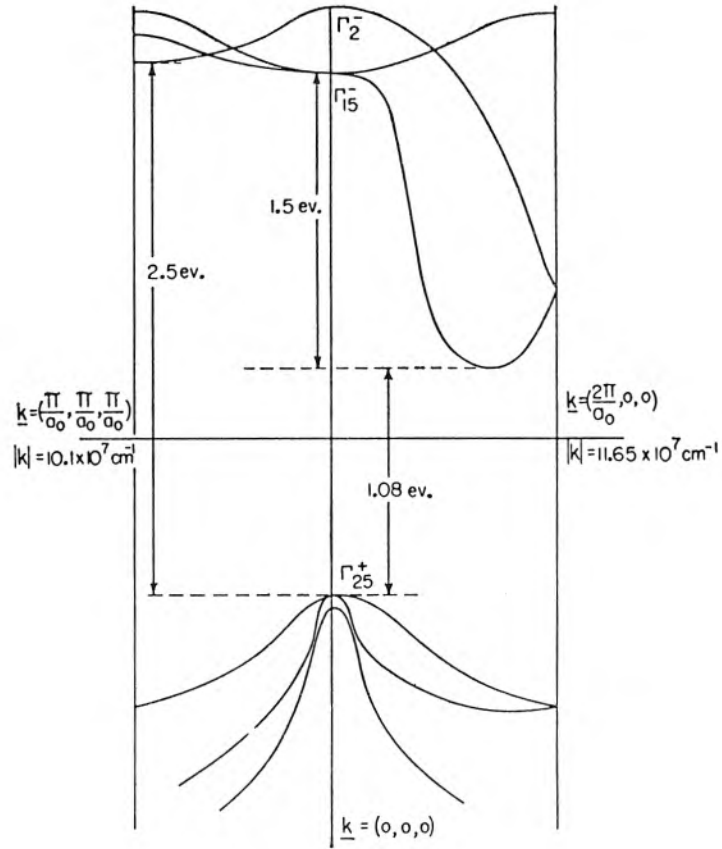


Fig. 1.7 Energy as a Function of Reduced Wave Vector for [100] and [111] Directions in Si (After H. Brooks, Ref. 14)

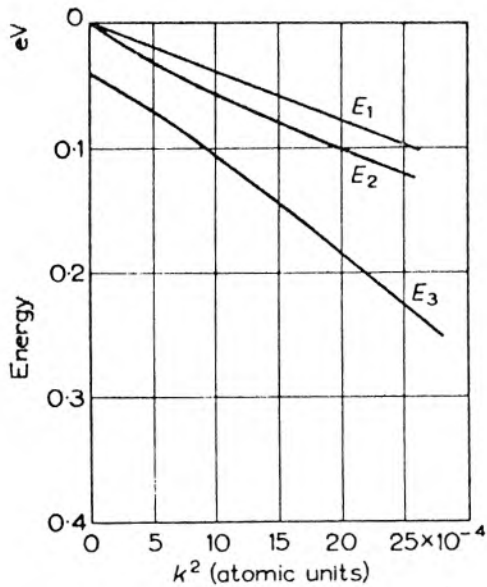


Fig. 1.8 Energy vs. k^2 for [100] Direction in the Valence Band of Si (After E. O. Kane, Ref. 15)

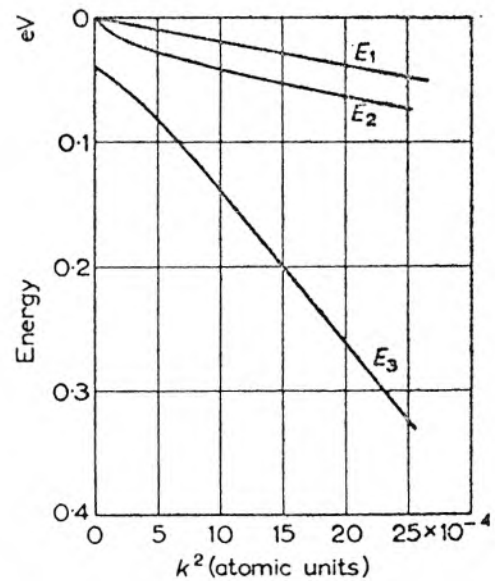


Fig. 1.9 Energy vs. k^2 for [111] Direction in the Valence Band of Si (After E. O. Kane, Ref. 15)

InSb does not possess a center of inversion symmetry.

One observes the following:

- 1) The conduction band edge occurs at $k = 0$ and belongs to the Γ_1 band.
- 2) The valence band edge no longer occurs at $k = 0$, but near $k = 0$.
- 3) The valence band is still fourfold degenerate at $k = 0$, but the degeneracy splits for even very small k . Thus the valence band edge is not degenerate.
- 4) The spin orbit coupling is very large and as a consequence the V_3 band is depressed relative to the V_1 bands by 0.9 ev. (4).
- 5) The separation between the band edges is quite small, $\epsilon_G = .175$ ev (19). (This complicates the analysis of the band structure--to be discussed later.)

The V_1 and V_2 bands are highly anisotropic but the expression 1.1.2 no longer holds. As a matter of fact, for certain directions the expressions for E contain terms linear in k . The nonparabolic effects for small k have again been considered by Kane (19) and are shown in Figure 1.11. In his calculations he assumed that the valence band maximum occurs at $k = 0$, which makes his results for the valence band somewhat unreliable, quantitatively.

1.2 Semiconductor Crystal in a Magnetic Field - Previous Investigations

It is a well known fact that if a free electron is placed in a magnetic field its energy becomes quantized in the direction perpendicular to the magnetic field with the energy levels $\hbar\omega_c$ apart (where $\omega_c = \frac{e\mathcal{H}}{mc}$, the cyclotron frequency) (20). A similar effect takes place when a semiconductor is placed in a magnetic field. However, the problem of determining the energy levels of electrons

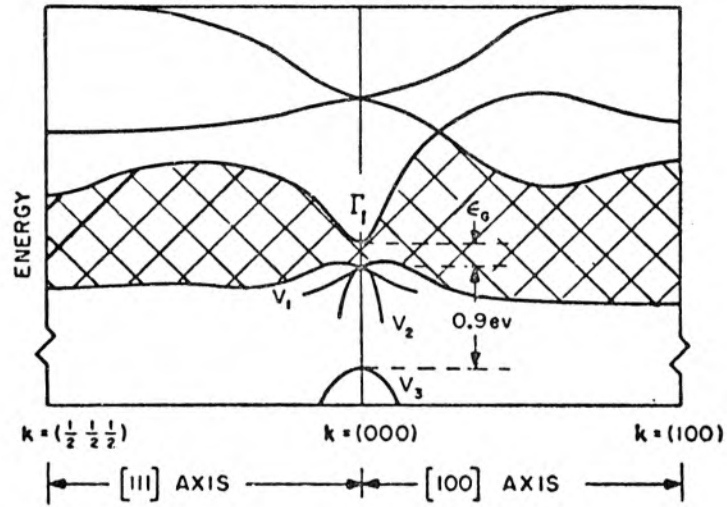


Fig. 1.10 Energy as a Function of Reduced Wave Vector for [100] and [111] Direction in InSb (After Burstein et al, ref. 4)

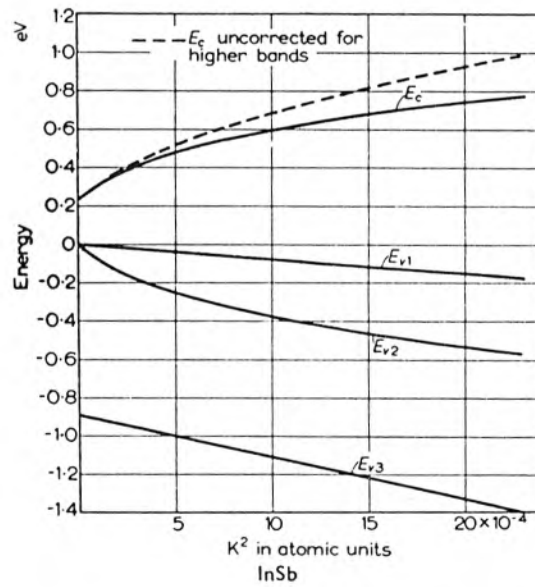


Fig. 1.11 Energy vs. k^2 for an Average Direction in InSb (After E. O. Kane, Ref. 19)

is considerably complicated by the degeneracies, anisotropies and the generally nonparabolic character of the energy bands.

A semi-classical approach to the problem of an electron in a lattice subjected to an external magnetic field has been adopted by Shockley (21), Dresselhaus, Kip and Kittel (6), Zeiger, Lax and Dexter (22), and others. This approach consists essentially of calculating quantum mechanically the energy band structure of a semiconductor without including the effects of the external magnetic field, and then considering the classical cyclotron motion of an electron (or a hole) in the force field of the lattice. One can confine his attention to the motion of a single carrier, in which case the problem is to solve the equations of motion:

$$\frac{d\bar{p}}{dt} + \frac{\bar{p}}{\tau} = e(\bar{E} + \frac{\bar{v} \times \bar{\mathcal{H}}}{c}) \quad (1.2.1)$$

$$\bar{v} = \nabla_{\bar{p}} \epsilon(\bar{p}) \quad (1.2.2)$$

where \bar{p} is the generalized momentum
 τ is the collision time
 \bar{E} is the externally applied electric field
 $\bar{\mathcal{H}}$ is the externally applied magnetic field
 $\epsilon(\bar{p})$ is the effective Hamiltonian

Alternatively, and more accurately, one can use the Boltzmann transport theory to solve the problem, as has been done by Zeiger, Lax and Dexter (22), in which case the following equation is to be solved:

$$\frac{\partial f}{\partial t} + \frac{f - f_0}{\tau} + \bar{v} \cdot \nabla_{\bar{r}} f + e(\bar{E} + \frac{\bar{v} \times \bar{\mathcal{H}}}{c}) \cdot \nabla_{\bar{p}} f = 0 \quad (1.2.3)$$

where again $\bar{v} = \nabla_{\bar{p}} \epsilon(\bar{p})$ and $f = f(\bar{p}, \bar{r}, t, \bar{\mathcal{H}}, \bar{E})$ is the distribution function.

The quantum mechanical effective mass formalism for treating problems of this sort has been developed by Luttinger and Kohn (1). The method has been used by Luttinger (2) to treat the problem of the valence band of a Ge crystal in a magnetic field. Since in the valence band of Ge the spin orbit splitting is rather large, Luttinger has been able to consider the V_1 and V_2 bands separately from the V_3 band which essentially amounts to the assumption that the V_1 and V_2 bands consist of purely $j = \frac{3}{2}$ states, which was also the assumption involved in deriving equation 1.1.2. Luttinger has written down a 4x4 matrix, a diagonalization of which should yield the energy levels for electrons in a Ge crystal which is subjected to a magnetic field in the [111] direction. He has also assumed that the momentum of the electrons in the direction of the magnetic field is zero. He has then simplified the problem further by assuming the energy bands to be isotropic. This reduced the problem to the solution of two 2x2 determinants which Luttinger has carried out. He also formulated a perturbation approach to the anisotropic problem. The numerical results have been given by Goodman (3) and are summarized in Figure 1.12.

It will be observed that the V_1 and V_2 bands split into four "ladders", two of which correspond to light holes and two to heavy holes. The spacing of the levels is no longer constant for all quantum numbers as it has been in the case of a free electron, but it becomes constant for higher quantum numbers where the classical limit is approached. However, we might expect that at even higher quantum numbers unevenness in the level spacings must again set in due to the nonparabolic effects. This, however, must be expected to occur at comparatively high energies relative to the band edge (see Figures 1.4, 1.5, 1.6). Calculations on

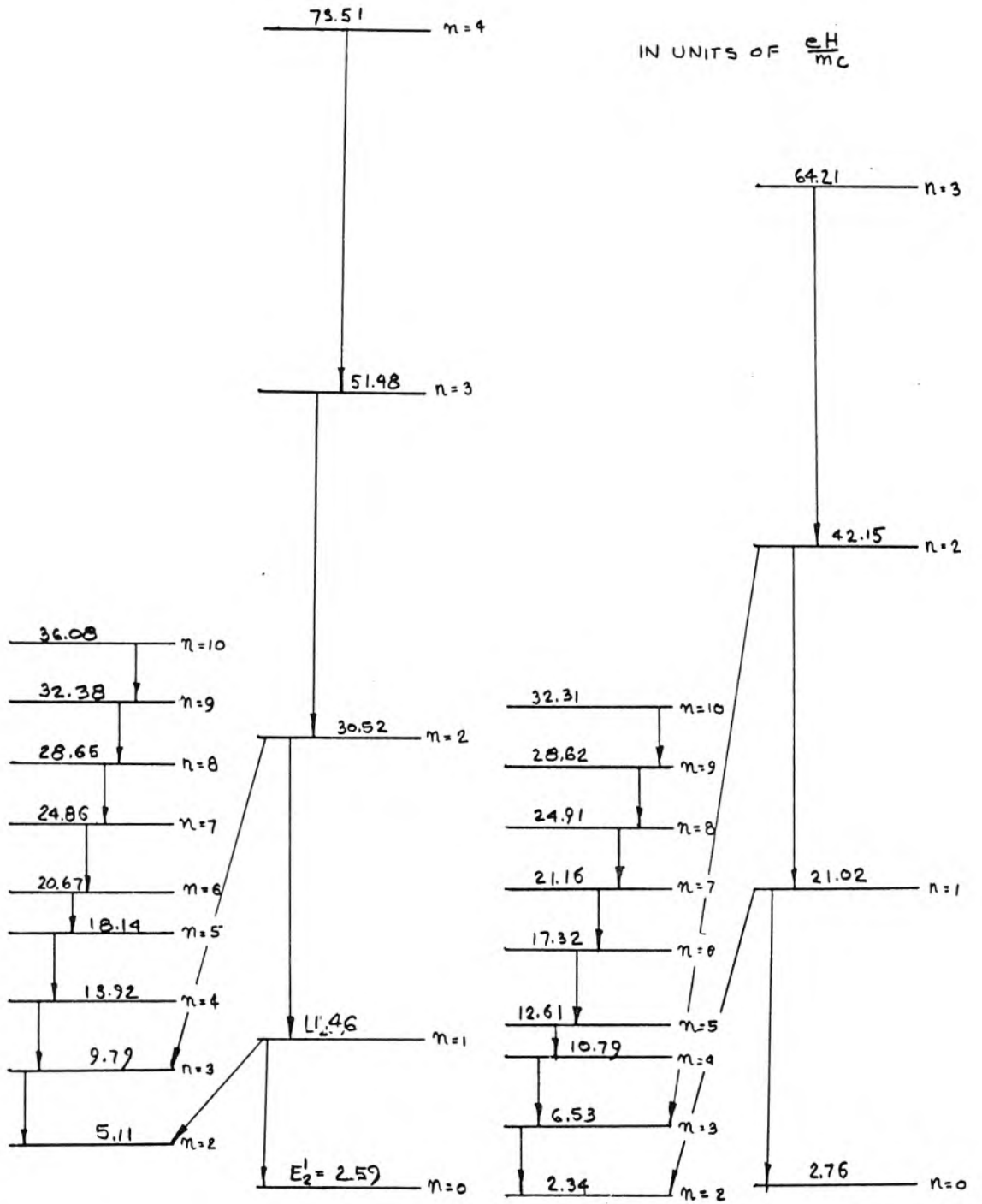


Fig. 1.12 Landau Levels in Ge at $k_H = 0$ for H in the [100] Direction (After R. R. Goodman, ref. 3)

the behavior of the Landau levels at values of $k_H \neq 0$ are not available at present. However, interesting effects are to be expected due to anisotropy of the energy bands. Thus in the direction where the constant energy contours are reentrant (see Figure 1.3), reordering of the Landau levels may take place; the levels corresponding to higher n numbers (angular momentum numbers of an electron orbiting on a magnetic field) appearing above those with lower quantum numbers. The effect may prove to be important from the applications point of view.

No calculations of the sort described above have been made for either Si or InSb. In the case of Si the analysis will be complicated by the small spin-orbit splitting. It appears that it may be necessary to consider all three valence bands together which will lead to the formulation of the general problem in terms of 6x6 matrices. It may be expected that in this case the energy levels will be much more unevenly spaced than in the case of Ge and the unevenness at high quantum numbers will set in at much lower energies. The above are assumed to be the effects of increased mixing of the V_1 and V_2 bands with the V_3 band and the strong nonparabolic effects. The anisotropy effects are of course expected to be even more pronounced for Si than for Ge.

The proximity of the Γ_1 conduction band to the valence band in InSb may necessitate rigorous inclusion of it in the solution of the valence band problem as has been done by Kane (15) for the no-magnetic-field case. This will lead to 8x8 matrices in the problem unless the V_3 band can be separated first. The absence of the center of symmetry will also complicate the analysis. The nonclassical effects (unevenness in the energy level spacings) will probably be strongly apparent in InSb.

The problem of energy band structure of Ge and Si in the presence of a magnetic field and thus the problems of cyclotron resonance and interband magnetoabsorption, is here considered from a quantum mechanical point of view. For the sake of clarity and completeness, some of the results of Luttinger and Kohn (1) and Luttinger (2) are rederived in Section 2 using a slightly different approach to the problem. Also, the analysis given makes use of a fewer number of approximations than has been previously made. Thus the assumption of decoupling of the states corresponding to $j = \frac{3}{2}$ and $j = \frac{1}{2}$ states in the tight binding limit is not made. This results in a 6x6 matrix operator in which the antisymmetric constant K is included. Spherically symmetric energy bands are not assumed, although approximations must of course be used in dealing with the resulting infinite matrices.

In Section 3 the Landau energy levels in Ge and Si subjected to a magnetic field in the $[001]$ direction are found at $k_H = 0$. No approximations other than those involved in the use of the second order perturbation theory are made in that section.

In Section 4, however, an approximation of the decoupling of the V_1 and V_2 bands from the V_3 band mentioned above is introduced. The Landau levels at $k_H = 0$ are then calculated and compared with the results in Section 3. Then the behavior of the energy levels for $k_H \neq 0$ is considered. Section 5 is devoted to the derivation of the matrices, the diagonalization of which should give the Landau level structures of Ge and Si for the cases of the magnetic field in the $[101]$ and the $[111]$ directions. No numerical results, however, are given. Section 6 is concerned with some possible practical applications of the Landau levels in semiconductors which have or have not been proposed before.

II. VALENCE BAND STRUCTURE OF DIAMOND TYPE SEMICONDUCTORS NEAR $k = 0$ ANALYTICAL FORMULATION OF THE PROBLEM

2.1 Perturbation Theory Approach to the Problem of Band Structure in the Absence of an External Magnetic Field

To analyze the energy level structure of a Ge or Si crystal in a magnetic field one must solve the following Schrödinger equation:

$$\begin{aligned} \frac{1}{2m} \left(\hat{p} + \frac{|e|\hbar}{c} \bar{A} \right)^2 \psi + \frac{\hbar}{4m^2 c^2} \left[\nabla V \times \left(\hat{p} + \frac{|e|\hbar}{c} \bar{A} \right) \right] \cdot \bar{\sigma} \psi + \\ + \frac{|e|\hbar}{2mc} \bar{\sigma} \cdot \bar{\mathcal{H}} \psi + V(r) \psi = E \psi \end{aligned} \quad (2.1.1)$$

This equation represents a one-electron approximation in which the potential $V(r)$ is chosen to account in the best possible fashion for the effect on a single electron of the nuclei of the crystal, the average electrostatic potentials due to the electrons in the crystal, and the exchange interactions. The choice of this potential is quite difficult and involves numerous assumptions. A discussion of the problem may be found in review papers by Callaway (23) and Reitz (13). However, it is often possible by using symmetry considerations and experimental data to avoid the explicit determination of the potential $V(r)$. This, as will be seen later, is the case for the problem considered here.

In the absence of the magnetic field, equation 2.1.1 simplifies to the following equation

$$\frac{1}{2m} \hat{p}^2 \psi_k + \frac{\hbar}{4m^2 c^2} \left[\nabla V \times \hat{p} \right] \cdot \bar{\sigma} \psi_k + V(r) \psi_k = E_k \psi_k \quad (2.1.2)$$

which has been solved quite accurately for Ge and Si in the region of the Brillouin zone near $k = 0$ with the help of the perturbation theory. The

method which has been suggested by Shockley (21) and has been carried out in detail by Dresselhaus, Kip and Kittel (6) and Kane (15), is based on the following considerations: The wave functions must be of the Bloch type, i.e., of the form

$$\psi_{\mathbf{k}} = e^{i\bar{\mathbf{k}} \cdot \bar{\mathbf{r}}} u_{\mathbf{k}}(\mathbf{r}) \quad (2.1.3)$$

where $u_{\mathbf{k}}(\mathbf{r})$ has the periodicity of the lattice. $\psi_{\mathbf{k}}$ may then be substituted into equation 2.1.2 with the following result:

$$\begin{aligned} -\frac{\hbar^2}{2m} \nabla^2 u_{\mathbf{k}} - \frac{i\hbar^2}{m} \bar{\mathbf{k}} \cdot \nabla u_{\mathbf{k}} - \frac{i\hbar^2}{4m^2 c^2} \left[\nabla V \times \nabla \right] \cdot \bar{\boldsymbol{\sigma}} u_{\mathbf{k}} + \\ + \frac{\hbar^2}{4m^2 c^2} \left[\nabla V \times \bar{\mathbf{k}} \right] \cdot \bar{\boldsymbol{\sigma}} u_{\mathbf{k}} + V(\mathbf{r}) u_{\mathbf{k}} = (E_{\mathbf{k}} - \frac{\hbar^2 k^2}{2m}) u_{\mathbf{k}} \end{aligned} \quad (2.1.4)$$

This can be solved by considering first the equation

$$-\frac{\hbar^2}{2m} \nabla^2 \epsilon_{\mathbf{i}} + V(\mathbf{r}) \epsilon_{\mathbf{i}} = E_{\mathbf{k}} \epsilon_{\mathbf{i}} \quad (2.1.5)$$

where $\epsilon_{\mathbf{i}}$ are the zero order u 's ($k = 0$), and treating all other terms as perturbations,

$$\hat{V}^{kp} = \frac{i\hbar^2}{m} \bar{\mathbf{k}} \cdot \nabla \quad (2.1.6)$$

$$\hat{V}^{so} = \frac{\hbar}{4m^2 c^2} \left[\nabla V \times \hat{\mathbf{p}} \right] \cdot \bar{\boldsymbol{\sigma}} \quad (2.1.7)$$

The effect of the $\frac{\hbar^2}{4m^2 c^2} \left[\nabla V \times \bar{\mathbf{k}} \right] \cdot \bar{\boldsymbol{\sigma}}$ term has been estimated by Kane (15) to be less than 1% of the effect of the \hat{V}^{kp} term, and thus may be neglected.

Equation 2.1.5 has been considered by Dresselhaus (24), and Dresselhaus, Kip and Kittel (6) for the case of the valence band of Ge and Si

which is the case of interest here. From Herman's (25) calculations, Dresselhaus, Kip and Kittel found that the energy levels in Ge at $k = 0$ and neglecting V^{so} are as shown in Figure 2.1, and are of a similar nature in Si. Using the fact that the valence band edge is six-fold degenerate and belongs to the Γ_{25^+} representation, Dresselhaus, Kip and Kittel (6) on the basis of Von der Lage and Bethe's work (26), chose for the zero order valence band wave functions the following:

$$\begin{aligned}\phi_1 &= \epsilon_1^+ S_{1/2} ; \quad \phi_2 = \epsilon_2^+ S_{1/2} ; \quad \phi_3 = \epsilon_3^+ S_{1/2} ; \\ \phi_4 &= \epsilon_1^+ S_{-1/2} ; \quad \phi_5 = \epsilon_2^+ S_{-1/2} ; \quad \phi_6 = \epsilon_3^+ S_{-1/2}\end{aligned}\quad (2.1.8)$$

where $S_{1/2}$ indicates the spin up wave function, $S_{-1/2}$ indicates the spin down wave function, and ϵ_1^+ , ϵ_2^+ , ϵ_3^+ transform as $\epsilon_1^+ \sim \frac{yz}{x^2 + y^2 + z^2}$, $\epsilon_2^+ \sim \frac{zx}{x^2 + y^2 + z^2}$, $\epsilon_3^+ \sim \frac{xy}{x^2 + y^2 + z^2}$.

Knowing the form of the zero order solutions, one can now introduce the perturbation Hamiltonians \hat{V}^{kp} and \hat{V}^{so} . Consider \hat{V}^{kp} first, although the order is immaterial (see Appendix 1). According to standard degenerate perturbation theory (27) the following determinantal equation must be solved to get the first order corrections to the energy.

$$\left| V_{ij}^{kp} - E_{kp}^{(1)} \delta_{ij} \right| = 0, \quad i, j = 1, 2, \dots, 6 \quad (2.1.9)$$

where

$$V_{ij}^{kp} = \sum_{\sigma_z} \int \phi_i^* \left(-\frac{i\hbar^2}{m} \vec{k} \cdot \nabla \right) \phi_j d\vec{r} \quad (2.1.10)$$

Keeping in mind the orthogonality condition for spin wave functions (where Leighton's (28) notation is employed):

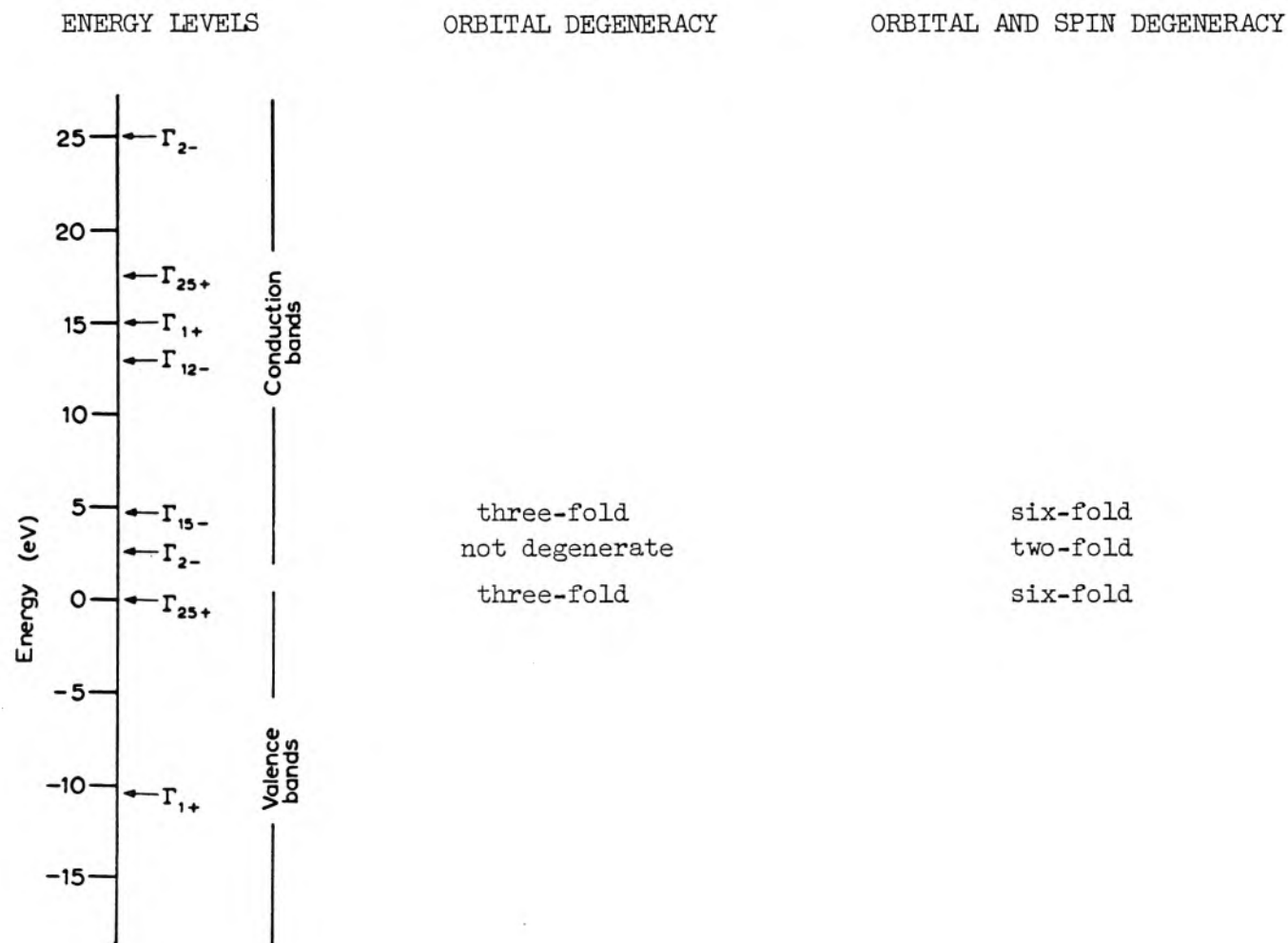


Figure 2.1 Energy Levels at $k = 0$. Standard Notation is Employed (See, for Example Ref. 40). After E. O. Kane (24).

$$\sum_{\sigma_z} S_{m_s}^* (\sigma_z) S_{m'_s} (\sigma_z) = \delta_{m_s m'_s} \quad (2.1.11)$$

It is obvious that all V_{ij} for which $i = 1, 2, 3$ and $j = 4, 5, 6$, and for which $i = 4, 5, 6$ and $j = 1, 2, 3$ are zero. For other V_{ij} one has

$$V_{ij}^{kp} = - \frac{i\hbar^2}{m} \int \epsilon_i^{+*} \bar{k} \cdot \nabla \epsilon_j^+ d\bar{r} \quad (2.1.12)$$

Using the transformation properties of ϵ_i^+ , it is easily shown that the above integral vanishes. Thus it is found that the first order correction to the energy due to \hat{V}^{kp} vanishes. One must therefore consider the second order corrections. These are found by solving the following:

$$\left| \sum_m \frac{V_{im}^{kp} V_{mj}^{kp}}{E_i^{(0)} - E_m^{(0)}} - E_{kp}^{(2)} \delta_{ij} \right| = 0 \quad i, j = 1, 2, \dots, 6 \quad (2.1.13)$$

where m refers to all states except those in the Γ_{25}^+ band. Consider

$$\sum_m \frac{V_{im}^{kp} V_{mj}^{kp}}{E_i^{(0)} - E_m^{(0)}} \equiv D_{ij} \quad (2.1.14)$$

$$D_{ij} = \frac{\hbar^2}{m^2} \sum_m \frac{(\bar{k} \cdot p_{im})(\bar{k} \cdot p_{mj})}{E_i^{(0)} - E_m^{(0)}} \quad (2.1.15)$$

where $\bar{p}_{im} = \sum_{\sigma_2} \int \phi_i \bar{p} \phi_m d\bar{r}$

$$D_{ij} = \frac{\hbar^2}{m^2} \sum_{\substack{\alpha, \beta = \\ x, y, z}} k_\alpha k_\beta \sum_m \frac{p_{im}^\alpha p_{mj}^\beta}{E_i^{(0)} - E_m^{(0)}} \quad (2.1.16)$$

If all $E_m^{(0)}$ were equal (to $E_k^{(0)}$) one could write

$$D'_{ij} = \frac{\hbar^2}{m} \sum_{\alpha, \beta} k_{\alpha} k_{\beta} \frac{(p^{\alpha} p^{\beta})_{ij}}{E_i^{(0)} - E_k^{(0)}} \quad (2.1.17)$$

Now using the transformation properties of ϵ_i^+ and the orthogonality condition for spin wave function, 2.1.11, the following is obtained:

$$D'_{11} = \mathcal{D}'_{11}{}^{xx} k_x^2 + \mathcal{D}'_{11}{}^{yy} k_y^2 + \mathcal{D}'_{11}{}^{zz} k_z^2 \quad \text{where } \mathcal{D}'_{11}{}^{yy} = \mathcal{D}'_{11}{}^{zz} \quad (2.1.18)$$

$$D'_{12} = \mathcal{D}'_{12}{}^{xy} k_x k_y + \mathcal{D}'_{12}{}^{yx} k_y k_x, \text{ etc.}$$

Since the form of D_{ij} does not depend on $E_m^{(0)}$, one has

$$D_{11} = \mathcal{D}_{11}{}^{xx} k_x^2 + \mathcal{D}_{11}{}^{yy} k_y^2 + \mathcal{D}_{11}{}^{zz} k_z^2 = Lk_x^2 + M(k_y^2 + k_z^2) \quad (2.1.19)$$

$$D_{12} = \mathcal{D}_{12}{}^{xy} k_x k_y + \mathcal{D}_{12}{}^{yx} k_y k_x = N k_x k_y, \text{ etc.}$$

Now $\|D_{ij}\|$ can be written as

$$\|D_{ij}\| = \begin{vmatrix} \|\mathcal{D}_{ln}\| & 0 \\ 0 & \|\mathcal{D}_{ln}\| \end{vmatrix} \quad (2.1.20)$$

where

$$\|\mathcal{D}_{ln}\| = \begin{vmatrix} Lk_x^2 + M(k_y^2 + k_z^2) & Vk_x k_y & Nk_x k_z \\ Nk_x k_y & Lk_y^2 + M(k_x^2 + k_z^2) & Nk_y k_z \\ Nk_x k_z & Nk_y k_z & Lk_z^2 + M(k_x^2 + k_y^2) \end{vmatrix} \quad (2.1.21)$$

Consider next the spin orbit interaction \hat{V}_{so} . Again the first

order correction is determined by solving

$$|V_{ij}^{so} - E_{so}^{(1)} \delta_{ij}| = 0 \quad (2.1.22)$$

where

$$V_{ij}^{so} = \sum_{\sigma_z} \int \phi_i^* \left(\frac{\hbar}{4m^2 c^2} \nabla V \times \hat{p} \cdot \vec{\sigma} \right) \phi_j d\vec{r} \quad (2.1.23)$$

Using the transformation properties of ϵ_i^+ , the Pauli spin matrices for $\vec{\sigma}$, and remembering that V is a symmetric function of the coordinates, the following results are obtained:

$$\begin{aligned} V_{11}^{so} &= 0 \\ V_{12}^{so} &\sim \frac{i\hbar^2}{4m^2 c^2} \int \frac{\partial V}{\partial x} \frac{2xy^2 z^2}{(x^2 + y^2 + z^2)^3} d\vec{r} \\ &= -i \frac{\Delta}{3}, \text{ etc.} \end{aligned} \quad (2.1.24)$$

Thus the matrix $||V_{ij}^{so}||$ which determines the first order correction to the energy arising from spin-orbit coupling may be written

$$||V_{ij}^{so}|| = -\frac{\Delta}{3} \begin{vmatrix} 0 & 1 & 0 & 0 & 0 & -1 \\ -1 & 0 & 0 & 0 & 0 & 1 \\ 0 & 0 & 0 & 1 & -1 & 0 \\ 0 & 0 & 1 & 0 & -1 & 0 \\ 0 & 0 & 1 & 1 & 0 & 0 \\ -1 & -1 & 0 & 0 & 0 & 0 \end{vmatrix} \quad (2.1.25)$$

According to Kane (15) $E_{kp}^{(0)}$ and $E_{so}^{(1)}$ are of the same order of magnitude. Hence one can add $||D_{ij}||$ and $||V_{ij}^{so}||$ (see Appendix 1), and

diagonalize the complete matrix thus obtaining the first nonvanishing correction due to both the $\bar{\mathbf{k}} \cdot \bar{\mathbf{p}}$ term and the spin-orbit term.

$||v_{ij}^{so}||$ can be diagonalized by transforming to the J, j_m representation. This is to be expected because all elements of $||v_{ij}^{so}||$ are expressible in terms of Δ which is the only quantity which depends on the lattice constant and because in the tight binding limit the spin-orbit interaction is diagonalized by transforming to the J, m_j representation. The transformation matrix is (see Kane)

$$U = \begin{pmatrix} -\frac{1}{\sqrt{2}} & 0 & 0 & 0 & \frac{1}{\sqrt{6}} & \frac{1}{\sqrt{3}} \\ -\frac{i}{\sqrt{2}} & 0 & 0 & 0 & -\frac{i}{\sqrt{6}} & -\frac{i}{\sqrt{3}} \\ 0 & \sqrt{\frac{2}{3}} & -\frac{1}{\sqrt{3}} & 0 & 0 & 0 \\ 0 & -\frac{1}{\sqrt{6}} & -\frac{1}{\sqrt{3}} & -\frac{1}{\sqrt{2}} & 0 & 0 \\ 0 & -\frac{i}{\sqrt{6}} & -\frac{i}{\sqrt{3}} & \frac{i}{\sqrt{2}} & 0 & 0 \\ 0 & 0 & 0 & 0 & \sqrt{\frac{2}{3}} & -\frac{1}{\sqrt{3}} \end{pmatrix} \quad (2.1.26)$$

U is unitary, i.e., $U = (U^+)^{-1}$, and therefore

$$U^{-1} = U^+ = (\tilde{U})^* \quad (2.1.27)$$

If $||D_{ij}||$ and $||v_{ij}^{so}||$ are now transformed using U to the J, m_j representation and added, and the energy is measured from the top of the valence band, the following is obtained for the final perturbation matrix

$$||v_{ij}|| = \begin{pmatrix} G & \Gamma \\ -\Gamma^* & G^* \end{pmatrix} \quad (2.1.28)$$

where

$$G = \left\| \begin{array}{ccc} \frac{\vartheta_{11} + \vartheta_{22} + i(\vartheta_{12} - \vartheta_{21})}{2} & \frac{-\vartheta_{13} + i\vartheta_{23}}{\sqrt{3}} & \frac{\vartheta_{13} - i\vartheta_{23}}{\sqrt{6}} \\ \frac{-\vartheta_{31} - i\vartheta_{32}}{\sqrt{3}} & \frac{\vartheta_{11} + \vartheta_{22} + 4\vartheta_{33} + i(\vartheta_{12} - \vartheta_{21})}{6} & \frac{\vartheta_{11} + \vartheta_{12} - 2\vartheta_{33} + i(\vartheta_{12} - \vartheta_{21})}{3\sqrt{2}} \\ \frac{\vartheta_{31} + i\vartheta_{32}}{\sqrt{6}} & \frac{\vartheta_{11} + \vartheta_{22} - 2\vartheta_{33} + i(\vartheta_{12} - \vartheta_{21})}{3\sqrt{2}} & \frac{\vartheta_{11} + \vartheta_{22} + \vartheta_{33} + i(\vartheta_{12} - \vartheta_{21})}{3} - \Delta \end{array} \right\| \quad (2.1.29)$$

and

$$r = \left\| \begin{array}{ccc} 0 & \frac{-\vartheta_{11} + \vartheta_{22} + i(\vartheta_{12} + \vartheta_{21})}{2\sqrt{3}} & \frac{-\vartheta_{11} + \vartheta_{22} + i(\vartheta_{12} + \vartheta_{21})}{\sqrt{6}} \\ \frac{\vartheta_{11} - \vartheta_{12} - i(\vartheta_{12} + \vartheta_{21})}{2\sqrt{3}} & \frac{\vartheta_{31} - \vartheta_{13} + i(\vartheta_{23} - \vartheta_{32})}{3} & \frac{\vartheta_{13} + 2\vartheta_{31} - i(\vartheta_{23} + 2\vartheta_{32})}{3\sqrt{2}} \\ \frac{\vartheta_{11} - \vartheta_{22} - i(\vartheta_{12} + \vartheta_{21})}{\sqrt{6}} & \frac{-2\vartheta_{13} - \vartheta_{31} + i(2\vartheta_{23} + \vartheta_{32})}{3\sqrt{2}} & \frac{\vartheta_{13} - \vartheta_{31} + i(\vartheta_{32} - \vartheta_{23})}{3} \end{array} \right\| \quad (2.1.30)$$

It is important to note that G^* and Γ^* represent matrices obtained by conjugating complex quantities explicitly appearing in G and Γ as written above, and not conjugating the \mathcal{O}_{ij} 's.

It now remains to diagonalize $\|V_{ij}\|$ using appropriate values of LMN to determine the energy band structure of Ge and Si near the center of the Brillouin zone.

The usefulness of the above approach of simultaneous diagonalization of two perturbation Hamiltonians has been discussed by Kane (15). He points out that in degenerate perturbation theory the convergence of the perturbation expansions is always hastened if perturbations which are of the same magnitude are considered together and act simultaneously to remove the degeneracy. This applies to the first order spin-orbit and second order $\bar{k} \cdot \bar{p}$ perturbations since these two are of the same order of magnitude.

2.2 Energy Band Structure in the Presence of an External Magnetic Field

Consider equation 2.1.1, i.e., the problem of a crystal in a magnetic field. The solutions are obviously no longer of the Bloch type, (equation 2.1.3). However, with the appropriate choice of gauge some arguments can still be made about the general form of the wavefunction ψ . Since the spin-orbit interaction and the spin-magnetic field interaction terms are not essential to these arguments, one may temporarily omit them and consider the equation

$$-\frac{\hbar^2}{2m} \left(\hat{p} + \frac{ie\hbar}{c} \vec{A} \right)^2 \psi + V(r)\psi = E\psi \quad (2.2.1)$$

Choose a coordinate system x_1, x_2, x_3 such that the magnetic field lies along x_3 and select the gauge (Landau gauge):

$$A_1 = -Hx_2 \quad A_2 = A_3 = 0 \quad (2.2.2)$$

In this coordinate system equation 2.2.1 becomes

$$-\frac{\hbar^2}{2m} \nabla^2 \psi + V(r)\psi - \frac{ie\hbar}{mc} \frac{\hbar}{i} x_2 \frac{\partial}{\partial x_1} \psi + \frac{e^2 \hbar^2}{2mc^2} x_2^2 \psi = E\psi \quad (2.2.3)$$

which can be written

$$-\frac{\hbar^2}{2m} \nabla^2 \psi + \hat{V}'(r)\psi = E\psi$$

if one defines

$$\hat{V}'(r) = V(r) - \frac{e\hbar^2}{mc} \frac{\hbar}{i} x_2 \frac{\partial}{\partial x_1} + \frac{e^2 \hbar^2}{2mc^2} x_2^2 \quad (2.2.5)$$

Equation 2.2.4 is now of the same form as Bloch's (2) equation 1 except

that now $\hat{V}'(r)$ is periodic in x_1 with the period a and in x_3 with the period c but is not periodic in x_2 . The periods a and c are those of the lattice in the x_1 and x_3 directions respectively.

The arguments of Bloch can now be repeated omitting those involving x_2 (or y in Bloch's notation), i.e., deleting the second equation in his equations 4 and 4', and $b_{\kappa\lambda}$'s in equations 5, 5' and 5". The following result is thus obtained

$$\psi = e^{i(k_1 x_1 + k_3 x_3)} \mathcal{U}_{k_1 k_3}(r) \quad (2.2.6)$$

where $\mathcal{U}_{k_1 k_3}(r)$ has the periodicity of the lattice in the x_1 and x_3 directions. The factor $e^{i(k_1 x_1 + k_3 x_3)}$ could also be obtained by noting that \hat{p}_{x_1} and \hat{p}_{x_3} commute with the Hamiltonian of equation 2.2.1 if the gauge is chosen according to equation 2.2.2.

Having determined the general form of the solution ψ one may go back to equation 2.2.1 and to the coordinate system in which x, y, z axes are along the $[100]$, $[010]$, $[001]$ directions of the crystal respectively. This is the coordinate system in which the functions given by equation 2.1.8 are the solutions of equation 2.1.5.

The two coordinate systems are related by

$$\begin{pmatrix} x \\ y \\ z \end{pmatrix} = \begin{pmatrix} A \end{pmatrix} \begin{pmatrix} x_1 \\ x_2 \\ x_3 \end{pmatrix} \quad (2.2.7)$$

where

$$||A|| = \begin{vmatrix} a_{x1} & a_{x2} & a_{x3} \\ a_{y1} & a_{y2} & a_{y3} \\ a_{z1} & a_{z2} & a_{z3} \end{vmatrix} \quad (2.2.8)$$

In view of the form of the solution to the Schrodinger equation for an electron in a magnetic field and otherwise free, i.e., equation 2.1.1 with $V = 0$, which is given in Appendix II, it is convenient to write $u_{k_1 k_3}(r)$ in the following way:

$$u_{k_1 k_3}(r) = \sum_i \sum_n \alpha_{in} f_n(x_2) \phi_i \quad (2.2.9)$$

where ϕ_i are given by equation 2.1.8 and f_n are the harmonic oscillator wave functions. This is seen to have the periodicity in the x_1 and x_3 directions required by equation 2.2.6, and is expressed in terms of a complete set of functions of x_2 . One thus gets

$$\psi = e^{i(k_1 x_1 + k_2 x_2)} \sum_i \sum_n \alpha_{in} f_n(x_2) \phi_i \quad (2.2.10)$$

The choice of gauge is still given by equation 2.2.2 and therefore

$$\begin{aligned} A_x &= a_{x1} A_1 = -a_{x1} \mathcal{H} x_2 \\ A_y &= a_{y1} A_1 = -a_{y1} \mathcal{H} x_2 \\ A_z &= a_{z1} A_1 = -a_{z1} \mathcal{H} x_2 \end{aligned} \quad (2.2.11)$$

Equations 2.2.10 and 2.2.11 may now be substituted into equation 2.1.1:

$$\begin{aligned} & \left\{ \frac{1}{2m} \left(\frac{\hbar}{i} \frac{\partial}{\partial x} - \frac{|e| a_{x1} \mathcal{H} x_2}{c} \right)^2 + \frac{1}{2m} \left(\frac{\hbar}{i} \frac{\partial}{\partial y} - \frac{|e| a_{y1} \mathcal{H} x_2}{c} \right)^2 \right. \\ & \quad \left. + \frac{1}{2m} \left(\frac{\hbar}{i} \frac{\partial}{\partial z} - \frac{|e| a_{z1} \mathcal{H} x_2}{c} \right)^2 \right. \\ & \quad \left. + \frac{\hbar}{4m^2 c^2} \left[\nabla \cdot \mathbf{v} \times \left(\frac{\hbar}{i} \frac{\partial}{\partial x} - \frac{|e| a_{x1} \mathcal{H} x_2}{c} \right) + \frac{\hbar}{i} \frac{\partial}{\partial y} - \frac{|e| a_{y1} \mathcal{H} x_2}{c} \right. \right. \\ & \quad \left. \left. + \frac{\hbar}{i} \frac{\partial}{\partial z} - \frac{|e| a_{z1} \mathcal{H} x_2}{c} \right) \right] \cdot \bar{\sigma} + \frac{|e|}{2mc} \bar{\sigma} \cdot \mathcal{H} + V(r) \Big\} \\ & \cdot e^{i(k_1 x_1 + k_3 x_3)} \sum_i \sum_n \alpha_{in} f_n \phi_i = E e^{i(k_1 x_1 + k_3 x_3)} \sum_i \sum_n \alpha_{in} f_n \phi_i \end{aligned} \quad (2.2.12)$$

Now if one calls

$$\frac{\partial x_1}{\partial x} = b_{1x}, \quad \frac{\partial x_2}{\partial x} = b_{2x}, \quad \frac{\partial x_3}{\partial x} = b_{3x}, \quad , \quad \text{etc.}$$

that is,

$$\begin{pmatrix} x_1 \\ y_1 \\ z_1 \end{pmatrix} = \|B\| \begin{pmatrix} x \\ y \\ z \end{pmatrix} \quad (2.2.13)$$

one obtains

$$\begin{aligned}
& \sum_i \sum_n \alpha_{in} \left[-\frac{\hbar^2}{2m} \left(f_n \frac{\partial^2 \phi_i}{\partial x^2} + f_n \frac{\partial^2 \phi_i}{\partial y^2} + f_n \frac{\partial^2 \phi_i}{\partial z^2} \right) + v(r) \phi_i f_n + \right. \\
& + \phi_i \left\{ -\frac{\hbar^2}{2m} \left[i(b_{1x}^{k_1} + b_{3x}^{k_3})(b_{1x}^{ik_1} f_n + b_{2x} \frac{\partial f_n}{\partial x_2} + b_{3x}^{ik_3} f_n) + b_{2x}(b_{1x}^{ik_1} \frac{\partial f_n}{\partial x_2} + b_{2x} \frac{\partial^2 f_n}{\partial x_2^2} + b_{3x}^{ik_3} \frac{\partial f_n}{\partial x_2}) \right] - \right. \\
& - \frac{1}{2m} \frac{2|e|a_{x1}\mathcal{H}}{c} x_2 \frac{\hbar}{i} (b_{1x}^{ik_1} f_n + b_{2x} \frac{\partial f_n}{\partial x_2} + b_{3x}^{ik_3} f_n) + \frac{|e|^2 a_{x1}^2 \mathcal{H}^2 x_2^2}{2mc^2} f_n \\
& - \frac{\hbar^2}{2m} \left[i(b_{1y}^{k_1} + b_{3y}^{k_3})(b_{1y}^{ik_1} f_n + b_{2y} \frac{\partial f_n}{\partial x_2} + b_{3y}^{ik_3} f_n) + b_{2y}(b_{1y}^{ik_1} \frac{\partial f_n}{\partial x_2} + b_{2y} \frac{\partial^2 f_n}{\partial x_2^2} + b_{3y}^{ik_3} \frac{\partial f_n}{\partial x_2}) \right] - \\
& - \frac{1}{2m} \frac{2|e|a_{y1}\mathcal{H}}{c} x_2 \frac{\hbar}{i} (b_{1y}^{ik_1} f_n + b_{2y} \frac{\partial f_n}{\partial x_2} + b_{3y}^{ik_3} f_n) + \frac{|e|^2 a_{y1}^2 \mathcal{H}^2 x_2^2}{2mc^2} f_n \\
& - \frac{\hbar^2}{2m} \left[i(b_{1z}^{k_1} + b_{3z}^{k_3})(b_{1z}^{ik_1} f_n + b_{2z} \frac{\partial f_n}{\partial x_2} + b_{3z}^{ik_3} f_n) + b_{2z}(b_{1z}^{ik_1} \frac{\partial f_n}{\partial x_2} + b_{2z} \frac{\partial^2 f_n}{\partial x_2^2} + b_{3z}^{ik_3} \frac{\partial f_n}{\partial x_2}) \right] \\
& - \frac{1}{2m} \frac{2|e|a_{z1}\mathcal{H}}{c} x_2 \frac{\hbar}{i} (b_{1z}^{ik_1} f_n + b_{2z} \frac{\partial f_n}{\partial x_2} + b_{3z}^{ik_3} f_n) + \frac{|e|^2 a_{z1}^2 \mathcal{H}^2 x_2^2}{2mc^2} f_n \Big\} \\
& - \frac{i\hbar^2}{m} \left\{ \left[b_{1x}^{k_1} f_n + b_{2x} \frac{1}{i} \frac{\partial f_n}{\partial x_2} + b_{3x}^{k_3} f_n - \frac{|e|a_{x1}\mathcal{H}}{\hbar c} x_2 f_n \right] \frac{\partial \phi_i}{\partial x} + \right. \\
& + \left[(b_{1y}^{k_1} - \frac{|e|a_{y1}\mathcal{H}}{c\hbar} x_2) f_n + b_{2y} \frac{1}{i} \frac{\partial f_n}{\partial x_2} + b_{3y}^{k_3} f_n \right] \frac{\partial \phi_i}{\partial y} + \\
& + \left[(b_{1z}^{k_1} - \frac{|e|a_{z1}\mathcal{H}}{c\hbar} x_2) f_n + b_{2z} \frac{1}{i} \frac{\partial f_n}{\partial x_2} + b_{3z}^{k_3} f_n \right] \frac{\partial \phi_i}{\partial z} \Big\} + \frac{\hbar}{4m^2 c^2} f_n \left[\nabla v \times (\bar{i} \frac{\hbar}{i} \frac{\partial \phi_i}{\partial x} + \bar{j} \frac{\hbar}{i} \frac{\partial \phi_i}{\partial y} + \bar{k} \frac{\hbar}{i} \frac{\partial \phi_i}{\partial z}) \right] \cdot \vec{\sigma} + \\
& + \phi_i \frac{\hbar^2}{4m^2 c^2} \nabla v \times \left[\bar{i} \left((b_{1x}^{k_1} - \frac{|e|a_{x1}\mathcal{H}}{c\hbar} x_2) f_n + b_{2x} \frac{1}{i} \frac{\partial f_n}{\partial x_2} + b_{3x}^{k_3} f_n \right) + \right. \\
& + \bar{j} \left((b_{1y}^{k_1} - \frac{|e|a_{y1}\mathcal{H}}{c\hbar} x_2) f_n + b_{2y} \frac{1}{i} \frac{\partial f_n}{\partial x_2} + b_{3y}^{k_3} f_n \right) + \\
& + \bar{k} \left((b_{1z}^{k_1} - \frac{|e|a_{z1}\mathcal{H}}{c\hbar} x_2) f_n + b_{2z} \frac{1}{i} \frac{\partial f_n}{\partial x_2} + b_{3z}^{k_3} f_n \right) \Big] \Big\} \cdot \vec{\sigma} + \frac{|e|}{2mc} \vec{\sigma} \cdot \mathcal{H} \phi_i f_n \Big] = E \sum_i \sum_n \alpha_{in} f_n \phi_i \quad (2.2.14)
\end{aligned}$$

The matrices to which $a_{\alpha i}$ and $b_{i\alpha}$ belong are orthogonal and $A = B^{-1}$. From orthogonality $B^{-1} = B$, $A^{-1} = A$, or $A = B$.

$b_{1x} = a_{x1}$, $b_{2x} = a_{x2}$, $b_{3x} = a_{x3}$, etc.; also

$$b_{1x}b_{1x} + b_{1y}b_{1y} + b_{1z}b_{1z} = 1$$

$$b_{2x}b_{2x} + b_{2y}b_{2y} + b_{2z}b_{2z} = 1$$

(2.2.15)

$$b_{3x}b_{3x} + b_{3y}b_{3y} + b_{3z}b_{3z} = 1$$

$$b_{1x}b_{2x} + b_{1y}b_{2y} + b_{1z}b_{2z} = 0, \text{ etc.}$$

Using these relations and defining the operators

$$\hat{k}_1 = k_1 - \frac{|e|\hbar x_2}{c\hbar}$$

(2.2.16)

$$\hat{k}_2 = \frac{1}{i} \frac{\partial}{\partial x_2}$$

$$\hat{k}_3 = k_3$$

which operate only on the harmonic oscillator wavefunctions f_n , and

$$\begin{pmatrix} \hat{k}_x \\ \hat{k}_y \\ \hat{k}_z \end{pmatrix} = \| A \| \begin{pmatrix} \hat{k}_1 \\ \hat{k}_2 \\ \hat{k}_3 \end{pmatrix}$$

(2.2.17)

the following is finally obtained

$$\begin{aligned}
& \sum_i \sum_n \alpha_{in} f_n \left[-\frac{\hbar^2}{2m} \nabla^2 \phi_i + V(r) \phi_i \right] + \sum_i \sum_n \alpha_{in} \phi_i \frac{\hbar^2}{2m} \hat{k}^2 f_n \\
& - \sum_i \sum_n \alpha_{in} \frac{i\hbar^2}{2m} (\hat{k} f_n) \cdot \nabla \phi_i + \sum_i \sum_n \alpha_{in} f_n \left[\nabla V \times \hat{p} \right] \cdot \vec{\sigma} \phi_i + \\
& + \sum_i \sum_n \alpha_{in} \frac{\hbar^2}{4m^2 c^2} \left[\nabla V \times \hat{k} f_n \right] \cdot \vec{\sigma} \phi_i + \sum_i \sum_n \alpha_{in} \frac{|e|\hbar}{2mc} \vec{\sigma} \cdot \vec{\mathcal{H}} \phi_i f_n = \\
& = E \sum_i \sum_n \alpha_{in} f_n \phi_i \tag{2.2.18}
\end{aligned}$$

One may again neglect the term involving $\left[\nabla V \times \hat{k} \right] \cdot \vec{\sigma}$, treat the first term as the zero order equation and all other terms as perturbations, thus restricting the calculation to the region close to the center of the Brillouin zone and to low Landau level quantum numbers.

The zero order equation is thus given by (ignoring $\frac{\hbar^2}{2m} \hat{k}^2$ and $\frac{|e|\hbar}{2mc} \vec{\sigma} \cdot \vec{\mathcal{H}}$ terms at this time)

$$\sum_i \sum_n \alpha_{in}^0 f_n \left[-\frac{\hbar^2}{2m} \nabla^2 \phi_i + V(r) \phi_i \right] = E^0 \sum_i \sum_n \alpha_{in}^0 f_n \phi_i \tag{2.2.19}$$

Since all f_n are linearly independent one must write

$$\sum_i \alpha_{in}^0 \left[-\frac{\hbar^2}{2m} \nabla^2 \phi_i + V(r) \phi_i \right] = E^0 \sum_i \alpha_{in}^0 \phi_i \tag{2.2.20}$$

for each n . This is essentially equation 2.1.5 and therefore the solutions are given by equation 2.1.8 and the zero order energy levels are as indicated in Fig. 2.1.

In calculating the effects of the perturbation terms we first restrict our attention to the case with the external magnetic field applied in the [001] direction, i.e., along the z-axis. We thus have

$$a_{x1} = a_{y2} = a_{z3} = 1 \quad (2.2.21)$$

all other a's in 2.2.8 being zero and

$$A_x = -\mathcal{H}_y \quad A_y = A_z = 0 \quad (2.2.22)$$

$$\psi = e^{i(k_x x + k_z z)} \sum_i \sum_n \alpha_{in} f_n(y) \phi_i \quad (2.2.23)$$

$$\left. \begin{aligned} \hat{k}_x &= k_x - \frac{ie\hbar y}{c\hbar} \\ \hat{k}_y &= \frac{1}{i} \frac{\partial}{\partial y} \\ \hat{k}_z &= k_z \end{aligned} \right\} \quad (2.2.24)$$

Since \hat{k} operates only on f_n one can carry out the $k \cdot p$ and the spin-orbit perturbation analysis exactly as before in the no-magnetic field case, substituting \hat{k}_α for k_α in the final result and operating with the resulting matrix on some linear combination of functions f_n . There will be only one modification which arises from the noncommutivity of \hat{k}_α whereas k_α do commute. Consider \mathcal{D}_{12} given by 2.1.15 and entering into 2.1.20. When k_x and k_y commute $\mathcal{D}_{12} = N k_x k_y$. Actually, by 2.1.15

$$\mathcal{D}_{12} = \mathcal{D}_{12}^{xy} \hat{k}_x \hat{k}_y + \mathcal{D}_{12}^{yx} \hat{k}_y \hat{k}_x \quad (2.2.25)$$

Defining

$$K = \mathcal{D}_{12}^{xy} - \mathcal{D}_{12}^{yx} \quad (2.2.26)$$

one can write

$$\mathcal{D}_{12} = N \left\{ \hat{k}_x \hat{k}_y \right\} + \frac{1}{2} K (\hat{k}_x, \hat{k}_y) \quad (2.2.27)$$

where $\left\{ \hat{k}_x \hat{k}_y \right\}$ is the symmetrized product of \hat{k}_x and \hat{k}_y and (\hat{k}_x, \hat{k}_y) is the commutator of \hat{k}_x and \hat{k}_y . Similar relations hold for all \mathcal{D}_{ij} with $i \neq j$. K is the antisymmetric constant introduced by Luttinger (2). The commutators of \hat{k}_α are given by

$$\begin{aligned} (\hat{k}_x, \hat{k}_y) &= \frac{1}{i} \frac{|\mathbf{e}| \hbar}{c \hbar} \\ (\hat{k}_x, \hat{k}_z) &= 0 \\ (\hat{k}_y, \hat{k}_z) &= 0 \end{aligned} \quad (2.2.28)$$

One now has the new definitions of \mathcal{D}_{ij} :

$$\begin{aligned} \mathcal{D}_{11} &= L \hat{k}_x^2 + M (\hat{k}_y^2 + \hat{k}_z^2) \\ \mathcal{D}_{12} &= N \left\{ \hat{k}_x \hat{k}_y \right\} - i \frac{K}{2} \frac{|\mathbf{e}| \hbar}{c \hbar} \\ \mathcal{D}_{13} &= N \left\{ \hat{k}_x \hat{k}_z \right\} = N \hat{k}_x k_z \\ \mathcal{D}_{21} &= N \left\{ \hat{k}_x \hat{k}_y \right\} + i \frac{K}{2} \frac{|\mathbf{e}| \hbar}{c \hbar} \\ \mathcal{D}_{22} &= L \hat{k}_y^2 + M (\hat{k}_x^2 + \hat{k}_z^2) \\ \mathcal{D}_{23} &= N \left\{ \hat{k}_y \hat{k}_z \right\} = N \hat{k}_y k_z \\ \mathcal{D}_{31} &= N \left\{ \hat{k}_x \hat{k}_z \right\} = N \hat{k}_x k_z \end{aligned} \quad (2.2.29)$$

$$\begin{aligned} \mathcal{D}_{32} &= N \left\{ \hat{k}_y \hat{k}_z \right\} = N \hat{k}_y k_z \\ \mathcal{D}_{33} &= L \hat{k}_z^2 + M (\hat{k}_x^2 + \hat{k}_y^2) \end{aligned} \quad (2.2.29)$$

It is obvious that the spin-orbit perturbation matrix $\| V_{ij}^{\text{so}} \|$ is unaffected by the change from k_α to \hat{k}_α . The transformation given by equation 2.1.26 can therefore be used on both the new D_{ij} and V_{ij}^{so} to transform them to the $J m_j$ representation. The energy is again measured from the top of the valence band. The transformed matrix is once more given by equation 2.1.28 with G and Γ defined by equations 2.1.29 and 2.1.30. The important differences in the new results will arise from the fact that in the presence of the magnetic field one no longer has $\mathcal{D}_{ij} = \mathcal{D}_{ji}$. One now gets for the elements of G and Γ :

$$\begin{aligned} \frac{\mathcal{D}_{11} + \mathcal{D}_{22} + i(\mathcal{D}_{12} - \mathcal{D}_{21})}{2} &= \frac{1}{2} P - \frac{i}{2} K \frac{|e|\hbar}{c\hbar} \\ -\frac{\mathcal{D}_{13} + i\mathcal{D}_{23}}{\sqrt{3}} &= -i\mathcal{L} \\ \frac{\mathcal{D}_{13} - i\mathcal{D}_{23}}{\sqrt{6}} &= \frac{1}{\sqrt{2}} \mathcal{L} \\ -\frac{\mathcal{D}_{31} - i\mathcal{D}_{23}}{\sqrt{3}} &= i\mathcal{L}^* \\ \frac{\mathcal{D}_{11} + \mathcal{D}_{22} + 4\mathcal{D}_{33} + i(\mathcal{D}_{12} - \mathcal{D}_{21})}{6} &= \frac{1}{6} P + \frac{2}{3} Q - i \frac{1K}{6} \frac{|e|\hbar}{c\hbar} \end{aligned} \quad (2.2.30)$$

$$\frac{\mathcal{D}_{11} + \mathcal{D}_{22} - 2\mathcal{D}_{33} + i(\mathcal{L}_{12} - \mathcal{L}_{21})}{3\sqrt{2}} = \frac{1}{3\sqrt{2}} (P - 2Q) - i \frac{iK}{3\sqrt{2}} \frac{|e|\mathcal{H}}{c\hbar}$$

$$\frac{\mathcal{D}_{31} + i\mathcal{D}_{32}}{\sqrt{6}} = -\frac{i}{\sqrt{2}} \mathcal{L}^*$$

$$\frac{\mathcal{D}_{11} + \mathcal{D}_{22} + \mathcal{D}_{33} + i(\mathcal{L}_{12} - \mathcal{L}_{21})}{3} - \Delta = \frac{1}{3} (P + Q) - i \frac{iK}{3} \frac{|e|\mathcal{H}}{c\hbar} - \Delta$$

$$\frac{-\mathcal{D}_{11} + \mathcal{D}_{22} + i(\mathcal{D}_{12} + \mathcal{L}_{21})}{2\sqrt{3}} = -\mathcal{M}$$

$$\frac{-\mathcal{D}_{11} + \mathcal{D}_{22} + i(\mathcal{L}_{12} + \mathcal{D}_{21})}{\sqrt{6}} = -\sqrt{2} \mathcal{M}$$

$$\frac{\mathcal{D}_{11} - \mathcal{D}_{22} - i(\mathcal{D}_{12} + \mathcal{L}_{21})}{2\sqrt{3}} = \mathcal{M}$$

$$\frac{\mathcal{D}_{31} - \mathcal{D}_{13} + i(\mathcal{D}_{23} - \mathcal{D}_{32})}{3} = 0$$

$$\frac{\mathcal{D}_{13} + 2\mathcal{D}_{31} - i(\mathcal{D}_{23} + 2\mathcal{D}_{32})}{3\sqrt{2}} = i\sqrt{\frac{3}{2}} \mathcal{L}$$

$$\frac{\mathcal{L}_{11} - \mathcal{D}_{22} - i(\mathcal{L}_{12} + \mathcal{L}_{21})}{\sqrt{6}} = \sqrt{2} \mathcal{M}$$

$$\frac{-2\mathcal{D}_{13} - \mathcal{D}_{31} + i(2\mathcal{D}_{23} + \mathcal{D}_{32})}{3\sqrt{2}} = -i\sqrt{\frac{3}{2}} \mathcal{L}$$

$$\frac{\mathcal{D}_{13} - \mathcal{D}_{31} + i(\mathcal{D}_{32} - \mathcal{D}_{23})}{3} = 0$$

(2.2.30)

The following definitions have been used (following in form Luttinger and Kohn (1)), although L,M,N, constants used here are different numerically from their A,B,C):

$$\begin{aligned}
 P &= (L + M)(\hat{k}_x^2 + \hat{k}_y^2) + 2M k_z^2 \\
 Q &= M(\hat{k}_x^2 + \hat{k}_y^2) + L k_z^2 \\
 \mathcal{L} &= \frac{iN}{\sqrt{3}} (\hat{k}_x - i\hat{k}_y)k_z \\
 \mathcal{M} &= \frac{1}{\sqrt{12}} \left[(L - M)(\hat{k}_x^2 - \hat{k}_y^2) - 2iN \left\{ \hat{k}_x \hat{k}_y \right\} \right]
 \end{aligned} \tag{2.2.31}$$

The matrix $\|V_{ij}\|$ may now be explicitly written. The ordering of terms in $\|V_{ij}\|$ as given by equation 2.1.28 is the following:

$$\left(\frac{3}{2}\right) \frac{3}{2} ; \left(\frac{3}{2}\right) \frac{1}{2} ; \left(\frac{1}{2}\right) \frac{1}{2} ; \left(\frac{3}{2}\right) - \frac{3}{2} ; \left(\frac{3}{2}\right) - \frac{1}{2} ; \left(\frac{1}{2}\right) - \frac{1}{2} \tag{2.2.32}$$

Reordering the matrix elements so as to conform with Luttinger and Kohn (1) one gets

$$\|v_{ij}\| = \left\| \begin{array}{cccccc} \frac{1}{2}P + \frac{K_S}{2} & -i\mathcal{L} & -m & 0 & \frac{1}{\sqrt{2}}\mathcal{L} & -\sqrt{2}m \\ i\mathcal{L}^* & \frac{1}{6}P + \frac{2}{3}Q + \frac{K_S}{6} & 0 & m & \frac{1}{3\sqrt{2}}(P - 2Q + K_S) & i\sqrt{\frac{3}{2}}\mathcal{L} \\ -m^* & 0 & \frac{1}{6}P + \frac{2}{3}Q - \frac{K_S}{6} & -i\mathcal{L} & i\sqrt{\frac{3}{2}}\mathcal{L}^* & \frac{1}{3\sqrt{2}}(P - 2Q - K_S) \\ 0 & m^* & i\mathcal{L}^* & \frac{1}{2}P - \frac{K_S}{2} & \sqrt{2}m^* & -\frac{i}{\sqrt{2}}\mathcal{L}^* \\ -\frac{i}{\sqrt{2}}\mathcal{L}^* & \frac{1}{3\sqrt{2}}(P - 2Q + K_S) & -i\sqrt{\frac{3}{2}}\mathcal{L} & \sqrt{2}m & \frac{1}{2}(P + Q) + \frac{K_S}{3} - \Delta & 0 \\ -\sqrt{2}m^* & -i\sqrt{\frac{3}{2}}\mathcal{L}^* & \frac{1}{3\sqrt{2}}(P - 2Q - K_S) & \frac{1}{\sqrt{2}}\mathcal{L} & 0 & \frac{1}{3}(P + Q) - \frac{K_S}{3} - \Delta \end{array} \right\| \begin{array}{l} (\frac{3}{2}) \frac{3}{2} \\ (\frac{3}{2}) \frac{1}{2} \\ (\frac{3}{2}) - \frac{1}{2} \\ (\frac{3}{2}) - \frac{3}{2} \\ (\frac{1}{2}) \frac{1}{2} \\ (\frac{1}{2}) - \frac{1}{2} \end{array}$$

(2.2.33)

where
$$s = \frac{|e|\hbar c}{c\hbar} \quad (2.2.34)$$

Now if $||V_{ij}||$ is transformed using the transformation $||\mathcal{U}||$:

$$||\mathcal{U}|| = \begin{vmatrix} 1 & 0 & 0 & 0 & 0 & 0 \\ 0 & 1 & 0 & 0 & 0 & 0 \\ 0 & 0 & -1 & 0 & 0 & 0 \\ 0 & 0 & 0 & 1 & 0 & 0 \\ 0 & 0 & 0 & 0 & 1 & 0 \\ 0 & 0 & 0 & 0 & 0 & 1 \end{vmatrix} \quad (2.2.35)$$

and K is set equal to zero, a matrix is obtained which is identical in form with the final result of Luttinger and Kohn (1).

The matrix $||V_{ij}||$ must now be allowed to operate on linear combinations of the harmonic oscillator wavefunctions f_n . This is most conveniently done by writing the operators \hat{k}_x and \hat{k}_y in terms of the raising and lowering operators.

The problem of a particle in a magnetic field is treated from the operator point of view in Appendix II. It is shown there that the raising and lowering operators are given by

$$\text{Raising Operator: } \frac{1}{\sqrt{2n}} \sqrt{\frac{\hbar c}{|e|\hbar}} (-\hat{k}_x - i\hat{k}_y) \quad (2.2.36)$$

$$\text{Lowering Operator: } \frac{1}{\sqrt{2n}} \sqrt{\frac{\hbar c}{|e|\hbar}} (-\hat{k}_x + i\hat{k}_y) \quad (2.2.37)$$

One may define:

$$a^+ = -\frac{1}{\sqrt{2}} \sqrt{\frac{\hbar c}{|e|\mathcal{H}}} (\hat{k}_x + i\hat{k}_y) \quad (2.2.38)$$

$$a = -\frac{1}{\sqrt{2}} \sqrt{\frac{\hbar c}{|e|\mathcal{H}}} (\hat{k}_x - i\hat{k}_y) \quad (2.2.39)$$

Then

$$f_n = n^{-1/2} a^+ f_{n-1} \quad \text{or} \quad a^+ f_n = (n+1)^{1/2} f_{n+1} \quad (2.2.40)$$

$$f_{n-1} = n^{-1/2} a f_n \quad \text{or} \quad a f_n = n^{1/2} f_{n-1} \quad (2.2.41)$$

a^+ and a being our raising and lowering operators respectively.

Using the following relations:

$$a^+ a = \frac{1}{2} \frac{\hbar c}{|e|\mathcal{H}} (\hat{k}_x^2 + \hat{k}_y^2 - \frac{|e|\mathcal{H}}{\hbar c})$$

$$a a^+ = \frac{1}{2} \frac{\hbar c}{|e|\mathcal{H}} (\hat{k}_x^2 + \hat{k}_y^2 + \frac{|e|\mathcal{H}}{\hbar c})$$

$$(a, a^+) = 1 \quad (2.2.42)$$

$$a^{+2} = \frac{1}{2} \frac{\hbar c}{|e|\mathcal{H}} (\hat{k}_x^2 - \hat{k}_y^2 + i\hat{k}_x \hat{k}_y + i\hat{k}_y \hat{k}_x)$$

$$a^2 = \frac{1}{2} \frac{\hbar c}{|e|\mathcal{H}} (\hat{k}_x^2 - \hat{k}_y^2 - i\hat{k}_x \hat{k}_y - i\hat{k}_y \hat{k}_x)$$

one obtains

$$\begin{aligned}
 \hat{k}_x^2 + \hat{k}_y^2 &= \frac{|e|\mathcal{H}}{\hbar c} (2aa^+ - 1) = \frac{|e|\mathcal{H}}{\hbar c} (2a^+a + 1) \\
 \hat{k}_x^2 - \hat{k}_y^2 &= \frac{|e|\mathcal{H}}{\hbar c} (a^2 + a^{+2}) \\
 \left\{ \hat{k}_x \hat{k}_y \right\} &= \frac{|e|\mathcal{H}}{\hbar c} \frac{1}{2i} (a^{+2} - a^2)
 \end{aligned} \tag{2.2.43}$$

Using the definitions

$$\begin{aligned}
 \frac{\hbar^2}{2m} \ell &= L & \frac{\hbar^2}{m} \chi &= K \\
 \frac{\hbar^2}{2m} \mu &= M & \sqrt{\frac{|e|\mathcal{H}}{\hbar c}} d &= \gamma s d = k_z \\
 \frac{\hbar^2}{2m} \nu &= N & \frac{\hbar |e|\mathcal{H}}{mc} \Delta' &= \Delta
 \end{aligned} \tag{2.2.44}$$

and relationships 2.2.43, one may write

$$\begin{aligned}
 P &= \frac{\hbar^2}{m} s \left[(\ell + \mu) (a^+a + \frac{1}{2}) + \mu d^2 \right] \\
 Q &= \frac{\hbar^2}{m} s \left[\mu (a^+a + \frac{1}{2}) + \frac{\ell}{2} d^2 \right] \\
 \mathcal{L} &= \frac{\hbar^2}{m} s \left(\frac{1}{\sqrt{6}} \nu \right) a d \\
 \mathcal{M} &= \frac{\hbar^2}{m} s \frac{1}{4\sqrt{3}} \left[(\ell - \mu - \nu) a^{+2} + (\ell - \mu + \nu) a^2 \right] \\
 \mathcal{L}^* &= - \frac{\hbar^2}{m} s \left(\frac{1}{\sqrt{6}} \nu \right) a^+ d \\
 \mathcal{M}^* &= \frac{\hbar^2}{m} s \frac{1}{4\sqrt{3}} \left[(\ell - \mu + \nu) a^{+2} + (\ell - \mu - \nu) a^2 \right]
 \end{aligned} \tag{2.2.45}$$

Now reordering the terms in V_{ij} again in a manner which will be found convenient and which is used by Luttinger (2) and by Burstein et al. (4) in their equation 27, one gets the result:

$$||v_{1,j}|| = \frac{\hbar |e| \mathcal{E}}{mc}$$

$$\begin{array}{ccccccc}
\frac{\ell+\mu}{2}(a^+a+\frac{1}{2}) + & -\frac{1}{4\sqrt{3}}[(\ell-\mu-\nu)a^{+2} + & \frac{1}{\sqrt{6}}\nu ad & 0 & -\frac{1}{2\sqrt{3}}\nu ad & -\frac{1}{4}\sqrt{\frac{2}{3}}[(\ell-\mu-\nu)a^{+2} + & (\frac{3}{2}) \frac{3}{2} \\
+ \frac{\mu}{2}d^2 + \frac{\chi}{2} & + (\ell-\mu+\nu)a^2] & & & & + (\ell-\mu+\nu)a^2] & \\
\\
-\frac{1}{4\sqrt{3}}[(\ell-\mu+\nu)a^{+2} + & \frac{1}{6}[(\ell+5\mu)(a^+a+\frac{1}{2}) + & 0 & \frac{1}{\sqrt{6}}\nu ad & \frac{1}{2}\nu a^+d & \frac{\ell-\mu}{3\sqrt{2}}(a^+a+\frac{1}{2}-d^2) - & (\frac{3}{2}) - \frac{1}{2} \\
+ (\ell-\mu-\nu)a^2] & + (\mu+2\ell)d^2 - \chi] & & & & - \frac{\chi}{3\sqrt{2}} & \\
\\
\frac{1}{\sqrt{6}}\nu a^+d & 0 & \frac{1}{6}[(\ell+5\mu)a^+a + \frac{1}{2}) + & \frac{1}{4\sqrt{3}}[(\ell-\mu-\nu)a^{+2} + & \frac{\ell-\mu}{3\sqrt{2}}(a^+a+\frac{1}{2}-d^2) + & -\frac{1}{2}\nu ad & (\frac{3}{2}) \frac{1}{2} \\
& & + (\mu+2\ell)d^2 + \chi] & + (\ell-\mu+\nu)a^2] & + \frac{\chi}{3\sqrt{2}} & & \\
\\
0 & \frac{1}{\sqrt{6}}\nu a^+d & \frac{1}{4\sqrt{3}}[(\ell-\mu+\nu)a^{+2} + & \frac{1}{2}[(\ell+\mu)(a^+a+\frac{1}{2}) + & \frac{1}{4}\sqrt{\frac{2}{3}}[(\ell-\mu+\nu)a^{+2} + & -\frac{1}{2\sqrt{3}}\nu a^+d & (\frac{3}{2}) - \frac{3}{2} \\
& & + (\ell-\mu-\nu)a^2] & + \mu d^2 - \chi] & + (\ell-\mu-\nu)a^2] & & \\
\\
-\frac{1}{2\sqrt{3}}\nu a^+d & \frac{1}{2}\nu ad & \frac{\ell-\mu}{3\sqrt{2}}(a^+a+\frac{1}{2}-d^2) + & \frac{1}{4}\sqrt{\frac{2}{3}}[(\ell-\mu-\nu)a^{+2} + & \frac{1}{3}[(\ell+2\mu)(a^+a+\frac{1}{2}+\frac{1}{2}d^2) + & 0 & (\frac{1}{2}) \frac{1}{2} \\
& & + \frac{\chi}{3\sqrt{2}} & + (\ell-\mu+\nu)a^2] & + \chi] - \Delta' & & \\
\\
-\frac{1}{4}\sqrt{\frac{2}{3}}[(\ell-\mu+\nu)a^{+2} + & \frac{\ell-\mu}{3\sqrt{2}}(a^+a+\frac{1}{2}-d^2) - & -\frac{1}{2}\nu a^+d & -\frac{1}{2\sqrt{3}}\nu ad & 0 & \frac{1}{3}[(\ell+2\mu)(a^+a+\frac{1}{2} + & (\frac{1}{2}) - \frac{1}{2} \\
+ (\ell-\mu-\nu)a^2] & + \frac{\chi}{3\sqrt{2}} & & & & + \frac{1}{2}d^2) - \chi] - \Delta' &
\end{array}$$

(2.2.46)

Now the terms $\frac{\hbar^2}{2m} \hat{k}^2$ and $\frac{|e|}{2mc} \vec{\sigma} \cdot \vec{\mathcal{H}}$ which appear in equation 2.2.18 and which have been ignored so far, must be introduced. In connection with the $\frac{\hbar^2}{2m} \hat{k}^2$ term, matrix elements of the following form must be evaluated:

$$V_{ij}^{k^2} = \int \phi_i^* \frac{\hbar^2}{2m} \hat{k}^2 \phi_j d\vec{r} \quad (2.2.47)$$

Since the operator \hat{k} is simply a multiplier as far as the wavefunctions ϕ_i are concerned, the result is

$$V_{ij}^{k^2} = \frac{\hbar^2}{2m} \hat{k}^2 \delta_{ij} \quad (2.2.48)$$

The 6×6 matrix $||V_{ij}^{k^2}||$ must now be transformed by U , equation 2.1.26 after which it may be added to $||V_{ij}||$. Again using equations 2.1.29 and 2.1.30 one obtains

$$\begin{aligned} \frac{V_{11}^{k^2} + V_{22}^{k^2} + i(V_{12}^{k^2} - V_{21}^{k^2})}{2} &= \frac{\hbar^2}{2m} \hat{k}^2 \\ \frac{V_{11}^{k^2} + V_{22}^{k^2} + 4V_{33}^{k^2} + i(V_{12}^{k^2} - V_{21}^{k^2})}{6} &= \frac{\hbar^2}{2m} \hat{k}^2 \\ \frac{V_{11}^{k^2} + V_{22}^{k^2} + V_{33}^{k^2} + i(V_{12}^{k^2} - V_{21}^{k^2})}{3} &= \frac{\hbar^2}{2m} \hat{k}^2 \end{aligned} \quad (2.2.49)$$

all other elements of G and Γ being zero. The transformed matrix is therefore

$$||V_{ij}^{k^2}|| = ||\frac{\hbar^2}{2m} \hat{k}^2 \delta_{ij}|| \quad (2.2.50)$$

$$\hat{k}^2 = \hat{k}_x^2 + \hat{k}_y^2 + \hat{k}_z^2 = \frac{e\hbar}{mc} \left[2(a^\dagger a + \frac{1}{2}) + d^2 \right] \quad (2.2.51)$$

Therefore,

$$||v_{1j}^k|| = \frac{\hbar e\hbar}{mc} \left| \left| \left[(a^\dagger a + \frac{1}{2}) + \frac{d^2}{2} \right] \delta_{1j} \right| \right| \quad (2.2.52)$$

These additional terms can be easily accounted for in the matrix of equation 2.2.46 by substituting in place of ℓ and μ , ℓ' and μ' defined as follows:

$$\ell' = \ell + 1 \quad \mu' = \mu + 1 \quad (2.2.53)$$

One must now evaluate the contribution of the $\frac{|e|}{2mc} \vec{\sigma} \cdot \vec{\mathcal{H}}$ term. In the ϕ_1 representation this is simply:

$$||v_{1j}^{\sigma \cdot \mathcal{H}}|| = \frac{\hbar(e)\hbar}{mc} \left| \left| \begin{array}{cccccc} 1/2 & 0 & 0 & 0 & 0 & 0 \\ 0 & 1/2 & 0 & 0 & 0 & 0 \\ 0 & 0 & 1/2 & 0 & 0 & 0 \\ 0 & 0 & 0 & -1/2 & 0 & 0 \\ 0 & 0 & 0 & 0 & -1/2 & 0 \\ 0 & 0 & 0 & 0 & 0 & -1/2 \end{array} \right| \right| \quad (2.2.54)$$

This must be transformed using U . Unfortunately equations 2.1.28, 2.1.29 and 2.1.30 can no longer be used. Instead one has to find how a matrix of the form

$$||v_{1j} \delta_{1j}|| \quad (2.2.55)$$

transforms under the transformation U . The result is:

$$U^{-1} \| v_{ij} \delta_{ij} \| U =$$

$$\begin{array}{cccccc}
\frac{v_{11} + v_{22}}{2} & 0 & 0 & 0 & \frac{-v_{11} + v_{22}}{2\sqrt{3}} & \frac{-v_{11} + v_{22}}{\sqrt{6}} & \left(\frac{3}{2}\right) \frac{3}{2} \\
0 & \frac{4v_{33} + v_{44} + v_{55}}{6} & \frac{-2v_{33} + v_{44} + v_{55}}{3\sqrt{2}} & \frac{v_{44} - v_{55}}{2\sqrt{3}} & 0 & 0 & \left(\frac{3}{2}\right) \frac{1}{2} \\
0 & \frac{-2v_{33} + v_{44} + v_{55}}{3\sqrt{2}} & \frac{v_{33} + v_{44} + v_{55}}{3} & \frac{v_{44} - v_{55}}{\sqrt{6}} & 0 & 0 & \left(\frac{1}{2}\right) \frac{1}{2} \\
0 & \frac{v_{44} - v_{55}}{2\sqrt{3}} & \frac{v_{44} - v_{55}}{\sqrt{6}} & \frac{v_{44} + v_{55}}{2} & 0 & 0 & \left(\frac{3}{2}\right) - \frac{3}{2} \\
\frac{-v_{11} + v_{22}}{2\sqrt{3}} & 0 & 0 & 0 & \frac{v_{11} + v_{22} + 4v_{66}}{6} & \frac{v_{11} + v_{22} - 2v_{66}}{3\sqrt{2}} & \left(\frac{3}{2}\right) - \frac{1}{2} \\
\frac{-v_{11} + v_{22}}{\sqrt{6}} & 0 & 0 & 0 & \frac{v_{11} + v_{22} - 2v_{66}}{3\sqrt{2}} & \frac{v_{11} + v_{22} + v_{66}}{3} & \left(\frac{1}{2}\right) - \frac{1}{2}
\end{array}$$

(2.2.56)

In the present case

$$\begin{aligned}
 \frac{V_{11}^{\sigma \cdot \mathcal{K}} + V_{22}^{\sigma \cdot \mathcal{K}}}{2} &= \frac{1}{2} & \frac{V_{44}^{\sigma \cdot \mathcal{K}} + V_{55}^{\sigma \cdot \mathcal{K}}}{2} &= -\frac{1}{2} \\
 \frac{-V_{11}^{\sigma \cdot \mathcal{K}} + V_{22}^{\sigma \cdot \mathcal{K}}}{2\sqrt{3}} &= 0 & \frac{-V_{11}^{\sigma \cdot \mathcal{K}} + V_{22}^{\sigma \cdot \mathcal{K}}}{2\sqrt{3}} &= 0 \\
 \frac{4V_{33}^{\sigma \cdot \mathcal{K}} + V_{44}^{\sigma \cdot \mathcal{K}} + V_{55}^{\sigma \cdot \mathcal{K}}}{6} &= \frac{1}{6} & \frac{V_{11}^{\sigma \cdot \mathcal{K}} + V_{22}^{\sigma \cdot \mathcal{K}} + 4V_{66}^{\sigma \cdot \mathcal{K}}}{6} &= -\frac{1}{6} \\
 \frac{-2V_{33}^{\sigma \cdot \mathcal{K}} + V_{44}^{\sigma \cdot \mathcal{K}} + V_{55}^{\sigma \cdot \mathcal{K}}}{3\sqrt{2}} &= -\frac{\sqrt{2}}{3} & \frac{V_{11}^{\sigma \cdot \mathcal{K}} + V_{22}^{\sigma \cdot \mathcal{K}} - 2V_{66}^{\sigma \cdot \mathcal{K}}}{3\sqrt{2}} &= \frac{\sqrt{2}}{3} \\
 \frac{V_{44}^{\sigma \cdot \mathcal{K}} - V_{55}^{\sigma \cdot \mathcal{K}}}{2\sqrt{3}} &= 0 & \frac{V_{11}^{\sigma \cdot \mathcal{K}} + V_{22}^{\sigma \cdot \mathcal{K}} + V_{66}^{\sigma \cdot \mathcal{K}}}{3} &= \frac{1}{6} \\
 \frac{V_{33}^{\sigma \cdot \mathcal{K}} + V_{44}^{\sigma \cdot \mathcal{K}} + V_{55}^{\sigma \cdot \mathcal{K}}}{3} &= -\frac{1}{6} & & (2.2.57)
 \end{aligned}$$

Reordering the terms one gets:

$$\left\| V_{ij}^{\sigma \cdot \mathcal{K}} \right\| = \frac{\hbar |e| \hbar}{mc} \left\| \begin{array}{cccccc} \frac{1}{2} & 0 & 0 & 0 & 0 & 0 \\ 0 & -\frac{1}{6} & 0 & 0 & 0 & \frac{\sqrt{2}}{3} \\ 0 & 0 & \frac{1}{6} & 0 & -\frac{\sqrt{2}}{3} & 0 \\ 0 & 0 & 0 & -\frac{1}{2} & 0 & 0 \\ 0 & 0 & -\frac{\sqrt{2}}{3} & 0 & -\frac{1}{6} & 0 \\ 0 & \frac{\sqrt{2}}{3} & 0 & 0 & 0 & \frac{1}{6} \end{array} \right\| \begin{array}{l} \left(\frac{3}{2} \right) \frac{3}{2} \\ \left(\frac{3}{2} \right) -\frac{1}{2} \\ \left(\frac{3}{2} \right) \frac{1}{2} \\ \left(\frac{3}{2} \right) -\frac{3}{2} \\ \left(\frac{1}{2} \right) \frac{1}{2} \\ \left(\frac{1}{2} \right) -\frac{1}{2} \end{array} \quad (2.2.58)$$

One may now write the complete perturbation Hamiltonian $\left\| V_{ij} \right\|$ by adding equations 2.2.46 and 2.2.58 and replacing ℓ by ℓ' and μ by μ' :

$$||V_{ij}|| = \frac{\hbar |e| \mathcal{H}}{mc}$$

$$\left| \begin{array}{ccccccc} \frac{\ell'+\mu'}{2}(a^+a+\frac{1}{2})+ & -\frac{1}{4\sqrt{3}}[(\ell'-\mu'-\nu)a^{+2}+ & \frac{1}{\sqrt{6}}\nu ad & 0 & -\frac{1}{2\sqrt{3}}\nu ad & -\frac{1}{4}\sqrt{\frac{2}{3}}[(\ell'-\mu'-\nu)a^{+2}+ & (\frac{3}{2})\frac{3}{2} \\ +\frac{\mu'}{2}d^2-\frac{3}{2}\kappa & +(\ell'-\mu'+\nu)a^2] & & & & +(\ell'-\mu'+\nu)a^2] & \\ -\frac{1}{4\sqrt{3}}[(\ell'-\mu'+\nu)a^{+2}+ & \frac{1}{6}[(\ell'+5\mu')(a^+a+\frac{1}{2})+ & 0 & \frac{1}{\sqrt{6}}\nu ad & \frac{1}{2}\nu a^+d & \frac{\ell'-\mu'}{3\sqrt{2}}(a^+a+\frac{1}{2}d^2)+ & (\frac{3}{2})-\frac{1}{2} \\ +(\ell'-\mu'-\nu)a^2] & +(\mu'+2\ell')d^2]+\frac{1}{2}\kappa & & & & +\frac{\kappa+1}{\sqrt{2}} & \\ \frac{1}{\sqrt{6}}\nu a^+d & 0 & \frac{1}{6}[(\ell'+5\mu')(a^+a+\frac{1}{2})+ & \frac{1}{4\sqrt{3}}[(\ell'-\mu'-\nu)a^{+2}+ & \frac{\ell'-\mu'}{3\sqrt{2}}(a^+a+\frac{1}{2}- & -\frac{1}{2}\nu ad & (\frac{3}{2})\frac{1}{2} \\ +(\mu'+2\ell')d^2]-\frac{1}{2}\kappa & +(\ell'-\mu'+\nu)a^2] & -d^2)-\frac{\kappa+1}{\sqrt{2}} & & & & \\ 0 & \frac{1}{\sqrt{6}}\nu a^+d & \frac{1}{4\sqrt{3}}[(\ell'-\mu'+\nu)a^{+2}+ & \frac{1}{2}[(\ell'+\mu')(a^+a+\frac{1}{2})+ & \frac{1}{4}\sqrt{\frac{2}{3}}[(\ell'-\mu'+\nu)a^{+2}+ & -\frac{1}{2\sqrt{3}}\nu a^+d & (\frac{3}{2})-\frac{3}{2} \\ (\ell'-\mu'-\nu)a^2] & +\mu'd^2]+\frac{3}{2}\kappa & +(\ell'-\mu'-\nu)a^2] & & & & \\ -\frac{1}{2\sqrt{3}}\nu a^+d & \frac{1}{2}\nu ad & \frac{\ell'-\mu'}{3\sqrt{2}}(a^+a+\frac{1}{2}- & \frac{1}{4}\sqrt{\frac{2}{3}}[(\ell'-\mu'-\nu)a^{+2}+ & \frac{1}{3}[(\ell'+2\mu')(a^+a+\frac{1}{2}+ & 0 & (\frac{1}{2})\frac{1}{2} \\ -d^2)-\frac{\kappa+1}{\sqrt{2}} & +(\ell'-\mu'+\nu)a^2] & +\frac{1}{2}d^2)]-\frac{2\kappa+1}{2}-\Delta' & & & & \\ -\frac{1}{4}\sqrt{\frac{2}{3}}[(\ell'-\mu'+\nu)a^{+2}+ & \frac{\ell'-\mu'}{3\sqrt{2}}(a^+a+\frac{1}{2}- & -\frac{1}{2}\nu a^+d & -\frac{1}{2\sqrt{3}}\nu ad & 0 & \frac{1}{3}[(\ell'+2\mu')(a^+a+\frac{1}{2}+ & (\frac{1}{2})-\frac{1}{2} \\ +(\ell'-\mu'-\nu)a^2] & -d^2)+\frac{\kappa+1}{\sqrt{2}} & & & & +\frac{1}{2}d^2)]+\frac{2\kappa+1}{2}-\Delta' & \end{array} \right|$$

(2.2.59)

Here the definition $\chi = -(3\kappa+1)$ was used.

To compare this result with Luttinger's (2) the following approximations are introduced.

- 1) 4×4 matrix in the upper left-hand corner may be decoupled from the 2×2 matrix in the lower right hand corner. This approximation seems to be valid in case small k_z (or d) and a small number of energy levels close to the band edge are of interest and in case Δ , the spin-orbit splitting, is appreciable.
- 2) $d = 0$ (i.e., $k_z = k_{z'} = 0$)
- 3) $\ell - \mu - \nu = 0$ which implies spherically symmetric energy bands. Luttinger makes this approximation in all cases except that of the magnetic field in the $[111]$ direction, and then treats $\ell - \mu - \nu \neq 0$ case by perturbation theory. This procedure seems to be applicable to Ge where $\ell - \mu - \nu$ is small but is questionable in case of Si.

One also defines

$$\begin{aligned} r_1 &= -\frac{1}{3} (\ell' + 2\mu') \\ r_2 &= -\frac{1}{6} (\ell' - \mu') \\ r_3 &= -\frac{1}{6} \nu \end{aligned} \tag{2.2.60}$$

r_1, r_2, r_3 being the constants used by Luttinger. Assumption 3) listed above implies

$$r_2 = r_3 = \bar{r} \tag{2.2.61}$$

The resulting 4×4 matrix is as follows:

$$\|v_{ij}^{4x4}\| = \frac{\hbar|e|\hbar}{mc} \left\| \begin{array}{cccc} -(\gamma_1 + \bar{\gamma})(a^\dagger a + \frac{1}{2}) - \frac{3}{2} \kappa & \sqrt{3} \bar{\gamma} a^2 & 0 & 0 \\ \sqrt{3} \bar{\gamma} a^{+2} & -(\gamma_1 - \bar{\gamma})(a^\dagger a + \frac{1}{2}) + \frac{1}{2} \kappa & 0 & 0 \\ 0 & 0 & -(\gamma_1 - \bar{\gamma})(a^\dagger a + \frac{1}{2}) - \frac{1}{2} \kappa & -\sqrt{3} \bar{\gamma} a^2 \\ 0 & 0 & -\sqrt{3} \bar{\gamma} a^{+2} & -(\gamma_1 + \bar{\gamma})(a^\dagger a + \frac{1}{2}) + \frac{3}{2} \kappa \end{array} \right\|$$

(2.2.62)

If the energy is measured in units of $\frac{\hbar|e|\hbar}{mc}$ as Luttinger does, and the sign of the above matrix is changed, i.e., one deals with holes instead of the electrons, one obtains a matrix which is identical with Luttinger's equation 71 with the exception of some signs. It is easily shown, however, that these signs do not affect the solutions.

III. LANDAU LEVEL STRUCTURE OF Ge AND Si AT $k_H = 0$ FOR H
IN THE [001] DIRECTION

In this section the energy levels in the valence bands of Ge and Si will be calculated for a special case of the external magnetic field H in the [001] direction and $k_H = 0$. This special case is analogous to the case of $k_z = 0$ but k_x and k_y finite in the no-magnetic-field problem. The resulting energy levels are the ones involved in the interband magneto-optical transitions and probably in most of the cyclotron resonance transitions. They are thus of primary importance in the interpretation of the experimental data.

Since no approximations, aside from the basic ones which have already been discussed, are being made in this calculation, it will serve as a basis of comparison for other calculations. The results should also indicate the behavior of the Landau levels as a function of the magnetic field and thus give the variation of the effective mass with the applied magnetic field.

3.1 Reduction of the Problem to an Algebraic One

Upon setting $d = 0$ (i.e., $k_H = k_z = 0$) in the matrix of equation 2.2.59 and changing its sign so as to deal with holes instead of electrons, the following two matrices are immediately obtained

$$||V_{ij,1}^{3 \times 3}|| = \frac{\hbar |e| \mathcal{H}}{mc} \left\| \begin{array}{ccc} \alpha(a^+a + \frac{1}{2}) + \frac{3}{2} \kappa & -(\beta a^2 + \delta a^{+2}) & -\sqrt{2} (\beta a^2 + \delta a^{+2}) \\ -(\beta a^{+2} + \delta a^2) & \xi(a^+a + \frac{1}{2}) - \frac{1}{2} \kappa & \rho(a^+a + \frac{1}{2}) - \frac{\kappa+1}{\sqrt{2}} \\ -\sqrt{2} (\beta a^{+2} + \delta a^2) & \rho(a^+a + \frac{1}{2}) - \frac{\kappa+1}{\sqrt{2}} & \lambda(a^+a + \frac{1}{2}) - \frac{2\kappa+1}{2} + \Delta' \end{array} \right\| \begin{array}{l} (\frac{3}{2}) \frac{3}{2} \\ (\frac{3}{2}) - \frac{1}{2} \\ (\frac{1}{2}) - \frac{1}{2} \end{array} \quad (3.1.1)$$

$$||V_{ij,2}^{3 \times 3}|| = \frac{\hbar |e| \mathcal{H}}{mc} \left\| \begin{array}{ccc} \xi(a^+a + \frac{1}{2}) + \frac{1}{2} \kappa & \beta a^2 + \delta a^{+2} & \rho(a^+a + \frac{1}{2}) + \frac{\kappa+1}{\sqrt{2}} \\ \beta a^{+2} + \delta a^2 & \alpha(a^+a + \frac{1}{2}) - \frac{3}{2} \kappa & \sqrt{2} (\beta a^{+2} + \delta a^2) \\ \rho(a^+a + \frac{1}{2}) + \frac{\kappa+1}{\sqrt{2}} & \sqrt{2} (\beta a^2 + \delta a^{+2}) & \lambda(a^+a + \frac{1}{2}) + \frac{2\kappa+1}{2} + \Delta' \end{array} \right\| \begin{array}{l} (\frac{3}{2}) \frac{1}{2} \\ (\frac{3}{2}) - \frac{3}{2} \\ (\frac{1}{2}) \frac{1}{2} \end{array} \quad (3.1.2)$$

where for convenience the following definitions have been used:

$$\begin{aligned} \alpha &= -\frac{\ell' + \mu'}{2} & \beta &= -\frac{\ell' - \mu' + \nu}{4\sqrt{3}} & \delta &= -\frac{\ell' - \mu' - \nu}{4\sqrt{3}} & \xi &= -\frac{\ell' + 5\mu'}{6} \\ \eta &= -\frac{\mu' + 2\ell'}{6} & \rho &= -\frac{\ell' - \mu'}{3\sqrt{2}} & \lambda &= -\frac{\ell' + 2\mu'}{3} \end{aligned} \quad (3.1.3)$$

Equations 3.1.1 and 3.1.2 must now be allowed to operate on some linear combination of the harmonic oscillator wave functions and then the result must be substituted into an equation of the form 2.1.9. This is equivalent to solving the following eigenvalue problem:

$$\|V_{ij}^{3 \times 3}\| F = E \|I\| F \quad (3.1.4)$$

where $\|I\|$ is the unit matrix and F can be taken to be of the form

$$F = \begin{pmatrix} \sum_i a_i f_i \\ \sum_j b_j f_j \\ \sum_k c_k f_k \end{pmatrix} \quad (3.1.5)$$

Letting $\frac{\hbar|e|\mathcal{H}}{mc} \epsilon = E$ measuring energy in units of $\frac{\hbar|e|\mathcal{H}}{mc}$, and remembering that

$$\begin{aligned} a \sum_i a_i f_i &= \sum_i a_i i^{1/2} f_{i-1} \\ a^+ \sum_i a_i f_i &= \sum_i a_i (i+1)^{1/2} f_{i+1} \\ a^+ a \sum_i a_i f_i &= \sum_i a_i i f_i \\ a^2 \sum_i a_i f_i &= \sum_i a_i [i(i-1)]^{1/2} f_{i-2} \\ a^{+2} \sum_i a_i f_i &= \sum_i a_i [(i+1)(i+2)]^{1/2} f_{i+2} \end{aligned} \quad (3.1.6)$$

one obtains by substituting equations 3.1.1 and 3.1.5 into 3.1.4, the following sets of equations:

$$\begin{aligned}
\text{I} \\
\sum_i \left[\alpha \left(i + \frac{1}{2} \right) + \frac{3}{2} \kappa - \epsilon \right] a_i f_i - \sum_j b_j \left\{ \beta [j(j-1)]^{1/2} f_{j-2} + \delta [(j+1)(j+2)]^{1/2} f_{j+2} \right\} - \\
- \sum_k \sqrt{2} c_k \left\{ \beta [k(k-1)]^{1/2} f_{k-2} + \delta [(k+1)(k+2)]^{1/2} f_{k+2} \right\} = 0
\end{aligned}$$

$$\begin{aligned}
\text{II} \\
- \sum_i a_i \left\{ \beta [(i+1)(i+2)]^{1/2} f_{i+2} + \delta [i(i-1)]^{1/2} f_{i-2} \right\} + \sum_j \left[\xi \left(j + \frac{1}{2} \right) - \frac{1}{2} \kappa - \epsilon \right] b_j f_j + \\
+ \sum_k c_k \left[\rho \left(k + \frac{1}{2} \right) - \frac{\kappa+1}{\sqrt{2}} \right] f_k = 0
\end{aligned}$$

$$\begin{aligned}
\text{III} \\
- \sum_i \sqrt{2} a_i \left\{ \beta [(i+1)(i+2)]^{1/2} f_{i+2} + \delta [i(i-1)]^{1/2} f_{i-2} \right\} + \sum_j b_j \left[\rho \left(j + \frac{1}{2} \right) - \frac{\kappa+1}{\sqrt{2}} \right] f_j + \\
+ \sum_k c_k \left[\lambda \left(k + \frac{1}{2} \right) - \frac{2\kappa+1}{2} + \Delta' - \epsilon \right] f_k = 0
\end{aligned} \tag{3.1.7}$$

TABLE 3.1

	b_1	c_1	a_1	b_1	c_1	a_1
I	$-\delta[(i+1) \times (i+2)]^{1/2}$	$\sqrt{2} \delta[(i+1) \times (i+2)]^{1/2}$	$\alpha(i + \frac{1}{2}) + \frac{3}{2}\kappa - \epsilon$	$-\beta[i(i-1)]^{1/2}$	$-\sqrt{2}\beta[i(i-1)]^{1/2}$	
II			$-\beta[(i+1) \times (i+2)]^{1/2}$	$-\xi(i + \frac{1}{2}) - \frac{1}{2}\kappa - \epsilon$	$\rho(i + \frac{1}{2}) - \frac{\kappa+1}{\sqrt{2}}$	$-\delta[i(i-1)]^{1/2}$
III			$-\sqrt{2}\beta[(i+1) \times (i+2)]^{1/2}$	$\rho(i + \frac{1}{2}) - \frac{\kappa+1}{\sqrt{2}}$	$\lambda(i + \frac{1}{2}) - \frac{2\kappa+1}{2} + \Delta' - \epsilon$	$-\sqrt{2}\delta[i(i-1)]^{1/2}$

The elements in any three rows of this matrix labeled I, II, III may be determined from Table 3.1. For example, the elements of the three rows labeled I f_2 , II f_4 , III f_4 are given by

$$\begin{array}{c}
 \begin{array}{cc|ccc|c}
 & b_0 & c_0 & a_2 & b_4 & c_4 & a_6 \\
 \text{I } f_2 & -\sqrt{2}\delta & -2\delta & \frac{5\alpha+3\kappa}{2} - \epsilon & -2\sqrt{3}\beta & -2\sqrt{6}\beta & 0 \\
 \text{II } f_4 & 0 & 0 & -2\sqrt{3}\beta & \frac{9\zeta - \kappa}{2} - \epsilon & \frac{9}{2}\rho - \frac{\kappa+1}{\sqrt{2}} & -\sqrt{30}\delta \\
 \text{III } f_4 & 0 & 0 & -2\sqrt{6}\beta & \frac{9}{2}\rho - \frac{\kappa+1}{\sqrt{2}} & \frac{9\lambda - 2\kappa - 1}{2} + \Delta' - \epsilon & -2\sqrt{15}\delta
 \end{array}
 \end{array}
 \quad (3.1.9)$$

It will be observed that the infinite set of equations can be decoupled into four independent sets (labeled A,B,C,D), which reduces the problem to the solution of four independent infinite determinants, two of each of the following types:

$$\begin{array}{c}
 \begin{array}{|c|} \hline \epsilon \rho \\ \hline \rho \epsilon \\ \hline \end{array}
 \begin{array}{|c|} \hline \delta \\ \hline \sqrt{2}\delta \\ \hline \end{array} \\
 \begin{array}{|c|c|} \hline \epsilon \beta & \sqrt{2}\beta \\ \hline \beta \epsilon & \rho \\ \hline \end{array}
 \begin{array}{|c|} \hline \delta \\ \hline \sqrt{2}\delta \\ \hline \end{array} \\
 \begin{array}{|c|c|c|} \hline \sqrt{2}\beta & \rho & \epsilon \\ \hline \delta & \sqrt{2}\delta & \epsilon \beta \\ \hline \end{array}
 \begin{array}{|c|} \hline \sqrt{2}\beta \\ \hline \epsilon \beta \\ \hline \end{array}
 \begin{array}{|c|} \hline \rho \\ \hline \epsilon \\ \hline \end{array}
 \end{array}
 \quad (3.1.10)$$

and

$$\begin{array}{c}
 \begin{array}{|ccc|} \hline \epsilon & \beta & \sqrt{2}\beta \\ \hline \beta & \epsilon & \rho \\ \hline \sqrt{2}\beta & \rho & \epsilon \\ \hline \end{array} & \begin{array}{c} \delta \\ \sqrt{2}\delta \end{array} & \\
 \delta \sqrt{2}\delta & \begin{array}{|ccc|} \hline \epsilon & \beta & \sqrt{2}\beta \\ \hline \beta & \epsilon & \rho \\ \hline \sqrt{2}\beta & \rho & \epsilon \\ \hline \end{array} & \begin{array}{c} \delta \\ \sqrt{2}\delta \end{array} \\
 & \delta \sqrt{2}\delta & \begin{array}{|ccc|} \hline \epsilon & \beta & \sqrt{2}\beta \\ \hline \beta & \epsilon & \rho \\ \hline \sqrt{2}\beta & \rho & \epsilon \\ \hline \end{array} & \begin{array}{c} \delta \\ \sqrt{2}\delta \end{array} \\
 & & \delta \sqrt{2}\delta & \begin{array}{|ccc|} \hline \epsilon & \beta & \sqrt{2}\beta \\ \hline \beta & \epsilon & \rho \\ \hline \sqrt{2}\beta & \rho & \epsilon \\ \hline \end{array}
 \end{array}
 \quad (3.1.11)$$

Each of these four determinants can be quite accurately solved by truncating it sufficiently far from the 3x3 block which gives rise to the eigenvalue of interest. This is possible because the terms involving δ are smaller than those in the main blocks. As will be discussed in greater detail later, in this process one must avoid the "decoupling" of levels close to each other in energy.

Now in a similar fashion, equations 3.1.2 and 3.1.5 can be substituted into 3.1.4, yielding the equations:

$$\begin{aligned}
 \text{I} \quad & \sum_i \left[\left(\zeta \left(i + \frac{1}{2} \right) + \frac{1}{2} \kappa - \epsilon \right) a_i f_i + \sum_j b_j \left\{ \beta [j(j-1)]^{1/2} f_{j-2} + \right. \right. \\
 & \left. \left. + \delta [(j+1)(j+2)]^{1/2} f_{j+2} \right\} + \sum_k \left[\rho \left(k + \frac{1}{2} \right) + \frac{\kappa+1}{\sqrt{2}} \right] c_k f_k = 0 \\
 \text{II} \quad & \sum_i a_i \left\{ \beta [(i+1)(i+2)]^{1/2} f_{i+2} + \delta [i(i-1)]^{1/2} f_{i-2} \right\} + \\
 & + \sum_j \left[\alpha \left(j + \frac{1}{2} \right) - \frac{3}{2} \kappa - \epsilon \right] b_j f_j + \\
 & + \sum_k \sqrt{2} c_k \left\{ \beta [(k+1)(k+2)]^{1/2} f_{k+2} + \delta [k(k-1)]^{1/2} f_{k-2} \right\} = 0 \quad (3.1.12)
 \end{aligned}$$

$$\begin{aligned}
 & \text{III} \\
 & \sum_1 a_1 \left[\rho \left(i + \frac{1}{2} \right) + \frac{\kappa+1}{\sqrt{2}} \right] f_1 + \sum_j \sqrt{2} b_j \left\{ \beta [j(j-1)]^{1/2} f_{j-2} + \right. \\
 & \left. + \delta [(j+1)(j+2)]^{1/2} f_{j+2} \right\} + \sum_k \left[\lambda \left(i + \frac{1}{2} \right) + \frac{2\kappa+1}{2} + \Delta - \epsilon \right] c_k f_k = 0
 \end{aligned} \tag{3.1.12}$$

Again, if $\delta = 0$ one may get $j = i+2$, $k = i$, obtaining for each i a set of three simultaneous equations. If, on the other hand, $\delta \neq 0$ as is actually the case, one proceeds as indicated in the previous case obtaining an infinite matrix of the form

	b_0	b_1	a_0	b_2	c_0	a_1	b_3	c_1	a_2	b_4	c_2	a_3	b_5	c_3	a_4	b_6	c_4	a_5	b_7
II f_0	ϵ	A							δ	$\sqrt{2}\delta$									
II f_1		ϵ	B									δ	$\sqrt{2}\delta$						
I f_0			ϵ	β	ρ														
II f_2			β	ϵ	$\sqrt{2}\beta$	C									δ	$\sqrt{2}\delta$			
III f_0			ρ	$\sqrt{2}\beta$	ϵ														
I f_1				ϵ	β	ρ													
II f_3				β	ϵ	$\sqrt{2}\beta$	D											δ	
III f_1				ρ	$\sqrt{2}\beta$	ϵ													
I f_2	δ						ϵ	β	ρ										
II f_4							β	ϵ	$\sqrt{2}\beta$	A									
III f_2	$\sqrt{2}\delta$						ρ	$\sqrt{2}\beta$	ϵ										
I f_3		δ						ϵ	β	ρ									
II f_5			δ					β	ϵ	$\sqrt{2}\beta$	B								
III f_3		$\sqrt{2}\delta$						ρ	$\sqrt{2}\beta$	ϵ									
I f_4			δ						ϵ	β	ρ								
II f_6				δ					β	ϵ	$\sqrt{2}\beta$	C							
III f_4			$\sqrt{2}\delta$						ρ	$\sqrt{2}\beta$	ϵ								
I f_5					δ							ϵ	β						
II f_7						δ						β	ϵ						
III f_5							$\sqrt{2}\delta$					ρ	$\sqrt{2}\beta$						

(3.1.13)

in which the elements are computed with the help of Table 3.2. This matrix also decouples into four infinite matrices which are solved by the same method as equations 3.1.10 and 3.1.11.

TABLE 3.2

	b_i	a_i	b_i	c_i	a_i	c_i
I	$\delta[(i+1) \times (i+2)]^{1/2}$	$\zeta(i + \frac{1}{2}) + \frac{1}{2} \kappa - \epsilon$	$\beta[i(i-1)]^{1/2}$	$\rho(i + \frac{1}{2}) + \frac{\kappa+1}{\sqrt{2}}$		
II		$\beta[(i+1)(i+2)]^{1/2}$	$\alpha(i + \frac{1}{2}) - \frac{3}{2} \kappa - \epsilon$	$\sqrt{2} \beta[(i+1)(i+2)]^{1/2}$	$\delta[i(i-1)]^{1/2}$	$\sqrt{2} \delta[i(i-1)]^{1/2}$
III	$\sqrt{2} \delta[(i+1) \times (i+2)]^{1/2}$	$(i + \frac{1}{2}) + \frac{\kappa+1}{\sqrt{2}}$	$\sqrt{2} \beta[i(i-1)]^{1/2}$	$\lambda(i + \frac{1}{2}) + \frac{2\kappa+1}{2} + \Delta' - \epsilon$		

3.2 The Numerical Constants Characterizing the Valence Bands of Ge and Si

The constants ℓ' , μ' , ν and κ which appear in the above analysis have not as yet been evaluated analytically. One must therefore rely on the experimentally determined values. The determinations based on experimental data have been made by Dresselhaus, Kip and Kittel (6), Dexter, Zeiger and Lax (7), Dexter and Lax (30), and Goodman (3). The first three estimates have been based on the "semi-classical" model of cyclotron resonance described briefly on page 11, while the last one by Goodman is based on fitting the quantum mechanical energy level calculation (for Ge at $k_H = 0$) to the data obtained by Fletcher, Yager and Merritt (31). The various estimates are summarized in Tables 3.3 and 3.4 for Ge and Si respectively. The following relations hold between the various constants quoted in the tables:

$$\begin{aligned} L &= A - 1 + 2B & A &= \frac{1}{3} (L + 2M) + \frac{\hbar^2}{2m} \\ M &= A - 1 - B & B &= \frac{1}{3} (L - M) \\ N &= -3 \left(\frac{1}{3} C^2 + B^2 \right)^{1/2} & C^2 &= \frac{1}{3} [N^2 - (L - M)^2] \end{aligned} \quad (3.2.1)$$

$$\begin{aligned} r_1 &= \frac{2m}{\hbar^2} \left[-\frac{1}{3} (L + 2M) - 1 \right] = -\frac{2m}{\hbar^2} A \\ r_2 &= \frac{2m}{\hbar^2} \left[-\frac{1}{6} (L - M) \right] = -\frac{1}{2} \frac{2m}{\hbar^2} B \end{aligned} \quad (3.2.2)$$

$$r_3 = \frac{2m}{\hbar^2} \left(-\frac{1}{6} N \right) = \frac{1}{2} \frac{2m}{\hbar^2} \left(\frac{1}{3} C^2 + B^2 \right)^{1/2}$$

$$\begin{aligned} \ell' &= \frac{2m}{\hbar^2} L + 1 \\ \mu' &= \frac{2m}{\hbar^2} M + 1 \\ \nu &= \frac{2m}{\hbar^2} N \end{aligned} \quad (3.2.3)$$

TABLE 3.3 NUMERICAL CONSTANTS, Ge

Source of Original Data					Remarks
DL (1954) Assuming $k_H = 0$	$A = -13.6 \frac{\hbar^2}{2m}$	$L = -32.8 \frac{\hbar^2}{2m}$	$r_1 = 13.6$		
	$B = -9.1 \frac{\hbar^2}{2m}$	$M = -5.5 \frac{\hbar^2}{2m}$	$r_2 = 4.55$		
	$ C = 11.2 \frac{\hbar^2}{2m}$	$N = -33.5 \frac{\hbar^2}{2m}$	$r_3 = 5.59$		
DKK (1955) Assuming $k_H = 0$	$A = -(13.0 \pm 0.2) \frac{\hbar^2}{2m}$	$L = -31.8 \frac{\hbar^2}{2m}$	$r_1 = 13.0$		IMN given by DKK (6)
	$B = -(8.9 \pm 0.1) \frac{\hbar^2}{2m}$	$M = -5.1 \frac{\hbar^2}{2m}$	$r_2 = 4.45$		
	$ C = (10.3 \pm 0.2) \frac{\hbar^2}{2m}$	$N = -32.1 \frac{\hbar^2}{2m}$	$r_3 = 5.36$		
DKK (1955) Considering thermal distribution around $k_H = 0$	$A = -(13.2 \pm 0.1) \frac{\hbar^2}{2m}$	$L = -32.0 \frac{\hbar^2}{2m}$	$r_1 = 13.2$	$l' = -31.0$	IMN used by Kane (15) $r_1 r_2 r_3$ used by Luttinger(2)
	$B = -(8.9 \pm 0.05) \frac{\hbar^2}{2m}$	$M = -5.3 \frac{\hbar^2}{2m}$	$r_2 = 4.45$	$\mu' = -4.3$	
	$C = (10.6 \pm 0.2) \frac{\hbar^2}{2m}$	$N = -32.4 \frac{\hbar^2}{2m}$	$r_3 = 5.4$	$v = -32.4$	
DZL (1956) Considering thermal distribution around $k_H = 0$	$A = -(13.1 \pm 0.4) \frac{\hbar^2}{2m}$	$L = -30.7 \frac{\hbar^2}{2m}$	$r_1 = 13.1$		
	$B = -(8.3 \pm 0.6) \frac{\hbar^2}{2m}$	$M = -5.8 \frac{\hbar^2}{2m}$	$r_2 = 4.15$		
	$C = (12.5 \pm 0.5) \frac{\hbar^2}{2m}$	$N = -33.0 \frac{\hbar^2}{2m}$	$r_3 = 5.5$		
FYM (1955)			$r_1 = 13.2$	$l' = -29.6$	Deduced by Goodman (3) from Fletcher, Yager, Merritt (31) data.
			$r_2 = 4.1$	$\mu' = -5.0$	
			$r_3 = 5.6$	$v = -33.6$	
			$\kappa = 3.9$		

TABLE 3.4a NUMERICAL CONSTANTS, Si

Source of Original Data						Remarks
DL (1954) Assuming $k_H = 0$	$A = -4.0 \frac{\hbar^2}{2m}$	$L = -7.6 \frac{\hbar^2}{2m}$	$r_1 = 4.0$			
	$B = -1.3 \frac{\hbar^2}{2m}$	$M = -3.7 \frac{\hbar^2}{2m}$	$r_2 = 0.65$			
	$ C = 3.6 \frac{\hbar^2}{2m}$	$N = -7.33 \frac{\hbar^2}{2m}$	$r_3 = 1.22$			
DKK (1955) Assuming $k_H = 0$	$A = -(4.1 \pm 0.2) \frac{\hbar^2}{2m}$	$L = -8.3 \frac{\hbar^2}{2m}$	$r_1 = 4.1$			
	$B = -(1.6 \pm 0.2) \frac{\hbar^2}{2m}$	$M = -3.5 \frac{\hbar^2}{2m}$	$r_2 = 0.8$			
	$ C = (3.3 \pm 0.5) \frac{\hbar^2}{2m}$	$N = -7.5 \frac{\hbar^2}{2m}$	$r_3 = 1.25$			
DKK (1955) Considering thermal distribution around $k_H = 0$	$A = -(4.0 \pm 0.2) \frac{\hbar^2}{2m}$	$L = -7.2 \frac{\hbar^2}{2m}$	$r_1 = 4.0$	$\ell' = -6.2$		LMN used by Kane (15)
	$B = -(1.1 \pm 0.5) \frac{\hbar^2}{2m}$	$M = -3.9 \frac{\hbar^2}{2m}$	$r_2 = 0.55$	$\mu' = -2.9$		$r_1 r_2 r_3$ close to values quoted by Luttinger (2) except he left signs of
	$ C = (4.0 \pm 0.5) \frac{\hbar^2}{2m}$	$N = -7.7 \frac{\hbar^2}{2m}$	$r_3 = 1.28$	$\nu = -7.7$		r_2 and r_3 undefined
DZL (1956) Considering thermal distribution around $k_H = 0$	$A = -(4.0 \pm 0.1) \frac{\hbar^2}{2m}$	$L = -7.2 \frac{\hbar^2}{2m}$	$r_1 = 4.0$			$r_1 r_2 r_3$ close to values quoted by Luttinger (2) except he left signs of
	$B = -(1.1 \pm 0.4) \frac{\hbar^2}{2m}$	$M = -3.9 \frac{\hbar^2}{2m}$	$r_2 = 0.55$			r_2 and r_3 undefined
	$ C = (4.1 \pm 0.4) \frac{\hbar^2}{2m}$	$N = -7.8 \frac{\hbar^2}{2m}$	$r_3 = 1.30$			

TABLE 3.4b

NUMERICAL CONSTANTS, S1

Source of Original Data				Remarks
DL (1954) Assuming $k_H = 0$	$A = -4.0 \frac{H^2}{2m}$	$L = -2.4 \frac{H^2}{2m}$	$r_1 = 4.0$	
	$B = 1.3 \frac{H^2}{2m}$	$M = -6.3 \frac{H^2}{2m}$	$r_2 = -0.65$	
	$ C = 3.6 \frac{H^2}{2m}$	$N = -7.33 \frac{H^2}{2m}$	$r_3 = 1.22$	
DKK (1955) Assuming $k_H = 0$	$A = -(4.1 \pm 0.2) \frac{H^2}{2m}$	$L = -1.9 \frac{H^2}{2m}$	$r_1 = 4.1$	LMN quoted by DKK (6)
	$B = (1.6 \pm 0.2) \frac{H^2}{2m}$	$M = -6.7 \frac{H^2}{2m}$	$r_2 = -0.8$	
	$ C = (3.3 \pm 0.5) \frac{H^2}{2m}$	$N = -7.5 \frac{H^2}{2m}$	$r_3 = 1.25$	
DKK (1955) Considering thermal distri- bution around $k_H = 0$	$A = -(4.0 \pm 0.2) \frac{H^2}{2m}$	$L = -2.8 \frac{H^2}{2m}$	$r_1 = 4.0$	$\ell' = -1.8$
	$B = (1.1 \pm 0.5) \frac{H^2}{2m}$	$M = -6.1 \frac{H^2}{2m}$	$r_2 = -0.55$	$\mu' = -5.1$
	$ C = (4.0 \pm 0.5) \frac{H^2}{2m}$	$N = -7.7 \frac{H^2}{2m}$	$r_3 = 1.28$	$\nu = -7.7$
DZL (1956) Considering thermal distri- bution around $k_H = 0$	$A = -(4.0 \pm 0.1) \frac{H^2}{2m}$	$L = -2.8 \frac{H^2}{2m}$	$r_1 = 4.0$	
	$B = (1.1 \pm 0.4) \frac{H^2}{2m}$	$M = -6.1 \frac{H^2}{2m}$	$r_2 = -0.55$	
	$ C = (4.1 \pm 0.4) \frac{H^2}{2m}$	$N = -7.8 \frac{H^2}{2m}$	$r_3 = 1.30$	

It should be noted that due to the difficulty of determining the A, B, C, constants for Si with sufficient degree of precision, there arises an ambiguity in the sign of the constant B. Dresselhaus, Kip and Kittel (6) chose the positive sign which gives rise to constants in Table 3.4b, while Kane (15) prefers the negative sign (Table 3.4a) since it makes the bands in Si similar qualitatively to those of Ge. Of course, more accurate cyclotron resonance data for Si should resolve this ambiguity. In the calculations which follow, the negative sign is chosen. All of the above constants, as well as the antisymmetric constant κ can be related to the constants (sums of matrix elements) F, G, H_1 , and H_2 defined by Dresselhaus, Kip and Kittel (6). If H_2 is taken to be zero, which is the value quoted by Dresselhaus, Kip and Kittel, the constant κ can be easily evaluated.

In summary, the following are the constants used in the subsequent calculations:

For Ge

$$\begin{aligned}\ell' &= -31.0 \\ \mu' &= -4.3 \\ \nu &= -32.4 \\ \kappa &= 3.3 \\ \Delta &= 0.29 \text{ ev (ref. 15)}\end{aligned}\tag{3.2.4}$$

For Si

$$\begin{aligned}\ell' &= -6.2 \\ \mu' &= -2.9 \\ \nu &= -7.7 \\ \kappa &= -0.016 \\ \Delta &= 0.0441 \text{ ev (ref. 32)}\end{aligned}\tag{3.2.5}$$

3.3 Numerical Results for Ge

The energy eigenvalues for the valence band of Ge at $k_H = 0$, as well as the coefficients in the corresponding wave function expansions, are determined by solving the various determinants specified by equations 3.1.8 and 3.1.13. Thus a total of eight eigenvalue problems must be solved. The four problems arising from equation 3.1.8 result in eigenvalues which correspond to the two ϵ_1 ladders of Luttinger (2). This is so because the eigenvalues involved have eigenfunctions composed of linear combinations of the harmonic oscillator functions multiplied by the $\phi_{3/2}^{(3/2)}$, $\phi_{-1/2}^{(3/2)}$, and $\phi_{-1/2}^{(1/2)}$ angular momentum functions only. Thus if one assumes $\delta = 0$ and Δ' very large so that in each 3x3 block the third row and the third column can be ignored, the remaining eigenfunctions are found to be of the form

$$af_{i-2} \phi_{3/2}^{(3/2)} + bf_i \phi_{-1/2}^{(3/2)} \quad (3.3.1)$$

which is exactly of the same form as the eigenfunctions characterizing the eigenvalues in the ϵ_1 ladders of Luttinger. Similarly, the eigenvalues arising from equation 3.1.13 correspond to the ϵ_2 ladders of Luttinger.

Although in the case treated here the eigenfunctions are considerably more complicated than 3.3.1, the eigenvalues can still be assigned to various ladders (mainly for the sake of convenience in applying the selection rules and in comparing with previously obtained results) according to the leading terms in the corresponding eigenfunction expansions.

As pointed out in Section 3.1, it is possible to solve fairly accurately the infinite determinants involved in this problem by truncating

them judiciously. In Appendix 3 are shown the numbers resulting from the solution of various size determinants corresponding to the eight eigenvalue problems described above. To illustrate the method by which accuracy of solutions has been estimated, consider the solutions to the "B" determinant of equation 3.1.8 given on page 175. It will be observed that the change from an 8x8 determinant to the 11x11 determinant has not affected the values of ϵ_1 and ϵ_2 . It is thus shown that the solution of the 8x8 determinant gives ϵ_1 and ϵ_2 essentially exactly. It may therefore be assumed that the solution of the 11x11 determinant gives ϵ_1 through ϵ_5 exactly. Assuming this, one finds that the 8x8 determinant gives values for ϵ_3 , ϵ_4 , and ϵ_5 which are inaccurate by considerably less than 1%. Following a similar procedure in other cases, it is found that in general for Ge in order to find the first n eigenvalues, a determinant of the order of $n + 3$ must be solved.

Another important consideration which in certain cases may render the above arguments invalid, is that of close-lying energy levels. Thus if a certain heavy hole level is close in energy to a light hole level arising from another basic 3x3 block, their decoupling during the truncating process may introduce larger than ordinary errors into the corresponding eigenvalues. This, of course, is completely analogous to the results of the higher order perturbation theory where the zero-order energy differences enter in the denominator of the correction. Thus on page 176 the effect on ϵ_2 ($\epsilon_{1+}(0,2)$) of going from 6x6 determinant to a 9x9 determinant is slightly greater than ordinary since ϵ_7

($\epsilon_{1-}(8,10)$) lies fairly close in value to ϵ_2 . However, this effect becomes smaller as the basic blocks which give rise to the close lying levels become farther separated. Thus for Ge there seem to be few if any cases where the above must be seriously considered.

The eigenvalues for Ge are plotted in Figures 3.1 through 3.4 as functions of the external magnetic field. The ordinate is normalized so that the actual energy of a given level above the band edge is given by

$$E = \frac{\hbar |e| \mathcal{H}}{mc} \epsilon \quad (3.3.2)$$

It will be observed that the energy levels for the heavy holes (ϵ_{1-} and ϵ_{2-} ladder) depend very little on the magnetic field. This is to be expected since the energy levels shown lie quite close to the band edge (thus the $\epsilon_{1-}(5,7)$ level is ~ 0.014 ev above the band edge at $H = 50$ kg) and therefore the interaction of these levels with the V_3 valence band is quite small. This interaction is, of course, the one responsible for the dependence of the energy eigenvalues on the magnetic field.

The light hole energy levels, on the other hand, show a more marked dependence on the magnetic field. This again is not surprising in view of the above arguments. On the average, the "effective mass" for the ϵ_{1+} holes increases by about a factor of 1.12 as the field changes from 1 kgauss to 50 kgauss. The corresponding increase in the mass of the ϵ_{2+} holes is by a factor of 1.07. The higher lying levels are, of course, affected more strongly than the low lying ones. Table 3.5 shows the values of the coefficients in the eigenfunction expansions for

TABLE 3.5

WAVE FUNCTION EXPANSION COEFFICIENTS

for Ge at $d = 0$ and $H = 5$ kg

for Ge at d = 0 and H = 5 kg																								
$\phi(3/2)$ 3/2												$\phi(3/2)$ -1/2												
	a ₀	a ₁	a ₂	a ₃	a ₄	a ₅	a ₆	a ₇	a ₈	a ₉		b ₀	b ₁	b ₂	b ₃	b ₄	b ₅	b ₆	b ₇	b ₈	b ₉	b ₁₀	b ₁₁	
ε ₁ -	(0,2)	1.0000				-.0608									.7731				-.0562					
	(1,3)		.9368				-.1013			.0980						1.000				-.1027				.0966
	(2,4)			.8194				-.1186				.0925		.2789			1.000				-.1255			
	(3,5)				.7570				-.1373				.0911				1.000					-.1531		
	(4,6)	.1728				.7334				-.1502				.0499				1.000					-.1724	
	(5,7)		.1367				.7072				-.1671					.0962			1.000					-.1976
	(6,8)			.1366				.6967								.1330				1.000				
	(7,9)				.1454				.6840												1.000			
ε ₁ +	(0)											1.000						-.0466						
	(1)												1.000					-.1619						
	(0,2)	-.7597				-.0549				.0169									.1479					
	(1,3)		1.000				-.1479													-.0817				
	(2,4)			1.000																	-.0575			
	(3,5)				1.000																	-.0503		
	(4,6)					1.000																	-.0476	
												.0240												
													.0296											
														.7700										
															.7362									

TABLE 3.5 Continued

Figure 1 displays two triangular matrices of correlation coefficients. The top matrix is for the negative correlation case (ϵ_2^-) and the bottom for the positive case (ϵ_2^+). Both matrices show correlation coefficients for pairs of variables (a_0 to a_{12} and b_0 to b_{12}) and their combinations. The diagonal elements are all 1.000. The off-diagonal elements are the correlation coefficients, with some values highlighted in boxes. The top matrix has a correlation coefficient of -0.3289 between a_2 and b_2 , and -0.4175 between a_3 and b_3 . The bottom matrix has a correlation coefficient of 0.3234 between a_0 and b_0 , and 0.4110 between a_1 and b_1 .

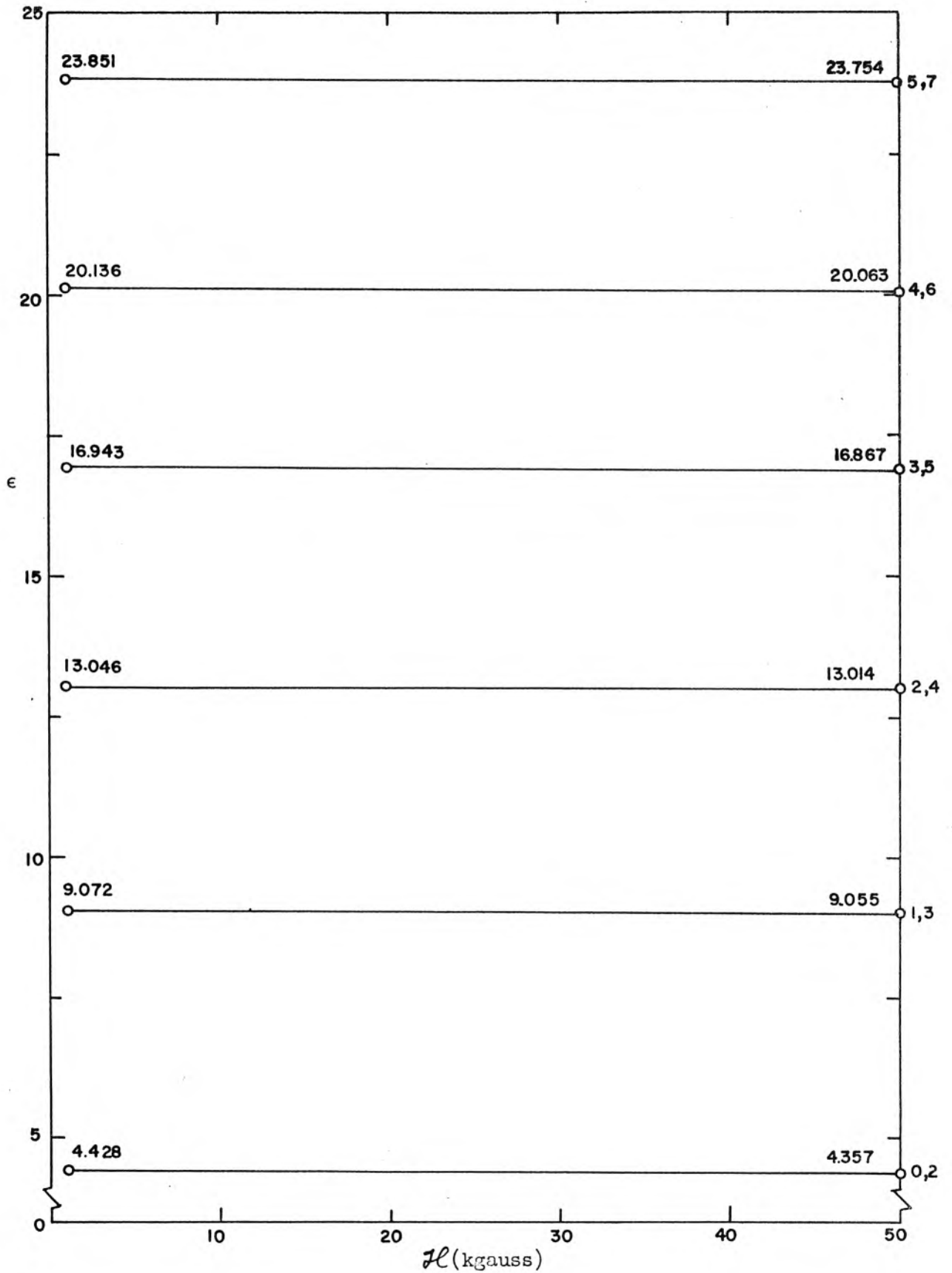


Fig. 3.1 Landau Levels belonging to the ϵ_1 - Ladder in Ge as Functions of the Magnetic Field

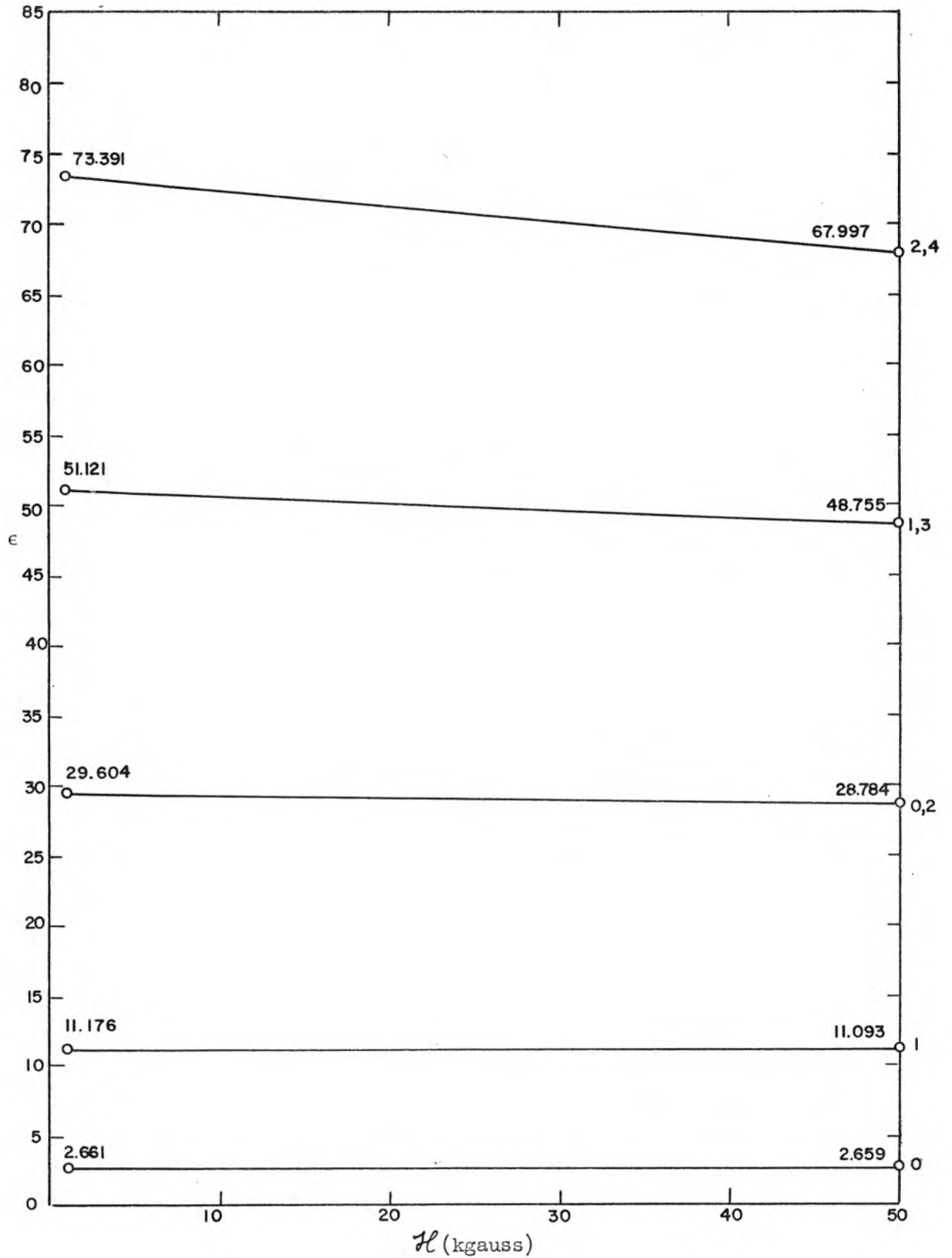


Fig. 3.2 Landau Levels belonging to the ϵ_1 Ladder in Ge as Functions of the Magnetic Field

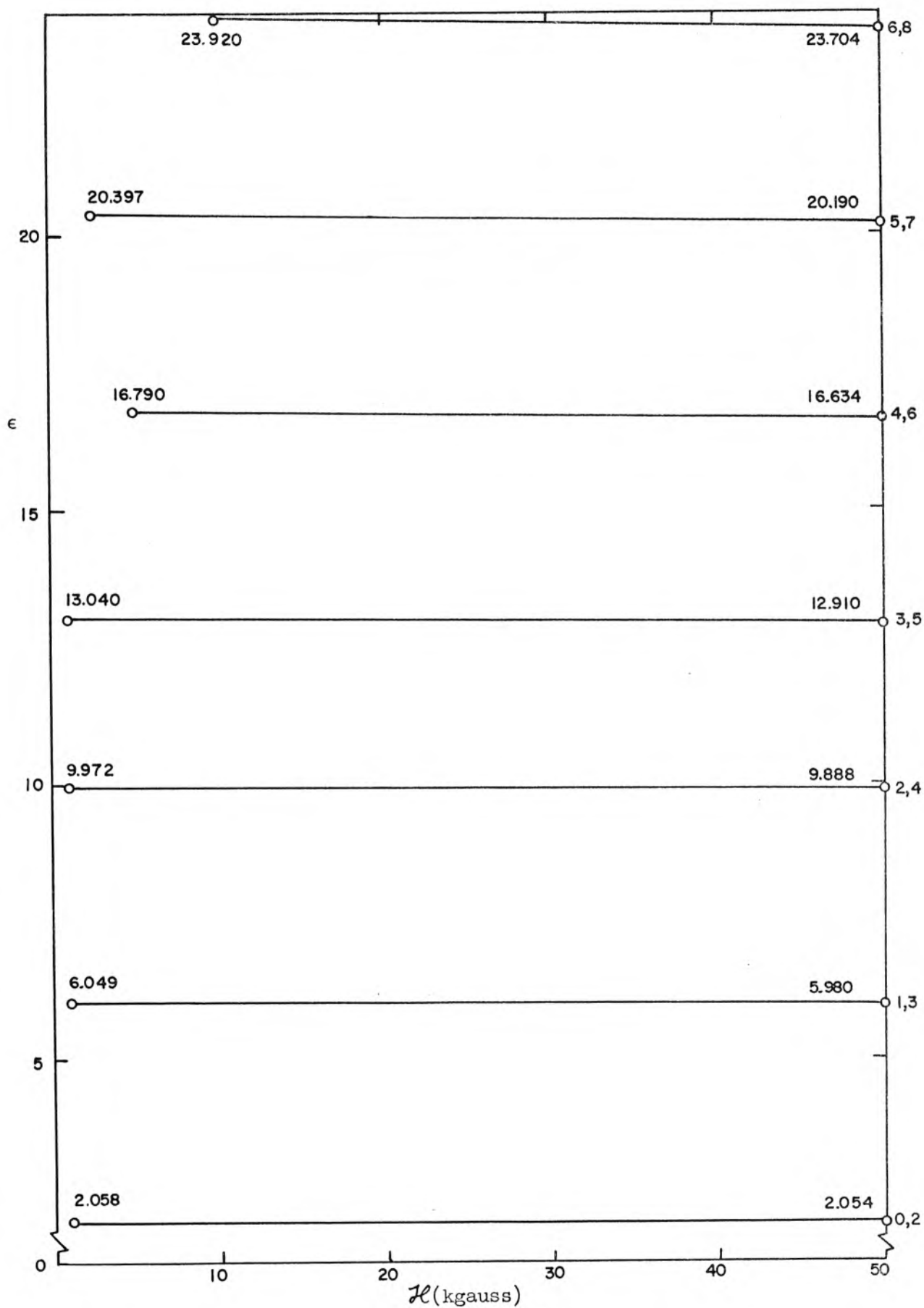


Fig. 3.3 Landau Levels belonging to the ϵ_2 - Ladder in Ge as Functions of the Magnetic Field.

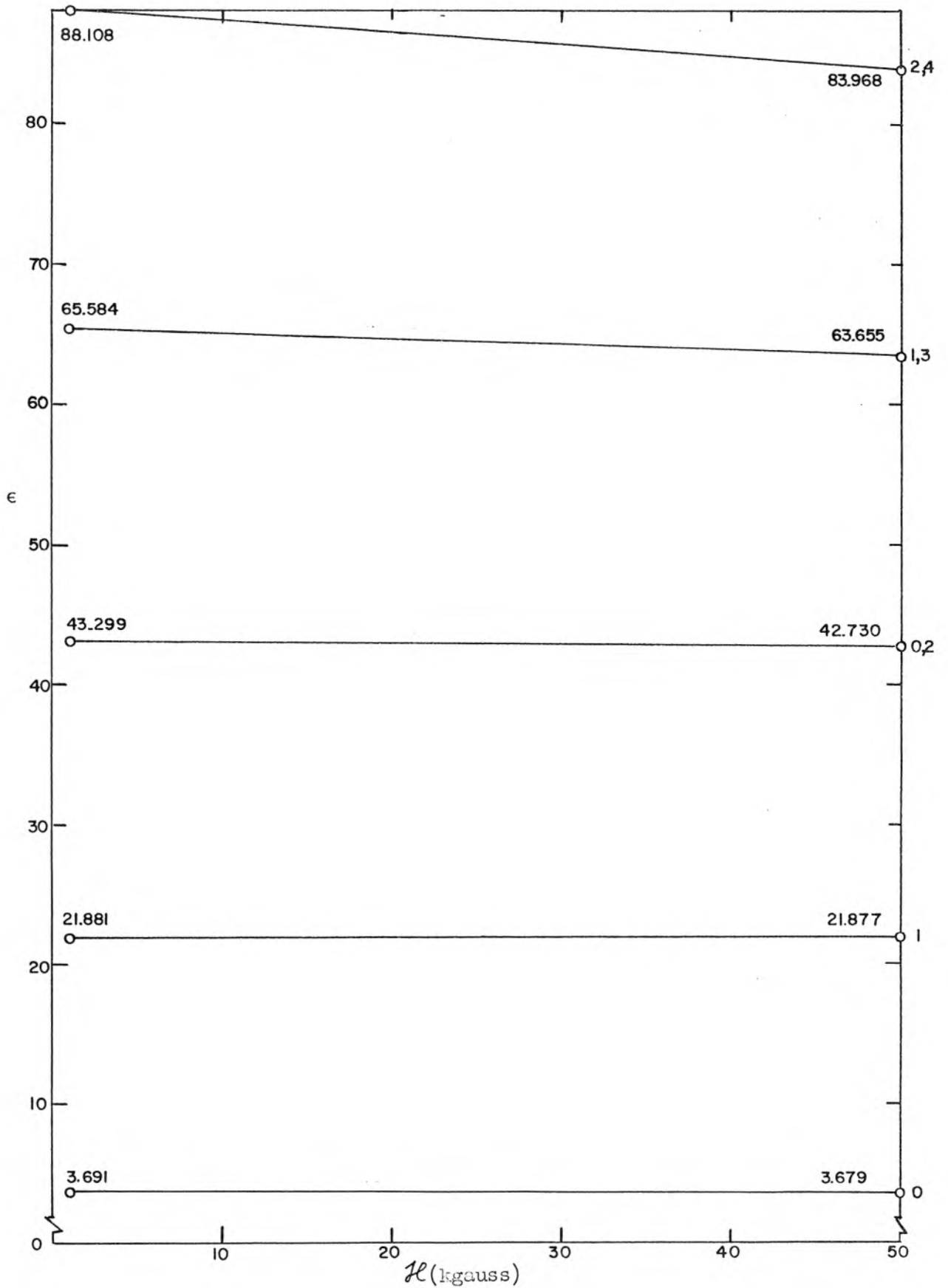


Fig. 3.4 Landau Levels belonging to the ϵ_{2+} Ladder in Ge as Functions of the Magnetic Field

the various levels. From the table it can be seen that although the leading coefficients for a given level are in most cases appreciably larger than the others, significant mixing does occur in some instances. In these cases transitions of relatively high probability may occur between an $\epsilon(n, n+2)$ level and the $\epsilon(n+3, n+5)$ or $\epsilon(n+5, n+7)$ levels. The $\epsilon(n, n+2)$ to $\epsilon(n+3, n+5)$ transition will be a negative mass transition, i.e., it will be caused by a circularly polarized photon with the sense of polarization opposite to that causing the normal cyclotron resonance transitions (8,4).

3.4 Numerical Results for Si

The calculations for this case are very similar to the ones described in Section 3.3. However, because the δ terms for Si are relatively larger than for Ge, larger determinants must be solved to obtain the same number of eigenvalues accurately. Thus to obtain the first n eigenvalues, it was found by a procedure similar to that described previously, that a determinant of the order of $n+6$ must be solved. Also the difficulties due to the proximity in energy of the heavy and light hole levels arise somewhat more frequently here than in the case of Ge. For example, on page 184, Appendix 4, the change in the value of ϵ_5 ($\epsilon_{1+}(4,6)$) caused by increasing the order of the determinant from 9 to 12 is 2.25%, whereas the corresponding change in the value of ϵ_4 ($\epsilon_{1-}(4,6)$) is only 0.23%. This is caused by the fact that ϵ_5 is very close in energy to $\epsilon_{10}(\epsilon_{1-}(12,14))$. Another example of very strong coupling is provided by the $\epsilon_{1+}(5,7)$ and the $\epsilon_{1-}(13,15)$ levels. The coupling between these increases to such an extent with the magnetic field, that

TABLE 3.6

WAVE FUNCTION EXPANSION COEFFICIENTS

for Si at $d = 0$ and $H = 5$ kg

$\rho^{(3/2)}_{3/2}$

$\rho^{(3/2)}_{-1/2}$

	a_0	a_1	a_2	a_3	a_4	a_5	a_6	a_7	a_8	a_9	a_{10}	a_{11}	a_{12}	a_{13}	b_0	b_1	b_2	b_3	b_4	b_5	b_6	b_7	b_8	b_9	b_{10}	b_{11}	b_{12}	b_{13}	b_{14}	b_{15}		
ϵ_1^- (0,2)	1.000				-.0487				.0034								.3287				-.0209											
(1,3)		1.000			-.1070				.0101						.1594			.5582				-.0538										
(2,4)			1.000		-.1725				-.2428						.3240				.7422			-.0977										
(3,5)				1.000					-.3152											.8931												
(4,6)					.9625					-.3434											1.000											
(5,7)						.7155					-.3155											.9024										
(6,8)							1.000															1.000										
(7,9)								.9139															1.000									
(8,10)									.8583															1.000								
(9,11)										.8163															1.000							
(10,12)											.8746																1.000					
ϵ_1^+ (0)																																
(1)																																
(0,2)																																
(1,3)																																
(2,4)																																
(3,5)																																
(4,6)																																
(5,7)																																
(6,8)																																
(7,9)																																
(8,10)																																
(9,11)																																
(10,12)																																
(11,13)																																
(12,14)																																

TABLE 3.6 (Continued)

$\phi^{(3/2)}_{1/2}$														$\phi^{(3/2)}_{-3/2}$																	
	a_0	a_1	a_2	a_3	a_4	a_5	a_6	a_7	a_8	a_9	a_{10}	a_{11}	a_{12}	a_{13}	b_0	b_1	b_2	b_3	b_4	b_5	b_6	b_7	b_8	b_9	b_{10}	b_{11}	b_{12}	b_{13}	b_{14}	b_{15}	
ϵ_2^-	(0,2)	1.000			-.0440													-.2304			.0144										
	(1,3)		1.000			-.0850									-.2163				-.3425			.0312									
	(2,4)			1.000																-.4271			.0529								
	(3,5)				1.000																-.5088			.0860							
	(4,6)	.2513																				-.4781									
	(5,7)		.2702																				-.5289								
	(6,8)			.2993																				-.5646							
	(7,9)				.3388																				-.5962						
	(8,10)					.3912																				-.6245					
	(9,11)						.4763																				-.6533				
															</																

one level actually changes gradually into the other as \mathcal{H} increases (see Figures 3.5 and 3.6). The above phenomenon manifests itself also in the behavior of the coefficients in the eigenfunction expansions quoted in Table 3.6. It will be observed that for the $\epsilon_{1+}(4,6)$ and the $\epsilon_{1+}(5,7)$ levels a_{12} and a_{13} are larger respectively than a_8 and a_9 , and b_{14} and b_{15} are larger than b_{10} and b_{11} .

The energy levels can be identified and classified in the same way as for Ge but in the present instance the task is somewhat more difficult since in many cases, as has just been pointed out, mixing is quite strong (see Table 3.6).

As may be seen from Figures 3.5 through 3.8 the effect of the magnetic field on the energy levels is in this case appreciably more pronounced than in the case of Ge. Thus for the ϵ_{1-} , ϵ_{1+} , ϵ_{2-} , and ϵ_{2+} ladders, the approximate changes in the effective masses are by factors of 1.03 to 1.4, 1.08 to 1.5, 1.01 to 1.05, and 1.08 to 1.5 respectively. This is due to the small spin-orbit splitting in Si and the consequent strong mixing between the V_1 and V_2 band levels, and the V_3 band levels. In Figures 3.5 through 3.8 the dotted lines indicate levels whose energies are not as accurately known as some of the others.

Since in Si mixing between the Landau levels is quite strong, as Table 3.6 demonstrates, many interesting transitions should be possible. Some of these are shown in Figures 3.9 and 3.10. In Figure 3.9 levels belonging to the ϵ_1 ladders are shown, together with those wave function expansion coefficients which are equal to or greater than 0.50. These coefficients specify the harmonic oscillator functions as well as the

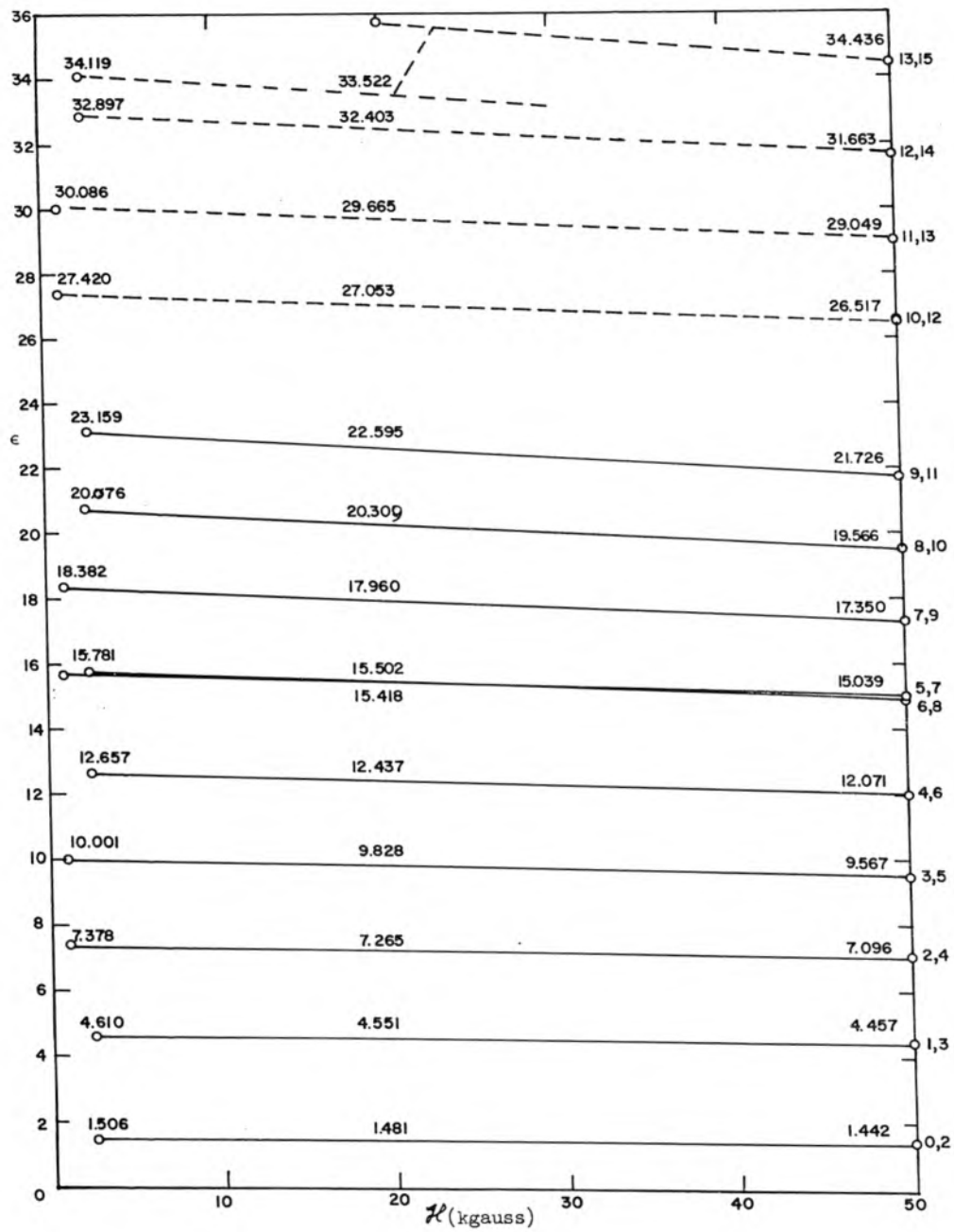


Fig. 3.5 Landau Levels belonging to the ϵ_1 - Ladder in Si as Functions of the Magnetic Field

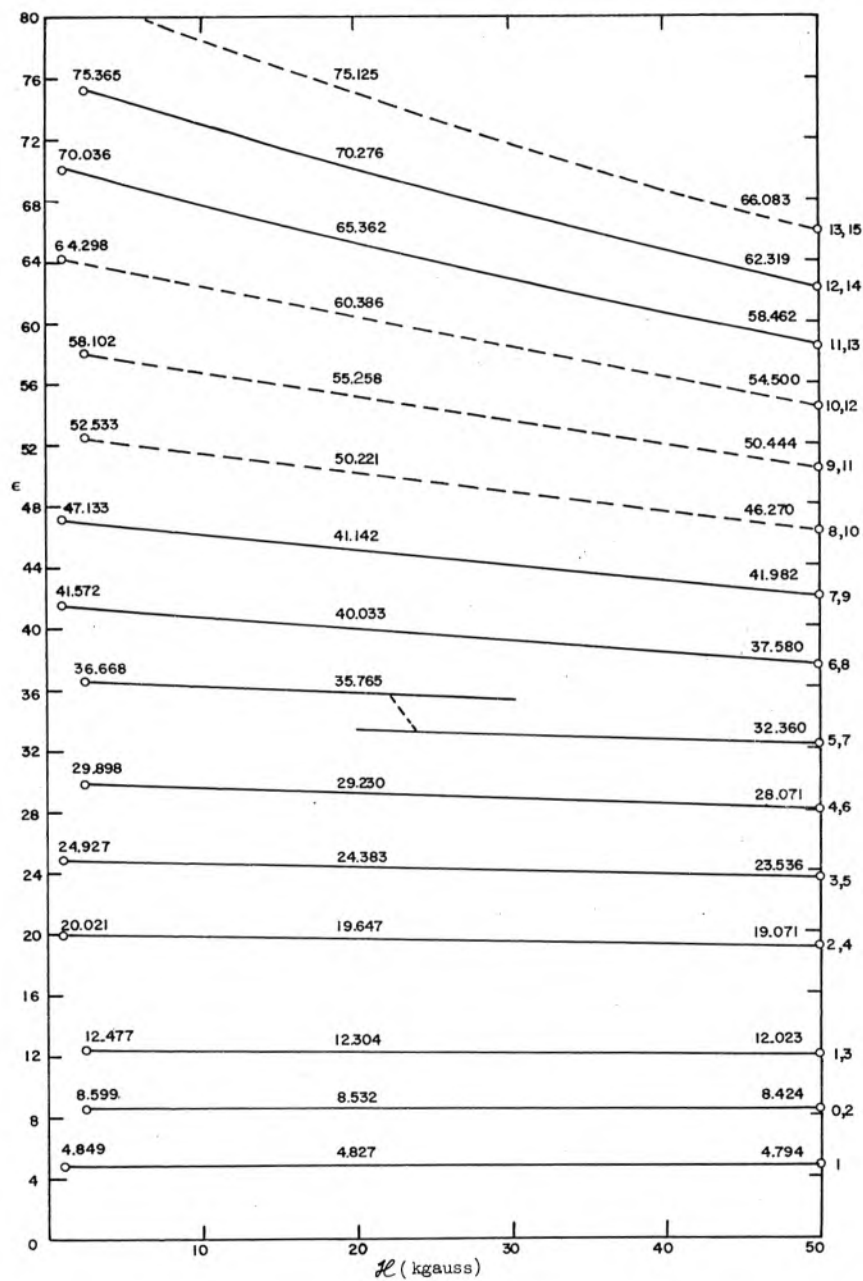


Fig. 3.6 Landau Levels belonging to the ϵ_{1+} Ladder in Si as Functions of the Magnetic Field

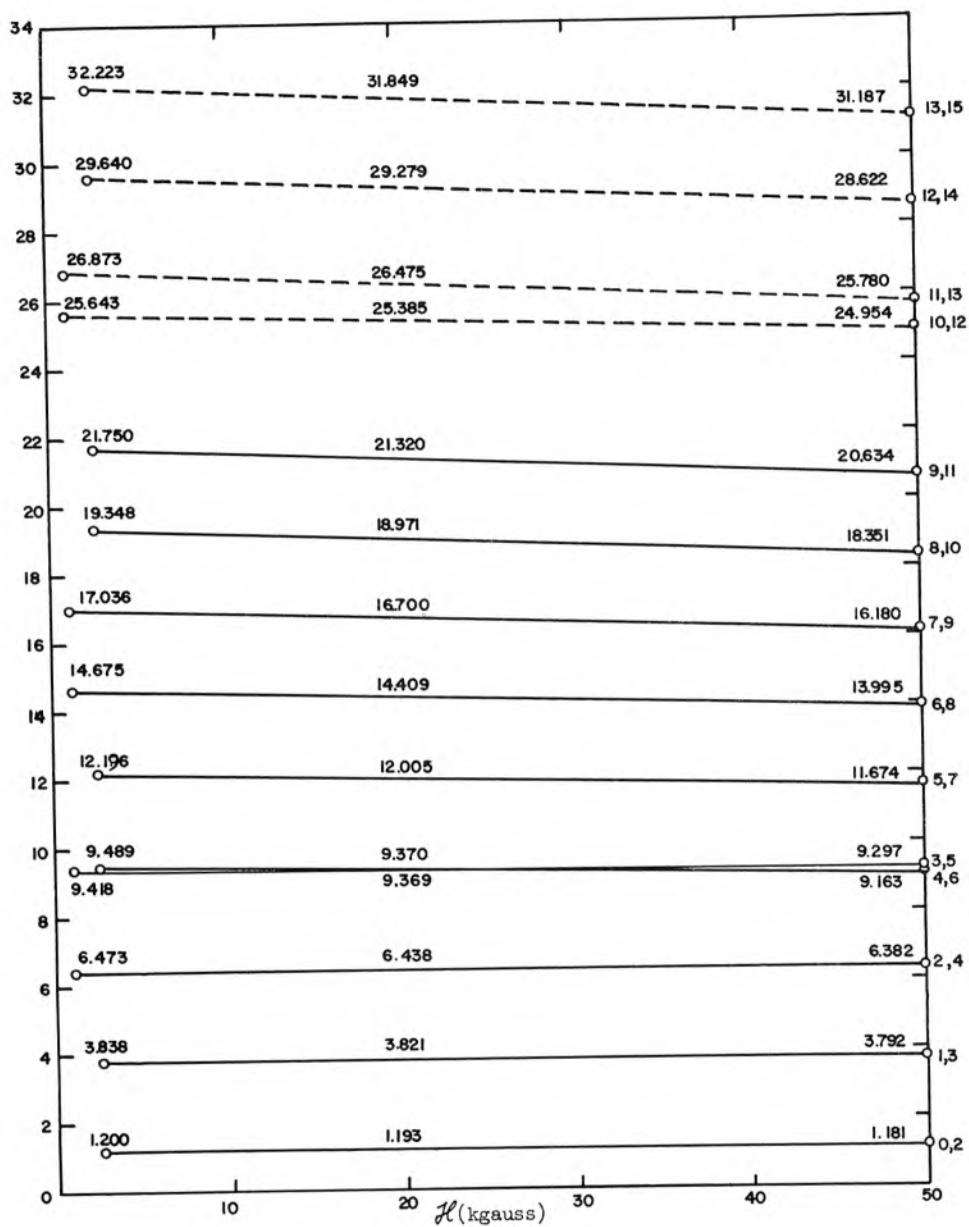


Fig. 3.7 Landau Levels belonging to the ϵ_2 - Ladder in Si as Functions of the Magnetic Field

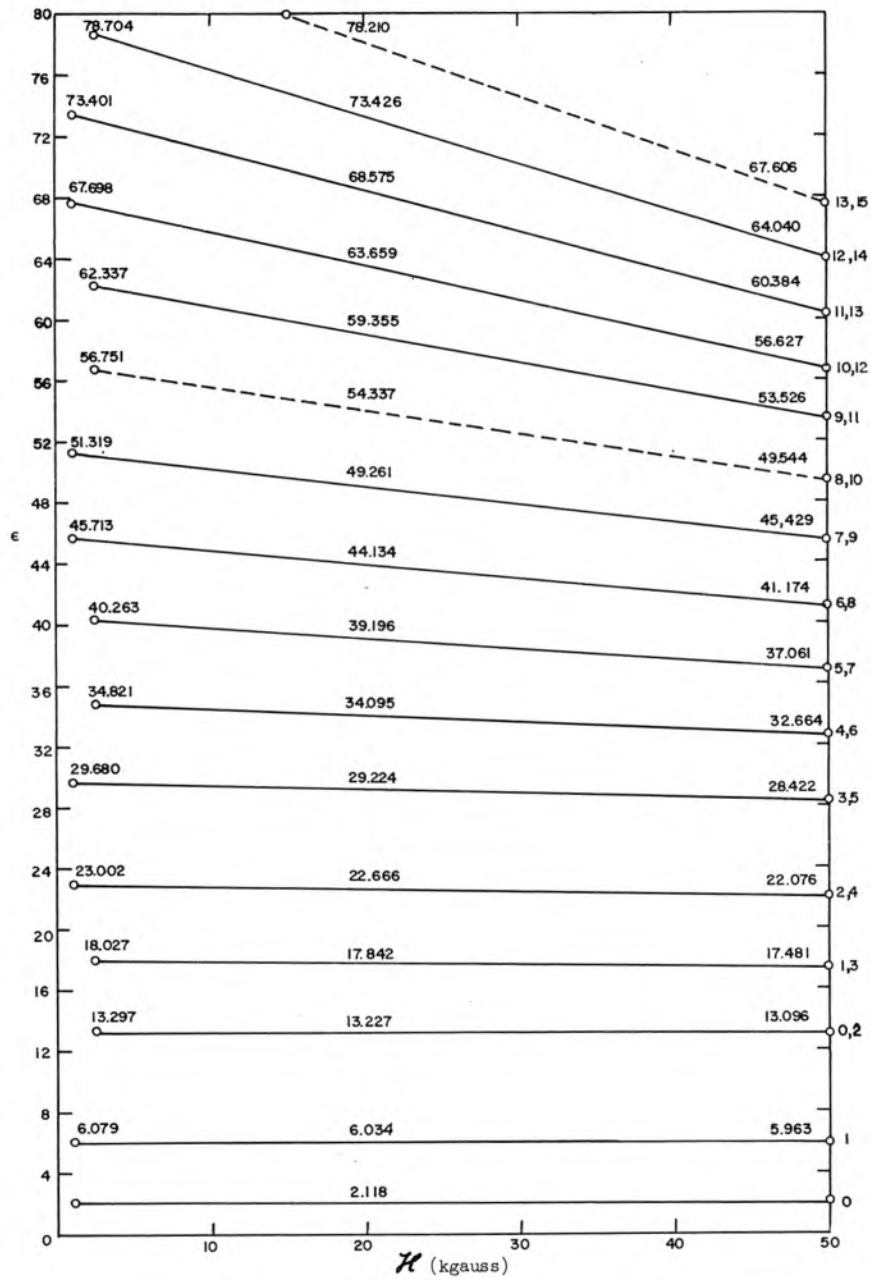


Fig. 3.8 Landau Levels belonging to the ϵ_{2+} Ladder in Si as Functions of the Magnetic Field

functions $\phi_m^{(J)}$ making up the wave function corresponding to a given level. Because only large coefficients have been considered, all of the transitions indicated should occur with a relatively high probability. It will be observed that some of the transitions are "negative mass" (NM) transitions, i.e., are caused by polarization of the incident radiation opposite to that causing ordinary transitions. They thus may be of a very high practical value. Figure 3.10 shows analogous transitions in the ϵ_2 ladders. No transitions between the ϵ_1 and ϵ_2 ladders are, of course, possible at $k_H = 0$.

Table 3.7 shows the expansion coefficients for the external magnetic field of 50 kgauss. Although in most cases there seem to be few qualitative changes as compared to coefficients in Table 3.6 (except for stronger coupling to the V_3 band), some levels do change the mixing pattern sufficiently so that their identity is essentially changed. Thus the absorption spectrum must be expected to be somewhat different at different values of the magnetic field. The high field transitions should therefore be examined in their own right for possible practically useful ones.

As was pointed out in the introduction, the "nonparabolic" effects in the V_2 band of Si appear at about .015 ev below the valence band edge according to the calculations of Kane (15). The deepest light hole energy level computed here is the ϵ_{2+} (12,14) level which lies about .017 ev away from the band edge at $\mathcal{H} = 20$ kgauss. Thus the "nonparabolic" effects should start manifesting themselves. However, in order to see them clearly a few additional deep lying levels would have to be calculated. This can be done by either solving larger determinants than the largest one solved here, or by truncating the infinite determinants at

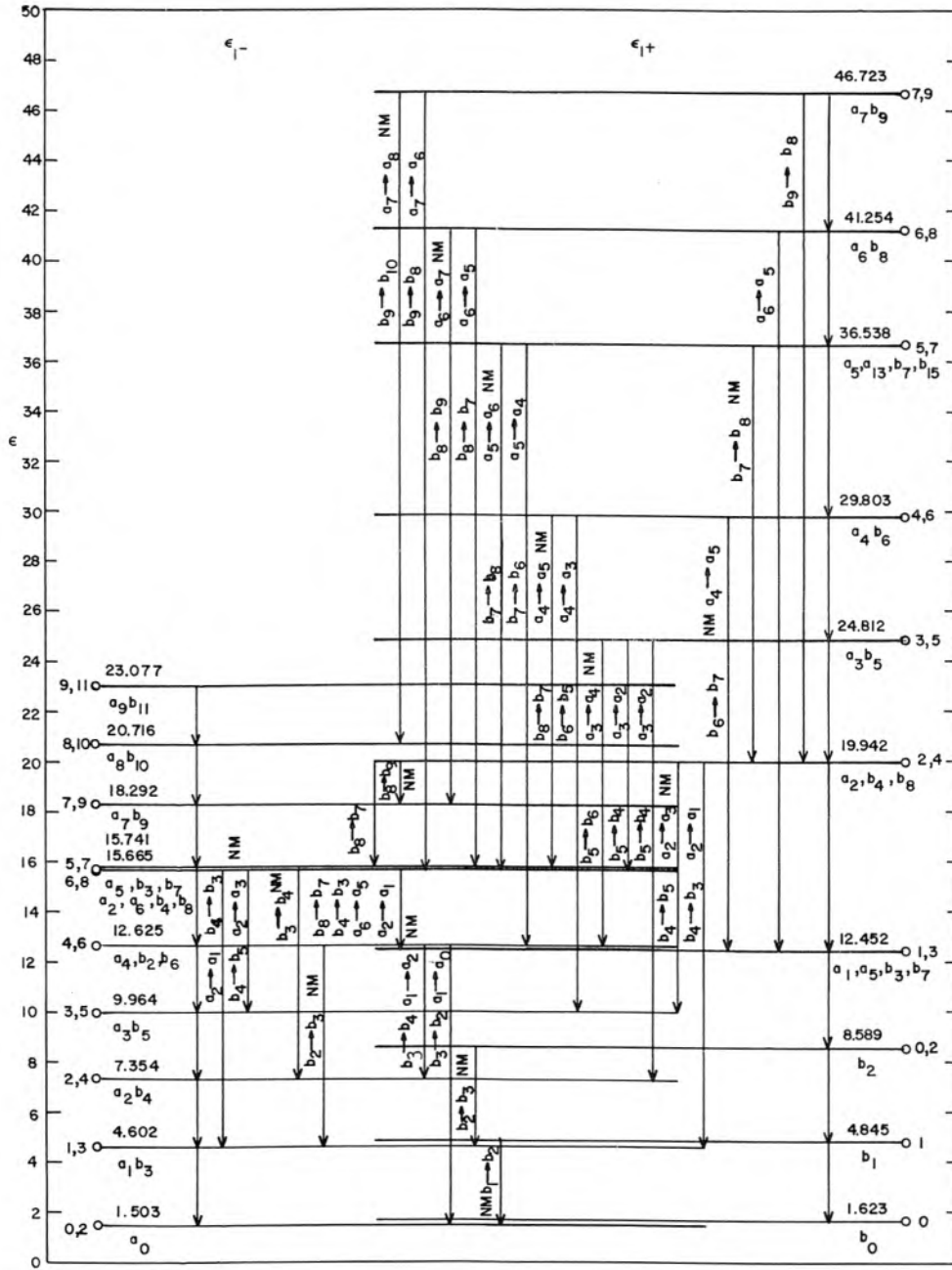


Fig. 3.9 Transitions between the Landau Levels belonging to the ϵ_1 Ladders in Si at $\mathcal{H} = 5$ kgauss. Expansion coefficients considered are approximately equal to or greater than 0.50. Transitions marked NM are of the "Negative Mass" type.

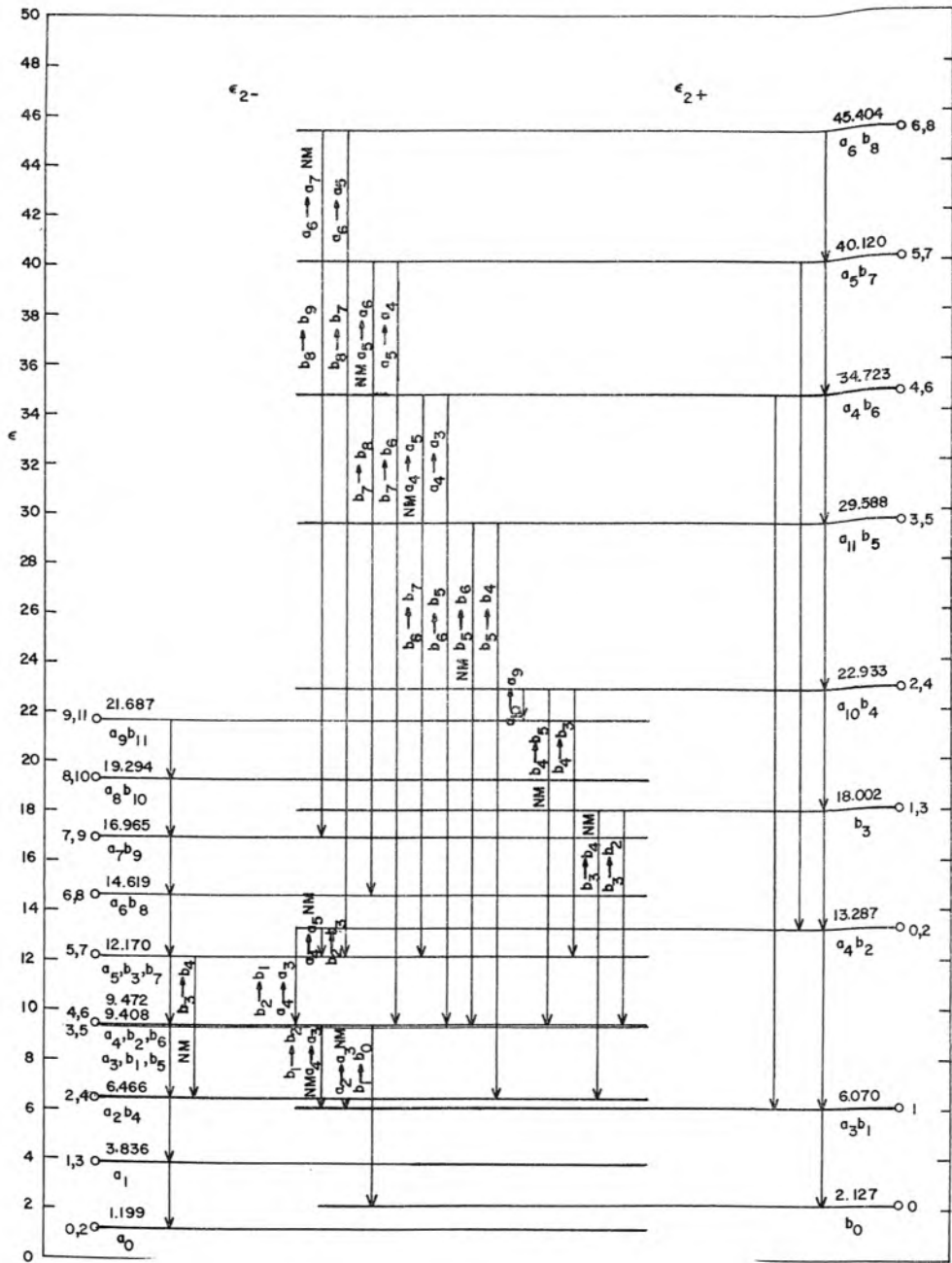


Fig. 3.10 Transitions between the Landau Levels belonging to the ϵ_2 ladders in Si at $\mathcal{H} = 5$ kgauss. Expansion Coefficients Considered are Approximately Equal to or Greater than 0.50. Transitions marked NM are of the "Negative Mass" type.

both ends. The latter method would allow one to go to arbitrarily large energies within the limits of validity of the perturbation theory.

for Si at $d = 0$ and $H = 50$ kg

-86-

TABLE 3.7 (Continued)

[illegible]

IV. VALENCE BAND LANDAU LEVELS AS FUNCTIONS OF k_H FOR H IN THE [001] DIRECTION

4.1 Check on the Validity of an Approximation Involving the Decoupling of the V_1 and V_2 Bands from the V_3 Band

Because of the complicated nature of equation 2.2.59, it is desirable to introduce some approximations before proceeding with further numerical computations. The approximation that has been extensively used so far involves an assumption that the states corresponding to $j = \frac{3}{2}$ and $j = \frac{1}{2}$ states in the tight binding limits couple only weakly and, therefore, may be assumed to be decoupled. According to Dresselhaus, Kip and Kittel (6), who used the assumption in computing the band structure of Ge and Si without the magnetic field, the error involved is of the order of k^4/Δ where Δ is the spin orbit splitting. Thus the assumption is good near the center of the Brillouin zone and should be much better for Ge than for Si. As far as the problem of a crystal in a magnetic field is concerned, this assumption is expected to be reasonably good for small k_H and for energy levels lying close to the band edge.

To check the extent of the validity of the approximation just discussed, one may simply compare the solutions to the exact and the approximate problems for some reasonably chosen special case. A convenient special case is that considered in Section III, i.e., the case of $k_H = 0$ and \mathcal{H} in the [001] direction. A calculation for this case provides sufficient information to enable one to deduce the extent to which the approximation is valid for $k_H \neq 0$.

The assumption that the $j = \frac{3}{2}$ and the $j = \frac{1}{2}$ states decouple, i.e., that the coupling matrix elements in the 2×4 and 4×2 strips in equation 2.2.59 may be neglected, reduces equation 2.2.59 to the following two matrices (see definitions on p. 51, equation 3.1.3).

$$\begin{aligned}
\|V_{ij}^{4x4}\| &= \frac{\hbar |e| \mathcal{H}}{mc} \left\| \begin{array}{cccc}
\alpha(a^+a + \frac{1}{2}) - & -(\beta a^2 + \delta a^{+2}) & -\frac{\nu}{\sqrt{6}} da & 0 \\
-\frac{\mu'}{2} d^2 + \frac{3}{2} \kappa & & & \\
-(\beta a^{+2} + \delta a^2) & \zeta(a^+a + \frac{1}{2}) + & 0 & -\frac{\nu}{\sqrt{6}} da \\
& + \eta d^2 - \frac{1}{2} \kappa & & \\
-\frac{\nu}{\sqrt{6}} da^+ & 0 & \zeta(a^+a + \frac{1}{2}) + & \beta a^2 + \delta a^{+2} \\
& & + \eta d^2 + \frac{1}{2} \kappa & \\
0 & -\frac{\nu}{\sqrt{6}} da^+ & \alpha(a^+a + \frac{1}{2}) - & \\
& & -\frac{\mu'}{2} d^2 - \frac{3}{2} \kappa &
\end{array} \right\| \begin{array}{l}
(\frac{3}{2}) \frac{3}{2} \\
(\frac{3}{2}) - \frac{1}{2} \\
(\frac{3}{2}) \frac{1}{2} \\
(\frac{3}{2}) - \frac{3}{2}
\end{array}
\end{aligned}
\tag{4.1.1}$$

and

$$\begin{aligned}
\|V_{ij}^{2x2}\| &= \frac{\hbar |e| \mathcal{H}}{mc} \left\| \begin{array}{cc}
\lambda(a^+a + \frac{1}{2} + \frac{1}{2} d^2) + \frac{2\kappa+1}{2} + \Delta, & 0 \\
0 & \lambda(a^+a + \frac{1}{2} + \frac{1}{2} d^2) - \frac{2\kappa+1}{2} + \Delta,
\end{array} \right\| \begin{array}{l}
(\frac{1}{2}) \frac{1}{2} \\
(\frac{1}{2}) - \frac{1}{2}
\end{array}
\end{aligned}
\tag{4.1.2}$$

The 4×4 matrix of equation 4.1.1 is of primary interest. In anticipation of the future needs $d = 0$ is not assumed at this point.

As in Section 3.1 the problem to be solved is the following:

$$||V_{ij}^{4 \times 4}|| F = E ||I|| F \quad (4.1.3)$$

where F is assumed to be

$$F = \left\| \begin{array}{c} \sum_i a_i f_i \\ \sum_j b_j f_j \\ \sum_k c_k f_k \\ \sum_l g_l f_l \end{array} \right\| \quad (4.1.4)$$

Making proper substitutions and carrying out the operations on f_n one obtains in units of $\frac{\hbar |e| \hbar}{mc}$

$$\begin{aligned} \text{I} \quad \sum_i \left[\alpha \left(1 + \frac{1}{2}\right) - \frac{\mu'}{2} d^2 + \frac{3}{2} \kappa - \epsilon \right] a_i f_i - \sum_j b_j \left\{ \beta [j(j-1)]^{1/2} f_{j-2} + \right. \\ \left. + \delta [(j+1)(j+2)]^{1/2} f_{j+2} \right\} - \sum_k \frac{\nu}{\sqrt{6}} d c_k k^{1/2} f_{k-1} = 0 \end{aligned}$$

II

$$\begin{aligned} - \sum_i a_i \left\{ \beta [(i+1)(i+2)]^{1/2} f_{i+2} + \delta [i(i-1)]^{1/2} f_{i-2} \right\} + \\ + \sum_j \left[\xi \left(j + \frac{1}{2}\right) + \eta d^2 - \frac{1}{2} \kappa - \epsilon \right] b_j f_j - \sum_l \frac{\nu}{\sqrt{6}} d g_l l^{1/2} f_{l-1} = 0 \end{aligned} \quad (4.1.5)$$

III

$$- \sum_i \frac{\nu}{\sqrt{6}} d a_i (i+1)^{1/2} f_{i+1} + \sum_k [\xi (k + \frac{1}{2}) + \eta d^2 + \frac{1}{2} \kappa - \epsilon] c_k f_k +$$

$$+ \sum_\ell g_\ell \left\{ \beta [\ell(\ell-1)]^{1/2} f_{\ell-2} + \delta [(\ell+1)(\ell+2)]^{1/2} f_{\ell+2} \right\} = 0$$

IV

$$- \sum_j \frac{\nu}{\sqrt{6}} d b_j (j+1)^{1/2} f_{j+1} + \sum_k c_k \left\{ \beta [(k+1)(k+2)]^{1/2} f_{k+2} + \right.$$

$$\left. + \delta [k(k-1)]^{1/2} f_{k-2} \right\} + \sum_\ell [\alpha (\ell + \frac{1}{2}) - \frac{\mu'}{2} d^2 - \frac{3}{2} \kappa - \epsilon] g_\ell f_\ell = 0 \quad (4.1.5)$$

In this case the assumption of $\delta = 0$ leads to the substitutions $j = i+2$
 $k = i+1$, $\ell = i+3$, which result in sets of four equations for each i .

In the case of $\delta \neq 0$ one has

	g_0	b_0	g_1	b_1	c_0	g_2	a_0	b_2	c_1	g_3	a_1	b_3	c_2	g_4	a_2	b_4	c_3	g_5	a_3	b_5	c_4	g_6	
IV f_0	ϵ												δ										
II f_0		ϵ	d											δ									
IV f_1		d	ϵ												δ								
II f_1				ϵ	d											δ							
III f_0					ϵ	β											δ						
IV f_0				d	β	ϵ												δ					
I f_0							ϵ	β	d														
II f_2							β	ϵ		d													
III f_1							d		ϵ	β													
IV f_3								d	β	ϵ													
I f_1									ϵ	β	d												
II f_3									β	ϵ		d											
III f_2	δ								d		ϵ	β											
IV f_4		δ								d	β	ϵ											
I f_2			δ								ϵ	β	d										
II f_4				δ							β	ϵ		d									
III f_3					δ						d		ϵ	β									
IV f_5						δ						d	β	ϵ									
I f_3							δ								ϵ	β	d						
II f_5								δ							β	ϵ		d					
III f_4									δ						d		ϵ	β					
IV f_6																d	β	ϵ					

(4.1.6)

TABLE 4.1

	b_1	g_1	a_1	b_1	c_1	g_1	a_1	c_1
I	$-\delta[(i+1)(i+2)]^{1/2}$	0	$\alpha(i+\frac{1}{2}) - \frac{\mu'}{2} d^2 + \frac{3}{2} \kappa - \epsilon$	$-\beta[i(i-1)]^{1/2}$	$-\frac{\nu}{\sqrt{6}} d i^{1/2}$	0	0	0
II	0	0	$-\beta[(i+1)(i+2)]^{1/2}$	$\zeta(i+\frac{1}{2}) + \eta d^2 - \frac{1}{2} \kappa - \epsilon$	0	$-\frac{\nu}{\sqrt{6}} d i^{1/2}$	$-\delta[i(i-1)]^{1/2}$	0
III	0	$\delta[(i+1)(i+2)]^{1/2}$	$-\frac{\nu}{\sqrt{6}} d(i+1)^{1/2}$	0	$(i+\frac{1}{2}) + d^2 + \frac{1}{2} \kappa - \epsilon$	$\beta[i(i-1)]^{1/2}$	0	0
IV	0	0	0	$-\frac{\nu}{\sqrt{6}} d(i+1)^{1/2}$	$\beta[(i+1)x(i+2)]^{1/2}$	$\alpha(i+\frac{1}{2}) - \frac{\mu'}{2} d^2 - \frac{3}{2} \kappa - \epsilon$	0	$\delta[i(i-1)]^{1/2}$

where the elements in any four rows labeled I,II,III,IV are determined from Table 4.1. The matrix as in Section III decouples into four independent ones of the following form:

$$\begin{array}{c}
 g_0 \ a_1 \ b_3 \ c_2 \ g_4 \ a_5 \ b_7 \ c_6 \ g_8 \ a_9 \ b_{11} \ c_{10} \ g_{12} \\
 \begin{array}{l}
 \text{IV } f_0 \\
 \text{I } f_1 \\
 \text{II } f_3 \\
 \text{III } f_2 \\
 \text{IV } f_4 \\
 \text{I } f_5 \\
 \text{II } f_7 \\
 \text{III } f_6 \\
 \text{IV } f_8 \\
 \text{I } f_9 \\
 \text{II } f_{11} \\
 \text{III } f_{10} \\
 \text{IV } f_{12}
 \end{array}
 \begin{array}{|c|c|c|c|c|c|c|c|c|c|c|c|c|}
 \hline
 \epsilon & & & & & & & & & & & & \\
 \hline
 & \epsilon & & d & & & & & & & & & \\
 \hline
 & \beta & \epsilon & & d & \delta & & & & & & & \\
 \hline
 \delta & d & & \epsilon & \beta & & & & & & & & \\
 \hline
 & & d & \beta & \epsilon & & & \delta & & & & & \\
 \hline
 & & & \delta & & & \epsilon & \beta & d & & & & \\
 \hline
 & & & & & & \beta & \epsilon & & d & \delta & & \\
 \hline
 & & & & & \delta & d & & \epsilon & \beta & & & \\
 \hline
 & & & & & & & d & \beta & \epsilon & & & \\
 \hline
 & & & & & & & & \delta & & & & \\
 \hline
 & & & & & & & & & \epsilon & \beta & d & \\
 \hline
 & & & & & & & & & \beta & \epsilon & & d \\
 \hline
 & & & & & & & & & d & & \epsilon & \beta \\
 \hline
 & & & & & & & & & & d & \beta & \epsilon \\
 \hline
 \end{array}
 \end{array}$$

(4.1.7)

$$\begin{array}{c}
 b_0 \ g_1 \ a_2 \ b_4 \ c_3 \ g_5 \ a_6 \ b_8 \ c_7 \ g_9 \ a_{10} \ b_{12} \ c_{11} \ g_{13} \\
 \begin{array}{l}
 \text{II } f_0 \\
 \text{IV } f_1 \\
 \text{I } f_2 \\
 \text{II } f_4 \\
 \text{III } f_3 \\
 \text{IV } f_5 \\
 \text{I } f_6 \\
 \text{II } f_8 \\
 \text{III } f_7 \\
 \text{IV } f_9 \\
 \text{I } f_{10} \\
 \text{II } f_{12} \\
 \text{III } f_{11} \\
 \text{IV } f_{13}
 \end{array}
 \begin{array}{|c|c|c|c|c|c|c|c|c|c|c|c|c|}
 \hline
 \epsilon & d & \delta & & & & & & & & & & \\
 \hline
 d & \epsilon & & & \delta & & & & & & & & \\
 \hline
 \delta & & \epsilon & \beta & d & & & & & & & & \\
 \hline
 & & & \epsilon & & d & \delta & & & & & & \\
 \hline
 \delta & & d & & \epsilon & \beta & & & & & & & \\
 \hline
 & & & d & \beta & \epsilon & & & \delta & & & & \\
 \hline
 & & & & \delta & & \epsilon & \beta & d & & & & \\
 \hline
 & & & & & & \beta & \epsilon & & d & \delta & & \\
 \hline
 & & & & & \delta & d & & \epsilon & \beta & & & \\
 \hline
 & & & & & & & d & \beta & \epsilon & & & \\
 \hline
 & & & & & & & & \delta & & & & \\
 \hline
 & & & & & & & & & \epsilon & \beta & d & \\
 \hline
 & & & & & & & & & \beta & \epsilon & & d \\
 \hline
 & & & & & & & & & d & & \epsilon & \beta \\
 \hline
 & & & & & & & & & & d & \beta & \epsilon \\
 \hline
 \end{array}
 \end{array}$$

(4.1.8)

$$\begin{array}{cccccccccccccccc}
 & b_1 & c_0 & g_2 & a_3 & b_5 & c_4 & g_6 & a_7 & b_9 & c_8 & g_{10} & a_{11} & b_{13} & c_{12} & g_{14} \\
 \text{II } f_1 & \epsilon & & d & & \delta & & & & & & & & & & \\
 \text{III } f_0 & & \epsilon & \beta & & & & & & & & & & & & \\
 \text{IV } f_2 & d & \beta & \epsilon & & & \delta & & & & & & & & & \\
 \text{I } f_3 & \delta & & & \epsilon & \beta & d & & & & & & & & & \\
 \text{II } f_5 & & & & \beta & \epsilon & & d & \delta & & & & & & & \\
 \text{III } f_4 & & \delta & & d & & \epsilon & \beta & & & & & & & & \\
 \text{IV } f_6 & & & & d & \beta & \epsilon & & & \delta & & & & & & \\
 \text{I } f_7 & & & & \delta & & & \epsilon & \beta & d & & & & & & \\
 \text{II } f_9 & & & & & & & \beta & \epsilon & & d & \delta & & & & \\
 \text{III } f_8 & & & & & \delta & & d & & \epsilon & \beta & & & & & \\
 \text{IV } f_{10} & & & & & & & d & \beta & \epsilon & & & \delta & & & \\
 \text{I } f_{11} & & & & & & & \delta & & & \epsilon & \beta & d & & & \\
 \text{II } f_{13} & & & & & & & & & & \beta & \epsilon & & d & & \\
 \text{III } f_{12} & & & & & & & & \delta & & d & & \epsilon & \beta & & \\
 \text{IV } f_{14} & & & & & & & & & & d & \beta & \epsilon & & & \\
 & & & & & & & & & & & \delta & & & &
 \end{array}$$

(4.1.9)

$$\begin{array}{cccccccccccccccc}
 & a_0 & b_2 & c_1 & g_3 & a_4 & b_6 & c_5 & g_7 & a_8 & b_{10} & c_9 & g_{11} & a_{12} & b_{14} & c_{13} & g_{15} \\
 \text{I } f_0 & \epsilon & \beta & d & & & & & & & & & & & & & \\
 \text{II } f_2 & \beta & \epsilon & & d & \delta & & & & & & & & & & & \\
 \text{III } f_1 & d & & \epsilon & \beta & & & & & & & & & & & & \\
 \text{IV } f_3 & & d & \beta & \epsilon & & \delta & & & & & & & & & & \\
 \text{I } f_4 & \delta & & & & \epsilon & \beta & d & & & & & & & & & \\
 \text{II } f_6 & & & & & \beta & \epsilon & & d & \delta & & & & & & & \\
 \text{III } f_5 & & \delta & & d & & \epsilon & \beta & & & & & & & & & \\
 \text{IV } f_7 & & & & d & \beta & \epsilon & & & & \delta & & & & & & \\
 \text{I } f_8 & & & & \delta & & & \epsilon & \beta & d & & & & & & & \\
 \text{II } f_{10} & & & & & & & \beta & \epsilon & & d & \delta & & & & & \\
 \text{III } f_9 & & & & & \delta & & d & & \epsilon & \beta & & & & & & \\
 \text{IV } f_{11} & & & & & & & d & \beta & \epsilon & & & \delta & & & & \\
 \text{I } f_{12} & & & & & & & \delta & & & \epsilon & \beta & d & & & & \\
 \text{II } f_{14} & & & & & & & & & & \beta & \epsilon & & d & & & \\
 \text{III } f_{13} & & & & & & & & \delta & & d & & \epsilon & \beta & & & \\
 \text{IV } f_{15} & & & & & & & & & & d & \beta & \epsilon & & & &
 \end{array}$$

(4.1.10)

The solutions are obtained by solving determinants of the order of $n+4$ if the first n energy eigenvalues are required (see Appendix 5). The eigenvalues for Ge are shown in Figure 4.1, while the eigenfunction

expansion coefficients are summarized in Table 4.2. The percentages quoted in Figure 4.1 represent the deviation of the eigenvalues given there from the "correct" ones given in Section III at $\mathcal{H} = 20$ kgauss. The deviations seem to range from .05% to 3.8 % increasing with the energy of the eigenvalue. This last result is, of course, to be expected since the higher lying energy levels are influenced more strongly by the V_3 band. However, for the levels considered, the errors introduced by decoupling the 4×4 and the 2×2 matrices seem to be sufficiently small to make the approximation an excellent one.

In Figure 4.2 are shown the eigenvalues for Ge calculated using Goodman's (3) parameters. The results are seen to agree very well (within 1%) with Goodman's results even though he used the first order perturbation theory to introduce the δ -terms. The only levels to show marked disagreement with Goodman's values are the $\epsilon_{1+}(0)$ and the $\epsilon_{2+}(0)$ levels. This may be due to the fact that the low-lying levels couple more strongly to the other levels (to be discussed below) and therefore the perturbation theory treatment of the δ terms introduces larger errors into the low-lying levels than into the other ones.

Similar calculations have been performed for Si with the results shown in Figure 4.3. Here the deviations from the eigenvalues given in Section III range from $\sim .15\%$ to $\sim 3.0\%$ at 10 kgauss and from $\sim 1.2\%$ to $\sim 15\%$ at 50 kgauss. The eigenfunctions given in Table 4.3 are quite appreciably in error compared to the correct ones at 50 kgauss. but are not as bad when compared to the 5 kgauss. eigenfunctions. The decoupling approximation may therefore be assumed to be satisfactory for low magnetic fields (below ~ 10 kgauss) especially since the ℓ' , μ' , ν and κ

TABLE 4.2
WAVE FUNCTION EXPANSION COEFFICIENTS
for Ge at $d = 0.0$

$\phi_{3/2}^{(3/2)}$											$\phi_{-1/2}^{(3/2)}$																		
$a_0 \quad a_1 \quad a_2 \quad a_3 \quad a_4 \quad a_5 \quad a_6 \quad a_7 \quad a_8 \quad a_9$											$b_0 \quad b_1 \quad b_2 \quad b_3 \quad b_4 \quad b_5 \quad b_6 \quad b_7 \quad b_8 \quad b_9 \quad b_{10} \quad b_{11}$																		
ϵ_{1-}	(0,2)	1.000				-.0604																							
	(1,3)		.934				-.1004																						
	(2,4)			.8172				-.1204																					
	(3,5)				.7549				-.1361																				
	(4,6)	.1721				.731				-.1487																			
	(5,7)		.1362				.704				-.1653																		
ϵ_{1+}	(0)																												
	(1)																												
	(0,2)	-.761			-.0547			.0036		.01672																			
	(1,3)		1.000		-.1475		.0740	-.0205		.0004																			
	(2,4)			1.000					.0102																				
ϵ_{2-}	(0,2)	1.000				-.0506																							
	(1,3)		1.000			-.0841			-.1165																				
	(2,4)			1.000			-.1397			-.1648																			
	(3,5)				1.000						-.1914																		
	(4,6)	.0890																											
	(5,7)		.1199																										
ϵ_{2+}	(0)																												
	(1)																												
	(0,2)	.323																											
	(1,3)		.4109																										
	(2,4)			.457																									

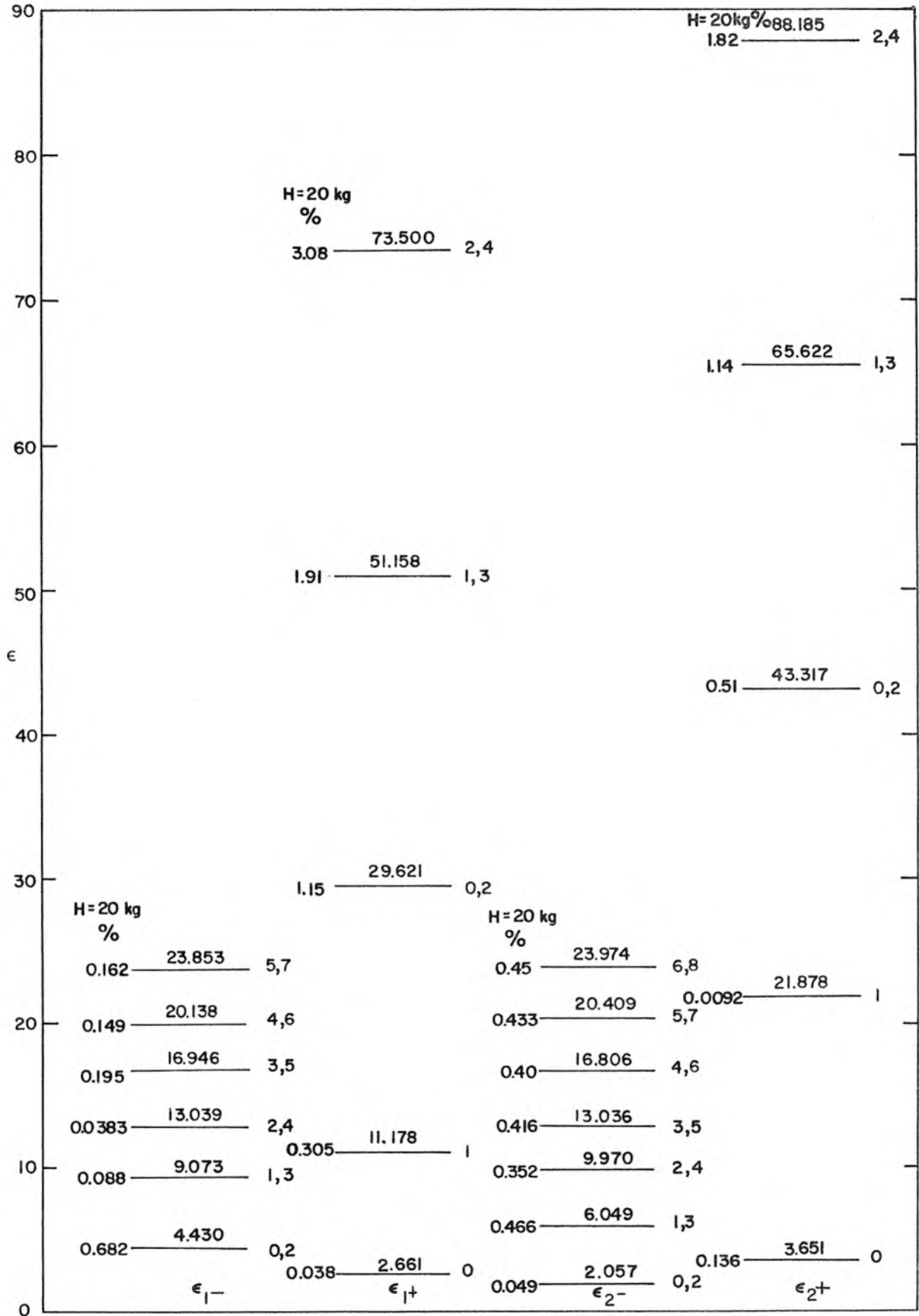


Fig. 4.1 Landau Levels in Ge at $d = k_H = 0$ for $7e$ in the [001] Direction. Percentage Figures Indicate Deviation from Results of Section III.

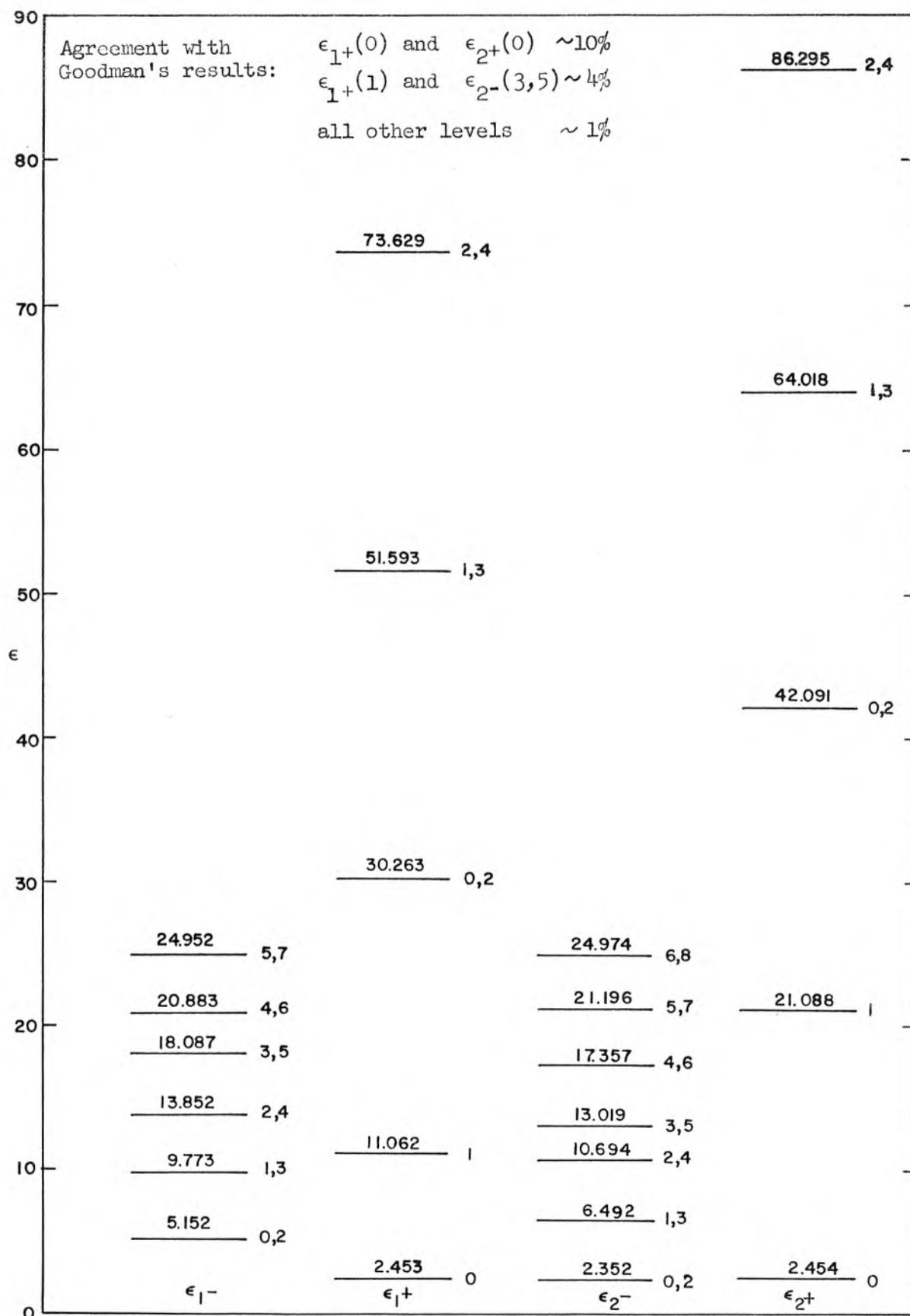


Fig. 4.2 Landau Levels in Ge at $d = k_H = 0$ for H in the $[001]$ Direction Calculated Using R.R. Goodman's (3) Parameters

parameters for Si are not very accurately known at the present time. Therefore, a more accurate calculation for Si involving the 6x6 matrix operator given by equation 2.2.59 is probably not warranted until more accurate experimental data is available.

Thus in the calculations which follow, the results for Ge may be assumed to be quite accurate for a wide range of magnetic fields, while those for Si are probably applicable only for the magnetic fields below ~ 10 kgauss and even then, may involve errors as large as $\sim 5\%$.

for Si at $d = 0.0$

-100-

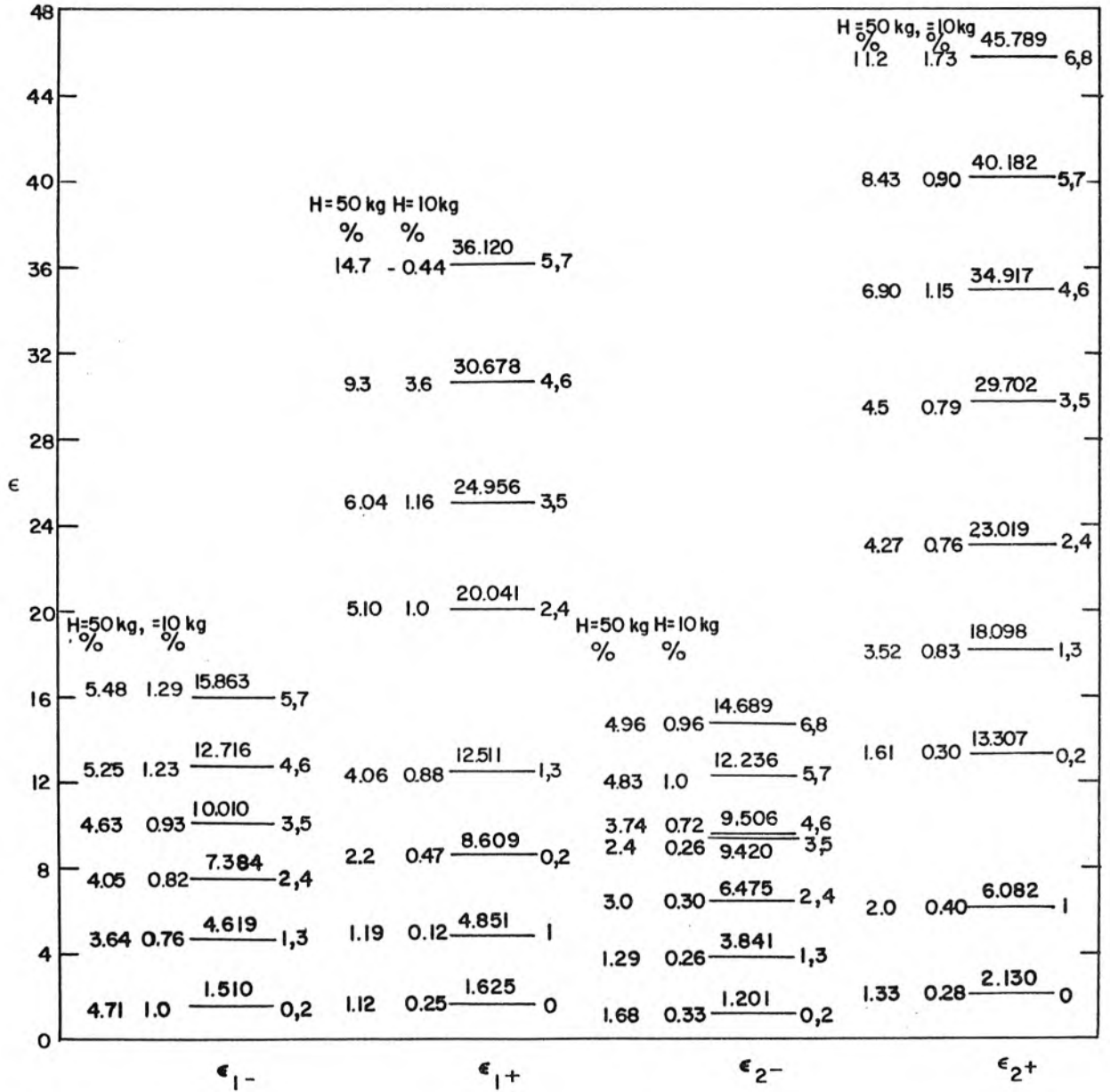


Fig. 4.3 Landau Levels in Si at $d = k_H = 0$ for H in the $[001]$ Direction. Percentage Figures Indicate Deviation from Results of Section 3.

4.2 Landau Levels as Functions of k_H in the Valence Band of Ge

Before proceeding with the complete calculations for Ge, it is instructive to compute some of the energy levels using the assumption $\delta = 0$. This corresponds to Luttinger's (2) D_0 of equation 81, where warping of the energy surfaces is included to zero order. The resulting levels contain some of the important features of the actual levels except, of course, for the coupling between them. The numerical results are tabulated in Appendix 6 and the energy levels resulting from the determinants of the types given by equations 4.1.7 through 4.1.10 are plotted in Figures 4.4 through 4.10. The following important features should be observed. The heavy hole levels seem to occur in pairs consisting of an $\epsilon_{1-}(n, n+2)$ level and an $\epsilon_{2-}(n+1, n+3)$ level. The separation between these levels at $d = 0$ decreases as n increases. One of the levels, the ϵ_{1-} level, has a curvature corresponding to negative mass in the k_H direction near $d = 0$, reaches a minimum at some finite value of d , and soon acquires the same curvature as the ϵ_{2-} member of the pair. The higher pairs seem to have smaller average curvatures than the lower ones and thus crossing of the levels occurs. Beyond the crossover, the cyclotron resonance effective mass is negative in the sense that the transitions are caused by radiation circularly polarized in the opposite sense to that causing the transitions before the crossover. The crossing over, however, is very gradual and occurs at relatively high values of d .

The character of the energy levels changes as d increases. The main change is in the leading coefficients in the eigenfunction expansions according to the following rule:

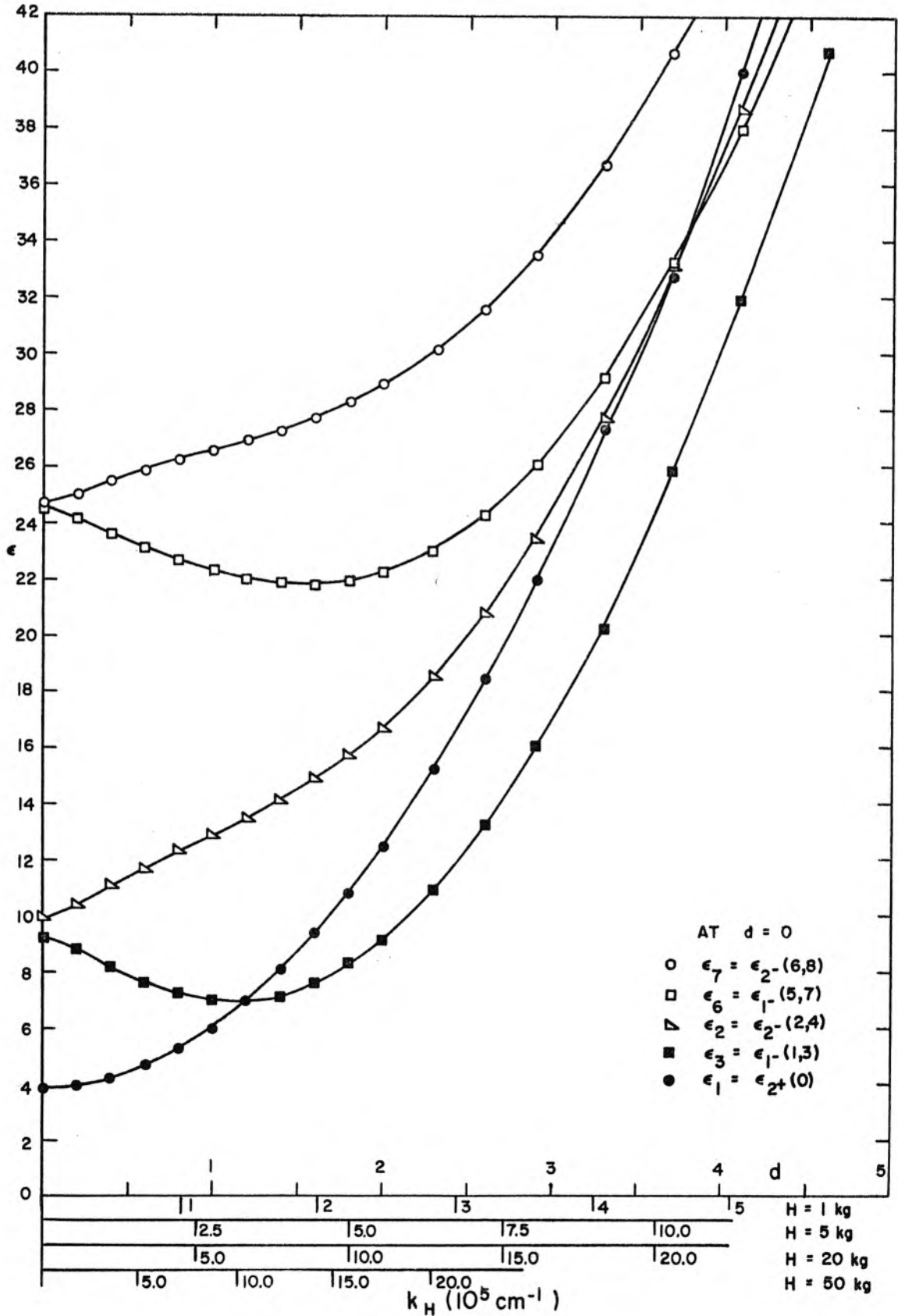


Fig. 4.4 Energy Sub-Bands Resulting from the Solution of Equation 4.1.7 (9x9 Determinant) for Ge Assuming $\delta = 0$

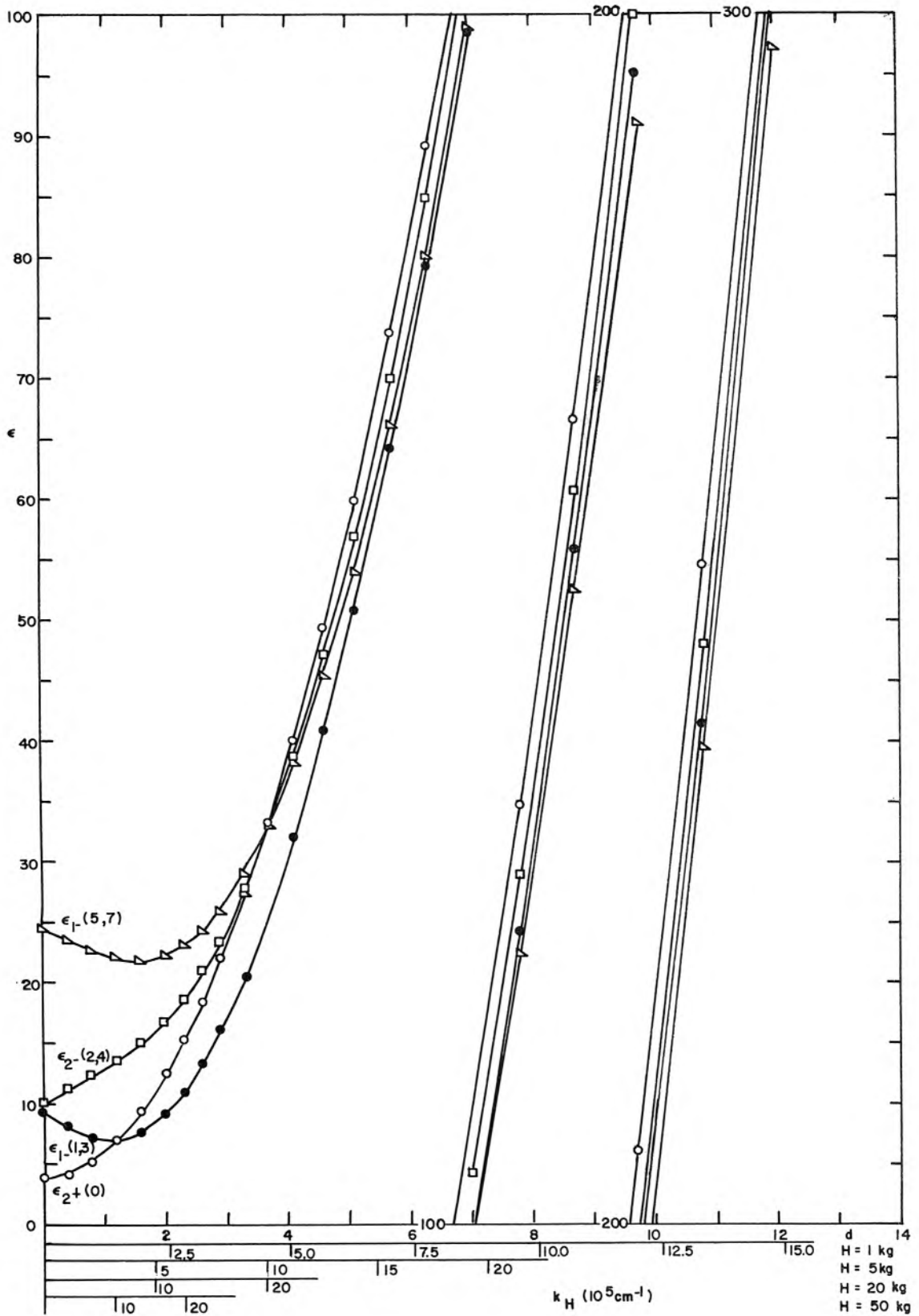


Fig. 4.5 Energy Sub-Bands Resulting from the Solution of Equation 4.1.7 (9×9 Determinant) for Ge, Assuming $\delta = 0$

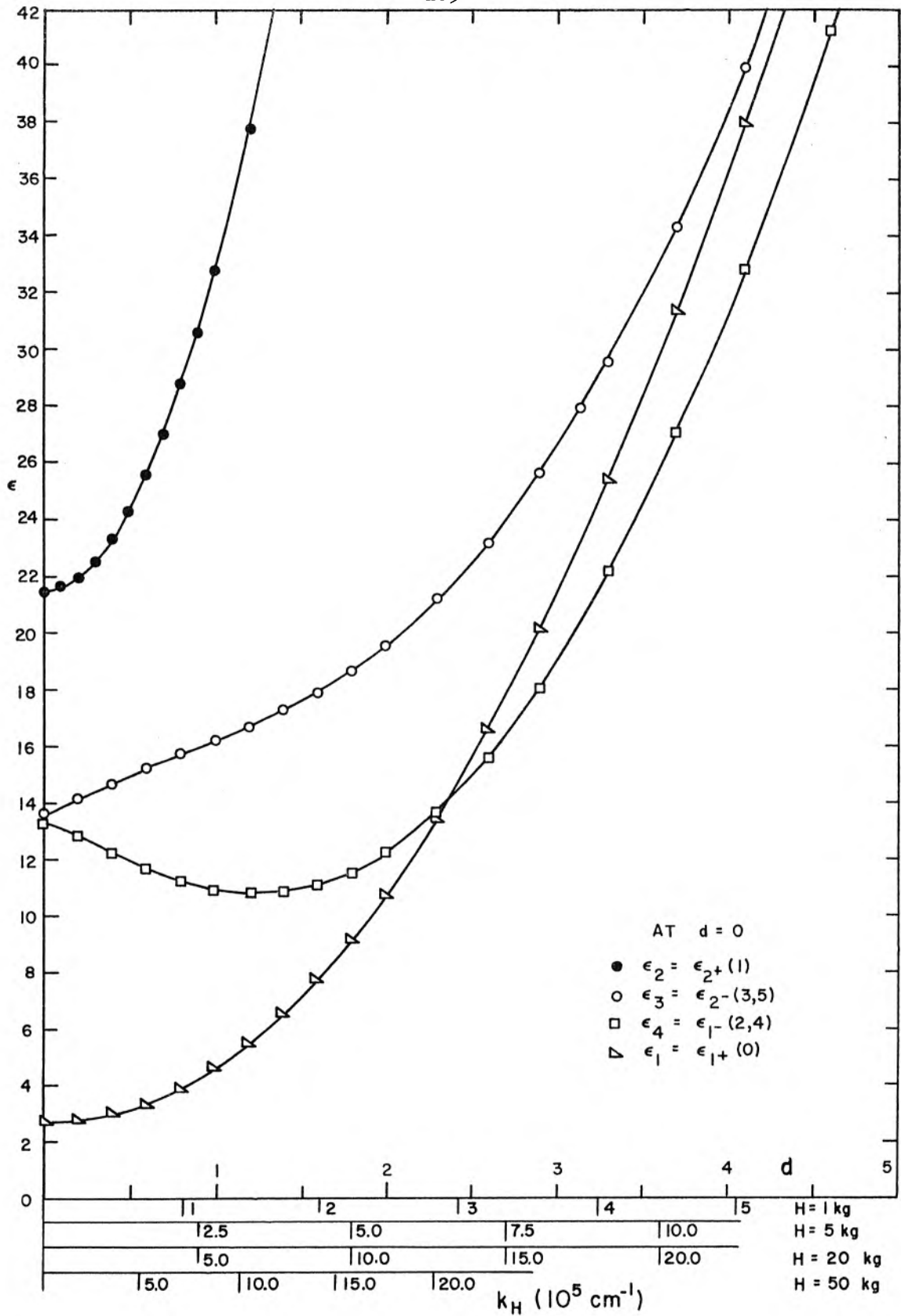


Fig. 4.6 Energy Sub-Bands Resulting from the Solution of Equation 4.1.8 (6x6 Determinant) for Ge, Assuming $\delta = 0$

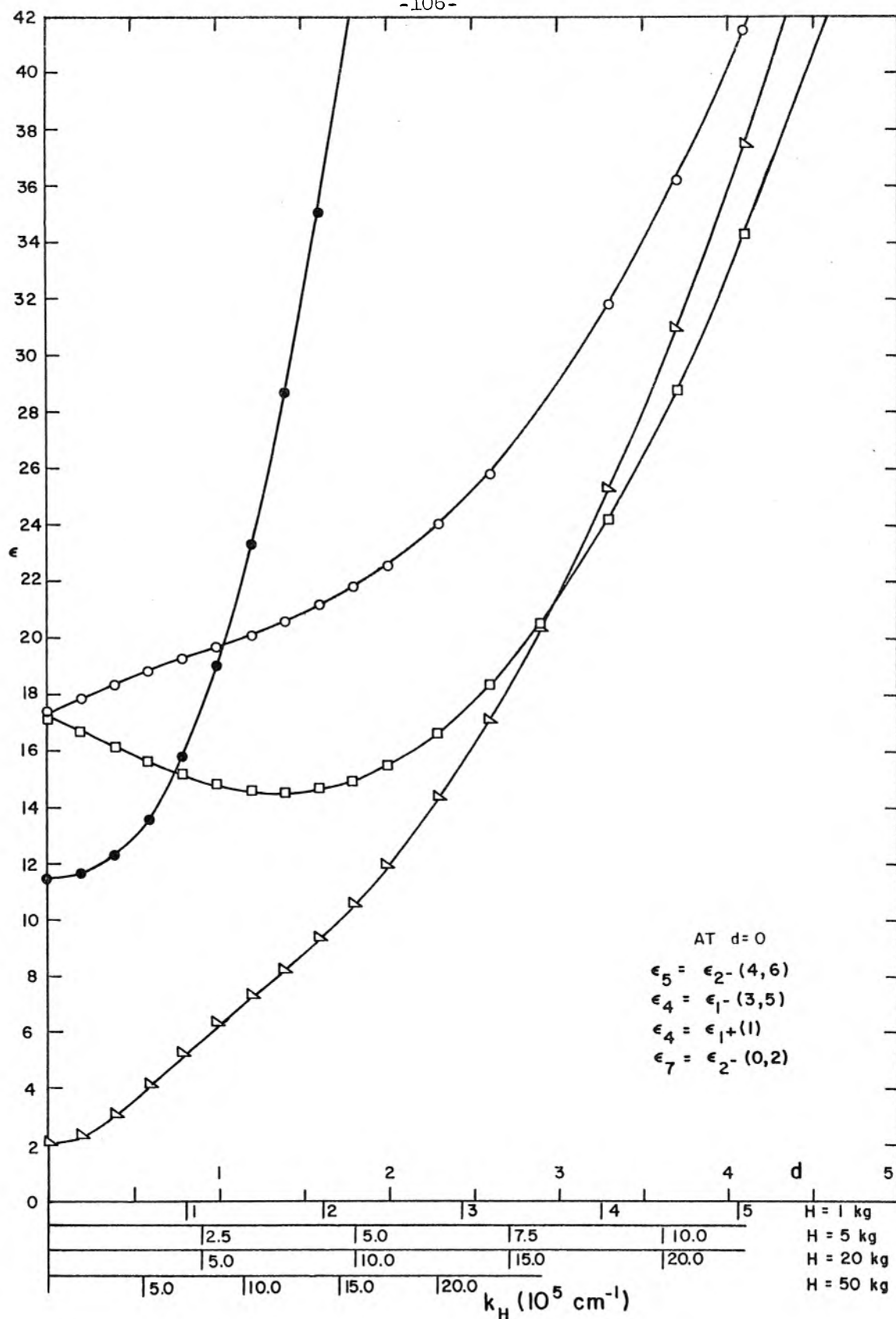


Fig. 4.7 Energy Sub-Bands Resulting from the Solution of Equation 4.1.9 (7x7 Determinant) for Ge, Assuming $\delta = 0$.

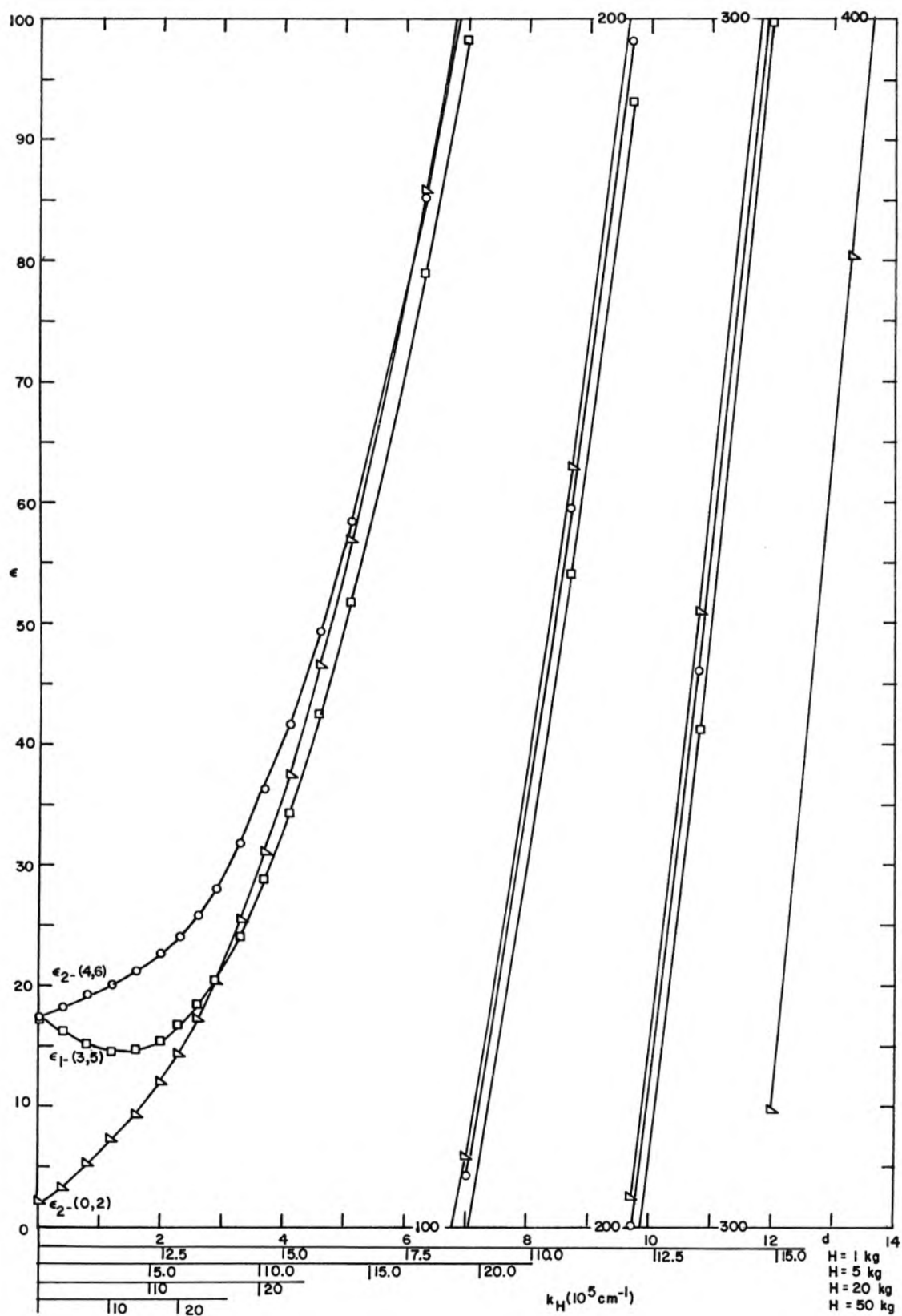


Fig. 4.8 Energy Sub-Bands Resulting from the Solution of Equation 4.1.9 (7x7 Determinant) for Ge, Assuming $\delta = 0$

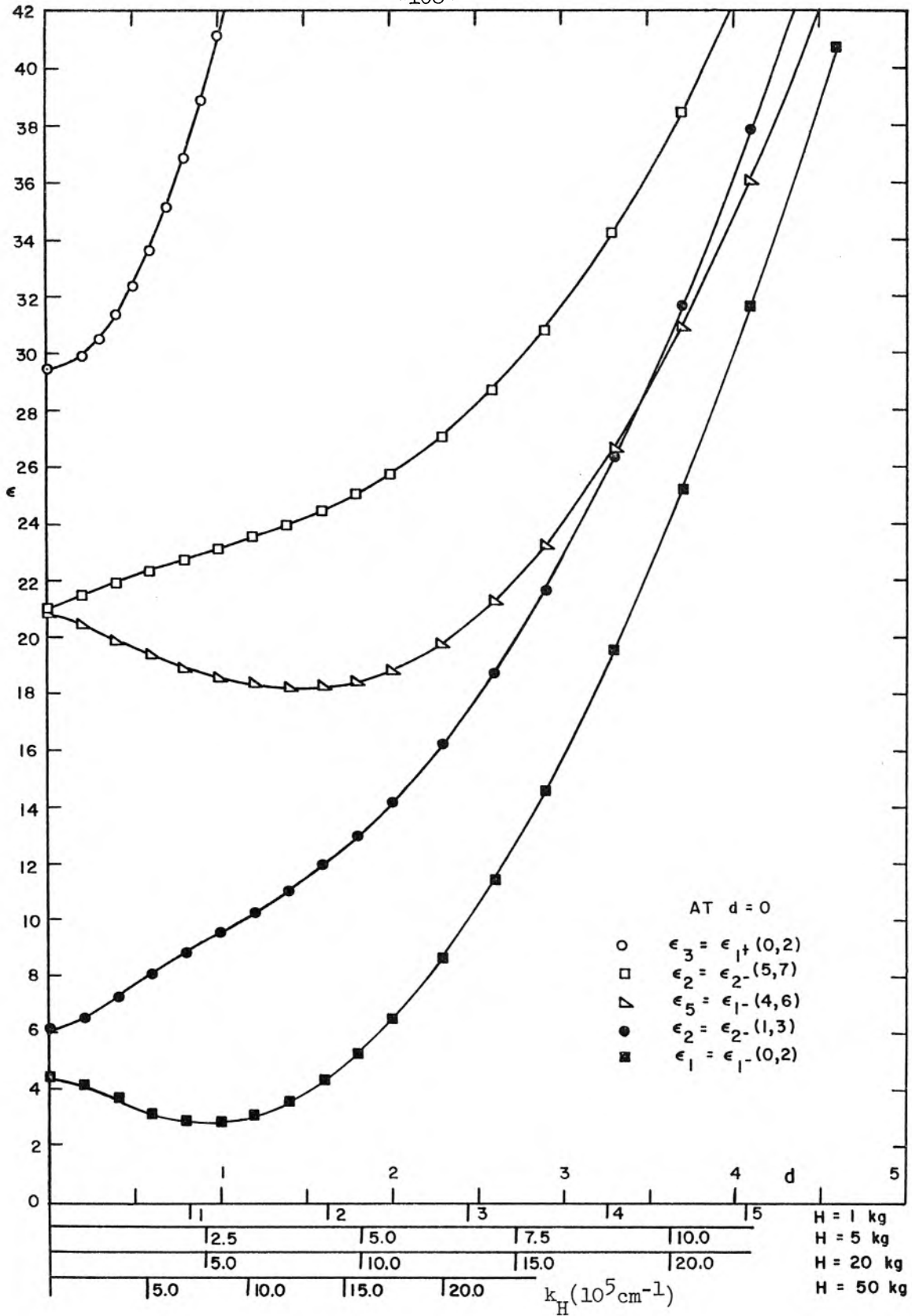


Fig. 4.9 Energy Sub-Bands Resulting from the Solution of Equation 4.1.10 (8x8 Determinant) for Ge, Assuming $\delta = 0$

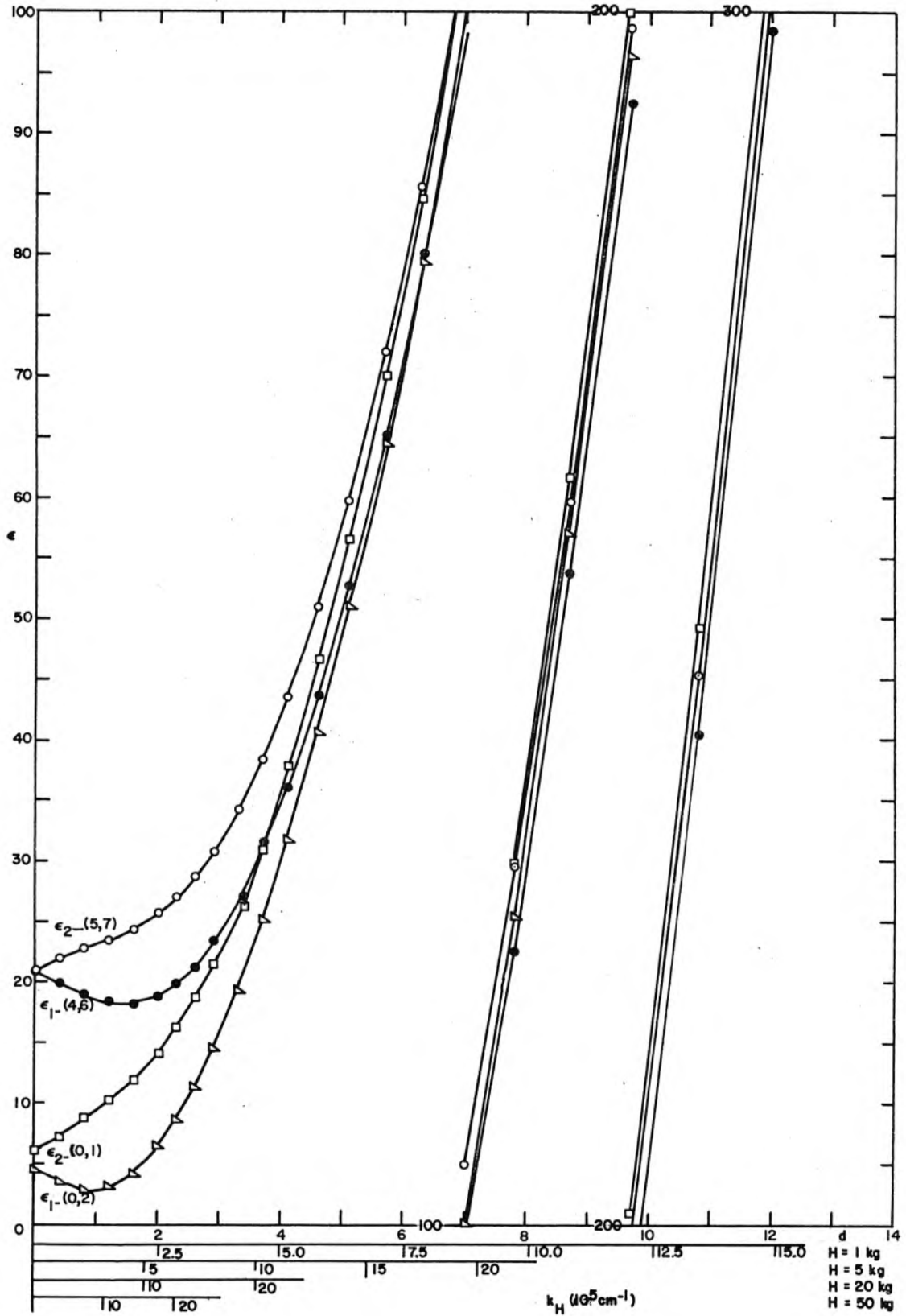


Fig. 4.10 Energy Sub-Bands Resulting from the Solution of Equation 4.1.10 (8×8 Determinant) for Ge, Assuming $\delta = 0$

	leading coeff. $d = 0$	leading coeff. d large
ϵ_1 levels	$a_i \quad b_{i+2}$	$a_i \quad c_{i+1}$
ϵ_2 levels	$c_i \quad g_{i+2}$	$b_{i+1} \quad g_{i+2}$

It should be noted that mixing occurs rather rapidly as a function of d . Thus at $d = 0$ the wave functions belonging to the ϵ_1 levels have $c_i = g_i \equiv 0$. However, at even small d (~ 0.3), certain c_i and g_i become appreciable even though the leading coefficients are still a_i and b_{i+2} . The expansion coefficients, in this as well as in all subsequent cases, have been actually computed for various values of d listed in Appendix 6, although they are not tabulated here. The above behavior of the eigenfunctions, however, is very easy to understand by inspecting the matrix elements in equations 4.1.7 through 4.1.10.

Let us now turn our attention to the complete Ge problem including the coupling terms δ . As was mentioned earlier, a determinant of $n+4$ order must be solved to obtain the first n eigenvalues. This can be seen by inspecting the numbers in Appendix 7. The solutions of various determinants are plotted in Figures 4.11 through 4.14. It will be observed that the general behavior of the levels is of the same nature as in the case of $\delta = 0$. The heavy hole levels still occur in pairs which approach each other and cross as d increases. However, the interaction between the levels does cause some important modifications. Thus in Figure 4.11 the $\epsilon_{2+}(0)$ and the $\epsilon_{1-}(1,3)$ levels no longer seem to cross at $d \approx 1.2$ but each simply changes gradually into the other as is illustrated in Figure 4.15. This figure also illustrates clearly the strong mixing which

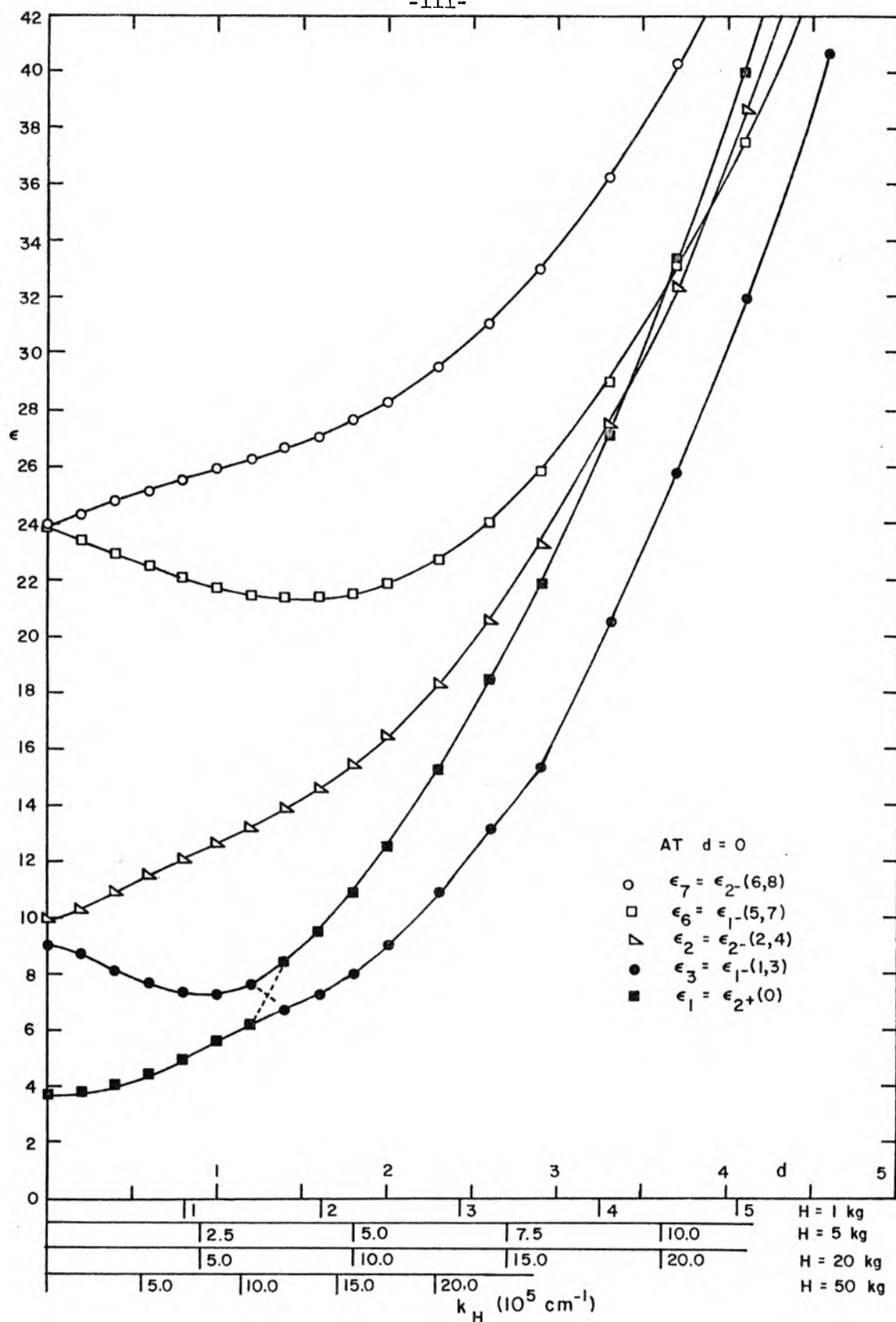


Fig. 4.11 Energy Sub-Bands Resulting from the Solution of Equation 4.1.7 (13x13 determinant) for Ge

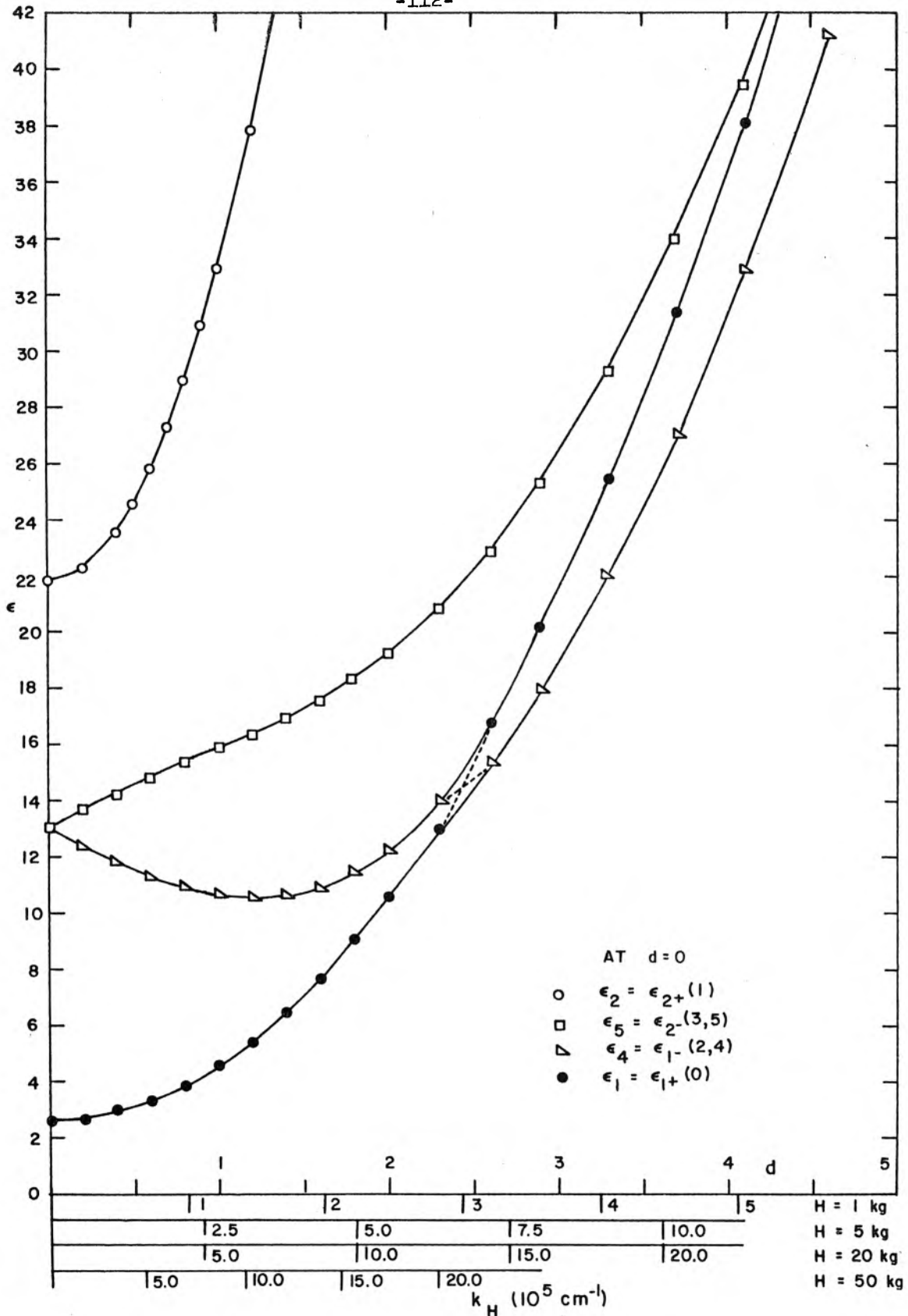


Fig. 4.12 Energy Sub-Bands Resulting from the Solution of Equation 4.1.8 (10x10 Determinant) for Ge

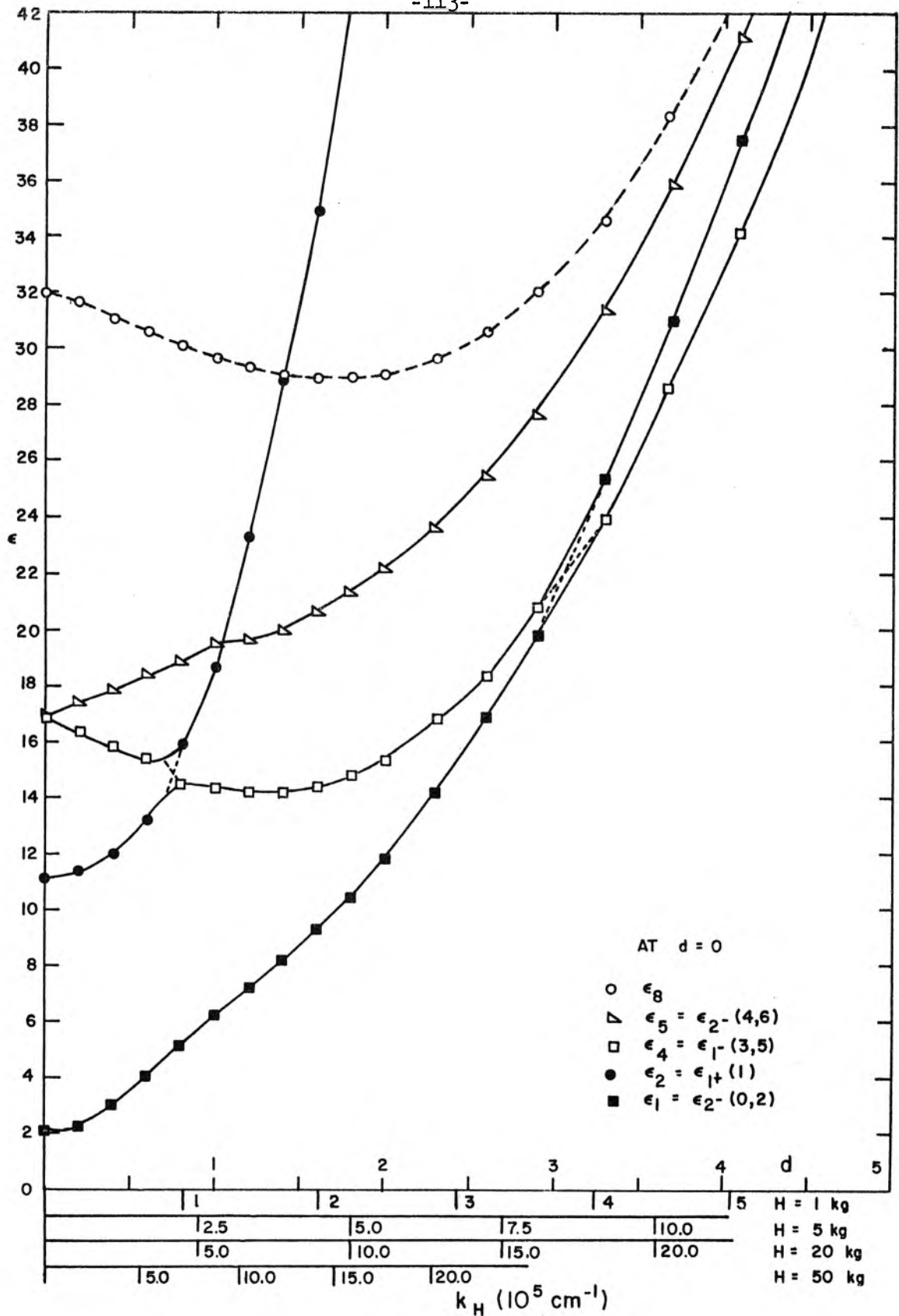


Fig. 4.13 Energy Sub-Bands Resulting from the Solution of Equation 4.1.9 (11x11 Determinant) for Ge

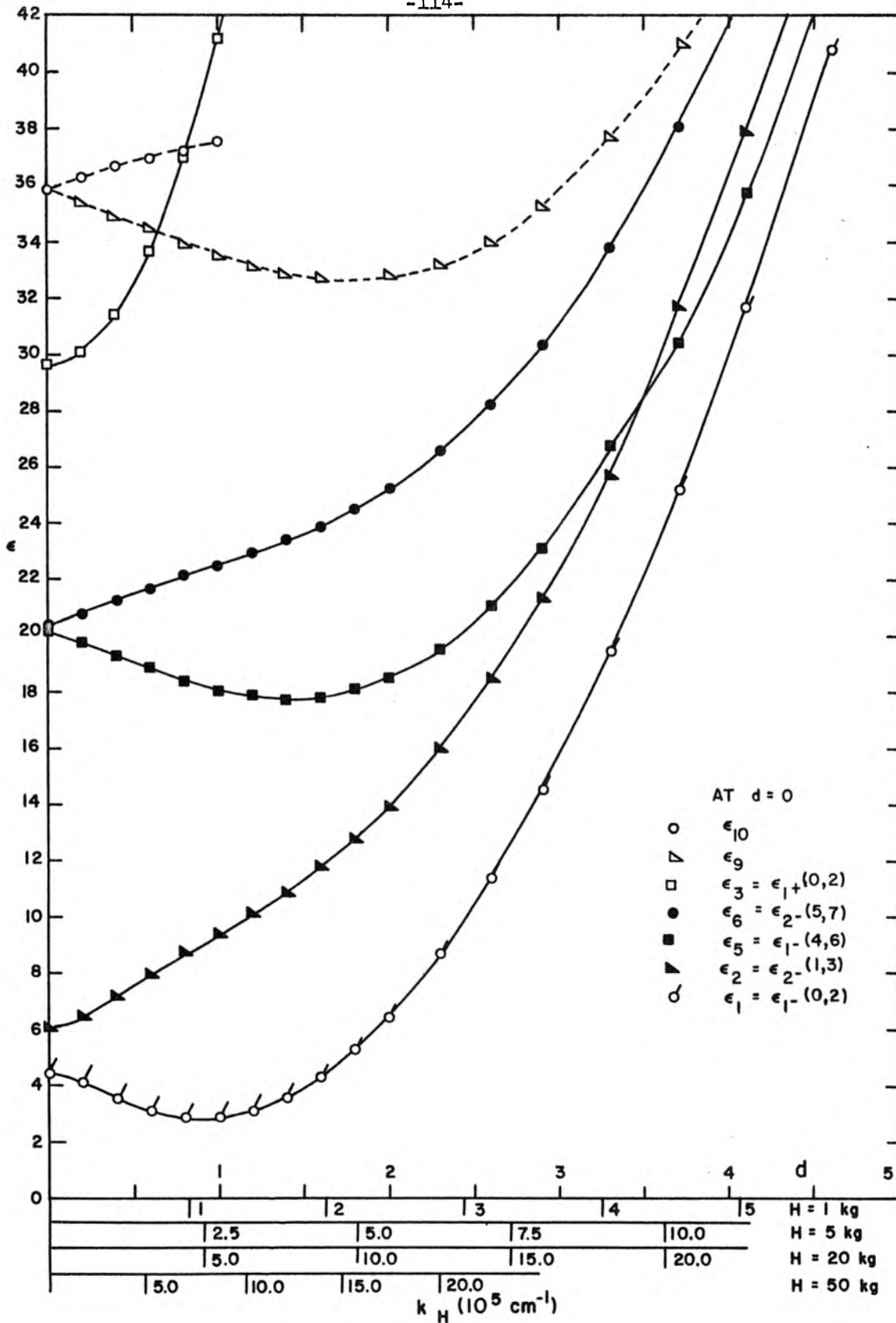


Fig. 4.14 Energy Sub-Bands Resulting from the Solution of Equation 4.1.10 (12×12 Determinant) for Ge

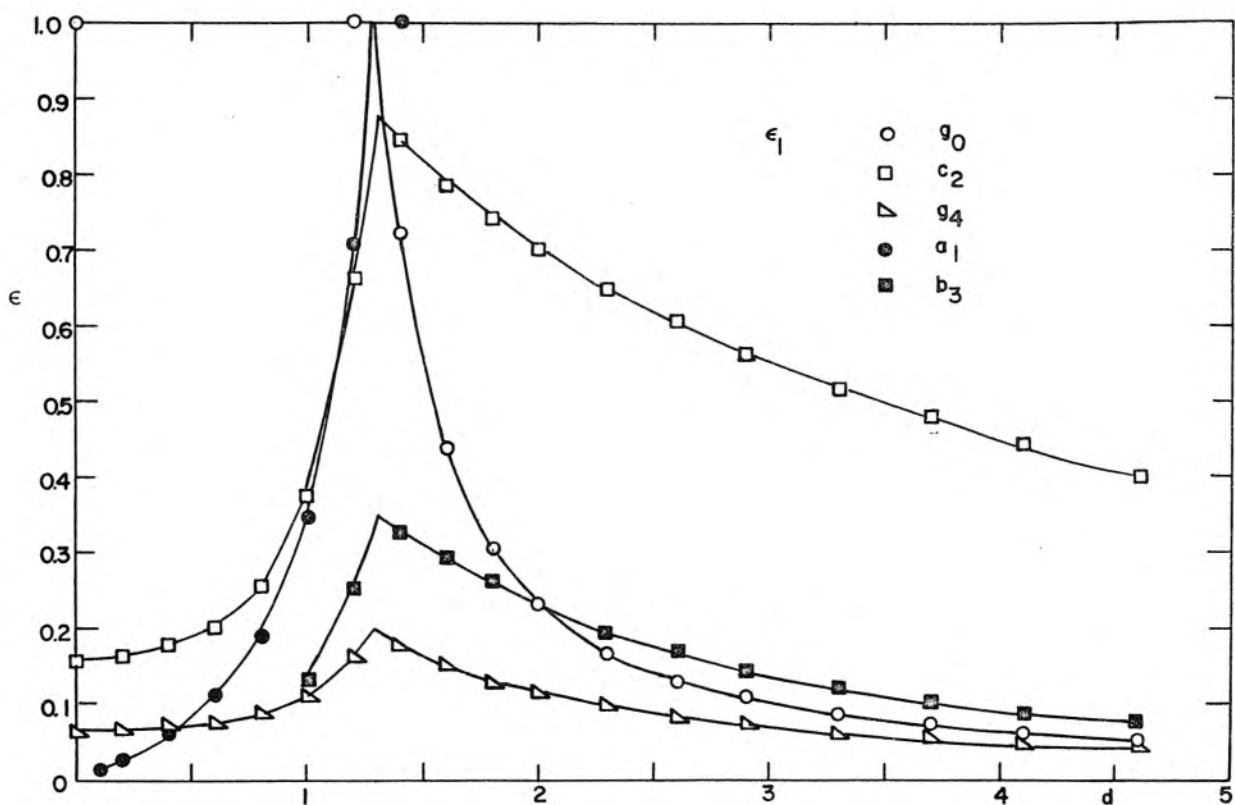
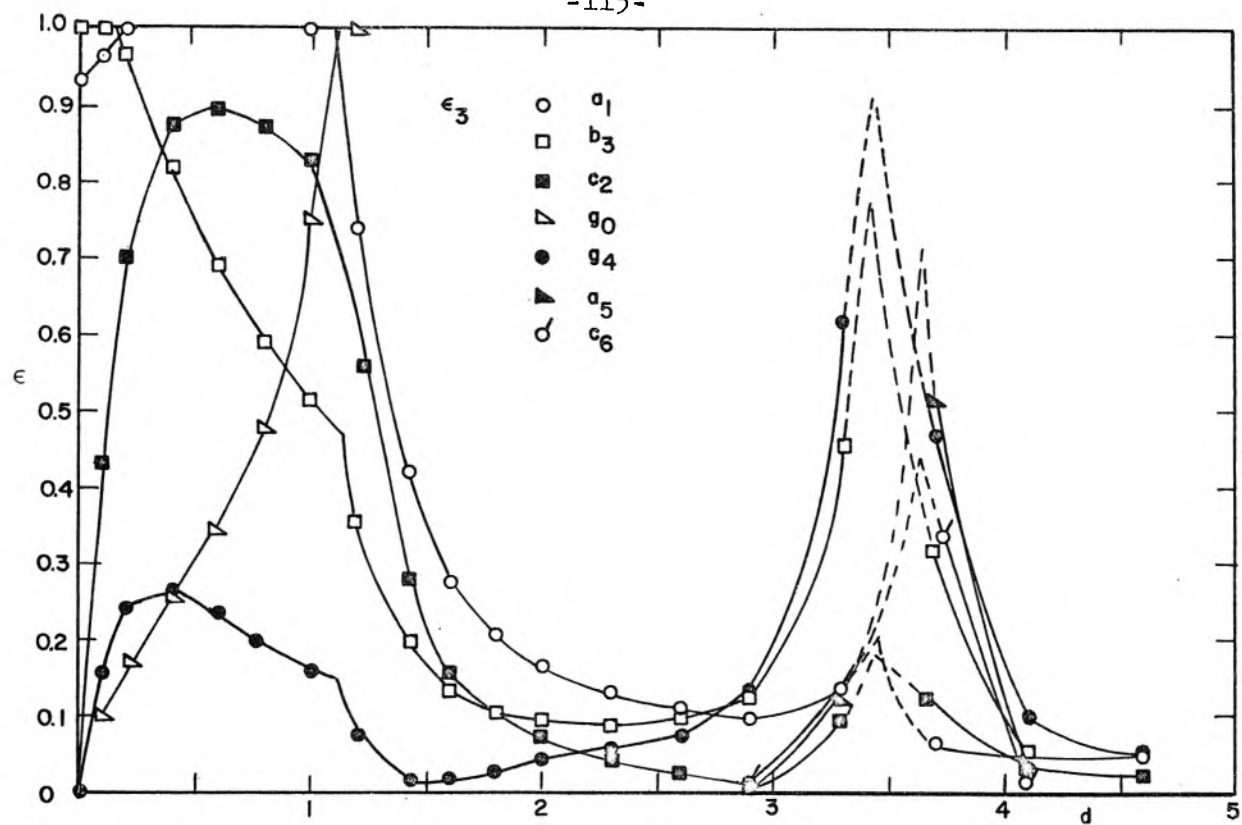


Fig. 4.15 Wave Function Expansion Coefficients for the ϵ_1 ($\epsilon_{2+}(0)$ at $d=0$) and ϵ_3 ($\epsilon_1 - (1,3)$ at $d=0$) Energy Levels Resulting from the Solution of Equation 4.1.7 (13×13 Determinant) for Ge

occurs whenever one level "crosses" another. (Observe peaks in values of certain coefficients at $d \approx 3.45$ and $d \approx 3.65$). In most cases whenever any two levels approach each other very closely and seem to cross over, their identity past such a region can be established only by looking at the leading coefficients in the eigenfunction expansions for the corresponding levels. This has been done in several cases in Figures 4.11 through 4.14.

In general, coupling between the heavy and the light hole levels seems to decrease as d increases and as the quantum numbers associated with them increase. Mathematically the former is due simply to the relative decrease in importance of the δ terms as d increases, while the latter is due to the fact that the heavy and light hole eigenvalues which coincide in energy come from the basic 4×4 blocks which are further removed from each other as quantum numbers increase. A simple physical reason for this can also be given: classically, when the orbit of an orbiting light hole (m_1) coincides with that of an orbiting heavy hole (m_2) we have, employing standard symbols:

$$\frac{1}{2} m_1 \omega_1^2 r_1^2 = \frac{1}{2} m_2 \omega_2^2 r_2^2$$

or

$$\frac{r_1}{r_2} = \sqrt{\frac{m_1}{m_2}}$$

from which $r_2 - r_1 = r_1 \left(\sqrt{\frac{m_2}{m_1}} - 1 \right) \sim \sqrt{E}$. Thus as energy increases the difference in the radii of the light hole and the heavy hole orbits increases, decreasing the interaction between them.

Because at large d $\delta = 0$ is such an excellent approximation, no

TABLE 4.4

WAVE FUNCTION EXPANSION COEFFICIENTS

for Ge at $d = 4.1$

		$\phi_{3/2}^{(3/2)}$										$\phi_{-1/2}^{(3/2)}$										
		a_0	a_1	a_2	a_3	a_4	a_5	a_6	a_7	a_8	a_9	b_0	b_1	b_2	b_3	b_4	b_5	b_6	b_7			
ϵ_{1-}	(0,1)	1.000				-.0356								.0540								
	(1,2)		1.000												.0876							
	(2,3)			1.000				-.0658								.1163						
	(3,4)				1.000												.1400					
	(4,5)					1.000				-.0979				.1474				.1557				
	(5,6)		.1012				1.000				-.1144				.3476				.1515			
ϵ_{1+}	(1)			.1100								-.3614				.1169						
	(0)											-.1422										
	(0,1)	.3353											-.2022									
	(1,2)		.4611											-.2489								
	(2,3)			.5521											-.2892							
	(3,4)				.6257											-.3232						
		$\phi_{1/2}^{(3/2)}$										$\phi_{-3/2}^{(3/2)}$										
		c_0	c_1	c_2	c_3	c_4	c_5	c_6	c_7	c_8	c_9	c_{10}	g_0	g_1	g_2	g_3	g_4	g_5	g_6	g_7	g_8	g_9
ϵ_{1-}	(0,1)		-.3248																			
	(1,2)			-.4408									-.0632									
	(2,3)				-.5212									-.1087								
	(3,4)					-.5855									-.1733							
	(4,5)						-.6421									-.2899				.0818		
	(5,6)							-.7037					.0948				-.5822				.1071	
ϵ_{1+}	(1)																					
	(0)	1.000				.0020								1.000					-.1524			.0176
	(0,1)		1.000												.0099							
	(1,2)			1.000												.0150						
	(2,3)				1.000												.0189					
	(3,4)					1.000												.0221				
							1.000												.0248			

Table 4.4 Cont'd.

[illegible]

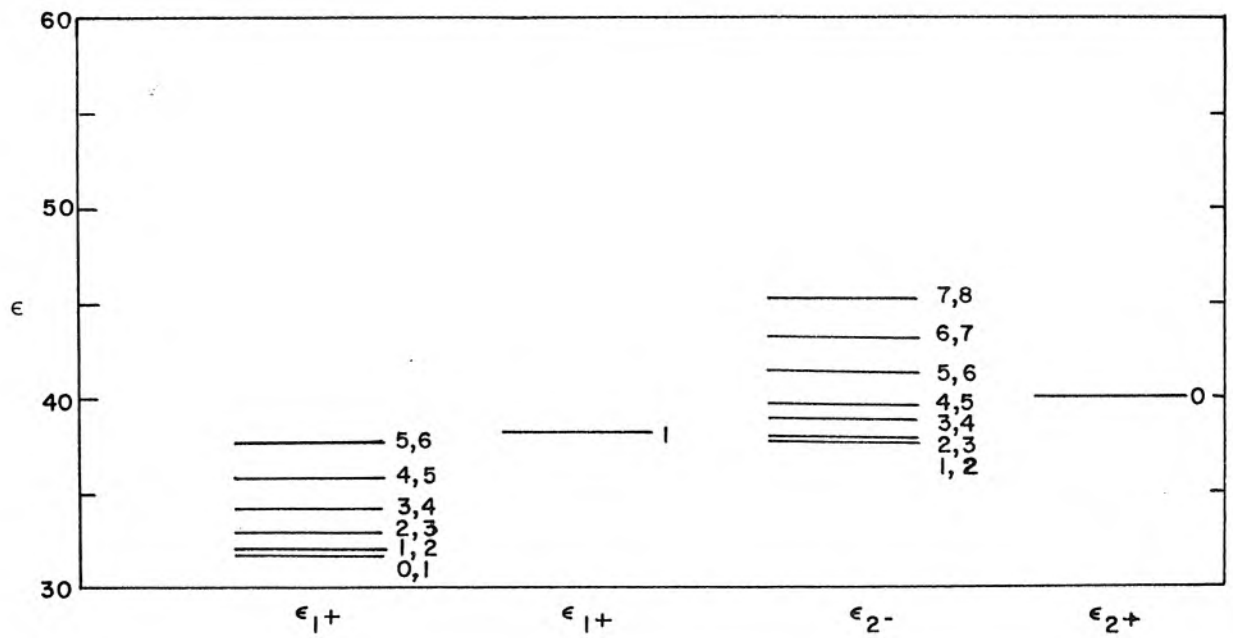


Fig. 4.16 London Levels in Ge at $d = 4.1$ for H in the [001] Direction

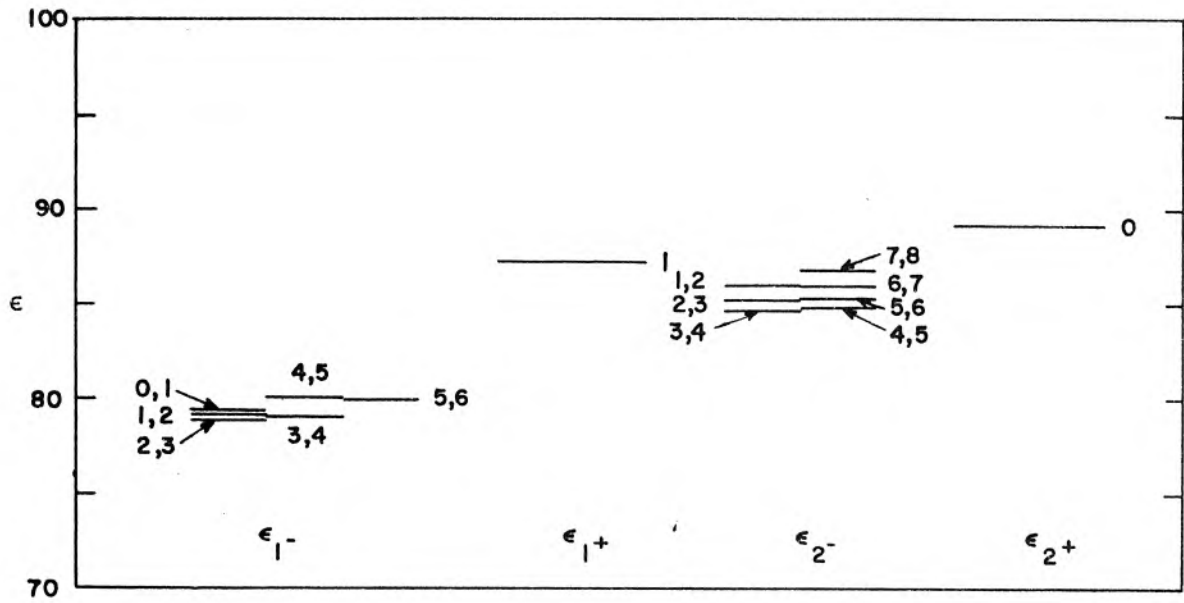


Fig. 4.17 Landau Levels in Ge at $d = 6.3$ for H in the $[001]$ Direction

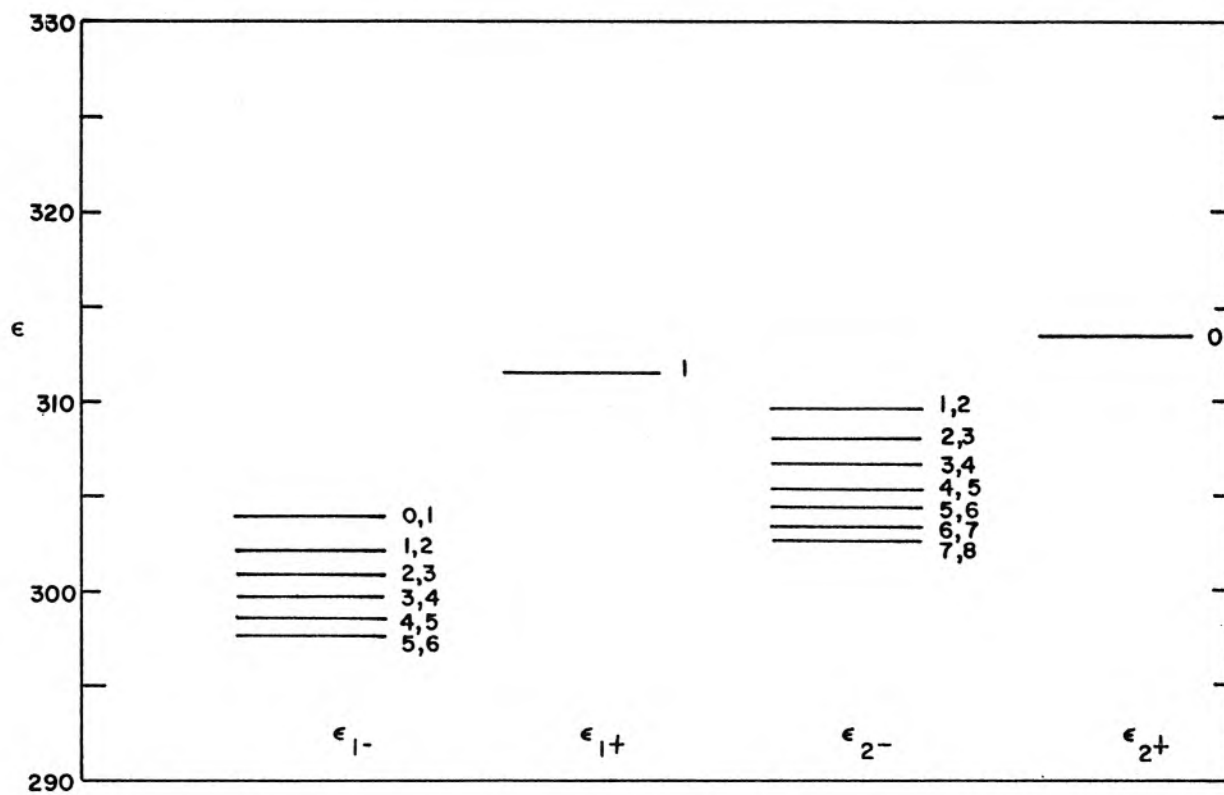


Fig. 4.18 Landau Levels in Ge at $d = 12.0$ for H in the $[001]$ Direction

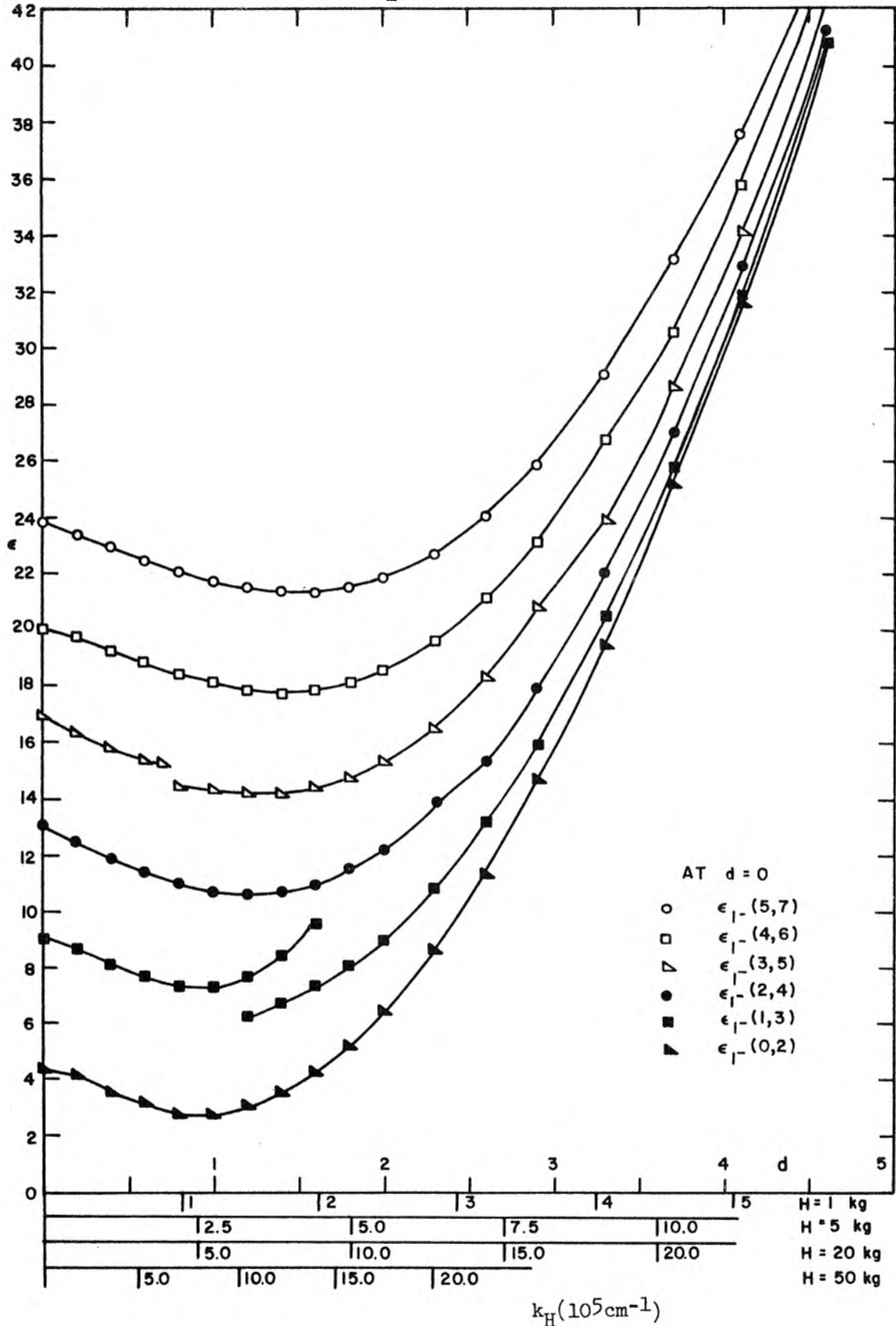


Fig. 4.19 Energy Sub-Bands Belonging to the ϵ_{1-} Ladder in Ge for H in the $[001]$ Direction

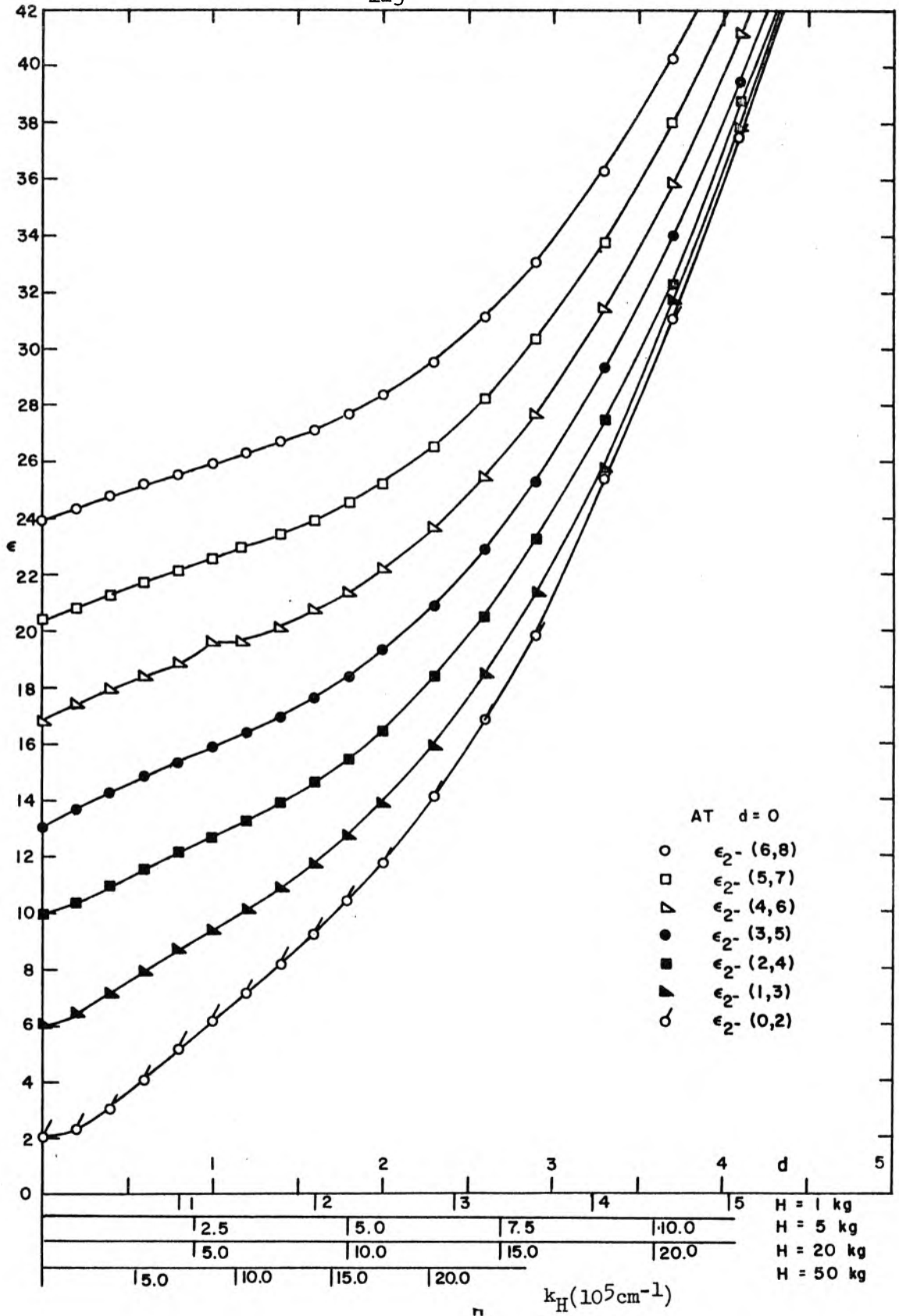


Fig. 4.20 Energy Sub-Bands Belonging to the ϵ_2^- Ladder in Ge for H in the $[001]$ Direction

plots have been made for $d > 5$ for the complete Ge problem.

The rule given on page 110 governing the change in the composition of the eigenfunctions as d increases still holds in the present case as it did in the case of $\delta = 0$, which is demonstrated in Table 4.4.

Although when $d \neq 0$ transitions can occur between all four ladders with relatively high degree of probability in some cases, it is still convenient to classify the various levels and plot them according to the ladders. This has been done for the heavy holes in Figures 4.19 and 4.20. In general, it can be said that the first order transitions take place between the adjoining levels.

It should be noted that, judging by the curvatures of the $\epsilon_{1+}(0)$ and the $\epsilon_{2+}(0)$ levels, their effective mass is much larger than that of the light holes, although they are assigned to the light hole ladders by Luttinger (2).

4.3 Landau Levels as Functions of k_H in the Valence Band of Si

Qualitatively the behavior of the Landau levels in the valence band of Si is similar to that in Ge. However, as can be seen from the plots in Figures 4.21 through 4.24 the couplings between levels are much stronger and therefore the levels are so strongly mixed--especially at low values of d and low quantum numbers, that the general pattern discussed in Section 4.2 is not always easily recognizable. This accounts for the rather confused appearance of the heavy hole ladder plots in Figs. 4.25 and 4.26. Here the levels at finite values of d were identified as belonging to a certain ladder defined by the levels at $d=0$ by inspecting the coefficients in the eigenfunction expansions. One such set of coefficients for $d=4.1$ is shown in Table 4.5. As is evident from the

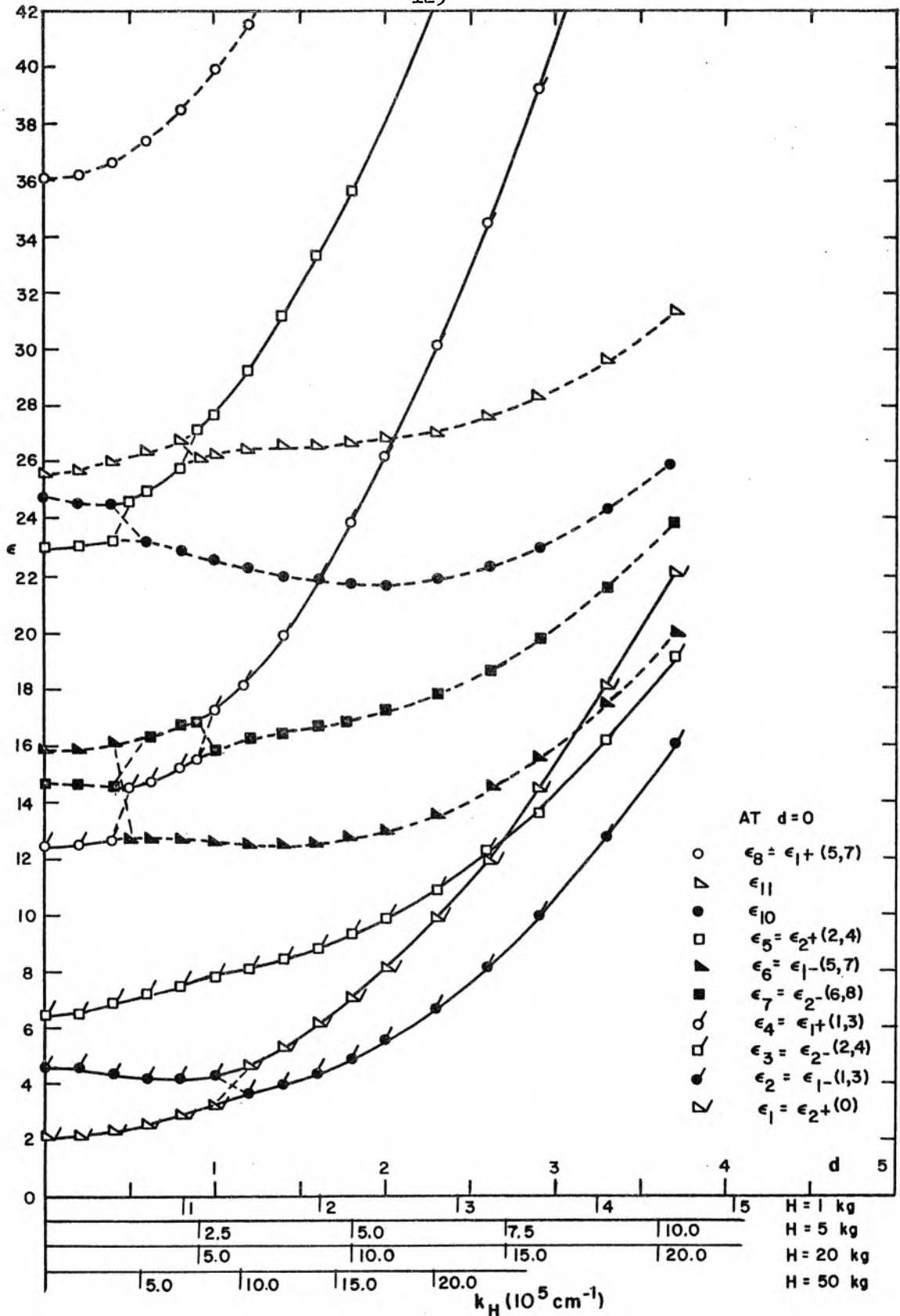


Fig. 4.21 Energy Sub-Bands Resulting from the Solution of Equation 4.1.7 (13x13 Determinant) for Si

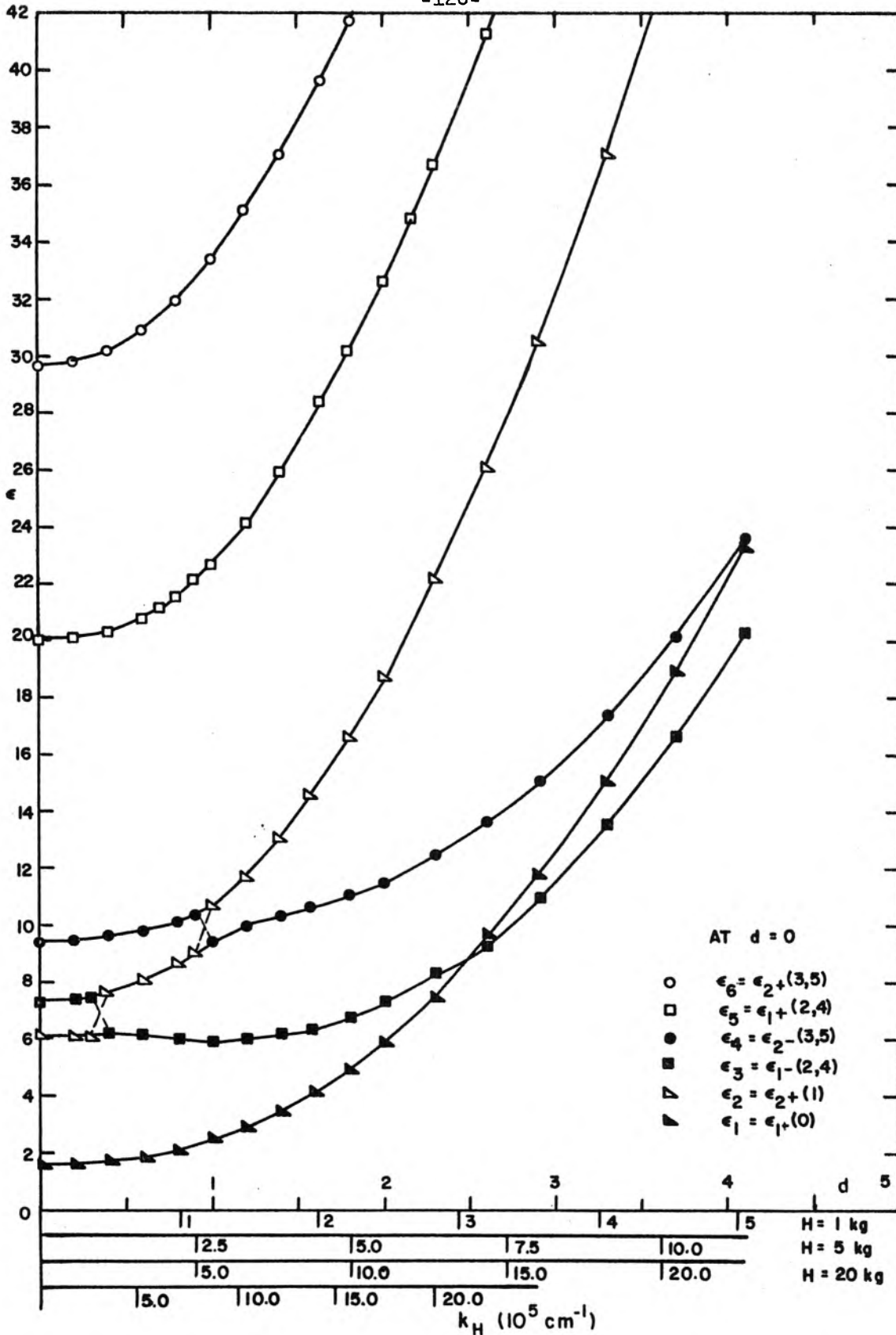


Fig. 4.22 Energy Sub-Bands Resulting from the Solution of Equation 4.1.8 (14×14 Determinant) for Si

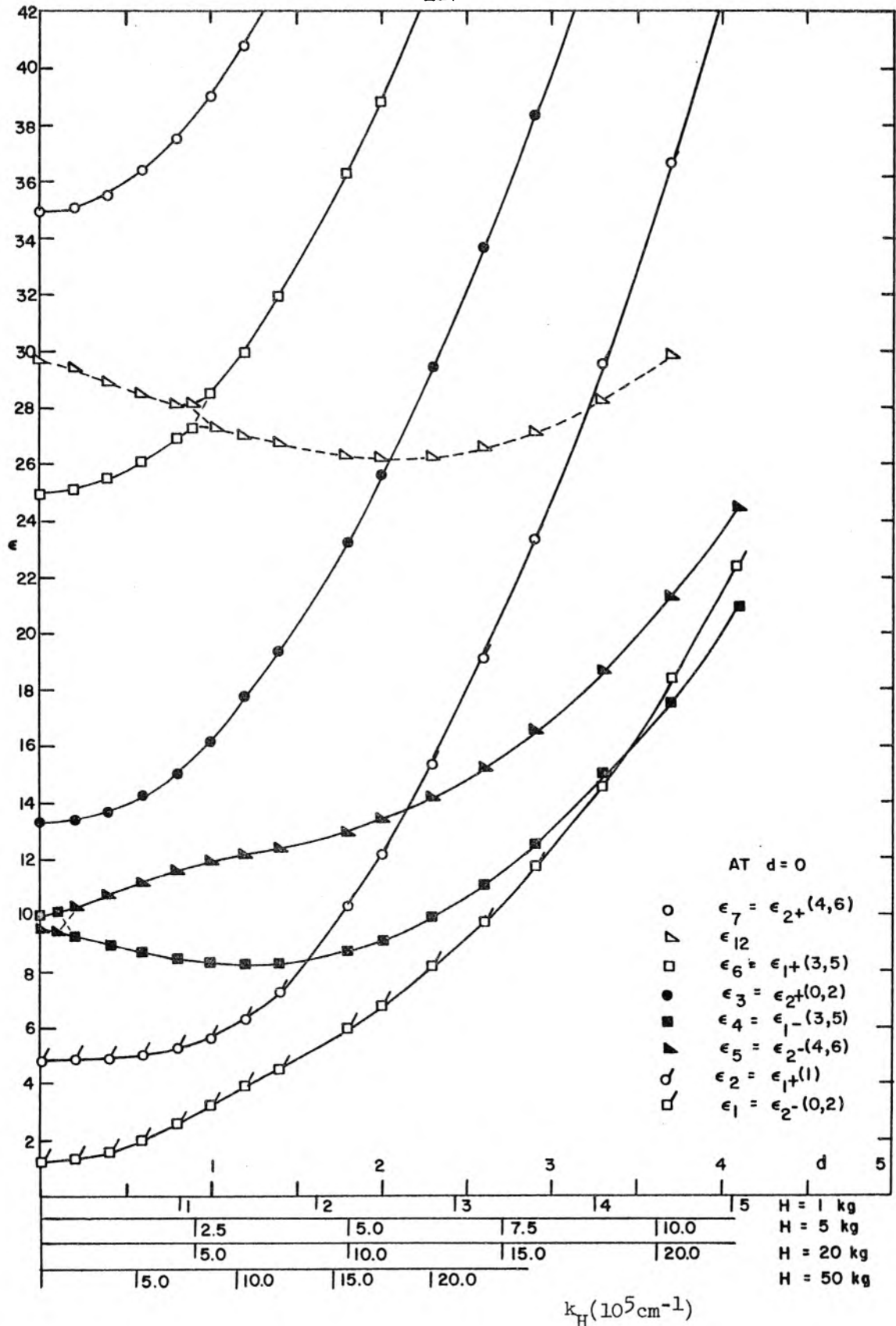


Fig. 4.23 Energy Sub-Bands Resulting from the Solution of Equation 4.1.9 (15x15 Determinant) for Si

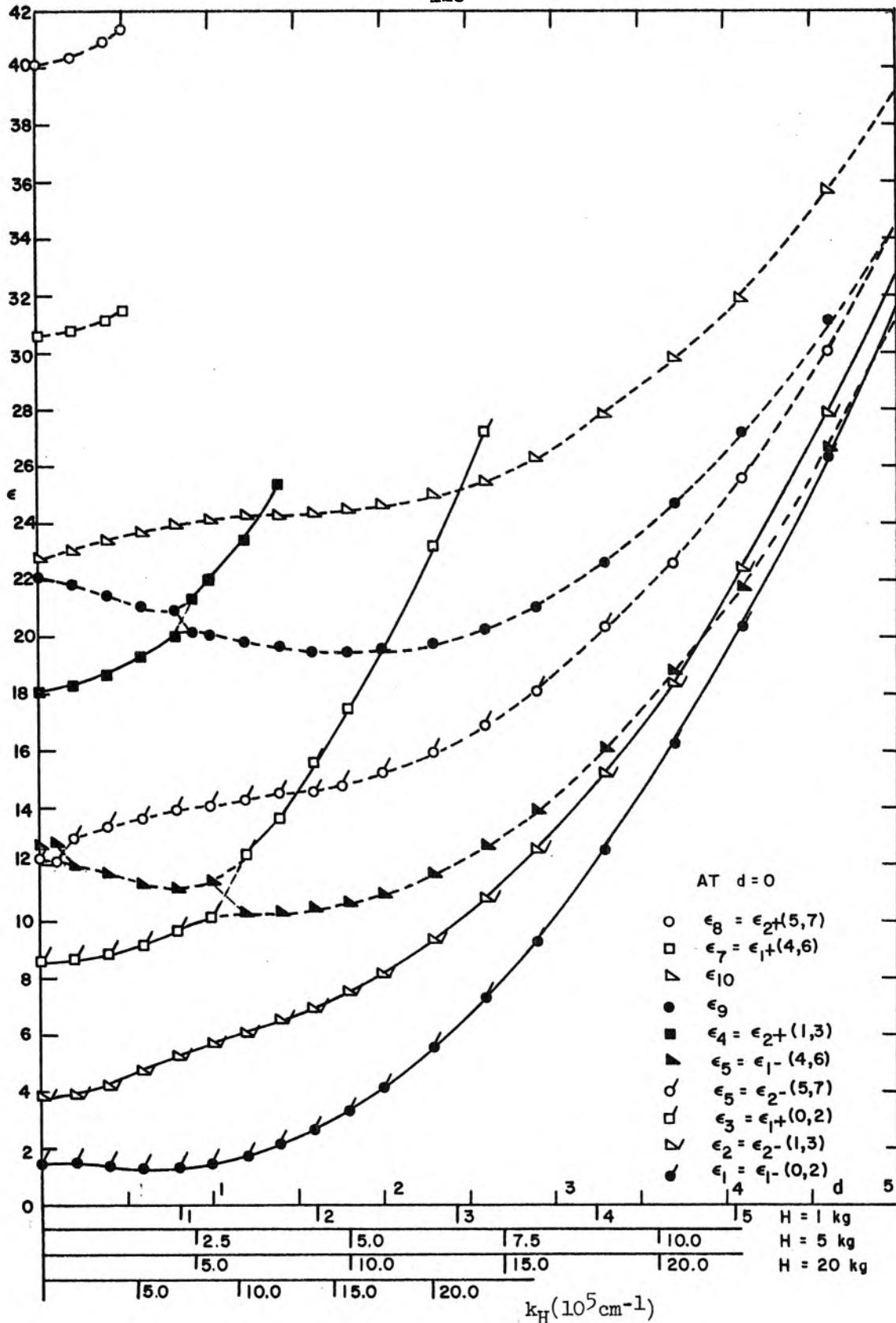


Fig. 4.24 Energy Sub-Bands Resulting from the Solution of Equation 4.1.10 (12x12 Determinant) for Si

TABLE 4.5

WAVE FUNCTION EXPANSION COEFFICIENTS

for Si at $d = 4.1$

		$\phi_{3/2}^{(3/2)}$										$\phi_{-1/2}^{(3/2)}$						
		a_0	a_1	a_2	a_3	a_4	a_5	a_6	a_7	a_8	a_9	b_0	b_1	b_2	b_3	b_4	b_5	b_6
ϵ_{1-}	(0,1)	1.000				-.0805												
	(1,2)		1.000															
	(2,3)			1.000														
	(3,4)				1.000													
	(4,5)	.1627				1.000				-.1100				.3060			.0998	
ϵ_{1+}	(1)			.2185														
	(0)											-.6130					.5640	
	(0,1)	.4780											-.1122					
	(1,2)		.6022											-.1548				
	(2,3)			.6778											-.1874			
	(3,4)				.7331											-.2146		
	(4,5)					.7767											-.2385	
																		-.2599
		$\phi_{1/2}^{(3/2)}$										$\phi_{-3/2}^{(3/2)}$						
		c_0	c_1	c_2	c_3	c_4	c_5	c_6	c_7	g_0	g_1	g_2	g_3	g_4	g_5	g_6	g_7	
ϵ_{1-}	(0,1)		-.4776															
	(1,2)			-.5964						-.0812								
	(2,3)				-.6703						-.1401				.0912			
	(3,4)					-.7280						-.2377				.1084		
	(4,5)						-.7925						-.4892				.1465	
ϵ_{1+}	(1)																	
	(0)	1.000							-.1330		1.000					-.6535		
	(0,1)		1.000									.0212						
	(1,2)			1.000									.0286					
	(2,3)				1.000									.0345				
	(3,4)					1.000									.0394			
	(4,5)						1.000						-.0489					
								1.000						-.0581				

Table 4.5 Cont'd.

$\phi_{3/2}^{(3/2)}$														$\phi_{-1/2}^{(3/2)}$													
		a_0	a_1	a_2	a_3	a_4	a_5	a_6	a_7	b_0	b_1	b_2	b_3	b_4	b_5	b_6											
ϵ_{2-}	(1,2)				.2456										.1377												
	(2,3)					.5086					- .7275						.1714										
	(3,4)						.5877					- .8125															
	(4,5)							.3064					- .7668														

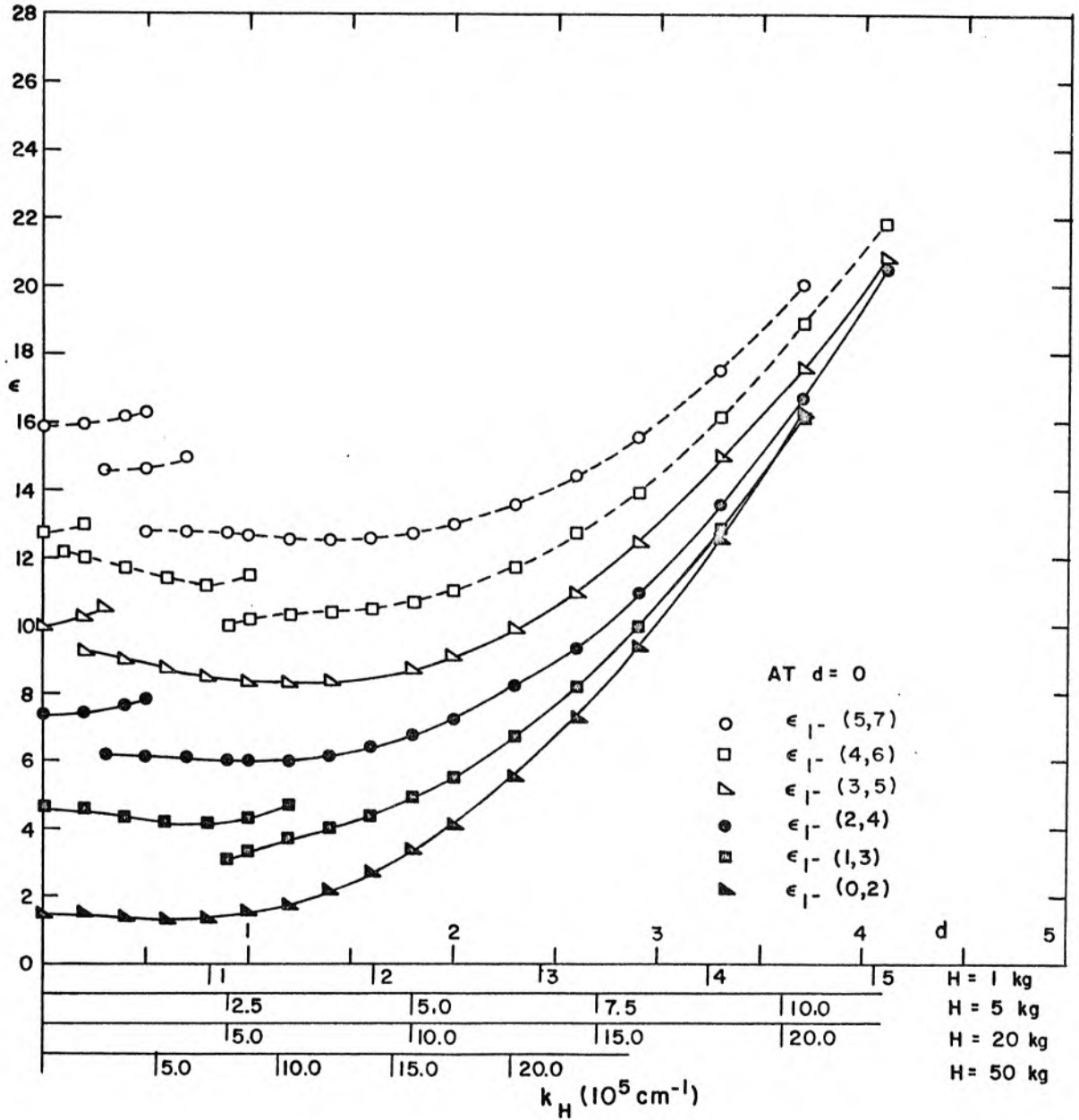


Fig. 4.25 Energy Sub-Bands Belonging to the ϵ_{1-} Ladder in Si for H in the $[001]$ Direction

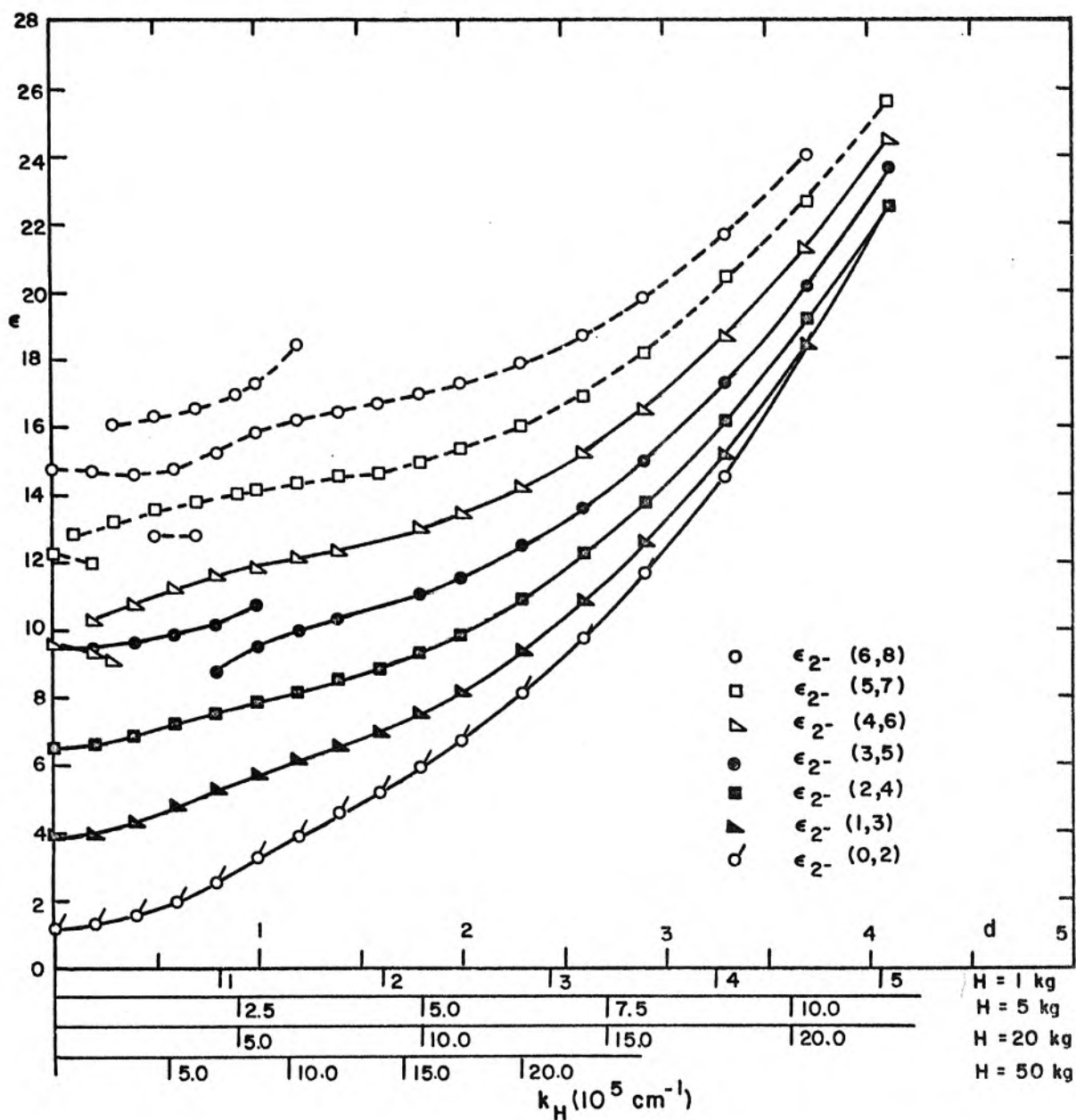


Fig. 4.26 Energy sub-Bands Belonging to the ϵ_{2-} Ladder in Si for H in the [001] Direction

plots and the table, the levels assume a more or less "normal" character as d increases.

V. VALENCE BAND LANDAU LEVEL STRUCTURE OF Ge AND Si FOR
IN THE [101] AND THE [111] DIRECTIONS

In this section the assumption of the decoupling of the V_1 and V_2 bands from the V_3 band will be retained. As has been shown, this assumption is a very good one in the case of Ge and is acceptable in the case of Si at low magnetic fields. This assumption will permit the use of certain canonical transformations suggested by Luttinger (2), which simplify the operator matrices obtained in the course of the solution of equation 2.2.18 by perturbation theory with \hat{k} given by 2.2.17. Thus following Luttinger, the matrix $||V_{1j}^{4 \times 4}||$ of equation 4.1.1 may be written as

$$||V^{4 \times 4}|| = \frac{\hbar^2}{m} \left\| -\frac{1}{4}(3\ell' + \mu') \frac{\hat{k}^2}{2} + \frac{1}{6}(\ell' - \mu')(\hat{k}_x^2 J_x^2 + \hat{k}_y^2 J_y^2 + \hat{k}_z^2 J_z^2) + \right. \\ \left. + \frac{1}{3} \nu \left(\left\{ \hat{k}_x \hat{k}_y \right\} \left\{ J_x J_y \right\} + \left\{ \hat{k}_y \hat{k}_z \right\} \left\{ J_y J_z \right\} + \left\{ \hat{k}_z \hat{k}_x \right\} \left\{ J_z J_x \right\} \right) + \right. \\ \left. + \frac{e}{\hbar c} \kappa J \cdot \mathcal{H} \right\| \quad (5.0.1)$$

where J 's are the $\frac{3}{2}$ angular momentum matrices.

Now, according to Luttinger whenever the transformation 2.2.17 is used one should also set

$$\left\| \begin{array}{c} J_x \\ J_y \\ J_z \end{array} \right\| = ||A|| \left\| \begin{array}{c} J_1 \\ J_2 \\ J_3 \end{array} \right\| \quad (5.0.2)$$

where

$$J_1 = \begin{vmatrix} 0 & 0 & \sqrt{3}/2 & 0 \\ 0 & 0 & 1 & 3/2 \\ \sqrt{3}/2 & 1 & 0 & 0 \\ 0 & 3/2 & 0 & 0 \end{vmatrix} \quad (5.0.3)$$

$$J_2 = \begin{vmatrix} 0 & 0 & -i\sqrt{3}/2 & 0 \\ 0 & 0 & i & -i\sqrt{3}/2 \\ i\sqrt{3}/2 & -i & 0 & 0 \\ 0 & i\sqrt{3}/2 & 0 & 0 \end{vmatrix} \quad (5.0.4)$$

$$J_3 = \begin{vmatrix} 3/2 & 0 & 0 & 0 \\ 0 & -1/2 & 0 & 0 \\ 0 & 0 & 1/2 & 0 \\ 0 & 0 & 0 & -3/2 \end{vmatrix} \quad (5.0.5)$$

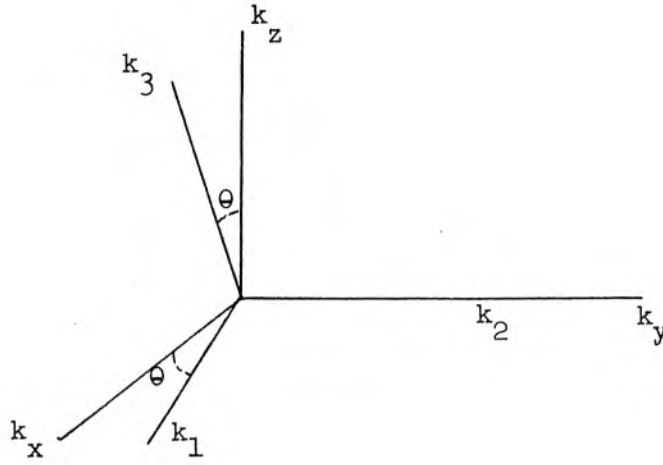
5.1 Magnetic Field in the [101] Direction

Considering first the case of the magnetic field in the [010] plane, one writes

$$\begin{aligned} \hat{k}_x &= c\hat{k}_1 + s\hat{k}_3 \\ \hat{k}_y &= \hat{k}_z \\ \hat{k}_z &= -s\hat{k}_1 + c\hat{k}_3 \end{aligned} \quad (5.1.1)$$

and

$$\begin{aligned} J_x &= cJ_1 + sJ_3 \\ J_y &= J_2 \\ J_z &= -sJ_1 + cJ_3 \end{aligned} \quad (5.1.2)$$



where $s = \sin \theta$ and $c = \cos \theta$.

Substitution of equations 5.1.1 and 5.1.2 into 5.0.1 gives

$$\begin{aligned}
 \|V^{4x4}\| &= \frac{\hbar^2}{m} \left\| -\frac{1}{4} (3\ell' + \mu') \frac{\hat{k}^2}{2} + \right. \\
 &+ \frac{1}{6} \left[\{[(\ell' - \mu')(s^4 + c^4) + 2\nu s^2 c^2] \hat{k}_1^2 + 2s^2 c^2 (\ell' - \mu' - \nu) \hat{k}_3^2 + \right. \\
 &+ 2sc(c^2 - s^2)(\ell' - \mu' - \nu) \hat{k}_1 \hat{k}_3 \} J_1^2 + (\ell' - \mu') k_2^2 J_2^2 + \\
 &+ \left\{ 2s^2 c^2 (\ell' - \mu' - \nu) k_1^2 + [(\ell' - \mu')(s^4 + c^4) + 2\nu s^2 c^2] \hat{k}_3^2 - \right. \\
 &- 2sc(c^2 - s^2)(\ell' - \mu' - \nu) \hat{k}_1 \hat{k}_3 \} J_3^2 + \\
 &+ 2\nu \left\{ \hat{k}_1 \hat{k}_2 \right\} \left\{ J_1 J_2 \right\} + 2\nu \left\{ \hat{k}_2 \hat{k}_3 \right\} \left\{ J_2 J_3 \right\} + \\
 &+ \left\{ 2sc(c^2 - s^2)(\ell' - \mu' - \nu) \hat{k}_1^2 - 2sc(c^2 - s^2)(\ell' - \mu' - \nu) \hat{k}_3^2 + \right. \\
 &+ \left. [(\ell' - \mu') 8c^2 s^2 + 2\nu (c^2 - s^2)^2] \hat{k}_1 \hat{k}_3 \right\} \left\{ J_1 J_3 \right\} \Big] + \frac{e\hbar}{\hbar c} \kappa J_3 \Big\| \quad (5.1.3)
 \end{aligned}$$

If the energy bands are now assumed to be spherically symmetric, one obtains

$$\begin{aligned} ||V^{4x4}|| = & \frac{\hbar^2}{m} \left\| -\frac{1}{4} (3\ell' + \mu') \frac{\hat{k}^2}{2} + \frac{1}{6} \nu (\hat{k}_1^2 J_1^2 + \hat{k}_2^2 J_2^2 + \hat{k}_3^2 J_3^2) + \right. \\ & + \frac{1}{2} \nu \left(\left\{ \hat{k}_1 \hat{k}_2 \right\} \left\{ J_1 J_2 \right\} + \left\{ \hat{k}_2 \hat{k}_3 \right\} \left\{ J_2 J_3 \right\} + \left\{ \hat{k}_1 \hat{k}_3 \right\} \left\{ J_1 J_3 \right\} \right) + \\ & \left. + \frac{e\hbar}{\hbar c} \kappa J_3 \right\| \quad (5.1.4) \end{aligned}$$

which should have been expected since for symmetrical bands the direction of the magnetic field is immaterial.

Consider now the special case of $\theta = 45^\circ$, i.e., \mathcal{H} in the [101] direction. Then $s = c = 1/\sqrt{2}$ and

$$\begin{aligned} ||V^{4x4}|| = & \frac{\hbar^2}{m} \left\| -\frac{1}{4} (3\ell' + \mu') \frac{\hat{k}^2}{2} + \frac{1}{6} \left[\left(\frac{\ell' - \mu' + \nu}{2} \hat{k}_1^2 + \frac{\ell' - \mu' - \nu}{2} \hat{k}_3^2 \right) J_1^2 + \right. \right. \\ & + (\ell' - \mu') \hat{k}_2^2 J_2^2 + \left. \left(\frac{\ell' - \mu' - \nu}{2} \hat{k}_1^2 + \frac{\ell' - \mu' + \nu}{2} \hat{k}_3^2 \right) J_3^2 + \right. \\ & \left. \left. + 2\nu \left\{ \hat{k}_1 \hat{k}_2 \right\} \left\{ J_1 J_2 \right\} + 2\nu \left\{ \hat{k}_2 \hat{k}_3 \right\} \left\{ J_2 J_3 \right\} + 2(\ell' - \mu') \left\{ \hat{k}_1 \hat{k}_3 \right\} \left\{ J_1 J_3 \right\} \right] \right. \\ & \left. + \frac{e\hbar}{\hbar c} \kappa J_3 \right\| \quad (5.1.5) \end{aligned}$$

$||V^{4x4}||$ may now be rewritten in terms of the raising and lowering operators using the following equalities:

$$\begin{aligned} \hat{k}_1 &= -\frac{1}{\sqrt{2}} \sqrt{\frac{|e|\hbar}{\hbar c}} (a^+ + a) \\ \hat{k}_2 &= \frac{1}{\sqrt{2}} \sqrt{\frac{|e|\hbar}{\hbar c}} (a^+ - a) \end{aligned} \quad (5.1.6)$$

$$\begin{aligned}
 \{\hat{k}_1 \hat{k}_2\} &= \frac{|e|\mathcal{H}}{\hbar c} \frac{1}{2i} (a^{+2} - a^2) \\
 \hat{k}_1^2 &= \frac{1}{2} \frac{|e|\mathcal{H}}{\hbar c} (2a^+ a + 1 + a^2 + a^{+2}) \\
 \hat{k}_2^2 &= \frac{1}{2} \frac{|e|\mathcal{H}}{\hbar c} (2a^+ a + 1 - a^2 - a^{+2}) \\
 \hat{k}_3 &= \sqrt{\frac{|e|\mathcal{H}}{\hbar c}} d
 \end{aligned} \tag{5.1.6}$$

The result is:

$$\begin{aligned}
 ||V^{4 \times 4}|| &= \frac{\hbar |e|\mathcal{H}}{mc} \left\| \left(-\frac{3\ell' + \mu'}{4} + \frac{\ell' - \mu' + \nu}{12} J_1^2 + \frac{\ell' - \mu'}{6} J_2^2 + \frac{\ell' - \mu' - \nu}{12} J_3^2 \right) (a^+ a + \frac{1}{2}) - \right. \\
 &\quad - \frac{3\ell' + \mu'}{4} \frac{d^2}{2} + \\
 &\quad + \frac{a^2 + a^{+2}}{2} \left(\frac{\ell' - \mu' + \nu}{12} J_1^2 - \frac{\ell' - \mu'}{6} J_2^2 + \frac{\ell' - \mu' - \nu}{12} J_3^2 \right) + \\
 &\quad + \frac{\ell' - \mu' - \nu}{12} d^2 J_1^2 + \frac{\ell' - \mu' + \nu}{12} d^2 J_3^2 + \\
 &\quad + i \frac{\nu}{6} (a^2 - a^{+2}) \{J_1 J_2\} - i \frac{\sqrt{2}}{6} \nu (a - a^+) d \{J_2 J_3\} - \\
 &\quad \left. - \frac{\sqrt{2}}{6} (\ell' - \mu')(a^+ + a) d \{J_1 J_3\} + \kappa J_3 \right\}
 \end{aligned} \tag{5.1.7}$$

If $\ell' - \mu' = \nu$ (spherical symmetry) and $d = 0$ (i.e., $k_H = 0$) are assumed Luttinger's equation 70 is obtained.

Substitution of equations 5.0.3, 5.0.4, and 5.0.5 into 5.1.7 gives

$$\begin{aligned}
\|v^{4x^4}\| = \frac{\hbar |e| \mathcal{H}}{mc} & \left\| \begin{array}{lll}
-\frac{1}{8}[(3\ell'+5\mu'+\nu)(a^+a+\frac{1}{2}) + & \frac{\sqrt{3}}{24}[\frac{1}{2}(2\nu+3\beta_1)a^2 - & -\frac{1}{6}\sqrt{\frac{3}{2}}[\beta_1 a + \delta_1 a^+] d \\
+(4\mu'+\delta_1)d^2 - \frac{1}{2}\delta_1(a^2+a^{+2})] + \frac{3}{2}\kappa & -\delta_1(a^+a+\frac{1}{2}-d^2-\frac{3}{2}a^{+2})] & 0 \\
\\
\frac{\sqrt{3}}{24}[\frac{1}{2}(2\nu+3\beta_1)a^{+2} - & -\frac{1}{8}[\frac{7\ell'+17\mu'-3\nu}{3}(a^+a+\frac{1}{2}) + \frac{5\ell'+7\mu'+3\nu}{3}d^2 + & 0 \\
-\delta_1(a^+a+\frac{1}{2}-d^2-\frac{3}{2}a^2)] & +\frac{1}{2}\delta_1(a^2+a^{+2})] - \frac{1}{2}\kappa & \frac{1}{6}\sqrt{\frac{3}{2}}[\beta_1 a + \delta_1 a^+] d \\
\\
-\frac{1}{6}\sqrt{\frac{3}{2}}[\beta_1 a^+ + \delta_1 a] d & 0 & -\frac{1}{8}[\frac{7\ell'+17\mu'-3\nu}{3}(a^+a+\frac{1}{2}) + \frac{5\ell'+7\mu'+3\nu}{3}d^2 + \\
& & +\frac{1}{2}\delta_1(a^2+a^{+2})] + \frac{1}{2}\kappa \\
\\
0 & \frac{1}{6}\sqrt{\frac{3}{2}}[\beta_1 a^+ + \delta_1 a] d & -\frac{\sqrt{3}}{24}[\frac{1}{2}(2\nu+3\beta_1)a^2 - \\
& & -\delta_1(a^+a+\frac{1}{2}-d^2-\frac{3}{2}a^{+2})] \\
\\
& & -\frac{1}{8}[(3\nu'+5\mu'+)(a^+a+\frac{1}{2}) + \\
& & +(4\mu'+\delta_1)d^2 - \frac{1}{2}\delta_1(a^2+a^{+2})] - \frac{3}{2}\kappa
\end{array} \right\|
\end{aligned}$$

(5.1.8)

where the definitions $(\ell' - \mu' - \nu) = \delta_1$ and $(\ell' - \mu' + \nu) = \beta_1$ have been used.

Now if $d \rightarrow 0$ Goodman's (3) equation 5.13 is obtained except for some differences in signs. The differences are superficial and arise from the fact that Goodman's 5.13 has been derived for \mathcal{H} in the $[110]$ instead of the $[101]$ direction.

For purposes of computation let

$$- \frac{3\ell' + 5\mu' + \nu}{8} = \alpha'$$

$$- \frac{4\mu' + \delta_1}{8} = \eta'$$

$$\frac{\sqrt{3}}{48} (2\nu + 3\beta_1) = \beta^+$$

$$- \frac{7\ell' + 17\mu' - 3\nu}{24} = \zeta'$$

$$- \frac{5\ell' + 7\mu' + 3\nu}{24} = \eta^+$$

$$\frac{\delta_1}{16} = \delta'$$

$$- \frac{\sqrt{3}}{24} \delta_1 = \delta^+$$

$$- \frac{1}{6} \sqrt{\frac{3}{2}} \delta_1 = \delta^*$$

$$- \frac{1}{6} \sqrt{\frac{3}{2}} \beta_1 = \beta' \tag{5.1.9}$$

Then,

$$\begin{aligned}
||V^{4x4}|| = \frac{\hbar |e| \hbar}{mc} & \left| \begin{array}{cccc}
\alpha'(a^+a + \frac{1}{2}) + \eta'd^2 + & \beta^+a^2 + \delta^+(a^+a + & (\beta'a + \delta^*a^+)d & 0 \\
+\delta'(a^2 + a^{+2}) + \frac{3}{2}\kappa & + \frac{1}{2} - d^2 - \frac{3}{2}a^{+2}) & & \\
\beta^+a^{+2} + \delta(a^+a + & \zeta'(a^+a + \frac{1}{2}) + \eta^+d^2 - & 0 & -(\beta'a + \delta^*a^+)d \\
+ \frac{1}{2} - d^2 - \frac{3}{2}a^2) & -\delta'(a^2 + a^{+2}) - \frac{1}{2}\kappa & & \\
(\beta'a^+ + \delta^*a)d & 0 & \zeta'(a^+a - \frac{1}{2}) + \eta^+d^2 - & \beta^+a^2 + \delta^+(a^+a + \frac{1}{2} - \\
& & -\delta'(a^2 + a^{+2}) + \frac{1}{2}\kappa & - d^2 - \frac{3}{2}a^{+2}) \\
0 & -(\beta'a^+ + \delta^*a)d & \beta^+a^{+2} + \delta^+(a^*a + \frac{1}{2} - & \alpha'(a^+a + \frac{1}{2}) + \eta'd^2 + \\
& & -d^2 - \frac{3}{2}a^2) & + \delta'(a^2 + a^{+2}) - \frac{3}{2}\kappa
\end{array} \right|
\end{aligned}$$

-171-

(5.1.10)

Assuming the solution:

$$F = \begin{pmatrix} \sum_i a_i f_i \\ \sum_j b_j f_j \\ \sum_k c_k f_k \\ \sum_l g_l f_l \end{pmatrix} \quad (5.1.11)$$

to the equation $\| V_{ij}^{4 \times 4} \| F = E \quad \| I \| F$ one gets:

$$\begin{aligned}
\text{I} \quad & \sum_i \left\{ [\alpha'(i + \frac{1}{2}) + \eta' d^2 + \frac{3}{2} \kappa - \epsilon] f_i + \delta' [i(i-1)]^{1/2} f_{i-2} + \delta' [(i+1)(i+2)]^{1/2} f_{i+2} \right\} a_i + \\
& + \sum_j b_j \left\{ \beta^+ [j(j-1)]^{1/2} f_{j-2} + \delta^+ (j + \frac{1}{2} - d^2) f_j - \frac{3}{2} \delta^+ [(j+1)(j+2)]^{1/2} f_{j+2} \right\} + \\
& + \sum_k c_k \left\{ \beta' k^{1/2} f_{k-1} + \delta^* (k+1)^{1/2} f_{k+1} \right\} d = 0
\end{aligned}$$

$$\begin{aligned}
\text{II} \quad & \sum_i a_i \left\{ \beta^+ [(i+1)(i+2)]^{1/2} f_{i+2} + \delta^+ (i + \frac{1}{2} - d^2) f_i - \frac{3}{2} \delta^+ [i(i-1)]^{1/2} f_{i-2} \right\} + \\
& + \sum_j b_j \left\{ [\xi' (j + \frac{1}{2}) + \eta' d^2 - \frac{1}{2} \kappa - \epsilon] f_j - \delta' [j(j-1)]^{1/2} f_{j-2} - \delta' [(j+1)(j+2)]^{1/2} f_{j+2} \right\} - \\
& - \sum_\ell g_\ell \left\{ \beta' \ell^{1/2} f_{\ell-1} + \delta^* (\ell+1)^{1/2} f_{\ell+1} \right\} d = 0
\end{aligned}$$

(5.1.12)

$$\begin{aligned}
\text{III} \quad \sum_i a_i \left\{ \beta'(i+1)^{1/2} f_{i+1} + \delta^* i^{1/2} f_{i-1} \right\} d + \sum_k c_k \left\{ \left[\zeta'(k + \frac{1}{2}) + \eta^+ d^2 + \frac{1}{2} \kappa - \epsilon \right] f_k - \right. \\
\left. - \delta'[k(k-1)]^{1/2} f_{k-2} - \delta'[(k+1)(k+2)]^{1/2} f_{k+2} \right\} + \sum_\ell g_\ell \left\{ \beta^+[\ell(\ell-1)]^{1/2} f_{\ell-2} + \right. \\
\left. + \delta(\ell + \frac{1}{2} - d^2) f_\ell - \frac{3}{2} \delta[(\ell+1)(\ell+2)]^{1/2} f_{\ell+2} \right\} = 0
\end{aligned}$$

$$\begin{aligned}
\text{IV} \quad - \sum_j b_j \left\{ \beta'(j+1)^{1/2} f_{j+1} + \delta^* j^{1/2} f_{j-1} \right\} d + \sum_k c_k \left\{ \beta^+[(k+1)(k+2)]^{1/2} f_{k+2} + \right. \\
\left. + \delta^+(k + \frac{1}{2} - d^2) f_k - \frac{3}{2} \delta[k(k-1)]^{1/2} f_{k-2} \right\} + \sum_\ell g_\ell \left\{ \left[\alpha'(\ell + \frac{1}{2}) + \eta^+ d^2 - \frac{3}{2} \kappa - \epsilon \right] f_\ell + \right. \\
\left. + \delta'[\ell(\ell-1)]^{1/2} f_{\ell-2} + \delta'[(\ell+1)(\ell+2)]^{1/2} f_{\ell+2} \right\} = 0
\end{aligned}$$

(5.1.12)

TABLE 5.1

	b_1	c_1	ε_1	a_1	b_1	c_1	ε_1	a_1	b_1	c_1	ε_1	a_1	b_1	c_1	ε_1	a_1	b_1	c_1	ε_1
I	$-\frac{3}{2}b^*\sqrt{(1+\frac{1}{2})(1+2)}$	0	0	$b^*\sqrt{(1+1)(1+2)}$	$b^*(1+\frac{1}{2}-d^2)$	$b^*\sqrt{(1+1)}d$	0	$\alpha^*(1+\frac{1}{2})+\eta^*d^2+$ $+\frac{3}{2}\kappa-\epsilon$	$b^*\sqrt{1(1-1)}$	$\beta^*\sqrt{1}d$	0	$b^*\sqrt{1(1-1)}$	0	0	0	0	0	0	0
II	0	0	0	0	$-b^*\sqrt{(1+1)(1+2)}$	0	$-b^*\sqrt{1+1}d$	$\sqrt{(1+1)(1+2)}\beta^*$	$\zeta^*(1+\frac{1}{2})+\eta^*d^2-$ $-\frac{1}{2}\kappa-\epsilon$	0	$-\beta^*\sqrt{1}d$	$b^*(1+\frac{1}{2}-d^2)$	$-b^*\sqrt{1(1-1)}$	0	0	$-\frac{3}{2}b^*\sqrt{1(1-1)}$	0	0	0
III	0	0	$-\frac{3}{2}b^*\sqrt{(1+1)(1+2)}$	0	0	$-b^*\sqrt{(1+1)(1+2)}$	$b^*(1+\frac{1}{2}-d^2)$	$\beta^*\sqrt{1+1}d$	0	$\zeta^*(1+\frac{1}{2})+\eta^*d^2+$ $+\frac{1}{2}\kappa-\epsilon$	$\beta^*\sqrt{1(1+1)}$	$b^*\sqrt{1}d$	0	$-b^*\sqrt{1(1-1)}$	0	0	0	$-\frac{3}{2}b^*\sqrt{1(1-1)}$	0
IV	0	0		0	0	0	$b^*\sqrt{(1+1)(1+2)}$	0	$-\beta^*\sqrt{1+1}d$	$\beta^*\sqrt{(1+1)(1+2)}$	$\alpha^*(1+\frac{1}{2})+\eta^*d^2-$ $-\frac{3}{2}\kappa-\epsilon$	0	$b^*\sqrt{1}d$	$b^*(1+\frac{1}{2}-d^2)$	$b^*\sqrt{1(1-1)}$	0	0	$-\frac{3}{2}b^*\sqrt{1(1-1)}$	0

These yield the determinant of the form

$$\begin{array}{cccccccccccccccccccc}
 & g_0 & b_0 & g_1 & b_1 & c_0 & g_2 & a_0 & b_2 & c_1 & g_3 & a_1 & b_3 & c_2 & g_4 & a_2 & b_4 & c_3 & g_5 & a_3 & b_5 & c_4 & g_6 \\
 \text{IV } f_0 & \boxed{\epsilon} & \\
 \text{II } f_0 & & \boxed{\epsilon \quad \beta'} & \\
 \text{IV } f_1 & & & \boxed{\beta' \quad \epsilon} & \\
 \text{II } f_1 & \delta^* & & & \boxed{\epsilon \quad \beta'} & & & & & & & & & & & & & & & & & & & \\
 \text{III } f_0 & \delta^+ & & & & \boxed{\epsilon \quad \beta^+} & & & & & & & & & & & & & & & & & & \\
 \text{IV } f_2 & \delta' & & & & & \boxed{\beta' \quad \beta^+ \quad \epsilon} & & & & & & & & & & & & & & & & & \\
 \text{I } f_0 & & \delta^+ & & & & & \boxed{\epsilon \quad \beta^+ \quad \beta'} & & & & & & & & & & & & & & & & \\
 \text{II } f_2 & & \delta' & \delta^* & & & & & \boxed{\beta^+ \quad \epsilon \quad \beta'} & & & & & & & & & & & & & & & \\
 \text{III } f_1 & & & \delta^+ & & & & & & \boxed{\beta' \quad \epsilon \quad \beta^+} & & & & & & & & & & & & & & \\
 \text{IV } f_3 & & & \delta' & & & & & & & \boxed{\beta' \quad \beta^+ \quad \epsilon} & & & & & & & & & & & & \\
 \text{I } f_1 & & & & \delta^+ & \delta^* & & & & & & \boxed{\epsilon \quad \beta^+ \quad \beta'} & & & & & & & & & & & \\
 \text{II } f_3 & & & & \delta' & & \delta^* & & & & & & \boxed{\beta^+ \quad \epsilon \quad \beta'} & & & & & & & & & & \\
 \text{III } f_2 & \delta^+ & & & & \delta' & \delta^+ & & & & & & & \boxed{\beta' \quad \epsilon \quad \beta^+} & & & & & & & & & \\
 \text{IV } f_4 & & & & & \delta' & & & & & & & & & \boxed{\beta' \quad \beta^+ \quad \epsilon} & & & & & & & & \\
 \text{I } f_2 & & \delta^+ & & & & \delta' & \delta^+ & \delta^* & & & & & & & \boxed{\epsilon \quad \beta^+ \quad \beta'} & & & & & & \\
 \text{II } f_4 & & & & & & \delta' & & \delta^* & & & & & & & & \boxed{\beta^+ \quad \epsilon \quad \beta'} & & & & & \\
 \text{III } f_3 & & & \delta^+ & & & & \delta' & \delta^+ & & & & & & & & & \boxed{\beta' \quad \epsilon \quad \beta^+} & & & & \\
 \text{IV } f_5 & & & & & & & \delta' & & & & & & & & & & & \boxed{\beta' \quad \beta^+ \quad \epsilon} & & & & \\
 \text{I } f_3 & & & & \delta^+ & & & & & \delta' & \delta^+ & \delta^* & & & & & & & & \boxed{\epsilon \quad \beta^+ \quad \beta'} & & \\
 \text{II } f_5 & & & & & & & & & \delta' & & \delta^* & & & & & & & & & \boxed{\beta^+ \quad \epsilon \quad \beta'} & & \\
 \text{III } f_4 & & & & & & \delta^+ & & & & \delta' & \delta^+ & & & & & & & & & & \boxed{\beta' \quad \epsilon \quad \beta^+} & \\
 \text{IV } f_6 & & & & & & & & & & & \delta' & & & & & & & & & & & \boxed{\beta' \quad \beta^+ \quad \epsilon}
 \end{array}$$

(5.1.13)

where the elements are determined from Table 5.1. This determinant decouples into two determinants of the following form:

	g_0	b_1	c_0	g_2	a_1	b_3	c_2	g_4	a_3	b_5	c_4	g_6	a_5	b_7	c_6	g_8	a_7	b_g	c_8	g_{10}	a_9	b_{11}	c_{10}
IV f_0	ϵ	δ^*	δ^+	δ'				δ^+															
II f_1	δ^*	ϵ		β'		δ^+	δ'		δ^+														
III f_0	δ^+		ϵ	β^+		δ^*	δ'																
IV f_2	δ'	β'	β^+	ϵ		δ^*	δ^+					δ^+											
I f_1		δ^+	δ^*		ϵ	β^+	β'		δ'														
II f_3		δ'		δ^*	β^+	ϵ		β'	δ^+	δ'			δ^+										
III f_2	δ^+		δ'	δ^+	β'		ϵ	β^+	δ^*	δ'													
IV f_4			δ'		β'	β^+	ϵ		δ^*	δ^+	δ'					δ'							
I f_3		δ^+			δ'	δ^+	δ^*		ϵ	β^+	β'		δ'										
II f_5				δ^+		δ'	δ^*	β^+	ϵ		β'	δ^+	δ'			δ^+							
III f_4					δ^+		δ'	δ^+	β'		ϵ	β^+	δ^*	δ'			δ^+						
IV f_6						δ^+		δ'	β'	β^+	ϵ		δ^*	δ^+	δ'				δ^+				
I f_5							δ^+	δ'	δ^+	δ^*		ϵ	β^+	β'		δ'							
II f_7								δ^+	δ'	δ^*	β^+	ϵ		β'	δ^+	δ'			δ^+				
III f_6								δ^+		δ'	δ^+	β'		ϵ	β^+	δ^*	δ'						
IV f_8									δ^+		δ'	β'	β^+	ϵ		δ^*	δ^+	δ'				δ^+	
I f_7										δ^+		δ'	δ^+	δ^*		ϵ	β^+	β'	δ'				
II f_9											δ^+		δ'	δ^*	β^+	ϵ		β'	δ^+	δ'			
III f_8												δ^+		δ'	δ^+	β'		ϵ	β^+	δ^*	δ'		
IV f_{10}													δ^+		δ'	β'	β^+	ϵ		δ^*	δ^+		
I f_9														δ^+		δ'	δ^+	δ^*	ϵ	β^+	β'		
II f_{11}															δ^+		δ'	δ^*	β^+	ϵ			
III f_{10}																δ^+		δ'	δ^+	β'		ϵ	
IV f_{12}																	δ^+			β'	β^+		

(5.1.14)

$b_0 \ g_1 \ a_0 \ b_2 \ c_1 \ g_3 \ a_2 \ b_4 \ c_3 \ g_5 \ a_4 \ b_6 \ c_5 \ g_7 \ a_6 \ b_8 \ c_7 \ g_9 \ a_8 \ b_{10} \ c_9 \ g_{11}$

II	f ₀	ϵ	β'	δ^+	δ'		δ^+												
IV	f ₁	β'	ϵ		δ^*	δ^+	δ'			δ^+									
I	f ₀	δ^+		ϵ	β^+	β'		δ'											
II	f ₂	δ'	δ^*	β^+	ϵ		β'	δ^+	δ'		δ^+								
III	f ₁		δ^+	β'		ϵ	β^+	δ^*		δ'									
IV	f ₃		δ'		β'	β^+	ϵ		δ^*	δ^+	δ'				δ^+				
I	f ₂	δ^+		δ'	δ^+	δ^*		ϵ	β^+	β'		δ'				δ^+			
II	f ₄			δ^+		δ'	δ^*	β^+	ϵ		β'	δ^+	δ'			δ^+			
III	f ₃		δ^+			δ'	δ^+	β'		ϵ	β^+	δ^*	δ'						
IV	f ₅					δ'		β'	β^+	ϵ		δ^*	δ^+	δ'		δ^+			
I	f ₄			δ^+			δ'	δ^+	δ^*		ϵ	β^+	β'	δ'					
II	f ₆						δ'		δ^*	β^+	ϵ		β'	δ^+	δ'		δ^+		
III	f ₅				δ^+			δ'	δ^+	β'		ϵ	β^+	δ^*	δ'				
IV	f ₇							δ'		β'	β^+	ϵ		δ^*	δ^+	δ'		δ^+	
I	f ₆						δ^+			δ'	δ^+	δ^*		ϵ	β^+	β'	δ'		
II	f ₈									δ'		δ^*	β^+	ϵ		β'	δ^+	δ'	
III	f ₇							δ^+			δ'	δ^+	β'		ϵ	β^+	δ^*	δ'	
IV	f ₉										δ'		β'	β^+	ϵ		δ^*	δ^+	δ'

$$(5.1.15)$$

The coupling between the various basic 4×4 blocks is seen to be quite strong and becomes stronger as d increases. This will undoubtedly make the convergence of the eigenvalues much slower than before and will probably completely invalidate the use of the first order perturbation theory for this case. No attempt has been made to solve the matrix numerically. Such solution will probably be of interest only after more experimental data is available.

5.2 Magnetic Field in the $[111]$ Direction

For this case the transformations to be used in equation 5.0.1 are as follows:

$$\begin{aligned}
 \hat{k}_x &= \frac{1}{\sqrt{6}} \hat{k}_1 - \frac{1}{\sqrt{2}} \hat{k}_2 + \frac{1}{\sqrt{3}} \hat{k}_3 \\
 \hat{k}_y &= \frac{1}{\sqrt{6}} \hat{k}_1 + \frac{1}{\sqrt{2}} \hat{k}_2 + \frac{1}{\sqrt{3}} \hat{k}_3 \\
 \hat{k}_z &= -\sqrt{\frac{2}{3}} \hat{k}_1 + \frac{1}{\sqrt{3}} \hat{k}_3
 \end{aligned} \tag{5.2.1}$$

and

$$\begin{aligned}
 J_x &= \frac{1}{\sqrt{6}} J_1 - \frac{1}{\sqrt{2}} J_2 + \frac{1}{\sqrt{3}} J_3 \\
 J_y &= \frac{1}{\sqrt{6}} J_1 + \frac{1}{\sqrt{2}} J_2 + \frac{1}{\sqrt{3}} J_3 \\
 J_z &= -\sqrt{\frac{2}{3}} J_1 + \frac{1}{\sqrt{3}} J_3
 \end{aligned} \tag{5.2.2}$$

The complete operator matrix has, however, already been derived by Goodman (3) and will therefore not be recomputed here. The result is shown in 5.2.4, where

$$\begin{aligned}
 \alpha'' &= -\frac{2\ell' + 4\mu' - \nu}{6} = r_1 + r_3 \\
 \eta'' &= -\frac{\ell' + 2\mu' - \nu}{6} = \frac{1}{2} (r_1 - 2r_3) \\
 \eta^* &= -\frac{\ell' + 2\mu' + \nu}{6} = \frac{1}{2} (r_1 + 2r_3) \\
 \beta'' &= -\frac{\ell' - \mu' + 2\nu}{6\sqrt{3}} = \frac{1}{\sqrt{3}} (r_2 + 2r_3) \\
 \beta^* &= -\frac{2\ell' - 2\mu' + \nu}{3\sqrt{6}} = \sqrt{\frac{2}{3}} (r_3 + 2r_2) \\
 \delta'' &= \frac{\ell' - \mu' - \nu}{3\sqrt{3}} = \frac{2}{\sqrt{3}} (r_3 - r_2) \\
 \delta^o &= \frac{\ell' - \mu' - \nu}{3\sqrt{6}} = \sqrt{\frac{2}{3}} (r_3 - r_2) \\
 \xi'' &= \frac{2\ell' + 2\mu' - \nu}{6} = r_1 - r_3
 \end{aligned} \tag{5.2.3}$$

$$||V_{ij}^{4 \times 4}|| = \frac{\hbar |e| \mathcal{H}}{mc} \left\| \begin{array}{cccc} \alpha''(a^+a + \frac{1}{2}) + \eta''d^2 + \frac{3}{2}\kappa & -\beta''a^2 - \delta''a^+d & -\delta^{\circ}a^{+2} - \beta^*ad & 0 \\ -\beta''a^{+2} - \delta''ad & \zeta''(a^+a + \frac{1}{2}) + \eta^*d^2 - \frac{1}{2}\kappa & 0 & \delta^{\circ}a^{+2} - \delta''a^+d \\ -\delta^{\circ}a^2 - \beta^*a^+d & 0 & \zeta''(a^+a + \frac{1}{2}) + \eta^*d^2 + \frac{1}{2}\kappa & -\beta''a^2 - \delta''a^+d \\ 0 & \delta^{\circ}a^2 + \beta^*a^+d & -\beta''a^{+2} - \delta''ad & \alpha''(a^+a + \frac{1}{2}) + \eta''d^2 - \frac{3}{2}\kappa \end{array} \right\|$$

(5.2.4)

Proceeding as before with the solution of the form given by equation 5.1.11, one gets

$$\text{I} \quad \sum_i a_i [\alpha''(i + \frac{1}{2}) + \eta'' d^2 + \frac{3}{2} \kappa - \epsilon] f_i - \sum_j b_j \left\{ \beta'' [j(j-1)]^{1/2} f_{j-2} + \delta'' d(j+1)^{1/2} f_{j+1} \right\} - \\ - \sum_k c_k \left\{ \delta^\circ [(k+1)(k+2)]^{1/2} f_{k+2} + \beta^* d k^{1/2} f_{k-1} \right\} = 0$$

$$\text{II} \quad - \sum_i a_i \left\{ \beta'' [(i+1)(i+2)]^{1/2} f_{i+2} + \delta'' d i^{1/2} f_{i-1} \right\} + \sum_j b_j [\zeta''(j + \frac{1}{2}) + \eta^* d^2 - \frac{1}{2} \kappa - \epsilon] f_j + \\ + \sum_\ell g_\ell \left\{ \delta^\circ [(\ell+1)(\ell+2)]^{1/2} f_{\ell+2} + \beta^* d \ell^{1/2} f_{\ell-1} \right\} = 0$$

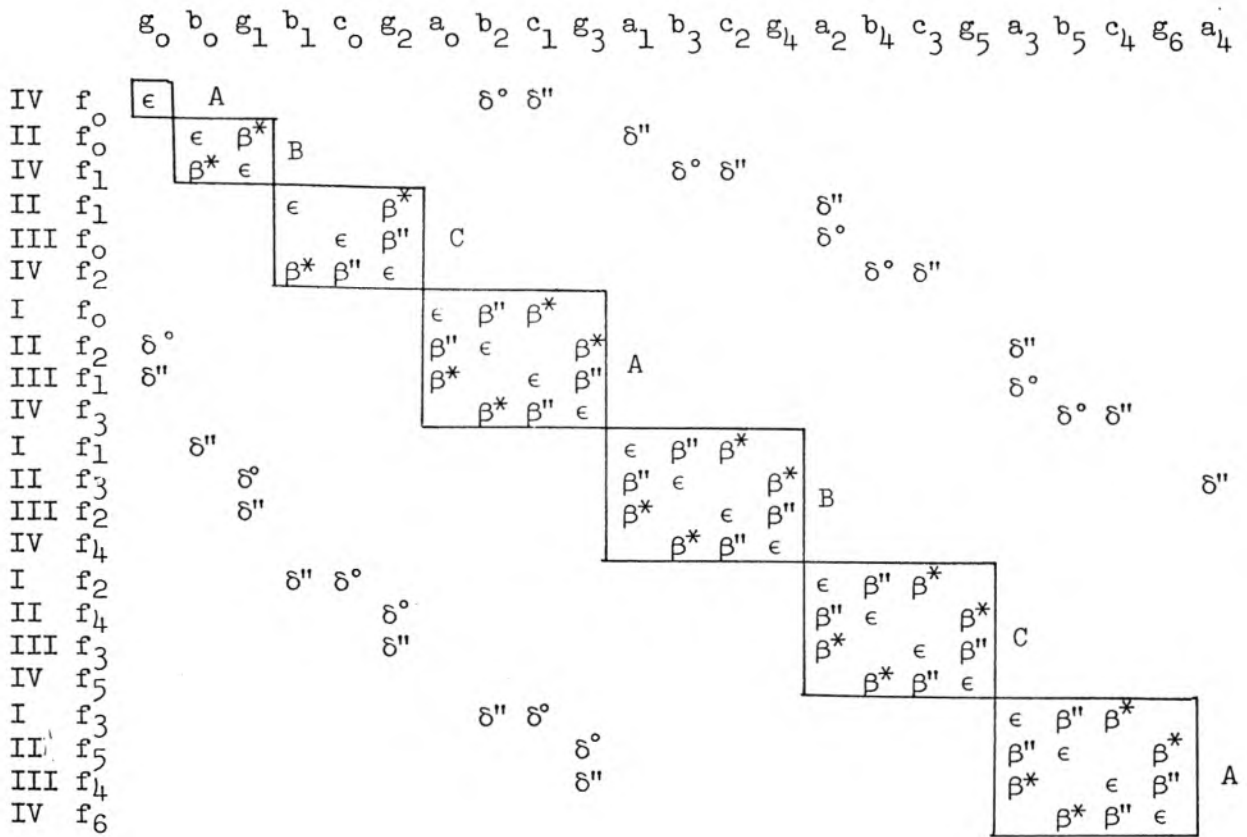
$$\text{III} \quad - \sum_i a_i \left\{ \delta^\circ [i(i-1)]^{1/2} f_{i-2} + \beta^* d(i+1)^{1/2} f_{i+1} \right\} + \sum_k c_k [\zeta''(k + \frac{1}{2}) + \eta^* d^2 + \frac{1}{2} \kappa - \epsilon] f_k \\ - \sum_\ell g_\ell \left\{ \beta'' [\ell(\ell-1)]^{1/2} f_{\ell-2} + \delta'' d(\ell+1)^{1/2} f_{\ell+1} \right\} = 0$$

$$\text{IV} \quad \sum_j b_j \left\{ \delta^\circ [j(j-1)]^{1/2} f_{j-2} + \beta^* d(j+1)^{1/2} f_{j+1} \right\} - \sum_k c_k \left\{ \beta'' [(k+1)(k+2)]^{1/2} f_{k+2} + \delta'' d k^{1/2} f_{k-1} \right\} + \\ + \sum_\ell g_\ell [\alpha''(\ell + \frac{1}{2}) + \eta'' d^2 - \frac{3}{2} \kappa - \epsilon] f_\ell = 0 \quad (5.2.5)$$

These equations yield the determinant (see Table 5.2 for elements).

TABLE 5.2

b_i	c_i	g_i	a_i	b_i	c_i	g_i	a_i	b_i	c_i
$-\delta'' d \sqrt{i+1}$	$-\delta^0 \sqrt{(i+1)(i+2)}$	0	$\alpha''(i + \frac{1}{2}) + \eta'' d^2 + \frac{3}{2} \kappa - \epsilon$	$-\beta'' \sqrt{i(i-1)}$	$-\beta^* d \sqrt{i}$	0	0	0	0
0	0	$\delta^0 \sqrt{(i+1)(i+2)}$	$-\beta'' \sqrt{(i+1)(i+2)}$	$\zeta''(i + \frac{1}{2}) + *d^2 - \frac{1}{2} \kappa - \epsilon$	0	$\beta^* d \sqrt{i}$	$-\delta'' d \sqrt{i}$	0	0
0	0	$-\delta'' d \sqrt{i+1}$	$-\beta^* d \sqrt{i+1}$	0	$\zeta''(i + \frac{1}{2}) + *d^2 + \frac{1}{2} \kappa - \epsilon$	$-\beta'' \sqrt{i(i-1)}$	$-\delta^0 \sqrt{i(i-1)}$	0	0
0	0	0	0	$\beta^* d \sqrt{i+1}$	$-\beta'' \sqrt{(i+1)(i+2)}$	$\alpha''(i + \frac{1}{2}) + \eta'' d^2 - \frac{3}{2} \kappa - \epsilon$	0	$\delta^0 \sqrt{i(i-1)}$	$-\delta'' d \sqrt{i}$



(5.2.6)

This determinant decouples into three independent ones as indicated, which will probably converge quite rapidly for small d . For large d , difficulties might arise since the δ'' coupling term is directly proportional to d .

The coupling patterns for the levels in this case will be different from both previous cases. Thus in general, transitions will be possible between all four "ladders" even at $d = 0$.

It should be noted that this problem is exactly solvable when $d = 0$. This can be seen more easily if the equations are arranged to give a determinant of the following form:

		b_0	b_1	a_0	b_2	g_0	a_1	b_3	g_1	a_2	b_4	c_0	g_2	a_3	b_5	c_1	g_3	a_4	b_6	c_2	g_4	a_5	b_7	c_3	
II	f_0	ϵ					δ''	β^*																	
II	f_1		ϵ					δ''		β^*															
I	f_0			ϵ	β''									δ''	β^*										
II	f_2			β''	ϵ	δ°									δ''	β^*									
IV	f_0				δ°	ϵ										δ''	β^*								
I	f_1	δ''				ϵ	β''											β^*							
II	f_3					β''	ϵ	δ°										δ''	β^*						
IV	f_1	β^*					δ°	ϵ											δ''	β^*					
I	f_2		δ''					ϵ	β''	δ°															
II	f_4							β''	ϵ		δ°														
III	f_0							δ°	ϵ	β''															
IV	f_2		β^*					δ°	β''	ϵ															
I	f_3			δ''					ϵ	β''	δ°														
II	f_5				β^*	δ''			β''	ϵ		δ°													
III	f_1					β^*	δ''			δ°	β''	ϵ													
IV	f_3							δ''			ϵ	β''	δ°												
I	f_4								β''	ϵ		δ°													
II	f_6								δ°	β''	ϵ		β''												
III	f_2						β^*	δ''					ϵ	β''	δ°										
IV	f_4							β^*	δ''					δ°	β''	ϵ									
I	f_5								δ''						ϵ	β''	δ°								
II	f_7									β^*	δ''				β''	ϵ		δ°							
III	f_3										β^*	δ''					δ°	β''							
IV	f_5											β^*	δ''					ϵ	β''	δ°					

(5.2.7)

Thus, since β^* and δ'' both contain d as a factor, the basic blocks decouple at $d = 0$ and can be solved exactly. As d increases, however, the coupling increases quite rapidly. For even small values of d transitions should be possible not only between adjacent levels but also between the $\epsilon(n+2, n+4)$ and the $\epsilon(n+4, n+6)$ levels, the former transition being of the "negative mass" type.

VI. SOME POSSIBLE PRACTICAL APPLICATIONS OF LANDAU LEVELS
IN Ge AND Si

In recent years there has been a number of proposals dealing with the practical applications of energy bands and Landau levels in semiconductors.

In 1958 Krömer (33,34) proposed to use the reentrant nature of the constant energy contours in the valence bands of Ge and Si (see Figure 1.3) to obtain a negative resistance element. This was to be achieved by populating with holes a region in k -space where the energy contours are reentrant, i.e., along $\langle 100 \rangle$ directions in Ge. Since in such a region the transverse (with respect to the direction in which the contours are reentrant) effective mass of the carriers is negative, their contribution to the resistance of the sample would be negative. Thus if sufficient number of carriers could be concentrated in a negative mass region, a negative resistance circuit element would in principle be obtained. Krömer estimated that such a device could be useful up to frequencies of about 1000 kmc/sec. His experiments, however, failed to show the effect. The failure was attributed to acoustical phonon scattering of the carriers out of the negative mass cone.

A few months later, G. C. Dousmanis (8) proposed to detect the negative mass carriers just mentioned by cyclotron resonance. Their effect on the spectrum would be a decrease in absorption rather than an increase. By the end of 1958 Dousmanis et al (9) reported an experiment which seemed to indicate the presence of negative mass carriers. It was soon pointed out by Kittel (35), Mattis and Stevenson (36), and Kaus (37)

that to obtain net emission by cyclotron resonance, one needs to populate preferentially certain regions in k -space. In terms of the Landau levels discussed in Section IV, negative mass cyclotron resonance corresponds to transitions between levels whose quantum number ordering is opposite to the normal ordering. Thus a negative mass CR absorption corresponds to an $f_n \rightarrow f_{n-1}$ transition. In Section IV such transitions were seen to occur in regions past the cross-over of the heavy hole levels.

In March 1960 Duncan (11) pointed out that if certain of these levels could be preferentially populated, a maser action between the negative mass levels could be achieved. This scheme would have the advantage over some other maser schemes (to be discussed below) of avoiding absorption by transitions between the heavily populated low lying positive effective mass levels. This could be done by using circularly polarized radiation of the sense that can induce negative mass transitions only.

In view of the results of Section IV, several objections can be raised in connection with the above scheme. As has already been pointed out, the crossing of the levels occurs rather slowly. That means that unless one works at fairly high k_H , the transition frequencies will be quite low even at high magnetic fields. Moreover, even at liquid helium temperatures the thermal distribution in k_H about some chosen k_{H0} may be sufficient to broaden the lines to the extent that they will not be easily identifiable. At the present time it appears that the relaxation times between Landau levels are rather

short (of the order of 10^{-12} sec). It is therefore difficult to obtain appreciable population inversion between these levels. The use of relatively high k_{H_0} necessary for the above scheme will make the task of maintaining proper level populations even harder. Another important consideration is that of the density of states. According to Burstein et al (4) for simple bands this is given by

$$N_n(\epsilon) = 2\left(\frac{s}{2\pi}\right)\left(\frac{2m^*}{h}\right)^{1/2} |\epsilon - \epsilon_n|^{-1/2} \quad (6.0.1)$$

where $s = e\hbar/kc$ and ϵ_n is the energy of the band at $k_H = 0$. Thus, as k_H increases, the density of states decreases rapidly.

A more straightforward way of utilizing the Landau levels in semiconductors, namely that of using them for a maser-type device, has been proposed by Lax (10). He pointed out that in the case of a free electron or an electron in a simple energy band, maser action between Landau levels is impossible since the levels are equally spaced. Thus after one of the levels is populated by the pump, the signal frequency would induce both emissive and absorptive transitions. In fact, since the matrix elements are proportional to $(n+1)^{1/2}$ the absorption transitions would in general predominate. However, Lax noted that according to calculations of Luttinger (2) and Goodman (3) the low lying Landau levels in degenerate bands (valence bands of Ge and Si) are unequally spaced due to quantum effects. Such levels could therefore be utilized in a maser type device. Oscillatory magnetoabsorption experiments (4,5) indicated that infrared pumping from the conduction band could probably be utilized to achieve level populations required for maser action. Assuming pump power of 10 - 100 mw and a relaxation time $\tau = 10^{-12}$ sec, Lax estimated the number of carriers that

can be excited at $\sim 10^6 \text{ cm}^{-3}$. Then using the formula of Shawlow and Townes (38)

$$n_{ex} = \frac{h(1 - \alpha)Ac}{v \tau 16\pi^2 \mu^2} \quad (6.0.2)$$

where A is the cavity wall area, α the reflection coefficient of the cavity walls, and μ is the electric dipole moment; and using $A = 1 \text{ cm}^2$ and $\mu = 10^{-14} \text{ e.s.u.}$, Lax concluded that the number of excited carriers necessary for emission is $\sim 10^8 \text{ cm}^{-3}$. Thus there is a factor of 10^2 difference between the required and the available number of carriers. The difficulty seems to arise mainly as a consequence of the very short relaxation times involved in cyclotron resonance transitions. Lax, however, suggested that the presently available estimates of the relaxation times may be somewhat too pessimistic and that better materials may result in longer relaxation times.

It has been suggested by Zeiger (10) that one does not necessarily need to populate a single discrete level thus if one has a set of levels which are equally spaced up to a certain energy, it should be possible to produce inverted populations in all of these. A scheme of this nature may be applicable to the light hole levels in Si where only a limited number of levels is nearly equally spaced, the higher lying ones being affected by the interaction with the V_3 band (see Section III).

Inspection of the results quoted in Section III and IV suggests several new schemes of utilizing the Landau levels in semiconductors. One of these is based on the fact that the ϵ_{1-} levels generally have a curvature corresponding to negative effective mass at $k_H = 0$. Thus if one were able to populate one of these preferentially, a negative resistance in the

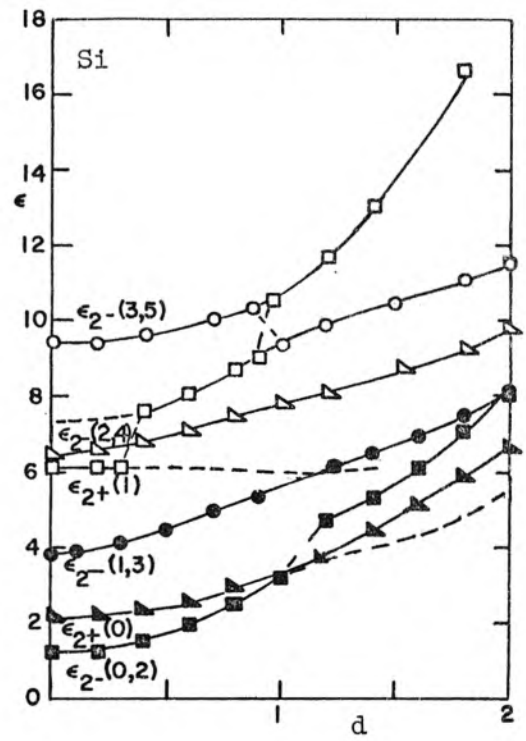
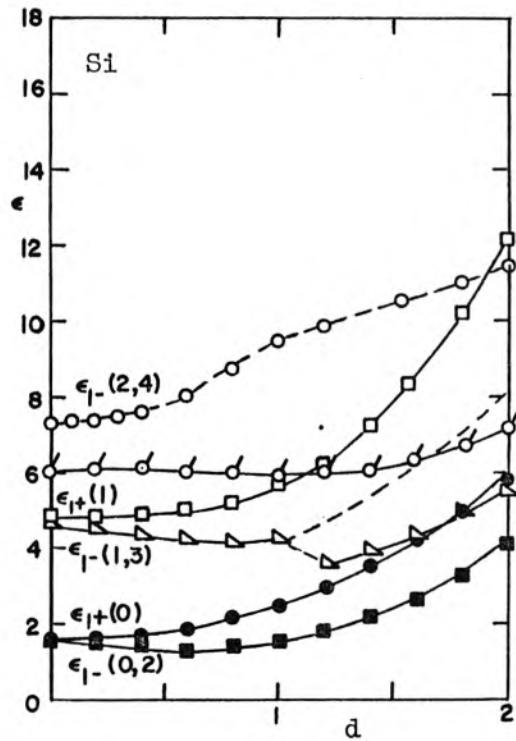
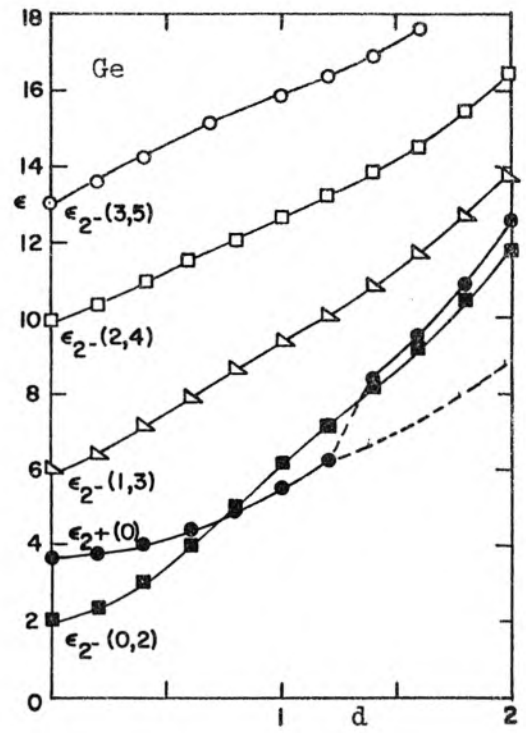
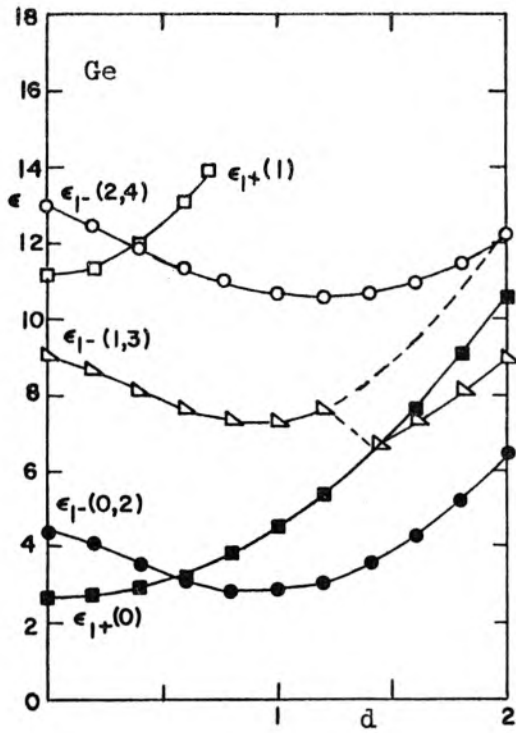


Fig. 6.1 Valence Band Landau Levels in Ge and Si near $k_H = 0$, some of which may have device applications--see text.

H direction could in principle be obtained. This scheme is similar in some respects to the proposal of Krömer. However, it seems to have some advantages over the latter scheme. Thus the negative effective masses occur at $k_H = 0$. The energy levels are continuous in only one direction and therefore the phonon scattering is possible only in that direction. The probability of successfully maintaining the desired population distribution seems to be greater in this case than in the case of no magnetic field.

Difficulties may arise in connection with this scheme due to the fact that the heavy hole levels seem to come in pairs (ϵ_{1-} and ϵ_{2-}), only one member of which (ϵ_{1-}) exhibits the negative mass characteristics. Thus in populating the ϵ_{1-} level it may, in general, be impossible to avoid populating the ϵ_{2-} level, in which case the positive resistance contribution of the ϵ_{2-} level may cancel the negative resistance contribution of the ϵ_{1-} level. It may therefore be necessary to use only the low lying ϵ_{1-} levels where the splitting between the ϵ_{1-} and ϵ_{2-} levels is appreciable. Thus the $\epsilon_{1-}(0,2)$ and the $\epsilon_{1-}(1,3)$ levels may be suitable.

It may be advantageous to use relatively high magnetic fields in connection with this scheme since high fields imply a wide range of k_H over which the effective masses in the ϵ_{1-} levels are negative. In addition, such fields will enable one to select the required level more easily.

There are several ways of populating the desired Landau levels. One of the most obvious ones is to use infrared excitation across the energy gap. This would create both holes and electrons. The holes will have a negative effective mass provided an excitation frequency can be selected

so that no hole levels except the desired ϵ_{1-} level are excited. The conductivity is then given by

$$\sigma = q(-\mu_p p + \mu_n n) = qp(\mu_n - \mu_p) \quad (6.0.3)$$

Thus to have negative over-all conductivity, the condition $\mu_p > \mu_n$ must be satisfied. But $\mu \sim \tau/m^*$, therefore (assuming for the moment the collision time τ to be the same for holes and electrons) one must have the absolute value of m^* for holes to be smaller than that for electrons. In addition, positive conductivity will be contributed by the holes which will be scattered into the positive effective mass regions.

For Ge it is easy to calculate that the effective mass of the holes is

$$m^* \approx -.074 m_0 \text{ in the } \epsilon_{1-}(0,2) \text{ level}$$

$$\text{and } m^* \approx -.071 m_0 \text{ in the } \epsilon_{1-}(1,3) \text{ level.}$$

The effective mass of electrons in the Γ_2 conduction band is

$$m^* \approx 0.04 m_0$$

and the effective masses in the L_1 band are

$$m_{\ell}^* = 1.58 m_0$$

$$m_t^* = 0.082 m_0 .$$

Thus if most of the electrons created in the conduction band drop to the conduction band edge (L_1) by means of phonon transitions, a negative resistance device should, in principle, be possible.

For Si the corresponding figures are

$$m^* = -0.67 m_0 \text{ for holes in } \epsilon_{1-}(0,2) \text{ level}$$

$$m^* = -0.315 m_0 \text{ for holes in } \epsilon_{1-}(1,3) \text{ level}$$

$$m_{\ell}^* = 0.97 m_0$$

$$m_t^* = 0.19 m_0 \text{ for electrons at conduction band edge}$$

The m^* at the band edge is given because the electrons, even if excited at $k_H = 0$, are most likely to drop to the band edge through phonon transitions. The above numbers indicate that one should be able to obtain negative resistance in Si for certain orientations of magnetic field quite easily, especially if the $\epsilon_{1-}(1,3)$ level is excited. A difficulty might arise due to the proximity of the $\epsilon_{1+}(0)$ and the $\epsilon_{1+}(1)$ levels to the $\epsilon_{1-}(0,2)$ and $\epsilon_{1-}(1,3)$ levels respectively. However, the difficulty may turn out to be not too great because of the high effective masses in the $\epsilon_{1+}(0)$ and $\epsilon_{1+}(1)$ levels and the consequently small contribution to the conductivity.

As an alternative excitation scheme one may use transitions to some impurity or exciton state in the energy gap. In this case the electron mobility should not enter the picture at all. This, of course, is a decided advantage. Another possible method of exciting the required ϵ_{1-} Landau level is to use cyclotron resonance transitions together with a shallow impurity which would create carriers in the valence band. However, before a specific set of levels can be selected for use with this scheme, the relative relaxation times between the various levels must be known.

Another interesting application possibility arises from the fact that there are many "negative mass" transitions even at $k_H = 0$. This is

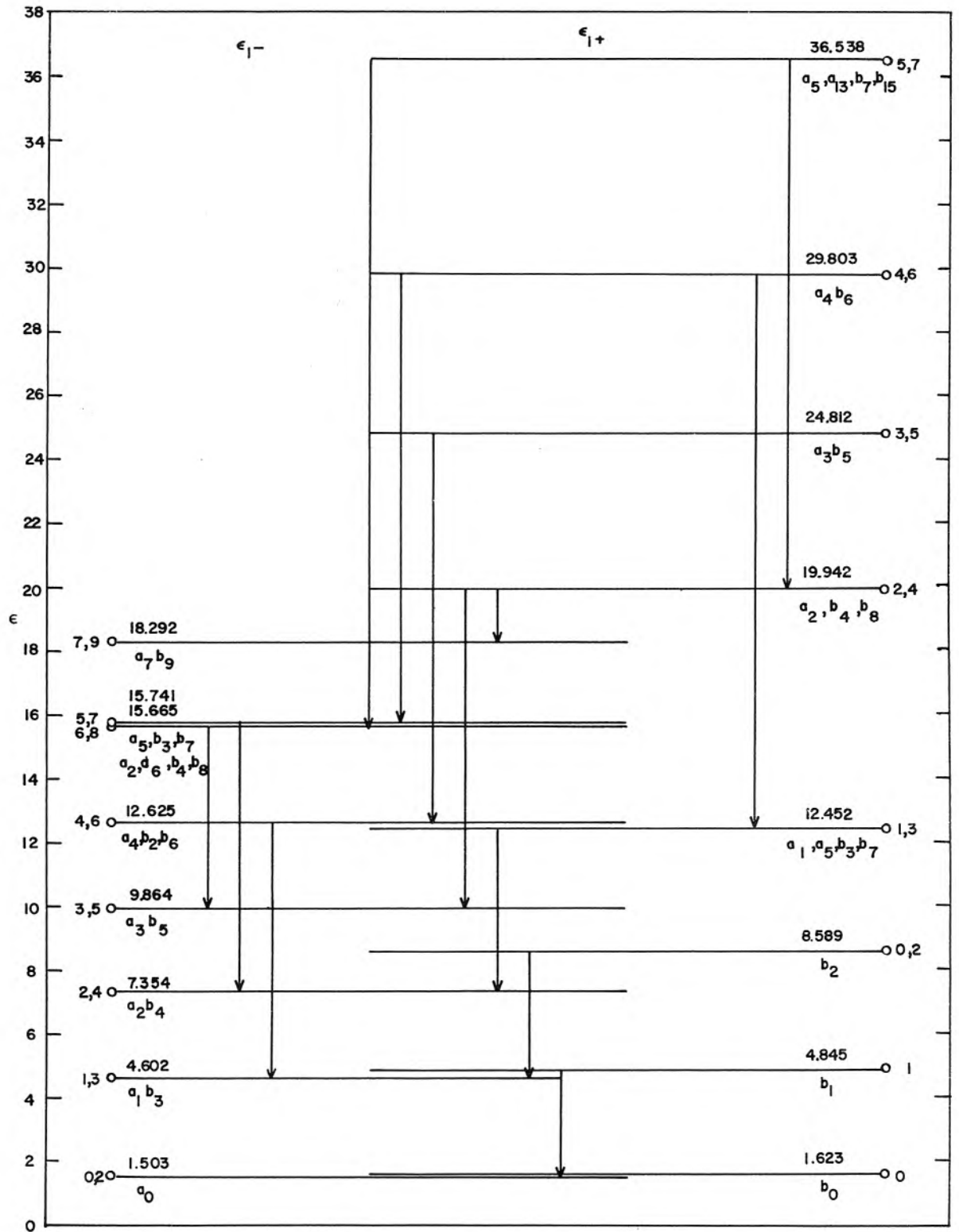


Fig. 6.2 "Negative Mass" Transitions between the Landau Levels belonging to the ϵ_1 Ladders in Si at $\mathcal{H} = 5$ kgauss. Expansion coefficients considered are approximately equal to or greater than 0.5

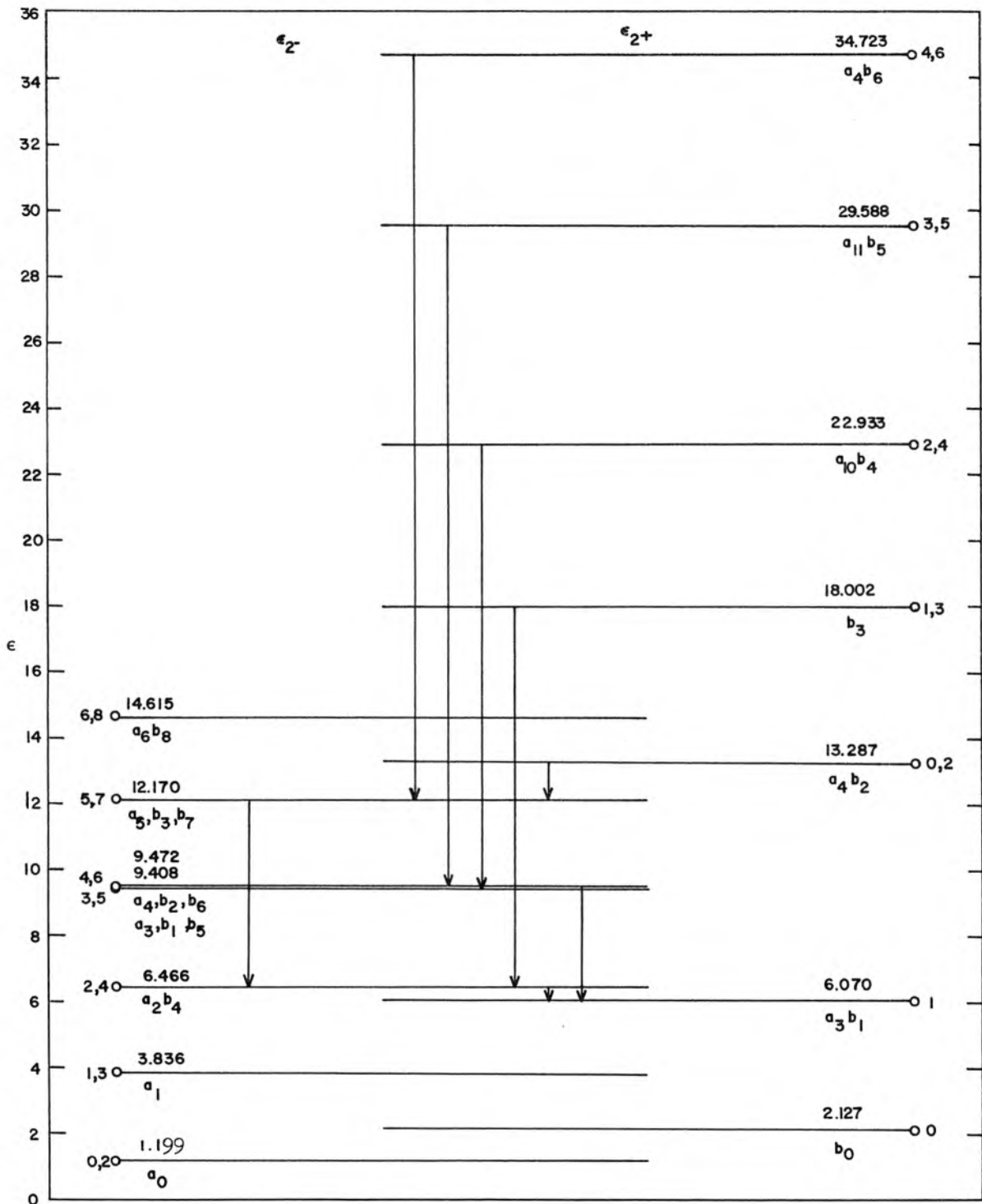


Fig. 6.3 "Negative Mass" Transitions between the Landau Levels belonging to the ϵ_2 Ladders in Si at $H = 5$ kgauss. Expansion coefficients considered are approximately equal to or greater than 0.5

especially true in the case of Si for which all of the "negative mass" transitions between the low lying levels have been summarized in Figs. 6.2 and 6.3. These transitions will be observed to vary quite widely in frequency, thus minimizing the problem of equal level spacings discussed in connection with Lax's maser proposals. The most interesting transitions seem to be those between the ϵ_{1-} and ϵ_{1+} levels and the ϵ_{2-} and ϵ_{2+} levels. In the case of Si, many of these fall into a very convenient frequency range. Thus at $H = 5$ kg the $\epsilon_{1+}(1,3) \rightarrow \epsilon_{1-}(2,4)$ transition occurs at 71 kmc. The considerable advantage of such transitions is that one may accidentally populate some of the levels which lie close to the desired one without causing any absorptive transitions. This, of course, will be true only if circularly polarized radiation is used for the signal

Because of the numerous second order transitions which are in general possible between the Landau levels--especially those of Si, possibilities seem to exist for low frequency pumping. Thus in most cases the $\epsilon(n,n+2) \rightarrow (n+3,n+5)$, as well as the $\epsilon(n,n+2) \rightarrow \epsilon(n+5,n+7)$ transition is possible, (see page 75). One could therefore use one of these as the signal transition while pumping at the cyclotron frequency. The requirement here (aside from the usual ones) is that there are to be no levels above the one to be populated separated from it by the cyclotron pump frequency. An example of such a level configuration in Si is shown in Fig. 6.4.

Many other level configurations suitable for application in a maser-type device could be found in both Ge and Si, especially if one also considers the levels arising from the application of the external magnetic field in other than the [001] direction. From Section V it can be seen that the [101] direction may be especially interesting, since the coupling

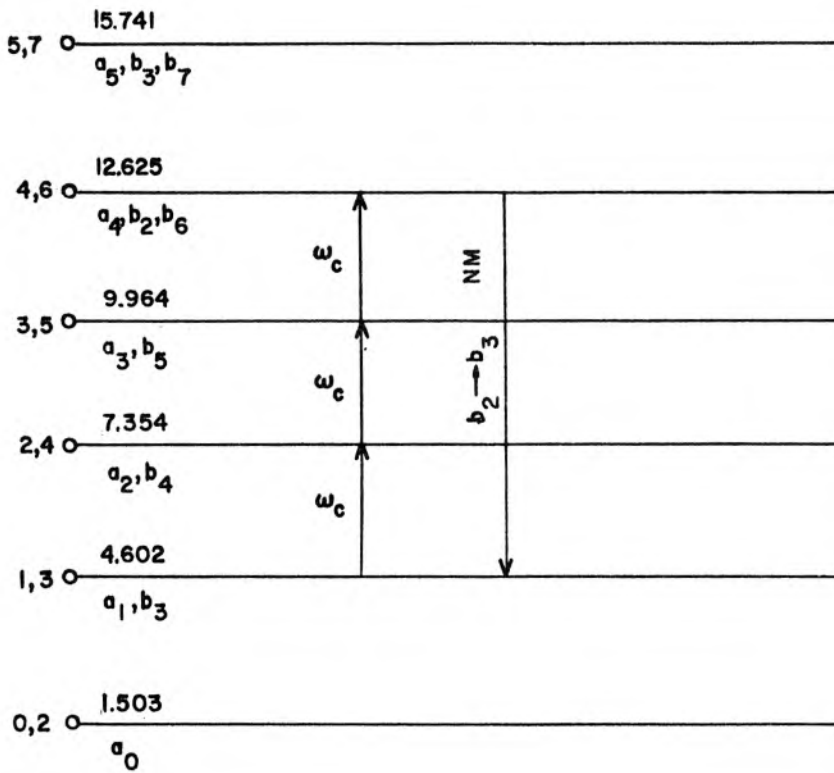


Fig. 6.4 An Example of a Set of Energy Levels in Si (ϵ_1 - Ladder at $\mathcal{H} = 5$ kgauss) Suitable, in Principle, for a Low-Frequency-Pump Maser

between the Landau levels for that case is quite strong. However, all of these possibilities, as well as the specific ones discussed above, will to a very large extent depend for their success on one's ability to find sufficiently powerful pump sources, and on the outcome of the relaxation time studies. Such studies will no doubt be necessary before any of the ideas presented above can be realized.

APPENDIX 1

SIMULTANEOUS DIAGONALIZATION OF TWO PERTURBATION HAMILTONIANS

The basic perturbation theory expansions are as follows (27):

$$\psi = \sum_{\ell} c_{\ell} \psi_{\ell}^{(0)} \quad (\text{A1.1})$$

$$(E - E_k^{(0)}) c_k = \sum_{\ell} V_{k\ell} c_{\ell} \quad (\text{A1.2})$$

$$E = E_k^{(0)} + E_k^{(1)} + E_k^{(2)} + \dots \quad (\text{A1.3})$$

$$c_{\ell} = c_{\ell}^{(0)} + c_{\ell}^{(1)} + c_{\ell}^{(2)} + \dots \quad (\text{A1.4})$$

where $\psi_{\ell}^{(0)}$ and $E_k^{(0)}$ are the zero order wave functions and energies respectively, $V_{k\ell}$ are the matrix elements between the zero order wave functions, and $E_k^{(1)}$, $E_k^{(2)}$, \dots , are the first, second, etc. order eigenvalue corrections.

Suppose the unperturbed (zero order) wave functions are

$$\psi_n^{(0)}, \psi_{n'}^{(0)} \dots \psi_m^{(0)} \dots \quad (\text{A1.5})$$

where all $\psi_n^{(0)}, \psi_{n'}^{(0)} \dots$ are degenerate. The problem is to find the corrections to $E_n^{(0)}$ to second order. The correct perturbed eigenfunction is given by

$$\psi = \sum_{n'} c_{n'} \psi_{n'}^{(0)} + \sum_m c_m \psi_m^{(0)} \quad (\text{A1.6})$$

In A1.2, letting $k = n, n' \dots$, one gets correct to second order the following set of equations:

$$(E_n^{(1)} + E_n^{(2)})(c_n^{(0)} + c_n^{(1)}) = \sum_{n'} V_{nn'}(c_{n'}^{(0)} + c_{n'}^{(1)}) + \sum_m V_{nm} c_m^{(1)} \quad (A1.7)$$

since $c_m^{(0)} = 0$.

Considering $k = m \neq n, n' \dots$, one obtains to first order,

$$(E_n^{(0)} - E_m^{(0)})c_m^{(1)} = \sum_{n'} V_{mn'} c_{n'}^{(0)} \quad (A1.8)$$

from which

$$c_m^{(1)} = \sum_{n'} \frac{V_{mn'} c_{n'}^{(0)}}{E_n^{(0)} - E_m^{(0)}} \quad (A1.9)$$

Substituting A1.9 into A1.7

$$\begin{aligned} (E_n^{(1)} + E_n^{(2)})(c_n^{(0)} + c_n^{(1)}) &= \sum_{n'} V_{nn'}(c_{n'}^{(0)} + c_{n'}^{(1)}) + \\ &+ \sum_m \sum_{n'} \frac{V_{nm} V_{mn'} c_{n'}^{(0)}}{E_n^{(0)} - E_m^{(0)}} \end{aligned} \quad (A1.10)$$

Now a third order term, $\sum_m \sum_{n'} \frac{V_{nm} V_{mn'} c_{n'}^{(1)}}{E_n^{(0)} - E_m^{(0)}}$, may be added to the right hand side of A1.10, with the result

$$(E_n^{(1)} + E_n^{(2)})(c_n^{(0)} + c_n^{(1)}) = \sum_{n'} (V_{nn'} + \sum_m \frac{V_{nm} V_{mn'}}{E_n^{(0)} - E_m^{(0)}})(c_{n'}^{(0)} + c_{n'}^{(1)}) \quad (A1.11)$$

For these equations to be compatible the following condition must be satisfied:

$$V_{nn'} + \sum_m \frac{V_{nm} V_{mn'}}{E_n^{(0)} - E_m^{(0)}} - (E_n^{(1)} + E_n^{(2)})\delta_{nn'} = 0 \quad (A1.12)$$

This gives the required corrections to second order.

Now consider a perturbation Hamiltonian V consisting of two parts:

$$\hat{V} = \hat{V}^1 + \lambda \hat{V}^2 \quad (\text{A1.13})$$

where λ is first order compared to unity.

Then

$$V_{nn'} = V_{nn'}^1 + \lambda V_{nn'}^2 \quad (\text{A1.14})$$

$$V_{nm} = V_{nm}^1 + \lambda V_{nm}^2 \quad (\text{A1.15})$$

$$V_{mn'} = V_{mn'}^1 + \lambda V_{mn'}^2 \quad (\text{A1.16})$$

$$\begin{aligned} V_{nm} V_{mn'} &= V_{nm}^1 V_{mn'}^1 + \lambda (V_{nm}^2 V_{mn'}^1 + V_{nm}^1 V_{mn'}^2) + \\ &\quad + \lambda^2 (V_{nm}^2 V_{mn'}^2) \\ &= V_{nm}^1 V_{mn'}^1 \end{aligned} \quad (\text{A1.17})$$

to second order. A1.12 then becomes

$$\left| V_{nn'}^1 + \lambda V_{nn'}^2 + \sum_m \frac{V_{nm}^1 V_{mn'}^1}{E_n^{(0)} - E_m^{(0)}} - (E_n^{(1)} + E_n^{(2)}) \delta_{nn'} \right| = 0 \quad (\text{A1.18})$$

In Section 2.1, $V^1 = V^{k \cdot p}$ and $\lambda V^2 = V^{so}$. In this case, $V_{nn'}^1 = 0$.

APPENDIX 2

ELECTRON IN A HOMOGENEOUS MAGNETIC FIELD

The problem of an electron in a constant homogeneous magnetic field has been solved by L. Landau (20)

The Hamiltonian is

$$\hat{H} = \frac{1}{2m} \left(\hat{p} + \frac{|e|\hat{A}}{c} \right)^2 + \frac{|e|\hbar}{2mc} \sigma \cdot \hat{\mathcal{H}} \quad (A2.1)$$

Landau chooses the gauge:

$$A_x = -\mathcal{H}y, \quad A_y = A_z = 0 \quad (A2.2)$$

Using this and observing that in A2.1 spin and coordinate parts of the Hamiltonian are separable, one gets

$$\left[\frac{1}{2m} \left(p_x - \frac{|e|\hbar y}{c} \right)^2 + \frac{\hat{p}_y^2}{2m} + \frac{\hat{p}_z^2}{2m} + \frac{|e|\hbar}{2mc} \sigma \mathcal{H} \right] \psi = E \psi \quad (A2.3)$$

where ψ is a function of coordinates only.

Now since \hat{p}_x and \hat{p}_z commute with \hat{H} one may write:

$$\psi = e^{\frac{i}{\hbar}(p_x x + p_z z)} \chi(y) \quad (A2.4)$$

where $\chi(y)$ satisfies the equation

$$-\frac{\hbar^2}{2m} \frac{\partial^2 \chi}{\partial y^2} + \frac{1}{2} m \left(\frac{|e|\hbar}{mc} \right)^2 (y - y_0)^2 \chi = \left(E - \frac{p_z^2}{2m} \right) \chi \quad (A2.5)$$

in which

$$y_0 \equiv -\frac{cp_x}{e\mathcal{H}} \quad (A2.6)$$

Recalling the equation for the harmonic oscillator:

$$-\frac{\hbar^2}{2m} \frac{\partial^2 \psi}{\partial q^2} + \frac{1}{2} m \omega^2 q^2 \psi = E \psi \quad (\text{A2.7})$$

The solution to the problem is obtained

$$\psi = e^{\frac{i}{\hbar}(p_x x + p_z z)} e^{-\frac{1}{2} \frac{|e|\hbar}{\hbar c} (y-y_0)^2} \left[H_n (y-y_0) \sqrt{\frac{|e|\hbar}{\hbar c}} \right] \quad (\text{A2.8})$$

$$= e^{\frac{i}{\hbar}(p_x x + p_z z)} f_n(y)$$

$$E = \left(n + \frac{1}{2}\right) \frac{|e|\hbar}{mc} + \frac{p_z^2}{2m} + \frac{|e|}{2mc} \sigma \hbar \quad (\text{A2.9})$$

The harmonic oscillator problem is conveniently treated using raising and lowering operators which have the following properties:

$$\text{Raising operator } a_r \equiv \frac{1}{\sqrt{2n}} \left(-\frac{\partial}{\partial \xi} + \xi \right) \quad (\text{A2.10})$$

$$\psi_n = a_r \psi_{n-1} \quad (\text{A2.11})$$

$$\text{Lowering operator } a_l \equiv \frac{1}{\sqrt{2n}} \left(\frac{\partial}{\partial \xi} + \xi \right) \quad (\text{A2.12})$$

$$\psi_{n-1} = a_l \psi_n \quad (\text{A2.13})$$

where $\xi = \sqrt{\frac{m\omega}{\hbar}} q$

Similar operators may be defined for the problem of an electron in a magnetic field. Comparing A2.7 with A2.5 one has

$$\omega \rightarrow \frac{|e|\hbar}{mc} \quad (\text{A2.14})$$

$$q \rightarrow y - y_0 \quad (\text{A2.15})$$

Therefore,

$$\text{Raising operator} = \frac{1}{\sqrt{2n}} \left[-\sqrt{\frac{\hbar c}{|e|\mathcal{H}}} \frac{\partial}{\partial y} + \sqrt{\frac{|e|\mathcal{H}}{\hbar c}} (y-y_0) \right] \quad (\text{A2.16})$$

$$\text{Lowering operator} = \frac{1}{\sqrt{2n}} \left[\sqrt{\frac{\hbar c}{|e|\mathcal{H}}} \frac{\partial}{\partial y} + \sqrt{\frac{|e|\mathcal{H}}{\hbar c}} (y-y_0) \right] \quad (\text{A2.17})$$

Using the definitions 2.2.24, the final results are obtained

$$\text{Raising operator} = \frac{1}{\sqrt{2n}} \sqrt{\frac{\hbar c}{|e|\mathcal{H}}} (-\hat{k}_x - i\hat{k}_y) \quad (\text{A2.18})$$

$$\text{Lowering operator} = \frac{1}{\sqrt{2n}} \sqrt{\frac{\hbar c}{|e|\mathcal{H}}} (-\hat{k}_x + i\hat{k}_y) \quad (\text{A2.19})$$

These operators have the properties

$$f_n(y) = \frac{1}{\sqrt{2n}} \sqrt{\frac{\hbar c}{|e|\mathcal{H}}} (-\hat{k}_x - i\hat{k}_y) f_{n-1}(y) \quad (\text{A2.20})$$

$$f_{n-1}(y) = \frac{1}{\sqrt{2n}} \sqrt{\frac{\hbar c}{|e|\mathcal{H}}} (-\hat{k}_x + i\hat{k}_y) f_n(y) \quad (\text{A2.21})$$

APPENDIX 3

Ge: Numerical Solution of Equation 3.1.8, Part A

5x5 Determinant

\mathcal{H} (kgauss)	Δ'	ϵ_1	ϵ_2	ϵ_3	ϵ_4	ϵ_5	ϵ_6	ϵ_7	ϵ_8
1	25×10^3	2.662	25010.4	13.361	73.392	25063.			
2.5	10	2.662	10010.4	13.361	73.228	10063.5			
5.0	5	2.662	5010.4	13.360	72.955	5063.7			
10	2.5	2.662	2510.4	13.359	72.407	2564.3			
15	1.66	2.661	1670.4	13.357	71.851	1724.9			
20	1.25	2.661	1260.4	13.355	71.307	1315.4			
30	.835	2.660	845.449	13.352	70.210	901.497			
50	.500	2.660	510.481	13.346	67.999	568.711			

8x8 Determinant

	$\epsilon_{1+}(0)$		$\epsilon_{1-}(2,4)$	$\epsilon_{1+}(2,4)$		$\epsilon_{1-}(6,8)$		
1	2.661	25010.4	13.046	73.391	25063.	28.387	163.874	25116.5
2.5	2.661	10010.4	13.045	73.227	10063.5	28.385	163.189	10117.
5.0	2.661	5010.4	13.044	72.953	5063.8	28.382	162.038	5118.3
10	2.661	2510.4	13.040	72.405	2564.3	28.377	159.709	2620.6
15	2.661	1670.4	13.037	71.849	1724.9	28.371	157.318	1783.0
20	2.660	1260.4	13.034	71.305	1315.4	28.366	154.958	1375.4
30	2.660	845.449	13.027	70.208	901.542	28.355	150.159	965.169
50	2.659	510.481	13.014	67.997	568.782	28.333	140.467	639.863

Ge: Numerical Solution of Equation 3.1.8, Part B

(kgauss)	Δ'	5x5 Determinant							
		ϵ_1	ϵ_2	ϵ_3	ϵ_4	ϵ_5	ϵ_6	ϵ_7	ϵ_8
1	25×10^3	11.189	25023.6	17.384	95.926	25076.6			
2.5	10	11.187	10023.6	17.382	95.666	10016.8			
5.0	5	11.182	5023.6	17.380	95.232	5077.3			
10	2.5	11.174	2523.7	17.375	94.358	2578.1			
15	1.66	11.166	1683.7	17.370	93.468	1735.0			
20	1.25	11.157	1273.7	17.365	92.595	1329.9			
30	.835	11.141	858.794	17.355	90.831	916.674			
50	.500	11.108	523.920	17.336	87.261	585.247			

8x8 Determinant

	$\epsilon_{1+}(1)$		$\epsilon_{1-}(3,5)$	$\epsilon_{1+}(3,5)$		$\epsilon_{1-}(7,9)$		
1	11.176	25023.6	16.943	95.400	25076.6	32.146	186.554	25129.8
2.5	11.173	10023.6	16.941	95.640	10076.8	32.144	185.681	10130.7
5.0	11.169	5023.6	16.937	95.206	5077.3	32.140	184.213	5132.1
10	11.161	2523.7	16.929	94.333	2578.2	32.133	181.235	2635.1
15	11.152	1683.7	16.921	93.444	1739.1	32.126	178.172	1798.2
20	11.144	1273.7	16.913	92.572	1330.0	32.119	175.144	1391.2
30	11.127	858.794	16.898	90.810	916.735	32.104	168.981	982.345
50	11.093	523.920	16.867	87.245	585.339	32.076	156.595	659.735

11x11 Determinant

Δ'	ϵ_1	ϵ_2	ϵ_3	ϵ_4	ϵ_5	ϵ_6	ϵ_7	ϵ_8	ϵ_9	ϵ_{10}	ϵ_{11}
$.500 \times 10^3$	10.898	523.920	16.850	87.245	585.339	30.845	156.570	659.874	47.059	213.408	747.069

Ge: Numerical Solution of Equation 3.1.8, Part C

3x3 Determinant

\mathcal{H} (kgauss)	Δ'	ϵ_1	ϵ_2	ϵ_3	ϵ_4	ϵ_5	ϵ_6	ϵ_7	ϵ_8	ϵ_9
1	25×10^2	4.511	29.471	25037.						
2.5	10	4.509	29.445	10037.						

6x6 Determinant

1	4.429	29.613	25037.	20.717	118.545	25090.
2.5	4.427	29.571	10037.	20.716	118.166	10090.

9x9 Determinant

	$\epsilon_{1-}(0,2)$	$\epsilon_{1+}(0,2)$	$\epsilon_{1-}(4,6)$	$\epsilon_{1+}(4,6)$					
1	4.428	29.604	25037.	20.136	118.496	25090.	35.912	209.233	25143.
2.5	4.426	29.579	10037.	20.134	118.117	10090.	35.909	208.149	10144.
5.0	4.422	29.537	5036.9	20.130	117.484	509099	35.905	206.325	5146.0
10	4.415	29.453	2537.1	20.123	116.207	2592.2	35.895	202.616	2649.7
15	4.408	29.368	1697.2	20.115	114.904	1753.5	35.886	198.792	1813.5
20	4.400	29.285	1287.3	20.108	113.623	1344.8	35.876	195.006	1407.3
30	4.386	29.119	872.582	20.093	111.026	932.417	35.858	187.304	1000.03
50	4.357	28.784	538.097	20.063	105.765	602.725	35.821	171.928	680.418

Ge: Numerical Solution of Equation 3.1.8, Part D

\mathcal{H} (kgauss)	Δ'	3x3 Determinant							
		ϵ_1	ϵ_2	ϵ_3	ϵ_4	ϵ_5	ϵ_6	ϵ_7	ϵ_8
1	25×10^3	9.265	51.083	25050.					
2.5	10	9.269	51.011	10050.					

6x6 Determinant							
1	9.076	51.117	25050.1	24.611	141.201	25103.2	
2.5	9.075	51.045	10050.2	24.610	140.681	10103.7	

9x9 Determinant									
	$\epsilon_{1-(1,3)}$	$\epsilon_{1+(1,3)}$		$\epsilon_{1-(5,7)}$	$\epsilon_{1+(5,7)}$				
1	9.072	51.121	25050.1	23.851	141.128	25103.2	39.650	231.909	25156.5
2.5	9.072	51.045	10050.2	23.848	140.608	10103.7	39.647	230.591	10151.8
5.0	9.071	50.929	5050.31	23.843	139.737	5104.56	39.642	228.370	5160.0
10	9.069	50.689	2550.61	23.833	137.978	2606.34	39.631	223.845	2664.52
15	9.067	50.446	1710.92	23.823	136.177	1768.16	39.620	219.170	1829.20
20	9.065	50.208	1301.22	23.813	134.403	1359.96	39.609	214.539	1423.82
30	9.062	49.727	886.828	23.794	130.800	948.595	39.588	205.123	1018.24
50	9.055	48.755	553.042	23.754	123.503	620.946	39.545	186.487	701.888

Ge: Numerical Solution of Equation 3.1.13, Part A

4x4 Determinant

\mathcal{H} (kgauss)	Δ'	ϵ_1	ϵ_2	ϵ_3	ϵ_4	ϵ_5	ϵ_6	ϵ_7	ϵ_8	ϵ_9	ϵ_{10}
1	25×10^3	3.694	10.162	87.943	25029.						
2.5	10×10^3	3.694	10.160	87.829	10029.						
5.0	5×10^3	3.693	10.157	87.639	5029.6						
10	2.5×10^3	3.692	10.151	87.251	2530.0						
15	1.66×10^3	3.691	10.144	86.849	1690.4						
20	1.25×10^3	3.690	10.138	86.447	1280.8						
30	$.835 \times 10^3$	3.688	10.126	85.613	866.65						
50	$.5 \times 10^3$	3.683	10.101	83.815	533.48						

7x7 Determinant

1	3.691	9.972	88.108	25029.	24.658	178.583	25082.
2.5	3.690	9.969	87.995	10029.4	24.653	178.004	10083.
5.0	3.690	9.965	87.804	5029.6	24.645	177.024	5084.0
10	3.689	9.956	87.415	2530.0	24.629	175.009	2586.0
15	3.687	9.948	87.012	1690.4	24.612	172.897	1748.1
20	3.686	9.939	86.609	1280.8	24.596	170.767	1340.3
30	3.684	9.922	85.772	866.647	24.564	166.288	429.798
50	3.679	9.888	83.968	533.471	24.498	156.613	604.558

10x10 Determinant

	$\epsilon_{2+}(0)$	$\epsilon_{2-}(2,4)$	$\epsilon_{2+}(2,4)$	$\epsilon_{2-}(6,8)$	$\epsilon_{2+}(6,8)$					
10						23.920				
15	3.687	9.943	87.013	1690.4	23.893	173.040	1748.1	39.459	255.201	1809.9
20	3.686	9.935	86.611	1280.8	23.867	171.105	1340.3	39.430	248.854	1405.3
30	3.684	9.917	85.773	866.647	23.813	166.430	929.773	39.377	238.634	1001.63
50	3.679	9.882	83.969	533.471	23.704	156.736	604.497	99.267	215.278	690.191

Ge: Numerical Solution of Equation 3.1.13, Part B

4x4 Determinant

\mathcal{H} (kgauss)	Δ'	ϵ_1	ϵ_2	ϵ_3	ϵ_4	ϵ_5	ϵ_6	ϵ_7	ϵ_8	ϵ_9	ϵ_{10}
1	25×10^3	21.917	13.312	110.564	25043.						
2.5	10	21.917	13.310	110.369	10043.						
5.0	5	21.916	13.305	110.039	5043.1						

7x7 Determinant

1	13.040	21.881	110.723	25043.	28.381	201.206	25096.
2.5	13.036	21.881	110.528	10043.	28.376	200.513	10096.
5.0	13.030	21.881	110.198	5043.06	28.366	199.237	5097.75
10	13.017	21.880	109.524	2543.7	28.348	196.608	2600.4
15	13.003	21.880	108.824	1704.46	28.329	193.845	1763.19
20	12.990	21.879	108.123	1295.16	28.310	191.054	1356.01
30	12.964	21.879	106.658	881.642	28.273	185.180	946.930
50	12.910	21.877	103.488	549.836	28.197	172.563	624.654

10x10 Determinant

	$\epsilon_{2+}(1)$	$\epsilon_{2-}(3,5)$	$\epsilon_{2+}(3,5)$		$\epsilon_{2-}(7,9)$	$\epsilon_{2+}(7,9)$				
10	21.877	13.009	109.525	2543.7	27.473	196.743	2600.4	43.225	281.445	2659.7
15	21.876	12.996	108.825	1704.46	27.440	193.984	1763.18	43.195	275.142	1826.03
20	21.876	12.982	108.124	1295.16	27.408	191.194	1355.99	43.166	268.752	1422.47
30	21.874	12.955	106.659	881.642	27.344	185.320	946.891	43.106	255.374	1020.96
50	21.872	12.900	103.489	549.836	27.213	172.678	624.562	42.986	227.937	713.653

Ge: Numerical Solution of Equation 3.1.13, Part C

3x3 Determinant

\mathcal{H} (kgauss)	Δ'	ϵ_1	ϵ_2	ϵ_3	ϵ_4	ϵ_5	ϵ_6	ϵ_7	ϵ_8	ϵ_9
1		2.100	43.090	25003.						
2.5		2.100	43.074	10003.						
5.0		2.100	43.047	5002.9						
10		2.100	42.993	2502.9						
15		2.099	42.937	1663.0						
20		2.099	42.882	1253.0						
30		2.099	42.768	838.16						
50		2.099	42.527	503.43						

6x6 Determinant

1	2.058	43.299	25002.8	17.207	133.224	25055.8
2.5	2.058	43.283	10002.8	17.204	132.923	10056.1
5.0	2.057	43.256	5002.86	17.198	132.416	5056.62
10	2.057	43.201	2502.92	17.187	131.378	2557.67
15	2.057	43.145	1662.98	17.175	130.296	1718.77
20	2.056	43.089	1253.04	17.164	129.210	1309.86
30	2.056	42.974	838.164	17.141	126.935	897.164
50	2.055	42.730	503.427	17.094	122.003	567.147

9x9 Determinant

	$\epsilon_{2-}(0,2)$	$\epsilon_{2+}(0,2)$	$\epsilon_{2-}(4,6)$	$\epsilon_{2+}(4,6)$			
5.0	2.057	43.263	5002.86	16.790	132.569	5056.62	32.050 221.383 5111.62
10	2.057	43.208	2502.92	16.773	131.531	2557.67	32.028 218.054 2614.97
15	2.056	43.152	1662.98	16.756	130.449	1718.76	32.006 214.548 1778.51
20	2.056	43.096	1253.04	16.739	129.361	1309.86	31.985 211.001 1372.09
30	2.055	42.981	838.164	16.704	127.083	897.155	31.942 203.537 964.611
50	2.054	42.737	503.427	16.634	122.140	567.125	31.855 187.635 645.648

Ge: Numerical Solution of Equation 3.1.13, Part D

		3x3 Determinant								
\mathcal{H} (kgauss)	Δ'	ϵ_1	ϵ_2	ϵ_3	ϵ_4	ϵ_5	ϵ_6	ϵ_7	ϵ_8	ϵ_9
1	25×10^3	6.157	65.406	25016.						
2.5	10	6.155	65.353	10016.						
5.0	5	6.152	65.263	5016.2						
10	2.5	6.147	65.081	2516.4						
15	1.66	6.141	64.893	1676.6						

6x6 Determinant							
1	6.049	65.584	25016.0	20.943	155.901	25069.1	
2.5	6.047	65.530	10016.1	20.939	155.472	10069.5	
5.0	6.044	65.440	5016.18	20.932	154.748	5070.25	
10	6.037	65.256	2516.37	20.919	153.263	2571.75	
15	6.030	65.067	1676.57	20.905	151.811	1733.32	
20	6.023	64.879	1266.76	20.891	150.149	1324.90	
30	6.008	64.489	852.59	20.861	146.869	912.212	
50	5.980	63.655	518.011	20.808	139.762	585.385	

9x9 Determinant									
	$\epsilon_{2-(1,3)}$	$\epsilon_{2+(1,3)}$		$\epsilon_{2-(5,7)}$	$\epsilon_{2+(5,7)}$				
2.5	6.046	65.532	10016.1	20.397	155.618	10069.5	35.790	245.448	10123.6
10	6.035	65.259	2516.37	20.365	153.411	2571.75	35.754	239.345	2629.71
15	6.028	65.070	1676.57	20.343	151.859	1733.32	35.729	235.002	1794.09
20	6.021	64.881	1266.76	20.321	150.296	1324.89	35.705	230.603	1388.52
30	6.006	64.491	852.159	20.278	147.014	913.196	35.651	221.355	982.843
50	5.978	63.657	518.011	20.190	139.893	585.347	35.559	201.859	667.508

APPENDIX 4

Si: Numerical Solution of Equation 3.1.8, Part A

		5x5 Determinant													
\mathcal{H} (kgauss)	Δ'	ϵ_1	ϵ_2	ϵ_3	ϵ_4	ϵ_5	ϵ_6	ϵ_7	ϵ_8	ϵ_9	ϵ_{10}	ϵ_{11}	ϵ_{12}	ϵ_{13}	ϵ_{14}
1	3.8×10^3	1.626	3802.49	7.645	19.325	3818.51									
2.5	1.52	1.625	1522.49	7.639	19.300	1538.54									
		8x8 Determinant													
1	3.8×10^3	1.625	3802.49	7.385	20.531	3818.51	16.355	41.489	3834.57						
2.5	1.52	1.624	1522.49	7.376	20.504	1538.55	16.339	41.367	1554.11						
		11x11 Determinant													
		$\epsilon_{1+}(0)$	$\epsilon_{1-}(2,4)$	$\epsilon_{1+}(2,4)$	$\epsilon_{1-}(6,8)$	$\epsilon_{1+}(6,8)$	$\epsilon_{1-}(10,12)$	$\epsilon_{1+}(10,12)$							
1	3.8×10^3	1.625	3802.49	7.378	20.021	3818.51	15.732	41.572	3834.59	27.420	64.248	3850.69			
2.5	1.52	1.624	1522.49	7.369	19.991	1538.55	15.707	41.453	1554.75	27.390	63.999	1571.00			
5.0	.76	1.623	762.488	7.354	19.942	778.618	15.665	41.254	795.022	27.341	63.496	811.519			
10	.38	1.621	382.491	7.324	19.843	398.752	15.581	40.851	415.558	27.244	62.472	432.583			
15	.253	1.619	255.495	7.294	19.745	271.886	15.499	40.442	289.094	27.148	61.428	306.672			
20	.190	1.618	192.499	7.265	19.647	209.018	15.418	40.033	226.520	27.053	60.386	244.764			
30	.127	1.614	129.507	7.208	19.454	146.278	15.261	39.213	164.645	26.870	58.332	183.938			
50	.076	1.607	78.523	7.096	19.071	95.791	14.961	37.580	115.587	26.517	54.500	137.087			
		14x14 Determinant													
20		1.618	192.499	7.265	19.563	209.018	15.356	40.327	226.624	24.882	60.246	245.311	36.638	79.909	264.435
30		1.614	129.507	7.208	19.358	146.278	15.183	39.533	164.656	24.535	58.266	184.576	36.365	76.155	205.455
50		1.607	78.523	7.096	18.954	95.792	14.847	37.994	115.625	23.889	54.504	137.662	35.813	69.762	161.623

Si: Numerical Solution of Equation 3.1.8, Part B

5x5 Determinant

\mathcal{H} (kgauss)	ϵ_1	ϵ_2	ϵ_3	ϵ_4	ϵ_5	ϵ_6	ϵ_7	ϵ_8	ϵ_9	ϵ_{10}	ϵ_{11}	ϵ_{12}	ϵ_{13}	ϵ_{14}
1	4.858	3806.49	10.445	24.729	3822.52									
2.5	4.856	1526.49	10.435	24.687	1542.57									

8x8 Determinant

1	4.850	3806.49	10.015	25.385	3822.53	19.382	47.162	3838.60
2.5	4.848	1526.49	10.002	25.342	1542.59	19.362	47.004	1558.77

11x11 Determinant

			$\epsilon_{1-}(3,5)$	$\epsilon_{1+}(3,5)$		$\epsilon_{1-}(7,9)$	$\epsilon_{1+}(7,9)$		$\epsilon_{1-}(11,13)$	$\epsilon_{1+}(11,13)$	
1	4.849	3806.49	10.001	24.927	3822.53	18.382	47.133	3838.62	30.086	70.036	3854.73
2.5	4.848	1526.49	9.987	24.884	1542.59	18.348	46.980	1558.82	30.052	69.680	1575.09
5.0	4.845	766.495	9.964	24.812	799.165	18.292	46.723	782.694	29.996	69.079	815.707
10	4.839	386.506	9.918	24.669	402.902	18.180	46.202	419.846	29.884	67.855	436.970
15	4.833	259.517	9.873	24.525	276.111	18.069	45.673	293.525	29.774	66.607	311.266
20	4.827	196.528	9.828	24.383	213.316	17.960	45.142	231.191	29.665	65.362	249.567
30	4.816	133.551	9.741	24.100	150.721	17.751	44.081	169.485	29.454	62.922	189.150
50	4.794	82.598	9.567	23.536	100.514	17.350	41.982	120.907	29.049	58.462	143.011

14x14 Determinant

30	4.816	133.551	9.739	23.890	150.721	17.604	44.233	169.502	26.887	62.834	189.791	39.067	80.394	211.111
50	4.794	82.598	9.565	23.303	100.514	17.141	42.146	120.960	26.156	58.458	143.491	38.569	73.365	168.078

Si: Numerical Solution of Equation 3.1.8, Part C

3x3 Determinant

\mathcal{H} (kgauss)	ϵ_1	ϵ_2	ϵ_3	ϵ_4	ϵ_5	ϵ_6	ϵ_7	ϵ_8	ϵ_9	ϵ_{10}	ϵ_{11}	ϵ_{12}
1	1.539	9.341	3810.49									
2.5	1.537	9.336	1530.50									
5.0	1.534	9.328	770.506									

6x6 Determinant

1	1.509	8.650	3810.49		13.301	30.253	3826.53	
2.5	1.507	8.645	1530.50		12.288	30.189	1546.61	

9x9 Determinant

1	1.509	8.606	3810.49		12.704	30.636	3826.54		22.132	52.858	3842.62	
2.5	1.506	8.600	1530.50		12.686	30.572	1546.64		22.109	52.658	1562.84	

12x12 Determinant

	$\epsilon_{1-}(0,2)$	$\epsilon_{1+}(0,2)$		$\epsilon_{1-}(4,6)$	$\epsilon_{1+}(4,6)$		$\epsilon_{1-}(8,10)$	$\epsilon_{1+}(8,10)$		$\epsilon_{1-}(12,14)$	$\epsilon_{1+}(12,14)$	
2.5	1.506	8.599	1530.50	12.657	29.898	1546.64	20.786	52.533	1562.91	32.897	75.365	1579.19
5.0	1.503	8.589	770.519	12.625	29.803	786.786	20.716	52.211	803.326	32.825	74.658	819.911
10	1.495	8.569	390.554	12.562	29.613	407.087	20.578	51.557	424.168	32.683	73.214	441.391
15	1.488	8.550	263.589	12.499	29.421	280.387	20.442	50.890	298.008	32.541	71.741	315.915
20	1.481	8.532	200.624	12.437	29.230	217.683	20.309	50.221	235.830	32.403	70.276	254.445
30	1.468	8.495	137.694	12.314	28.847	155.265	20.052	48.885	174.421	32.136	67.422	194.473
50	1.442	8.424	86.833	12.071	28.071	105.397	19.566	46.270	126.364	31.633	62.319	149.081

Si: Numerical Solution of Equation 3.1.8, Part D

3x3 Determinant

\mathcal{H} (kgauss)	ϵ_1	ϵ_2	ϵ_3	ϵ_4	ϵ_5	ϵ_6	ϵ_7	ϵ_8	ϵ_9	ϵ_{10}	ϵ_{11}	ϵ_{12}
1	4.738	14.135	3814.50									
2.5	4.734	14.123	1534.51									
5.0	4.727	14.102	774.539									

6x6 Determinant

1	4.617	12.720	3814.50	16.500	35.848	3830.55
2.5	4.612	12.709	1534.52	16.483	35.758	1550.65

9x9 Determinant

1	4.616	12.501	3814.50	15.848	36.060	3830.57	24.787	58.511	3846.56
2.5	4.610	12.487	1534.52	15.826	35.971	1550.69	24.761	58.324	1566.91

12x12 Determinant

	$\epsilon_{1-}(1,3)$	$\epsilon_{1+}(1,3)$		$\epsilon_{1-}(5,7)$	$\epsilon_{1+}(5,7)$		$\epsilon_{1-}(9,11)$	$\epsilon_{1+}(9,11)$		$\epsilon_{1-}(13,15)$	$\epsilon_{1+}(13,15)$	
2.5	4.610	12.477	1534.52	15.781	36.668	1550.69	23.159	58.102	1566.99	34.119	81.052	1583.30
5.0	4.602	12.452	774.560	15.741	36.538	790.895	23.077	57.707	807.504	34.036	80.229	824.132
10	4.585	12.402	394.636	15.661	36.278	411.305	22.913	56.903	428.525	33.868	78.546	445.899
15	4.568	12.353	267.712	15.581	36.021	284.715	22.752	56.082	302.542	33.696	76.829	320.621
20	4.551	12.304	207.787	15.502	35.769	222.119	22.595	55.258	240.537	33.522	75.125	259.401
30	4.519	12.209	141.936	15.346	33.162	159.911	22.293	53.615	179.952	35.287	71.832	199.909
50	4.457	12.023	91.231	15.039	32.360	110.435	21.726	50.444	131.951	34.436	66.083	155.287

Si: Numerical Solution of Equation 3.1.13, Part A

4x4 Determinant

\mathcal{H} (kgauss)	ϵ_1	ϵ_2	ϵ_3	ϵ_4	ϵ_5	ϵ_6	ϵ_7	ϵ_8	ϵ_9	ϵ_{10}	ϵ_{11}	ϵ_{12}	ϵ_{13}
1	2.132	6.623	22.644	3809.53									
2.5	2.131	6.622	22.620	1529.56									

7x7 Determinant

1	2.129	6.476	23.640	3809.53	15.186	44.995	3825.00
2.5	2.128	6.474	23.618	1529.56	15.175	44.877	1545.73

10x10 Determinant

	$\epsilon_{2+}(0)$	$\epsilon_{2-}(2,4)$	$\epsilon_{2+}(2,4)$		$\epsilon_{2-}(6,8)$	$\epsilon_{2+}(6,8)$		$\epsilon_{2-}(10,12)$	$\epsilon_{2+}(10,12)$	
1	2.129	6.473	23.002	3809.53	14.675	45.713	3825.60	25.643	67.698	3841.73
2.5	2.128	6.471	22.976	1592.56	14.654	45.599	1545.73	25.623	67.407	1562.05
5.0	2.127	6.466	22.933	769.601	14.619	45.404	785.952	25.590	66.911	802.593
10	2.124	6.456	22.846	389.688	14.549	44.999	406.402	25.523	65.875	423.732
15	2.121	6.447	22.756	262.779	14.479	44.574	279.869	25.454	64.784	297.932
20	2.118	6.438	22.666	199.871	14.409	44.134	217.346	25.385	63.659	236.170
30	2.113	6.415	22.479	137.062	14.271	43.206	155.335	25.245	61.331	175.734
50	2.102	6.382	22.076	86.483	13.995	41.174	106.467	24.954	56.627	129.935

13x13 Determinant

5.0	2.127	6.466	22.548	769.601	14.591	45.588	785.952	24.618	67.450	802.582	34.707	89.069	819.528
10	2.124	6.456	22.420	389.688	14.516	45.185	406.402	24.503	66.459	423.690	34.594	87.104	441.685
15	2.121	6.447	22.289	262.779	14.440	44.761	279.869	24.390	65.407	297.839	34.481	85.036	316.969
20	2.118	6.438	22.158	199.871	14.365	44.322	217.346	24.277	64.314	236.010	34.369	82.926	256.313
30	2.113	6.419	21.892	137.062	14.215	43.399	155.334	24.056	62.033	175.409	34.145	78.716	198.034
50	2.102	6.382	21.347	86.483	13.910	41.394	106.463	23.612	57.387	129.276	33.686	71.093	155.692

Si: Numerical Solution of Equation 3.1.13, Part B

70
(kgauss) ϵ_1 ϵ_2 ϵ_3 ϵ_4 ϵ_5 ϵ_6 ϵ_7 ϵ_8 ϵ_9 ϵ_{10} ϵ_{11} ϵ_{12} ϵ_{13}

1 6.112 | 9.654 28.170 3813.55 |
2.5 6.109 | 9.654 28.130 1533.59 |

7x7 Determinant

1 6.080 | 9.425 29.061 3813.55 | 17.723 50.651 3829.63 |
2.5 6.076 | 9.422 29.023 1533.59 | 17.709 50.497 1549.80 |

10x10 Determinant

	$\epsilon_{2+}(1)$	$\epsilon_{2-}(3,5)$	$\epsilon_{2+}(3,5)$		$\epsilon_{2-}(7,9)$	$\epsilon_{2+}(7,9)$		$\epsilon_{2-}(11,13)$	$\epsilon_{2+}(11,13)$	
1	6.079	9.418	29.680	3813.55	17.036	51.319	3829.63	26.873	73.401	3845.77
2.5	6.076	9.414	29.646	1533.59	17.010	51.171	1549.80	26.842	73.054	1566.15
5.0	6.070	9.408	29.588	773.663	16.965	50.918	790.083	26.791	72.461	806.798
10	6.058	9.395	29.470	393.814	16.877	50.392	410.670	26.688	71.223	428.159
15	6.046	9.383	29.348	266.969	16.788	49.837	284.278	26.582	69.919	302.596
20	6.034	9.370	29.224	204.129	16.700	49.261	221.900	26.475	68.575	241.077
30	6.010	9.346	28.968	141.460	16.526	48.049	160.187	26.256	65.817	181.127
50	5.963	9.297	28.422	91.188	16.180	45.429	111.927	25.780	60.384	136.174

13x13 Determinant

5.0	6.070	9.408	29.243	773.663	16.920	51.084	790.083	25.539	72.948	806.784	37.240	94.588	823.809
10	6.058	9.395	29.103	393.814	16.822	50.557	410.670	25.353	71.767	428.102	37.121	92.339	446.276
15	6.046	9.383	28.958	266.969	16.724	50.001	284.278	25.168	70.513	302.470	37.002	89.976	321.890
20	6.034	9.370	28.810	204.129	16.626	49.425	221.900	24.985	69.211	240.862	36.884	87.576	261.566
30	6.010	9.345	28.503	141.460	16.431	48.214	160.185	24.628	66.508	180.700	36.649	82.840	203.903
50	5.963	9.296	27.832	91.188	16.040	45.611	111.920	23.940	61.137	135.343	36.172	74.509	162.426

Si: Numerical Solution of Equation 3.1.13, Part C

3x3 Determinant

\mathcal{H} (kgauss)	ϵ_1	ϵ_2	ϵ_3	ϵ_4	ϵ_5	ϵ_6	ϵ_7	ϵ_8	ϵ_9	ϵ_{10}	ϵ_{11}	ϵ_{12}
1	1.221	11.892	3801.52									
2.5	1.221	11.888	1521.52									
5.0	1.220	11.882	761.530									

6x6 Determinant

1	1.201	13.569	3801.52	9.667	33.747	3817.56	
2.5	1.201	13.567	1521.52	9.660	33.686	1537.63	

9x9 Determinant

1	1.201	13.318	3801.52	9.504	34.569	3817.56	20.246	56.321	3833.66	
2.5	1.200	13.313	1521.52	9.494	34.509	1537.63	20.230	56.127	1553.87	

12x12 Determinant

	$\epsilon_{2-}(0,2)$ $\epsilon_{2+}(0,2)$			$\epsilon_{2-}(4,6)$ $\epsilon_{2+}(4,6)$			$\epsilon_{2-}(8,10)$ $\epsilon_{2+}(8,10)$			$\epsilon_{2-}(12,14)$ $\epsilon_{2+}(12,14)$		
2.5	1.200	13.297	1521.52	9.489	34.821	1537.63	19.348	56.751	1553.87	29.640	78.704	1570.26
5.0	1.199	13.287	761.530	9.472	34.723	777.742	19.294	56.433	794.232	29.589	78.005	811.023
10	1.197	13.267	381.543	9.438	34.521	397.974	19.186	55.768	414.974	29.487	76.545	432.627
15	1.195	13.247	254.558	9.404	34.311	271.215	19.078	55.066	288.743	29.383	75.006	307.323
20	1.193	13.227	191.572	9.369	34.095	208.460	18.971	54.337	226.529	29.279	73.426	246.069
30	1.189	13.185	128.602	9.301	33.645	145.971	18.762	52.803	165.151	29.068	70.208	186.643
50	1.181	13.096	77.668	9.163	32.664	96.089	18.351	49.544	117.557	28.622	64.040	142.554

Si: Numerical Solution of Equation 3.1.13, Part D

3x3 Determinant

\mathcal{H} (kgauss)	ϵ_1	ϵ_2	ϵ_3	ϵ_4	ϵ_5	ϵ_6	ϵ_7	ϵ_8	ϵ_9	ϵ_{10}	ϵ_{11}	ϵ_{12}
1	3.910	17.198	3805.52									
2.5	3.910	17.186	1525.54									

6x6 Determinant

1	3.841	18.395	3805.52	12.565	39.359	3821.58	
2.5	3.839	18.386	1525.54	12.555	39.271	1541.68	

9x9 Determinant

1	3.840	18.090	3805.52	12.225	40.126	3821.58	22.817	62.004	3837.69
2.5	3.838	18.077	1525.54	12.210	40.041	1541.68	22.799	61.764	1557.96

12x12 Determinant

	$\epsilon_{2-}(1,3)$ $\epsilon_{2+}(1,3)$			$\epsilon_{2-}(5,7)$ $\epsilon_{2+}(5,7)$			$\epsilon_{2-}(9,11)$ $\epsilon_{2+}(9,11)$			$\epsilon_{2-}(13,15)$ $\epsilon_{2+}(13,15)$		
2.5	3.838	18.027	1525.54	12.196	40.263	1541.68	21.750	62.337	1557.95	32.223	84.355	1574.38
5.0	3.836	18.002	765.557	12.170	40.120	781.838	21.687	61.945	798.398	32.170	83.542	815.266
10	3.831	17.950	385.598	12.115	39.824	402.170	21.564	61.125	419.314	32.063	81.839	437.135
15	3.826	17.896	258.641	12.060	39.515	275.514	21.441	60.257	293.263	31.956	80.046	312.113
20	3.821	17.842	195.685	12.005	39.196	212.866	21.320	59.355	231.232	31.849	78.210	251.148
30	3.811	17.729	132.776	11.895	38.526	150.596	21.085	57.465	170.226	31.634	74.506	192.280
50	3.792	17.481	81.977	11.674	37.061	101.183	20.634	53.526	123.344	31.187	67.606	149.064

APPENDIX 5

Ge: Numerical Solutions for $d = 0$

Solution of Eq. 4.1.7	5x5 Determinant	$\epsilon_{2+}(0)$	$\epsilon_{2-}(2,4)$	$\epsilon_{1-}(1,3)$	$\epsilon_{1+}(1,3)$	$\epsilon_{2+}(2,4)$	$\epsilon_{1-}(5,7)$	$\epsilon_{2-}(6,8)$						
	9x9 Determinant	3.694	10.163	9.269	51.131	88.018								
	13x13 Determinant	3.691	9.974	9.076	51.165	88.184	24.612	24.661	141.547	178.966				
		3.691	9.970	9.073	51.168	88.185	23.853	23.974	141.473	179.102	39.538	39.652	232.780	270.214
Solution of Eq. 4.1.8	6x6 Determinant	$\epsilon_{1+}(0)$	$\epsilon_{2+}(1)$	$\epsilon_{2-}(3,5)$	$\epsilon_{1-}(2,4)$	$\epsilon_{1+}(2,4)$	$\epsilon_{2+}(3,5)$							
	10x10 Determinant	2.662	21.917	13.362	13.314	73.501	110.694							
	14x14 Determinant	2.661	21.881	13.043	13.047	73.501	110.853	28.388	28.385	164.329	201.763			
		2.661	21.878	13.036	13.039	73.500	110.855	27.538	27.451	164.228	201.888	43.426	43.285	255.619
Solution of Eq. 4.1.9	7x7 Determinant	$\epsilon_{2-}(0,2)$	$\epsilon_{1+}(1)$	$\epsilon_{2+}(0,2)$	$\epsilon_{1-}(3,5)$	$\epsilon_{2-}(4,6)$	$\epsilon_{1+}(3,5)$	$\epsilon_{2+}(4,6)$						
	11x11 Determinant	2.058	11.191	43.310	17.385	17.210	96.100	133.423						
		2.057	11.178	43.317	16.946	16.806	96.074	133.576	32.069	32.149	187.133	224.572		
Solution of Eq. 4.1.10	8x8 Determinant	$\epsilon_{1-}(0,2)$	$\epsilon_{2-}(1,3)$	$\epsilon_{1+}(0,2)$	$\epsilon_{2+}(1,3)$	$\epsilon_{1-}(4,6)$	$\epsilon_{2-}(5,7)$	$\epsilon_{1+}(4,6)$	$\epsilon_{2+}(5,7)$					
	12x12 determinant	4.431	6.051	29.655	65.619	20.717	20.946	118.797	156.114					
		4.430	6.049	29.621	65.622	20.138	20.409	118.747	156.330	35.802	35.914	209.951	247.389	

Ge: Numerical Solutions for $d = 0$

R. R. Goodman's (3) Parameters

		$\epsilon_{2+}(0)$	$\epsilon_{2-}(2,4)$	$\epsilon_{1-}(1,3)$	$\epsilon_{1+}(1,3)$	$\epsilon_{2+}(2,4)$	$\epsilon_{1-}(5,7)$	$\epsilon_{2-}(6,8)$					
Solution of Eq. 4.1.7	5x5 Determinant	2.464	11.180	10.251	51.449	85.856							
	9x9 Determinant	2.454	10.716	9.791	51.555	86.281	26.541	26.659	140.994	175.807			
	13x13 Determinant	2.454	10.694	9.773	51.593	86.295	24.952	24.974	140.814	176.139	43.025	43.389	231.378 266.118

		$\epsilon_{1+}(0)$	$\epsilon_{2+}(1)$	$\epsilon_{1-}(2,4)$	$\epsilon_{2-}(3,5)$	$\epsilon_{1+}(2,4)$								
Solution of Eq. 4.1.8	6x6 Determinant	2.456	21.322	14.631	13.599	73.613	108.279							
	10x10 Determinant	2.453	21.116	13.891	13.047	73.622	108.681	30.692	30.875	163.558	198.363			
	14x14 Determinant	2.453	21.088	13.852	13.019	73.629	108.693	28.788	28.778	163.310	196.663	47.663	47.224	254.015 288.726

		$\epsilon_{2-}(0,2)$	$\epsilon_{1+}(1)$	$\epsilon_{2+}(0,2)$	$\epsilon_{2-}(4,6)$	$\epsilon_{1-}(3,5)$	$\epsilon_{1+}(3,5)$						
Solution of Eq. 4.1.9	7x7 Determinant	2.354	11.109	42.010	18.279	19.100	95.991	130.757					
	11x11 Determinant	2.352	11.062	42.091	17.357	18.087	95.935	131.139	39.626	35.069	186.147	220.935	

		$\epsilon_{1-}(0,2)$	$\epsilon_{2-}(1,3)$	$\epsilon_{1+}(0,2)$	$\epsilon_{2+}(1,3)$	$\epsilon_{1-}(4,6)$	$\epsilon_{2-}(5,7)$						
Solution of Eq. 4.1.10	8x8 Determinant	5.158	6.501	30.438	63.998	22.138	22.432	118.465	153.269				
	12x12 Determinant	5.152	6.492	30.263	64.018	20.883	21.196	118.349	153.629	38.844	39.299	208.755	243.521

Si: Numerical Solutions for $d = 0$

		$\epsilon_{2+}(0)$	$\epsilon_{1-}(1,3)$	$\epsilon_{2-}(2,4)$	$\epsilon_{1+}(1,3)$	$\epsilon_{2+}(2,4)$	$\epsilon_{1-}(5,7)$	$\epsilon_{2-}(6,8)$						
Solution	5x5 Determinant	2.132	4.741	6.623	14.143	22.659								
of	9x9 Determinant	2.130	4.621	6.478	12.727	23.655	16.512	15.194	35.908	45.073				
Eq. 4.1.7	13x13 Determinant	2.130	4.619	6.475	12.511	23.019	15.863	14.689	36.120	45.789	24.805	25.657	58.735	67.889
		$\epsilon_{1+}(0)$	$\epsilon_{2+}(1)$	$\epsilon_{1-}(2,4)$	$\epsilon_{2-}(3,5)$	$\epsilon_{1+}(2,4)$	$\epsilon_{2+}(3,5)$							
Solution	6x6 Determinant	1.626	6.114	7.650	9.654	19.341	28.197							
of	10x10 Determinant	1.625	6.082	7.391	9.428	20.549	29.087	16.366	17.732	41.571	50.752			
Eq. 4.1.8	14x14 Determinant	1.625	6.082	7.384	9.420	20.041	29.702	15.749	17.054	41.651	51.417	26.893	27.440	64.496 73.688
		$\epsilon_{2-}(0,2)$	$\epsilon_{1+}(1)$	$\epsilon_{2+}(0,2)$	$\epsilon_{1-}(3,5)$	$\epsilon_{2-}(4,6)$	$\epsilon_{1+}(3,5)$	$\epsilon_{2+}(4,6)$						
Solution	7x7 Determinant	1.202	4.859	13.571	10.451	9.672	24.757	33.788						
of	11x11 Determinant	1.201	4.851	13.321	10.024	9.511	25.414	34.609	19.395	20.256	47.267	56.449		
Eq. 4.1.9	15x15 Determinant	1.201	4.851	13.307	10.010	9.506	24.956	34.917	18.405	19.402	47.234	57.061	29.691 30.108 70.271 79.379	
		$\epsilon_{1-}(0,2)$	$\epsilon_{2-}(1,3)$	$\epsilon_{1+}(0,2)$	$\epsilon_{2+}(1,3)$	$\epsilon_{1-}(4,6)$	$\epsilon_{2-}(5,7)$	$\epsilon_{1+}(4,6)$	$\epsilon_{2+}(5,7)$					
Solution	8x8 Determinant	1.510	3.842	8.653	18.402	12.572	13.309	30.295	39.417					
of	12x12 Determinant	1.510	3.841	8.609	18.098	12.716	12.236	30.678	40.182	22.147	22.828	52.991	62.162	
Eq. 4.1.10														

APPENDIX 6

Ge: Numerical Solution of Equation 4.1.7, Assuming $\delta = 0$

9x9 Determinant

d	$\epsilon_{2+}(0)$	$\epsilon_{2-}(2,4)$	$\epsilon_{1-}(1,3)$	$\epsilon_{1+}(1,3)$	$\epsilon_{2+}(2,4)$	$\epsilon_{1-}(5,7)$	$\epsilon_{2-}(6,8)$	$\epsilon_{1+}(5,7)$	$\epsilon_{2+}(6,8)$
0.0	3.875	9.985	9.269	51.131	88.015	24.535	24.679	141.465	178.921
0.1	3.897	10.137	9.118	51.259	88.150	24.358	24.850	141.600	179.057
0.2	3.961	10.432	8.826	51.643	88.554	24.119	25.067	142.004	179.465
0.3	4.069	10.757	8.510	52.282	89.227	23.874	25.279	142.678	180.145
0.4	4.219	11.083	8.200	53.176	90.165	23.627	25.483	143.620	181.095
0.5	4.413	11.401	7.911	54.321	91.367	23.382	25.678	144.827	182.313
0.6	4.649	11.710	7.650	55.716	92.828	23.142	25.865	146.298	183.798
0.7	4.929	12.009	7.425	57.357	94.544	22.912	26.045	148.032	185.547
0.8	5.251	12.301	7.239	59.243	96.513	22.694	26.220	150.023	187.559
0.9	5.617	12.589	7.099	61.369	98.728	22.491	26.393	152.271	189.829
1.0	6.025	12.877	7.006	63.731	101.186	22.308	26.565	154.772	192.355
1.2	6.977	13.470	6.971	69.153	106.816	22.014	26.919	160.520	198.163
1.4	8.089	14.115	7.169	75.483	113.373	21.838	27.306	167.242	204.958
1.6	9.379	14.859	7.592	82.701	120.832	21.801	27.752	174.915	212.716
1.8	10.841	15.720	8.250	90.791	129.175	21.926	28.280	183.515	221.415
2.0	12.475	16.728	9.145	99.742	138.385	22.227	28.913	193.024	231.035
2.3	15.249	18.553	10.926	114.770	153.807	23.039	30.105	208.957	247.155
2.6	18.409	20.791	13.224	131.711	171.138	24.312	31.637	226.855	265.260
2.9	21.957	23.467	16.026	150.562	190.369	26.067	33.553	246.688	285.316
3.3	27.289	27.735	20.518	178.679	218.964	29.178	36.760	276.109	315.049
3.7	32.810	33.177	25.847	210.218	250.941	33.309	40.758	308.910	348.171
4.1	40.017	38.690	31.984	245.195	286.316	38.062	45.574	345.082	384.666
4.6	49.369	47.154	40.757	293.777	335.337	45.398	52.763	395.043	435.020
5.1	59.796	56.836	50.720	347.785	389.723	54.073	61.253	450.292	490.645
5.7	73.728	70.028	64.212	419.786	462.110	66.207	73.141	523.608	564.380
6.3	89.208	84.905	79.346	499.660	542.305	80.171	86.856	604.617	645.771
7.0	109.225	104.354	98.714	602.823	645.775	99.047	105.119	708.908	750.459
7.8	134.681	128.909	124.227			122.798	129.298		
8.7	166.609	160.778	155.920			153.492	159.310		
9.7	206.169	199.958	195.285			191.973	197.513		
10.8	254.651	248.122	243.607			239.532	244.816		
12.0	313.475	306.683	302.300			297.576	302.633		
13.3	384.188	377.181	372.908			367.640	372.497		
14.7	468.468	461.285	457.103			451.381	456.067		
16.3	575.108	567.774	563.670			557.551	562.083		
18.1	708.236	700.775	696.737			690.281	694.679		
	$\epsilon_{2+}(0)$	$\epsilon_{2-}(3,4)$	$\epsilon_{1-}(1,2)$	$\epsilon_{1+}(1,2)$	$\epsilon_{2+}(3,4)$	$\epsilon_{1-}(5,6)$	$\epsilon_{2-}(7,8)$	$\epsilon_{1+}(5,6)$	$\epsilon_{2+}(7,8)$

Ge: Numerical Solution of Equation 4.1.8 Assuming $\delta = 0$

6x6 Determinant

d	$\epsilon_{1+}(0)$	$\epsilon_{2+}(1)$	$\epsilon_{2-}(3,5)$	$\epsilon_{1-}(2,4)$	$\epsilon_{1+}(2,4)$	$\epsilon_{2+}(3,5)$
0.0	2.725	21.525	13.715	13.310	73.490	110.685
0.1	2.742	21.640	13.883	13.138	73.622	110.821
0.2	2.795	21.983	14.159	12.851	74.018	111.227
0.3	2.883	22.555	14.444	12.552	74.677	111.903
0.4	3.009	23.353	14.723	12.257	75.597	112.847
0.5	3.172	24.378	14.994	11.975	76.776	114.056
0.6	3.375	25.627	15.255	11.711	78.211	115.528
0.7	3.618	27.100	15.508	11.472	79.899	117.258
0.8	3.903	28.795	15.855	11.261	81.836	119.244
0.9	4.231	30.711	15.999	11.084	84.019	121.482
1.0	4.602	32.848	16.244	10.944	86.445	123.967
1.2	5.477	37.781	16.751	10.791	92.008	129.666
1.4	6.530	43.592	17.308	10.825	98.499	136.312
1.6	7.764	50.278	17.947	11.064	105.894	143.879
1.8	9.177	57.841	18.697	11.520	114.173	152.347
2.0	10.769	66.281	19.581	12.200	123.323	161.170
2.3	13.491	20.587	21.203	13.648	138.658	177.347
2.6	16.610	96.872	23.221	15.612	155.908	194.923
2.9	20.125	115.137	25.667	18.090	175.061	214.406
3.3	25.424	142.574	29.625	22.175	203.560	243.336
3.7	31.419	173.539	34.398	27.132	235.449	275.637
4.1	38.107	208.035	39.988	32.934	270.743	311.318
4.6	47.441	256.121	48.117	41.340	319.675	360.692
5.1	57.855	309.727	57.496	50.990	373.984	415.894
5.7	71.775	381.343	70.368	64.164	446.291	488.114
6.3	87.245	460.913	84.968	79.036	526.418	568.594
7.0	107.254	563.976	104.143	98.487	629.823	672.347
7.8	132.703		128.828	123.438		
8.7	164.624		160.073	154.930		
9.7	204.180		199.045	194.121		
10.8	252.659		247.030	242.298		
12.0	311.480		305.440	300.870		
13.3	382.191		375.811	371.379		
14.7	466.469		459.810	455.492		
16.3	573.107		566.206	561.989		
18.1	706.234		699.129	694.997		
	$\epsilon_{1+}(1)$	$\epsilon_{2+}(0,1)$	$\epsilon_{2-}(4,5)$	$\epsilon_{1-}(2,3)$	$\epsilon_{1+}(2,3)$	$\epsilon_{2+}(4,5)$

Ge: Numerical Solution of Equation 4.1.9, Assuming $\delta = 0$

7x7 Determinant

d	$\epsilon_{2-}(0,2)$	$\epsilon_{1+}(1)$	$\epsilon_{2+}(0,2)$	$\epsilon_{1-}(3,5)$	$\epsilon_{2-}(4,6)$	$\epsilon_{1+}(3,5)$	$\epsilon_{2+}(4,6)$
0.0	2.100	11.475	43.100	17.131	17.395	96.069	133.405
0.1	2.166	11.522	43.230	16.951	17.568	96.203	133.541
0.2	2.360	11.665	43.620	16.681	17.823	96.604	133.949
0.3	2.673	11.919	44.266	16.402	18.077	97.271	134.626
0.4	3.086	12.302	45.167	16.125	18.323	98.203	135.573
0.5	3.577	12.843	46.317	15.856	18.561	99.397	136.787
0.6	4.116	13.576	47.713	15.599	18.790	100.851	138.265
0.7	4.675	14.533	49.350	15.359	19.012	102.561	140.004
0.8	5.231	15.742	51.222	15.141	19.228	104.526	142.001
0.9	5.769	17.222	53.326	14.948	19.442	106.741	144.254
1.0	6.287	18.980	55.658	14.785	19.656	109.202	146.757
1.2	7.281	23.323	60.992	14.562	20.099	114.852	152.504
1.4	8.285	28.718	67.202	14.497	20.587	121.446	159.214
1.6	9.370	35.109	74.296	14.613	21.147	128.962	166.861
1.8	10.584	42.456	82.205	14.926	21.808	137.379	175.424
2.0	11.956	50.733	90.985	15.446	22.593	146.678	184.883
2.3	14.344	64.863	105.751	16.635	24.047	162.255	200.720
2.6	17.149	81.022	122.433	18.326	25.878	179.760	218.501
2.9	20.381	99.195	141.041	20.525	28.124	199.173	238.202
3.3	25.353	126.544	168.861	24.246	31.804	228.015	267.450
3.7	31.075	157.446	200.136	28.855	36.296	260.234	300.030
4.1	37.538	191.895	234.885	34.333	41.612	295.838	336.001
4.6	46.643	239.938	283.225	42.371	49.414	345.123	385.716
5.1	56.874	293.512	337.031	51.693	58.489	399.747	440.734
5.7	70.621	365.101	408.835	64.527	71.033	472.383	513.794
6.3	85.958	444.650	488.550	79.108	85.343	552.791	594.574
7.0	105.814	547.516	591.565	98.275	104.224	656.473	698.629
7.8	131.188	678.340	722.518	122.961	128.625	788.038	830.522
8.7	163.020	842.426	886.711	154.213	159.608	952.775	995.620
9.7	202.501	1045.741	1090.116	193.195	198.344	1156.648	1199.789
10.8	250.919			241.192	246.123		
12.0	309.691			299.613	304.356		
13.3	380.363			369.996	374.578		
14.7	464.609			454.005	458.451		
16.3	571.220			560.411	564.737		
18.1	704.324			693.342	697.566		
20.0	852.944			848.825	852.966		
	$\epsilon_{2-}(1,2)$	$\epsilon_{1+}(0)$	$\epsilon_{2+}(1,2)$	$\epsilon_{1-}(3,4)$	$\epsilon_{2-}(5,6)$	$\epsilon_{1+}(3,4)$	$\epsilon_{2+}(5,6)$

Ge: Numerical Solution of Equation 4.1.10, Assuming $\delta = 0$

8x8 Determinant

d	$\epsilon_{1-}(0,2)$	$\epsilon_{2-}(1,3)$	$\epsilon_{1+}(0,2)$	$\epsilon_{2+}(1,3)$	$\epsilon_{1-}(4,6)$	$\epsilon_{2-}(5,7)$	$\epsilon_{1+}(4,6)$	$\epsilon_{2+}(5,7)$
0.0	4.513	6.158	29.487	65.442	20.857	21.046	118.743	156.154
0.1	4.412	6.276	29.601	65.576	20.677	21.219	118.876	156.290
0.2	4.174	6.563	29.943	65.976	20.423	21.454	119.281	156.698
0.3	3.891	6.928	30.515	66.642	20.163	21.685	119.952	157.377
0.4	3.613	7.321	31.320	67.562	19.902	21.907	120.890	158.386
0.5	3.365	7.718	32.361	68.756	19.646	22.121	122.092	159.542
0.6	3.160	8.109	33.639	70.197	19.398	22.396	123.557	161.024
0.7	3.004	8.488	35.156	71.888	19.162	22.524	125.281	162.769
0.8	2.905	8.856	36.910	73.825	18.942	22.718	127.262	169.775
0.9	2.864	9.215	38.902	76.003	18.742	22.908	129.496	167.037
1.0	2.884	9.571	41.128	78.417	18.566	23.099	131.981	169.553
1.2	3.111	10.295	46.271	83.940	18.300	23.493	137.688	175.335
1.4	3.586	11.074	52.319	90.364	18.170	23.925	144.356	182.093
1.6	4.308	11.951	59.254	97.671	18.199	24.423	151.961	189.802
1.8	5.271	12.960	67.062	105.843	18.404	25.011	160.480	198.440
2.0	6.468	14.125	75.737	114.870	18.802	25.714	169.896	207.988
2.3	8.685	16.200	90.367	130.004	19.783	27.026	185.668	223.978
2.6	11.390	18.699	106.935	147.041	21.247	28.697	203.386	241.934
2.9	14.562	21.637	125.444	165.981	23.209	30.768	223.024	261.824
3.3	19.494	26.246	153.154	194.202	26.606	34.199	252.172	291.319
3.7	25.200	31.644	184.340	225.833	30.896	38.433	284.695	324.192
4.1	31.660	37.820	219.014	260.891	36.068	43.491	320.592	360.433
4.6	40.769	46.617	267.278	309.560	43.747	50.979	370.222	410.476
5.1	51.010	56.590	321.024	363.640	52.742	59.757	425.162	465.803
5.7	64.769	70.082	392.770	435.715	65.226	71.971	495.137	539.202
6.3	79.503	85.210	472.440	515.648	80.118	85.984	578.842	620.287
7.0	100.017	104.559	575.414	618.867	98.364	104.902	682.821	724.656
7.8	125.373	130.070	706.330	750.003	122.758	128.661	814.672	856.886
8.7	157.217	161.750	870.494	914.355	153.742	159.360	979.671	1022.243
9.7	196.708	201.102			192.485	197.839		
10.8	245.135	249.413			240.274	245.389		
12.0	303.914	308.097			298.519	303.423		
13.3	374.592	378.696			368.752	373.475		
14.7	458.843	462.883			452.636	457.205		
16.3	565.459	569.444			558.933	563.364		
18.1	698.566	702.506			691.771	696.083		
20.0	854.189	858.092			847.179	851.395		
	$\epsilon_{1-}(0,1)$	$\epsilon_{2-}(2,3)$	$\epsilon_{1+}(0,1)$	$\epsilon_{2+}(2,3)$	$\epsilon_{1-}(4,5)$	$\epsilon_{2-}(6,7)$	$\epsilon_{1+}(4,5)$	$\epsilon_{2+}(6,7)$

APPENDIX 7

Ge: Numerical Solution of Equation 4.1.7

5x5 Determinant

d	ϵ_1	ϵ_2	ϵ_3	ϵ_4	ϵ_5	ϵ_6	ϵ_7	ϵ_8	ϵ_9	ϵ_{10}	ϵ_{11}	ϵ_{12}	ϵ_{13}
0.0	3.694	10.163	9.269	51.131	88.018								
0.1	3.715	10.287	9.147	51.259	88.153								
0.2	3.776	10.552	8.888	51.643	88.557								
0.3	3.877	10.858	8.597	52.283	89.230								
0.4	4.019	11.170	8.309	53.177	90.168								
0.5	4.200	11.479	8.042	54.323	91.369								
4.1	40.054	38.674	31.957	245.200	286.316								
12.0	313.478	306.683	302.297										

9x9 Determinant

0.1	3.711	10.088	8.963	51.292	88.313	24.377	24.890	141.682	179.102				
0.2	3.772	10.338	8.728	51.675	88.722	24.115	25.133	142.087	179.510				
0.3	3.874	10.628	8.444	52.312	89.393	23.852	25.368	142.761	180.189				
0.4	4.015	10.927	8.170	53.202	90.329	23.590	25.593	143.703	181.138				
0.5	4.195	11.223	7.915	54.345	91.528	23.333	25.807	144.910	182.356				
4.1	40.054	38.816	31.938	245.199	286.369	37.710	45.687	345.137	384.671				
12.0	313.478	306.694	302.297			297.550	302.624						

13x13 Determinant

	$\epsilon_{2+}(0)$	$\epsilon_{2-}(2,4)$	$\epsilon_{1-}(1,3)$	$\epsilon_{1+}(1,3)$	$\epsilon_{2+}(2,4)$	$\epsilon_{1-}(5,7)$	$\epsilon_{2-}(6,8)$						
0.0	3.691	9.970	9.073	51.168	88.185	23.853	23.974	141.473	179.102	39.538	39.652	232.780	270.214
0.1	3.711	10.084	8.960	51.296	88.370	23.669	24.154	141.608	179.239	39.371	39.810	232.916	270.350
0.2	3.772	10.333	8.717	51.678	88.723	23.433	24.377	142.013	179.647	39.151	40.003	233.323	270.759
0.3	3.874	10.623	8.441	52.315	89.394	23.194	24.595	142.687	180.326	38.921	40.188	234.000	271.439
0.4	4.015	10.922	8.167	53.205	90.331	22.956	24.805	143.630	181.226	38.686	40.362	234.947	272.390
0.5	4.195	11.218	7.913	54.346	91.530	22.723	25.008	144.838	182.494	38.449	40.525	236.163	273.611
4.1	40.054	38.777	31.938	245.199	286.369	37.598	45.148	345.123	384.785	47.825	55.670	441.429	480.253
12.0	313.478	306.695	302.130			297.578	302.727			295.084	300.266		
	$\epsilon_{2+}(0)$	$\epsilon_{2-}(3,4)$	$\epsilon_{1-}(1,2)$	$\epsilon_{1+}(1,2)$	$\epsilon_{2+}(3,4)$	$\epsilon_{1-}(5,6)$	$\epsilon_{2-}(7,8)$						

Ge: Numerical Solution of Equation 4.1.8

6x6 Determinant

d	ϵ_1	ϵ_2	ϵ_3	ϵ_4	ϵ_5	ϵ_6
0.0	2.662	21.917	13.362	13.314	73.501	110.694
0.1	2.679	22.024	13.669	13.011	73.663	110.830
0.2	2.732	22.347	13.998	12.692	74.030	111.236
4.1	38.097	208.044	40.035	32.873	270.757	311.319
12.0	311.484		305.439	300.863		

Ge: Numerical Solution of Equation 4.1.8

10x10 Determinant

d	$\epsilon_{1+}(0)$	$\epsilon_{2+}(1)$	$\epsilon_{2-}(3,5)$	$\epsilon_{1-}(2,4)$	$\epsilon_{1+}(2,4)$	$\epsilon_{2+}(3,5)$				
0.0	2.661	21.881	13.043	13.047	73.500	110.853	28.388	28.385	164.329	201.763
0.1	2.679	21.989	13.359	12.734	73.632	110.988	28.623	28.142	164.465	201.899
0.2	2.731	22.313	13.673	12.430	74.028	111.394	28.851	27.892	164.870	202.307
0.3	2.819	22.856	13.981	12.137	74.686	112.069	29.070	27.640	165.546	202.987
0.4	2.943	23.620	14.281	11.858	75.606	113.012	29.277	27.327	166.489	203.937
0.5	3.105	24.605	14.569	11.596	76.784	114.220	29.474	27.140	167.700	205.156
0.6	3.307	25.800	14.846	11.356	78.219	115.689	29.662	26.913	169.176	206.642
0.7	3.548	27.334	15.112	11.141	79.907	117.418	29.842	26.580	170.915	208.393
0.8	3.831	28.952	15.369	10.956	81.844	119.402	30.022	26.393	172.915	210.407
0.9	4.157	30.880	15.621	10.804	84.028	121.637	30.147	26.185	175.172	212.681
1.0	4.525	32.977	15.872	10.688	86.453	124.120	30.326	25.992	177.685	215.213
1.2	5.392	37.875	16.389	10.581	92.017	129.813	30.655	25.666	183.463	221.039
1.4	6.435	43.663	16.955	10.660	98.509	136.453	31.004	25.447	190.225	227.860
1.6	7.651	50.334	17.603	10.945	105.904	144.014	31.339	25.356	197.949	235.655
1.8	9.033	57.886	18.361	11.455	114.185	152.475	31.866	25.415	206.613	244.401
2.0	10.565	66.318	19.255	12.215	123.335	161.818	32.429	25.640	216.196	254.078
2.3	12.990	80.615	20.890	13.985	138.671	177.460	33.498	26.319	232.259	270.302
2.6	16.767	96.894	22.918	15.311	155.921	195.027	34.889	27.442	250.308	288.533
2.9	20.197	115.155	25.370	17.888	175.074	214.502	36.651	29.037	270.306	308.731
3.3	25.454	142.588	29.322	22.028	203.573	243.422	39.636	31.929	299.964	338.674
3.7	31.426	173.550	34.054	27.014	235.461	275.715	43.401	35.734	333.013	372.022
4.1	38.091	208.044	39.493	32.835	270.755	311.388	47.981	40.541	369.435	408.748
4.6	48.249	256.128	47.397	41.257	319.686	360.752	54.876	46.955	419.703	459.394
5.1	57.968	309.732	57.349	50.916	373.994	415.448	63.082	55.469	475.247	515.304
5.7	71.814	381.348	70.246	64.097	446.299	488.160	74.651	67.318	548.892	589.365
6.3	87.768	460.917	84.832	78.968	526.425	568.635	88.079	81.005	630.202	671.059
7.0	107.272	563.800	103.970	98.391	629.829	672.382	106.056	99.277	734.805	776.068
7.8	132.715		128.527	123.502			129.653	122.901		
8.7	164.634		160.288	154.934			159.227	153.365		
9.7	204.187		199.118	194.118			197.281	191.588		
10.8	252.664		247.064	242.292			244.359	238.908		
12.0	311.484		305.458	300.865			301.958	296.743		
13.3	387.914		375.821	371.374			371.626	366.624		
14.7	466.472		459.816	455.488			455.026	450.211		
16.3	573.109		566.210	561.985			560.888	556.244		
	$\epsilon_{1+}(1)$	$\epsilon_{2+}(0,1)$	$\epsilon_{2-}(4,5)$	$\epsilon_{1-}(2,3)$	$\epsilon_{1+}(2,3)$	$\epsilon_{2+}(4,5)$				

14x14 Determinant

	$\epsilon_{1+}(0)$	$\epsilon_{2+}(1)$	$\epsilon_{2-}(3,5)$	$\epsilon_{1-}(2,4)$	$\epsilon_{1+}(2,4)$									
0.0	2.661	21.878	13.036	13.039	73.500	110.855	275.38	27.451	164.228	201.888	43.426	43.295	255.619	293.046
4.1	38.091	208.044	39.415	32.835	270.755	311.388	47.358	40.409	369.414	408.871	50.497	58.398	465.205	503.907

Ge: Numerical Solution of Equation 4.1.9

7x7 Determinant											
d	ϵ_1	ϵ_2	ϵ_3	ϵ_4	ϵ_5	ϵ_6	ϵ_7	ϵ_8	ϵ_9	ϵ_{10}	ϵ_{11}
0.0	2.058	11.191	43.310	17.385	17.210	96.100	133.423				
4.1	37.541	191.895	239.907	34.224	41.667	295.864	336.003				
11x11 Determinant											
	$\epsilon_{2-(0,2)}$	$\epsilon_{1+(1)}$	$\epsilon_{2+(0,2)}$	$\epsilon_{1-(3,5)}$	$\epsilon_{2-(4,6)}$	$\epsilon_{1+(3,5)}$	$\epsilon_{2+(4,6)}$				
0.0	2.057	11.178	43.317	16.946	16.806	96.074	133.576	32.069	32.149	187.133	224.572
0.1	2.122	11.224	43.445	16.593	17.156	96.207	133.712	31.872	32.338	187.268	224.708
0.2	2.314	11.368	43.830	16.323	17.418	96.608	134.119	31.633	32.553	187.674	225.116
0.3	2.623	11.520	44.469	16.057	17.676	97.275	134.796	31.389	32.758	188.350	225.796
0.4	3.030	11.998	45.361	15.802	17.925	98.207	135.742	31.142	32.953	189.296	226.746
0.5	3.512	12.524	46.501	15.570	18.166	99.402	136.955	30.895	33.137	190.509	227.966
0.6	4.041	13.207	47.885	15.386	18.401	100.857	138.431	30.651	33.311	191.988	229.453
0.7	4.589	13.983	49.511	15.350	18.632	102.568	140.170	30.413	33.476	193.731	231.207
0.8	5.134	15.899	51.372	14.440	18.866	104.534	142.166	30.184	33.634	195.736	233.224
0.9	5.661	17.163	53.465	14.450	19.127	106.750	144.416	29.966	33.781	198.000	235.502
1.0	6.169	18.625	55.787	14.363	19.593	109.212	146.918	29.762	33.933	200.522	238.040
1.2	7.151	23.374	61.103	14.218	19.612	114.864	152.661	29.413	34.228	206.323	243.881
1.4	8.147	28.727	67.298	14.206	20.140	121.461	159.366	29.164	34.541	213.118	250.726
1.6	9.226	35.123	74.359	14.366	20.715	128.979	167.009	29.018	34.888	220.885	258.553
1.8	10.433	42.460	82.277	14.719	21.394	137.397	175.507	29.017	35.314	229.601	267.340
2.0	11.794	50.736	91.049	15.279	22.192	146.698	185.020	29.170	35.822	239.247	277.069
2.3	14.151	64.864	105.803	16.537	23.665	162.276	200.849	29.722	36.794	255.423	293.386
2.6	16.875	81.023	122.478	18.341	25.513	179.782	218.622	30.697	38.071	273.604	311.728
2.9	19.839	99.196	141.075	20.834	27.772	199.196	238.315	32.125	39.704	293.751	332.055
3.3	25.461	126.544	168.892	23.931	31.461	228.038	267.534	34.773	42.499	323.626	362.190
3.7	31.106	157.446	200.163	28.638	35.945	260.256	300.125	38.303	46.059	356.905	395.745
4.1	37.537	191.895	234.907	34.160	41.213	295.859	336.087	42.752	50.423	393.564	432.689
4.6	46.616	239.938	283.243	42.230	48.763	345.142	385.793	49.745	57.044	444.122	483.612
5.1	56.803	293.512	337.046	51.572	58.537	399.765	440.080	57.174	64.977	499.960	539.797
	$\epsilon_{2-(1,2)}$	$\epsilon_{1+(0)}$	$\epsilon_{2+(1,2)}$	$\epsilon_{1-(3,4)}$	$\epsilon_{2-(5,6)}$	$\epsilon_{1+(3,4)}$	$\epsilon_{2+(5,6)}$				

Ge: Numerical Solution of Equation 4.1.10

8x8 Determinant

d	ϵ_1	ϵ_2	ϵ_3	ϵ_4	ϵ_5	ϵ_6	ϵ_7	ϵ_8	ϵ_9	ϵ_{10}	ϵ_{11}	ϵ_{12}
0.0	4.431	6.051	29.655	65.619	20.717	20.946	118.797	156.184				
4.1	31.653	37.847	219.014	260.928	35.887	43.570	320.632	360.438				

12x12 Determinant

	$\epsilon_{1-(0,2)}$	$\epsilon_{2-(1,3)}$	$\epsilon_{1+(0,2)}$	$\epsilon_{2+(1,3)}$	$\epsilon_{1-(4,6)}$	$\epsilon_{2-(5,7)}$	$\epsilon_{1+(4,6)}$	$\epsilon_{2+(5,7)}$				
0.0	4.430	6.049	29.621	65.622	20.138	20.409	118.747	156.330	35.802	35.914	209.951	247.389
0.1	4.332	6.162	29.731	65.755	19.988	20.558	118.882	156.466	35.627	36.080	210.086	247.525
0.2	4.101	6.440	30.062	66.153	19.755	20.790	119.286	156.873	35.399	36.282	210.483	247.934
0.3	3.826	6.794	30.619	66.816	19.513	21.029	119.957	157.552	35.163	36.476	211.170	248.613
0.4	3.555	7.174	31.405	67.740	19.274	21.264	120.896	158.500	34.924	36.659	212.116	249.564
0.5	3.313	7.559	32.423	68.922	19.041	21.493	122.099	159.716	34.686	36.832	213.331	250.785
0.6	3.113	7.938	33.661	70.358	18.816	21.715	123.565	161.198	34.466	36.996	214.812	252.273
0.7	2.963	8.307	35.218	72.043	18.605	21.929	125.291	162.242	34.170	37.153	216.559	254.028
0.8	2.868	8.667	36.904	73.974	18.410	22.137	127.273	164.946	33.956	37.339	218.857	256.048
0.9	2.831	9.020	38.946	76.145	18.234	22.340	129.509	167.208	33.738	37.414	230.838	258.330
1.0	2.854	9.370	41.156	78.554	18.081	22.542	131.995	169.723	33.531	37.557	223.365	260.871
1.2	3.085	10.088	46.285	84.064	17.862	22.955	137.705	175.502	33.163	37.827	229.186	266.726
1.4	3.565	10.865	52.327	90.478	17.775	23.404	144.376	182.257	32.879	38.110	236.007	273.590
1.6	4.290	11.742	59.258	97.778	17.845	23.917	151.984	189.962	32.701	38.428	243.808	281.444
1.8	5.255	12.751	67.064	105.937	18.090	24.521	160.506	198.597	32.648	38.806	252.568	290.266
2.0	6.454	13.915	75.738	114.956	18.526	25.239	169.924	208.140	32.790	39.265	262.267	300.037
2.3	8.673	15.985	90.367	130.079	19.563	26.574	185.699	224.128	33.181	40.150	278.540	316.435
2.6	11.379	18.466	106.935	147.107	21.088	28.266	203.418	242.071	34.025	41.325	296.836	334.876
2.9	14.553	21.359	124.444	166.039	23.131	30.355	223.057	261.954	35.307	42.847	317.115	355.318
3.3	19.486	25.755	153.154	194.252	26.782	33.805	252.205	291.439	37.738	45.462	347.185	385.625
3.7	25.193	31.765	184.339	225.876	30.492	38.047	284.727	324.303	41.030	48.830	380.675	419.372
4.1	31.653	37.838	219.014	260.928	35.792	43.094	320.623	360.535	45.212	52.992	417.554	456.518
4.6	40.762	46.591	267.278	309.591	43.537	50.495	370.251	410.569	51.748	59.352	468.398	507.702
	$\epsilon_{1-(0,1)}$	$\epsilon_{2-(2,3)}$	$\epsilon_{1+(0,1)}$	$\epsilon_{2+(2,3)}$	$\epsilon_{1-(4,5)}$	$\epsilon_{2-(6,7)}$	$\epsilon_{1+(4,5)}$	$\epsilon_{2+(6,7)}$				

APPENDIX 8

Si: Numerical Solution of Equation 4.1.7

5x5 Determinant

d	ϵ_1	ϵ_2	ϵ_3	ϵ_4	ϵ_5	ϵ_6	ϵ_7	ϵ_8	ϵ_9
0.0	2.132	4.741	6.623	14.143	22.659				
0.1	2.146	4.716	6.660	14.164	22.708				
0.2	2.185	4.649	6.761	14.229	22.852				
0.3	2.251	4.557	6.909	14.341	23.091				
0.4	2.343	4.457	7.086	14.505	23.420				
0.5	2.459	4.364	7.275	14.729	23.856				
4.1	26.691	20.093	23.028	62.668	76.673				

9x9 Determinant

0.0	2.130	4.621	6.478	12.727	23.655	16.512	15.194	35.908	45.073
0.1	2.143	4.599	6.509	12.743	23.695	16.544	15.168	35.949	45.123
0.2	2.183	4.540	6.595	12.792	23.816	16.631	15.100	36.070	45.269
0.3	2.248	4.458	6.722	12.868	24.019	16.750	15.019	36.273	45.513
0.4	2.340	4.369	6.873	12.960	24.302	16.883	14.959	36.556	45.850
0.5	2.455	4.285	7.036	14.955	24.666	13.049	17.017	36.919	46.280
4.1	26.691	20.074	23.230	62.666	76.829	22.691	27.423	91.809	104.220

Si: Numerical Solution of Equation 4.1.7

13x13 Determinant

d	$\epsilon_{2+}(0)$	$\epsilon_{1-}(1,3)$	$\epsilon_{2-}(2,4)$	$\epsilon_{1+}(1,3)$	$\epsilon_{2+}(2,4)$	$\epsilon_{1-}(5,7)$	$\epsilon_{2-}(6,8)$	$\epsilon_{1+}(5,7)$	$\epsilon_{2+}(6,8)$				
0.0	2.130	4.619	6.475	12.511	23.019	15.863	14.689	36.120	45.789	24.805	25.657	58.735	67.889
0.1	2.143	4.597	6.506	12.525	23.047	15.885	14.674	36.155	45.837	24.764	25.704	58.778	67.937
0.2	2.183	4.539	6.592	12.565	23.125	15.947	14.637	36.263	45.982	24.673	25.822	58.910	68.082
0.3	2.248	4.457	6.718	12.624	23.229	16.035	14.599	36.443	46.222	24.593	25.971	59.129	68.321
0.4	2.340	4.367	6.869	12.692	23.312	16.138	14.589	36.698	46.555	24.594	26.128	59.434	68.656
0.5	2.455	4.284	7.030	14.635	24.739	12.752	16.250	37.031	46.980	23.315	26.288	59.824	69.082
0.6	2.593	4.217	7.194	14.760	25.037	12.787	16.370	37.441	47.492	23.231	26.439	60.300	69.600
0.7	2.751	4.176	7.354	14.970	25.440	12.789	16.507	37.932	48.090	23.093	26.605	60.858	70.207
0.8	2.924	4.169	7.507	15.248	25.873	12.762	16.677	38.502	48.769	22.930	26.827	61.497	70.900
0.9	3.106	4.207	7.659	15.553	27.206	12.716	16.917	39.152	49.527	22.760	26.219	62.216	71.677
1.0	3.288	4.301	7.807	17.273	27.794	12.663	15.830	39.879	50.360	22.591	26.416	63.013	72.535
1.2	4.685	3.628	8.105	18.402	29.364	12.570	16.206	41.561	52.241	22.280	26.585	64.834	74.486
1.4	5.310	3.966	8.432	19.961	31.251	12.530	16.446	43.527	54.391	22.029	26.660	66.944	76.733
1.6	6.116	4.369	8.815	21.701	33.383	12.570	16.669	45.760	56.793	21.971	26.716	69.328	79.259
1.8	7.065	4.875	9.275	23.956	35.738	12.706	16.926	48.240	59.432	21.739	26.790	71.974	82.047
2.0	8.142	5.502	9.829	26.282	38.302	12.948	17.245	50.955	62.297	21.734	26.910	74.868	85.084
2.3	9.978	6.685	10.867	30.181	42.523	13.526	17.875	55.440	66.998	21.928	27.194	79.653	90.081
2.6	11.954	8.166	12.292	34.518	47.182	14.380	18.720	60.398	72.165	22.371	27.671	84.944	95.581
2.9	14.547	9.947	13.637	39.292	52.268	15.520	19.808	65.809	77.781	23.081	28.364	90.718	101.561
3.3	18.124	12.792	16.167	46.324	59.708	17.495	21.665	73.707	85.949	24.461	29.669	99.139	110.250
3.7	22.173	16.169	19.187	54.115	67.895	20.024	24.013	82.369	94.880	26.354	31.444	108.356	119.731
4.1	26.690	20.073	23.154	62.666	76.829	22.660	26.869	91.786	104.563	28.773	33.712	118.352	129.984
4.6	32.551	25.685	28.119	74.428	89.049	27.445	31.166	104.610	117.717	32.994	37.271	131.919	143.867
5.1	40.024	32.087	34.082	87.387	102.444	32.899	36.278	118.600	132.032	37.184	41.652	146.664	158.921
5.7	49.418	40.373	42.324	104.533	120.078	40.954	43.446	136.930	150.743	43.941	48.008	165.902	178.520
6.3	59.856	50.804	52.318	123.429	139.427	49.173	51.689	156.948	171.131	51.454	55.576	186.818	199.787
7.0	73.354	63.237	64.460			60.866	63.754			62.302	65.946		
7.8	90.521	79.822	80.388			75.986	78.134			75.986	80.606		
8.7		101.126				96.228	98.213			94.820	97.145		
$\epsilon_{2+}(0)$	$\epsilon_{1-}(1,2)$	$\epsilon_{2-}(3,4)$	$\epsilon_{1+}(1,2)$	$\epsilon_{2+}(3,4)$	$\epsilon_{1-}(5,6)$	$\epsilon_{2-}(7,8)$	$\epsilon_{1+}(5,6)$	$\epsilon_{2+}(7,8)$					

Sl: Numerical Solution of Equation 4.1.8

6x6 Determinant

d	ϵ_1	ϵ_2	ϵ_3	ϵ_4	ϵ_5	ϵ_6	ϵ_7	ϵ_8	ϵ_9	ϵ_{10}	ϵ_{11}	ϵ_{12}	ϵ_{13}	ϵ_{14}
0.0	1.626	6.114	7.650	9.654	19.341	28.197								
0.1	1.633	6.124	7.652	9.676	19.371	28.246								
4.1	23.321	52.464	20.370	23.900	70.409	83.838								

10x10 Determinant

0.0	1.625	6.082	7.391	9.428	20.549	29.087	16.366	17.732	41.571	50.752
0.1	1.631	6.090	7.399	9.444	20.565	29.131	16.353	17.755	41.612	50.801
4.1	23.261	52.464	20.339	23.623	70.404	84.040	24.417	28.869	98.593	110.772

14x14 Determinant

	$\epsilon_{1+}(0)$	$\epsilon_{2+}(1)$	$\epsilon_{1-}(2,4)$	$\epsilon_{2-}(3,5)$	$\epsilon_{1+}(2,4)$	$\epsilon_{2+}(3,5)$								
0.0	1.625	6.082	7.384	9.420	20.041	29.702	15.749	17.054	41.651	51.417	26.893	27.440	64.496	73.628
0.1	1.631	6.090	7.393	9.436	20.057	29.734	15.737	17.075	41.689	51.466	26.824	27.512	64.540	73.676
0.2	1.651	6.109	7.425	9.482	20.114	29.829	15.625	17.138	41.805	51.612	26.671	27.675	64.672	73.820
0.3	1.686	6.128	7.496	9.553	20.211	29.989	15.640	17.237	41.999	51.855	26.485	27.873	64.893	74.059
0.4	1.736	7.623	6.135	9.643	20.354	30.220	15.562	17.366	42.272	52.192	26.285	28.083	65.200	74.392
0.5	1.804	7.819	6.124	9.748	20.553	30.528	15.469	17.516	42.624	52.621	26.077	28.288	65.594	74.818
0.6	1.891	8.081	6.097	9.867	20.818	30.923	15.368	17.648	43.057	53.139	25.866	28.473	66.072	75.334
0.7	1.999	8.402	6.061	10.003	21.160	31.409	15.262	17.829	43.571	53.744	25.656	28.631	66.635	75.940
0.8	2.131	8.763	6.027	10.169	21.584	31.985	15.155	17.973	44.165	54.432	25.449	28.756	67.280	76.632
0.9	2.288	9.134	6.000	10.388	22.095	32.649	15.053	18.100	44.838	55.201	25.250	28.852	68.005	77.410
1.0	2.471	10.701	5.987	9.474	22.689	33.394	14.959	18.211	45.590	56.046	25.063	28.922	68.809	78.269
1.2	2.919	11.696	6.021	9.966	24.060	35.105	14.805	18.396	47.318	57.955	24.786	29.003	70.645	80.225
1.4	3.483	13.080	6.152	10.318	25.952	37.084	14.718	18.560	49.334	60.140	24.393	29.042	72.775	82.482
1.8	4.972	16.622	6.761	11.069	30.196	41.748	14.773	18.954	54.154	65.268	24.011	29.085	77.857	87.831
2.0	5.899	18.696	7.257	11.551	32.648	44.406	14.960	19.234	56.927	68.184	23.966	29.177	80.784	90.893
2.3	7.504	22.198	8.267	12.454	36.733	48.775	15.444	19.787	61.510	72.969	24.086	29.413	85.625	95.937
2.6	9.717	26.137	9.252	13.604	41.270	53.587	16.193	20.554	66.572	78.228	24.451	29.824	90.980	101.494
2.9	11.789	30.518	10.962	15.020	46.244	58.832	17.220	21.555	72.095	83.943	25.076	30.445	96.825	107.538
3.3	15.133	37.045	13.568	17.344	53.543	66.488	19.039	23.286	80.149	92.251	26.337	31.645	105.350	116.324
3.7	18.990	44.359	16.688	20.183	61.597	74.891	21.388	25.500	88.975	101.328	28.104	33.307	114.681	125.911
4.1	23.257	52.464	20.338	23.608	70.404	84.041	24.291	28.215	98.559	111.161	30.392	35.458	124.796	136.277
	$\epsilon_{1+}(1)$	$\epsilon_{2+}(0,1)$	$\epsilon_{1-}(2,3)$	$\epsilon_{2-}(4,5)$	$\epsilon_{1+}(2,3)$	$\epsilon_{2+}(4,5)$								

Si: Numerical Solution of Equation 4.1.9

7x7 Determinant

d	ϵ_1	ϵ_2	ϵ_3	ϵ_4	ϵ_5	ϵ_6	ϵ_7	ϵ_8	ϵ_9	ϵ_{10}	ϵ_{11}	ϵ_{12}	ϵ_{13}	ϵ_{14}	ϵ_{15}
0.0	1.202	4.859	13.571	10.451	9.672	24.757	33.788								
0.1	1.224	4.861	13.591	10.523	9.617	24.792	33.837								
4.1	22.482	44.630	61.317	21.010	24.888	77.774	90.784								

11x11 Determinant

0.0	1.201	4.851	13.321	10.024	9.511	25.414	34.609	19.395	20.256	47.267	56.449				
0.1	1.224	4.853	13.342	10.111	9.439	25.438	34.655	19.343	20.313	47.310	56.498				
4.1	22.475	44.630	61.317	20.962	24.502		91.033	25.765	30.409	105.264	117.242				

15x15 Determinant

	$\epsilon_{2-(0,1)}$	$\epsilon_{1+(1)}$	$\epsilon_{2+(0,2)}$	$\epsilon_{1-(3,5)}$	$\epsilon_{2-(4,6)}$	$\epsilon_{1+(3,5)}$	$\epsilon_{2+(4,6)}$								
0.0	1.201	4.851	13.307	10.010	9.506	24.956	34.917	18.405	19.402	47.234	57.061	29.691	30.108	70.271	79.379
0.1	1.224	4.853	13.328	10.097	9.433	24.984	34.957	18.374	19.434	47.275	57.110	29.585	30.208	70.316	79.427
0.2	1.291	4.859	13.393	9.286	10.285	25.069	35.079	18.292	19.519	47.396	57.257	29.381	30.392	70.449	79.570
0.3	1.402	4.872	13.506	9.127	10.509	25.215	35.284	18.177	19.636	47.599	57.502	29.156	30.585	70.670	79.808
0.4	1.556	4.897	13.673	8.972	10.744	25.424	35.573	18.045	19.767	47.884	57.841	28.925	30.766	70.980	80.140
0.5	1.752	4.937	13.903	8.826	10.977	25.700	35.947	17.906	19.900	48.251	58.274	28.695	30.929	71.376	80.564
0.6	1.986	4.998	14.202	8.694	11.197	26.044	36.407	17.766	20.028	48.700	58.797	28.472	31.070	71.857	81.080
0.7	2.256	5.088	14.578	8.576	11.397	26.451	36.951	17.630	20.145	49.230	59.407	28.266	31.187	72.423	81.684
0.8	2.556	5.215	15.032	8.474	11.573	26.897	37.577	17.500	20.249	49.842	60.102	28.107	31.280	73.072	82.376
0.9	2.879	5.388	15.559	8.392	11.727	28.117	38.282	17.383	20.341	50.533	60.879	27.260	31.350	73.801	83.153
1.0	3.217	5.619	16.146	8.330	11.864	27.316	39.064	17.291	20.421	51.303	61.733	28.519	31.402	74.611	84.013
1.2	3.902	6.293	17.730	8.277	12.111	29.956	40.842	16.937	20.560	53.080	63.667	27.040	31.472	76.461	85.973
1.4	4.567	7.277	19.326	8.345	12.357	31.960	42.885	16.874	20.696	55.126	65.881	26.736	31.302	78.608	88.238
1.8	5.946	10.325	23.327	8.655	12.976	36.280	47.691	16.872	20.998	60.036	71.084	26.312	31.426	83.735	93.616
2.0	6.742	12.164	25.621	9.059	13.396	38.841	50.427	17.007	21.240	62.862	74.045	26.225	31.478	86.690	96.700
2.3	8.132	15.394	29.435	9.887	14.174	43.083	54.921	17.407	21.738	67.530	78.906	26.275	31.659	91.580	101.786
2.6	9.782	19.089	33.680	11.010	15.215	47.784	59.866	18.063	22.433	72.686	84.249	26.566	32.008	96.993	107.393
2.9	11.692	23.356	38.353	12.451	16.509	52.925	65.249	18.990	23.365	78.309	90.053	27.112	32.562	102.904	113.496
3.3	14.514	29.563	45.247	15.009	18.660	60.451	73.094	20.666	24.971	86.505	98.489	28.261	33.663	111.524	122.371
3.7	18.440	36.686	52.900	17.516	21.315	68.733	81.691	22.862	27.061	95.480	107.701	29.909	35.218	120.961	132.056
4.1	22.475	44.630	61.317	20.961	24.485	77.765	91.034	25.593	29.646	105.217	117.674	32.074	37.257	131.188	142.528
	$\epsilon_{2-(1,2)}$	$\epsilon_{1+(0)}$	$\epsilon_{2+(1,2)}$	$\epsilon_{1-(3,4)}$	$\epsilon_{2-(5,6)}$	$\epsilon_{1+(3,4)}$	$\epsilon_{2+(5,6)}$								

S1: Numerical Solution of Equation 4.1.10

8x8 Determinant

d	ϵ_1	ϵ_2	ϵ_3	ϵ_4	ϵ_5	ϵ_6	ϵ_7	ϵ_8	ϵ_9	ϵ_{10}	ϵ_{11}	ϵ_{12}
0.0	1.510	3.842	8.653	18.402	12.572	13.309	30.295	39.417				
0.1	1.499	3.876	8.666	18.435	12.498	13.387	30.334	39.466				
4.1	20.420	22.514	54.307	69.310	21.873	26.086	84.885	97.565				

12x12 Determinant

	$\epsilon_{1-}(0,2)$	$\epsilon_{2-}(1,3)$	$\epsilon_{1+}(0,2)$	$\epsilon_{2+}(1,3)$	$\epsilon_{1-}(4,6)$	$\epsilon_{2-}(5,7)$	$\epsilon_{1+}(4,6)$	$\epsilon_{2+}(5,7)$				
0.0	1.510	3.841	8.609	18.098	12.716	12.236	30.678	40.182	22.147	22.828	52.991	62.162
0.1	1.499	3.875	8.622	18.133	12.799	12.155	30.710	40.230	22.076	22.898	53.034	62.211
0.2	1.470	3.972	8.662	18.238	11.991	12.966	30.804	40.372	21.913	23.054	53.164	62.356
0.3	1.430	4.122	8.731	18.413	11.811	13.150	30.963	40.609	21.718	23.236	53.381	62.596
0.4	1.390	4.311	8.835	18.660	11.636	13.330	31.192	40.937	21.516	23.418	53.683	62.932
0.5	1.359	4.526	8.980	18.975	11.476	13.497	31.493	41.354	21.321	23.591	54.069	63.360
0.6	1.343	4.754	9.170	19.351	11.337	13.648	31.870	41.858	21.144	23.747	54.539	63.878
0.7	1.347	4.985	9.406	19.758	11.231	13.783	32.326	42.446	21.017	23.884	55.092	64.486
0.8	1.376	5.213	9.676	20.097	11.177	13.903	32.862	43.113	21.041	24.000	55.725	65.178
0.9	1.432	5.433	9.944	21.386	11.216	14.011	33.479	43.857	20.194	24.097	56.436	65.954
1.0	1.517	5.646	10.148	21.978	11.414	14.111	34.175	44.676	20.122	24.177	57.225	66.811
1.2	1.780	6.061	12.341	23.456	10.300	14.307	35.795	46.522	19.886	24.331	59.026	68.754
1.4	2.171	6.491	13.678	25.386	10.355	14.568	37.701	48.631	19.677	24.280	61.112	70.989
1.6	2.694	6.970	15.596	27.385	10.463	14.579	39.871	50.985	19.539	24.391	63.469	73.497
1.8	3.351	7.526	17.479	29.621	10.664	14.924	42.287	53.572	19.489	24.501	66.082	76.261
2.0	4.142	8.176	19.661	32.072	10.975	15.296	44.932	56.378	19.505	24.653	68.940	79.269
2.3	5.581	9.356	23.261	36.113	11.665	16.007	49.306	60.985	19.803	25.008	73.662	84.213
2.6	7.320	10.802	27.341	40.587	12.640	16.941	54.144	66.048	20.332	25.553	78.882	89.650
2.9	9.356	12.524	31.861	45.487	13.910	18.125	59.429	71.555	21.732	26.324	84.578	95.559
3.3	12.530	15.251	38.568	52.678	16.084	20.428	67.153	79.570	22.640	27.740	92.884	104.143
3.7	16.221	18.407	46.049	60.618	18.886	22.615	75.635	88.342	24.667	29.633	101.979	113.510
4.1	20.419	22.497	54.307	69.310	21.814	25.622	84.869	97.862	27.226	32.027	111.845	123.642
4.6	26.340	27.925	65.727	81.238	26.678	30.111	97.464	110.810	31.187	35.747	125.245	137.367
5.1	33.149	34.179	78.374	94.352	32.236	36.028	111.228	124.920	35.405	40.292	139.819	152.259
5.7	42.239	43.263	95.180	111.669	40.081	42.774	129.291	143.387	42.519	46.850	158.848	171.659
	$\epsilon_{1-}(0,1)$	$\epsilon_{2-}(2,3)$	$\epsilon_{1+}(0,1)$	$\epsilon_{2+}(2,3)$	$\epsilon_{1-}(4,5)$	$\epsilon_{2-}(6,7)$	$\epsilon_{1+}(4,5)$	$\epsilon_{2+}(6,7)$				

REFERENCES

1. J. M. Luttinger and W. Kohn, Phys. Rev. 97, 869-883 (Feb. 1955)
2. J. M. Luttinger, Phys. Rev. 102, 1030-1041 (May 1956)
3. R. R. Goodman, doctoral dissertation, University of Michigan, 1958
4. E. Burstein, G. S. Picus, R. F. Wallis and F. Blatt, Phys. Rev. 113 15-33 (Jan. 1959)
5. S. Zwerdling, B. Lax, L. M. Roth, and K. J. Button, Phys. Rev. 114, 80-89 (April 1959)
6. G. Dresselhaus, A. F. Kip, and C. Kittel, Phys. Rev. 98, 368-384, (April 1955)
7. R. N. Dexter, H. J. Zeiger and B. Lax, Phys. Rev. 104, 637-644 (Nov. 1956)
8. G. C. Dousmanis, Phys. Rev. Letters 1, 55-56 (July 1958)
9. G. C. Dousmanis, R. C. Duncan Jr., J. J. Thomas, and R. C. Williams, Phys. Rev. Letters 1, 404-407 (Dec. 1958)
10. B. Lax, Quantum Electronics--A Symposium, ed. C. H. Townes, Columbia University Press, New York, 1960.
11. R. C. Duncan and B. Rosenblum, Bulletin of the American Phys. Society Series II, 5, 177 (March 1960)
12. C. Kittel, Introduction to Solid State Physics, John Wiley and Sons Inc., New York 1956.
13. J. R. Reitz, Solid State Physics VI, ed. F. Seitz and D. Turnbull, Academic Press Inc., New York 1955
14. H. Brooks, Advances in Electronics and Electron Physics V.7, ed. L. Marton, Academic Press Inc., New York 1955
15. E. O. Kane, J. Phys. and Chem. of Solids 1, 82-99 (1956)
16. G. Dresselhaus, quoted by E. Burstein et al, Ref. 4
17. L. M. Roth, B. Lax, S. Zwerdling, Phys. Rev. 114, 90-104 (April 1959)
18. H. Kromer, Private Communication
19. E. O. Kane, J. Phys. and Chem. of Solids 1, 249-261 (1957)
20. L. D. Landau, Z. Physik 64, 629 (1930)
21. W. Shockley, Phys. Rev. 78, 173 (1950)
22. H. J. Zeiger, B. Lax, and R. N. Dexter, Phys. Rev. 105, 495-501 (Jan. 1957)
23. J. Callaway, Solid State Phys. V7, ed. F. Seitz and D. Turnbull, Academic Press Inc., New York 1958
24. G. Dresselhaus, doctoral dissertation, University of California, Berkeley, 1955
25. F. Herman, Physica 20, 801-812 (1954)

26. F. C. Von der Lage and H. Bethe, Phys. Rev. 71, 612-622 (May 1947)
27. L. D. Landau and E. M. Lifschitz, Quantum Mechanics, Addison-Wesley Publishing Co., Reading, Mass. 1958
28. R. B. Leighton, Principles of Modern Physics, McGraw-Hill Book Co., Inc., New York, 1959
29. F. Bloch, Z. Physik 52, 555 (1928)
30. R. N. Dexter, B. Lax, Phys. Rev. 96, 223 (1954)
31. R. C. Fletcher, W. A. Yager, and R. F. Merritt, Phys. Rev. 100, 747, (1955)
32. S. Zwerdling, K. J. Button, B. Lax and L. M. Roth, Phys. Review Letters 4, 173-176 (Feb. 1960)
33. H. Kromer, Phys. Rev. 109, 1856 (March 1958)
34. H. Kromer, Proc. IRE 47, 397 (March 1959)
35. C. Kittel, Proc. of Natl. Academy of Sci. 45, 744-747 (May 1959)
36. D. C. Mattis and M. J. Stevenson, Phys. Rev. Letters 3, 18 (1959)
37. P. Kaus, Phys. Rev. Letters 3, 20 (1959)
38. A. L. Schawlow and C. H. Townes, Phys. Rev. 112, 1940-1949 (1958)
39. F. Herman, Rev. Mod. Phys. 30, 102-121, (Jan. 1958)
40. L. P. Bouckaert, R. Smoluchowski and E. Wigner, Phys. Rev. 50, 58-67 (1936)

DISTRIBUTION LIST

Chief of Naval Research Navy Department - CODE 427 Washington 25, D. C.	2	Thermionics Branch Signal Corps Eng. Labs. Evans Signal Lab, Bldg. 42 Belmar, New Jersey	5	Chief, West Coast Office Signal Corps Eng. Labs. 75 So. Grand Avenue Pasadena, 2, California	
Director, Naval Research Lab. Washington 25, D. C.		Commanding General Air Research and Dev. Command ATTN: RDSBTL(Hq.Tech.Library) Andrews Air Force Base Washington 25, D. C.	1	Periodicals Librarian General Library California Inst. of Technology Lincoln Laboratory Massachusetts Inst. of Tech. Cambridge 39, Massachusetts	1
Attn: CODE 5240 CODE 7130 CODE 2000 CODE 5430	1 1 1 1	Commanding General WCLC Wright Air Devel.Center WCLRC Wright-Patterson AF Base, Ohio	1 1	Signal Corps Resident Engineer Electronic Defense Lab. P.O. Box 205 Mountain View, California	1
Commanding Officer ONR Branch Office 1000 Geary Street San Francisco, California	1	Commanding General CRRE AF Cambridge Research Center 230 Albany Street Cambridge 39, Massachusetts	1	Cornell Aeronautical Laboratory Cornell Research Foundation Buffalo 21, New York	1
Scientific Liaison Officer ONR, London c/o Navy 100, Box 39, FPO New York, New York	25	Commanding General RCRW Rome Air Development Center Griffiss Air Force Base Rome, New York	1	Director, Electronics Defense Engineering Research Inst. University of Michigan Ann Arbor, Michigan	1
Commanding Officer ONR Branch Office 1030 E. Green Street Pasadena, California	1	Commander Armed Services Tech. Info. ATTN: TIPDR Arlington Hall Station Arlington 12, Virginia	5	Georgia Inst. of Technology Atlanta, Georgia Attn: Librarian	1
Commanding Officer ONR Branch Office The John Crerar Library Bldg. 86 E. Randolph Street Chicago, 1, Illinois	1	Director CR4582 Air University Library Maxwell AF Base, Alabama	1	Fred D. Wilimek Varian Associates 611 Hansen Way Palo Alto, California	1
Commanding Officer ONR Branch Office 346 Broadway New York 13, New York	1	Chief, Western Division Air Research and Devel.Command Office of Scientific Research P.O.Box 2035, Pasadena, Calif.	1	John Dyer Airborne Instrument Laboratory Mineola, L.I., New York	1
Officer-in-Charge Office of Naval Research Navy No. 100 Fleet Post Office New York, New York	3	Microwave Laboratory Stanford University Stanford, California Attn: F.V.L. Pindar	1	Bell Telephone Laboratories Murray Hill, New Jersey Attn: J. R. Pierce	1
Chief, Bureau Aeronautics Navy Department Washington 25, D.C.	EL4 1 EL43 1 EL45 1	University of Michigan Electron Tube Laboratory Ann Arbor, Michigan Attn: J. Rowe	1	Hughes Aircraft Company Culver City, California Attn: Mr.Milek, Tech.Librarian	1
Chief, Bureau of Ordnance Navy Department Washington 25, D. C.	Re 4 1 Re 9 1	Mr. John S. McCullough Eitel-McCullough, Inc. San Bruno, California	1	RCA Laboratories Princeton, New Jersey Attn: Dr.W.M.Webster	1
Chief of Naval Operations Navy Department Washington 25, D.C.	Op 20X 1 Op 421 1 Op 55 1	Johns Hopkins University Radiation Laboratory 1315 St. Paul Street Baltimore 2, Maryland Attn: M. Poole, Librarian	1	Federal Tele. Laboratories 500 Washington Avenue Nutley, New Jersey Attn: W. Derrick K. Wing	1 1
Director, Naval Ordnance Lab. White Oak, Maryland	1			Technical Library G.E. Microwave Laboratory 601 California Avenue Palo Alto, California	1
Director, Naval Electronics Lab San Diego 52, California	1			Columbia Radiation Laboratory 538 W. 120th Street New York 27, New York	1
Dept. of Electronics Physics U.S.Naval Post Grad. School Monterey, California	1			Countermeasures Laboratory Gilfillan Brothers, Inc 1815 Venice Boulevard Los Angeles, California	1
Commander Code 366 Naval Air Missile Test Center Point Mugu, California	1	Cascade Research 5245 San Fernando Road Los Angeles 39, California	1	The Rand Corporation 1700 Main Street Santa Monica, California Attn: Librarian	1
U.S. Naval Proving Ground Attn: W. H. Benson Dahlgren, Virginia	1	Engineering Library Stanford University Stanford, California	1	Technical Library Research and Development Board Pentagon Building Washington 25, D. C.	1
Commander U.S.Naval Air Development Center Johnsville, Pennsylvania	1	Research Lab.of Electronics Massachusetts Inst. of Tech. Cambridge 39, Massachusetts	1	Motorola Riverside Res. Lab. 8330 Indiana Avenue Riverside, California Attn: Mr. John Byrne	1
Committee on Electronics Research and Development Board Department of Defense Washington 25, D. C.	1	Sloane Physics Laboratory Yale University New Haven, Connecticut Attn: R. Beringer	1	Chief, Bureau of Ships Department of the Navy Washington, D. C.	1 1 1
Director, Natl. Bureau of Stds. Washington 25, D. C. Attn: Div.14.0 CRPL, Librarian	1	Mr. H. J. Reich Department of Elec. Eng. Yale University New Haven, Connecticut	1	Advisory Group on Electron Tubes 346 Broadway (8th Floor) New York 13, New York	1
Commanding Officer Engineering Res.and Dev. Lab. Fort Belvoir, Virginia	1	Electron Tube Section Electrical Engineering Dept. University of Illinois Champaign, Illinois	1	Supervisor of Research Lab. Electrical Engineering Bldg. Purdue University Lafayette, Indiana	1
Ballistics Research Labs. Aberdeen Proving Ground Maryland Attn: D.W.H. Delsasso	2	Chairman, Div. of Elec. Eng. University of California Berkeley 4, California	1	W. E. Lear University of Florida Department of Electrical Eng. Gainesville, Florida	1
Chief, Ordnance Develop. Div. Natl. Bureau of Standards Connecticut Av, Van Ness St, NW Washington 25, D. C.	2	Technical Report Collection 303A, Pierce Hall Harvard University Cambridge 38, Massachusetts	1		
Commanding Officer Frankford Arsenal Bridesburg, Philadelphia, Pa.	1	Laboratory for Insulation Res. Massachusetts Inst. of Tech. Cambridge 39, Massachusetts Attn: A. von Hippel	1		

W. E. Lear	1	Countermeasures Laboratory	1
University of Florida		Gilfillan Brothers, Inc.	
Department of Electrical Eng.		1815 Venice Boulevard	
Gainesville, Florida		Los Angeles, California	
Director Electronics Defense	1	The Rand Corporation	1
Engineering Research Inst.		1700 Main Street	
University of Michigan		Santa Monica, California	
Ann Arbor, Michigan		ATTN: Librarian	
Cornell Aeronautical Lab	1	Motorola Riverside Res. Lab.	1
Cornell Research Foundation		8330 Indiana Avenue	
Buffalo 21, New York		Riverside, California	
Director, Microwave Res.Inst.	1	ATTN: Mr. John Byrne	
Polytechnic Inst.of Brooklyn		Ramo-Wooldridge Corporation	1
55 Johnson Street		Control Systems Division	
Brooklyn 1, New York		P.O. Box 900B	
University of Washington		Hawthorne, California	
Department of Elec. Eng.		ATTN: Librarian	
Seattle, Washington		Microwave Physics Laboratory	1
ATTN: E. A. Harrison	1	Sylvania Electric Products	
A. V. Eastman	1	P. O. Box 1296	
University of Colorado	1	Mountain View, California	
Department of Elec. Eng.		Dr. J. E. Shepherd	1
Boulder, Colorado		Sperry Gyroscope Company	
University of Colorado	1	Great Neck, New York	
Engineering Experiment Sta.		W. L. Maxson Corporation	1
Boulder, Colorado		460 West 34th Street	
ATTN: W. G. Worcester		New York 1, New York	
Electrical Engineering Dept.	1	ATTN: M. Simpson	
Princeton University		Bertram G. Ryland, Manager	1
Princeton, New Jersey		Spencer Laboratory	
Professor W. P. Dyke	1	Raytheon Manufacturing Co.	
Linfield College		Burlington, Massachusetts	
McMinnville, Oregon		Westinghouse Electric Corp.	1
Research Lab.of Electronics	1	Electronic Tube Division	
Chalmers Institute of Tech.		Elmira, New York	
Gothenburg, Sweden		ATTN: Mr. S.S.King, Librarian	
ATTN: Librarian		Mr. Gilbert Kelton	1
Columbia Radiation Lab.	1	Security Officer	
538 W. 120th Street		Philips Laboratories	
New York 27, New York		Irrington-on-Hudson, New York	
Mr. John S. McCullough	1	R. E. McGuire, Librarian	1
Eitel-McCullough, Inc.		Boeing Airplane Company	
San Bruno, California		P.O. Box 3707	
Cascade Research	1	Seattle 24, Washington	
5245 San Fernando Road		Dr. Donald W. Kerst	1
Los Angeles 39, California		General Atomic	
Fred D. Wilimek	1	P. O. Box 608	
Varian Associates		San Diego, California	
611 Hansen Way		Image Instruments, Inc.	1
Palo Alto, California		2300 Washington Street	
John Dyer	1	Newton Lower Falls 62, Mass.	
Airborne Instrument Lab		Sylvania Electric Prod. Inc.	1
Mineola, New York		Waltham, Massachusetts	
Bell Telephone Laboratories	1	ATTN: Charles A. Thornhill	
Murray Hill, New Jersey		Research Division Library	1
ATTN: J. R. Pierce		Raytheon Company	
Hughes Aircraft Company	1	28 Seyon Street	
Culver City, California		Waltham 54, Massachusetts	
ATTN: Mr. Milek, Librarian		ITT Laboratories	1
Hughes Aircraft Company	1	15151 Bledsoe Street	
Microwave Laboratory		San Fernando, California	
Culver City, California		Technical Research Group Inc.	1
ATTN: Dr. A. D. Berk		2 Aerial Way	
Bell Telephone Laboratories	1	Syosset, New York	
Technical Information Library		American Systems Incorporated	1
463 W. Street		3412 Century Boulevard	
New York 14, New York		Inglewood, California	
RCA Laboratories	1	ATTN: M. D. Adcock	
Princeton, New Jersey		Microwave Physics Laboratory	1
ATTN: Dr. W. M. Webster		Sylvania Electric Products	
Federal Telecommunic. Labs	1	P.O. Box 1296	
500 Washington Avenue		Mountain View, California	
Nutley, New Jersey		U. S. Atomic Energy Commission	1
ATTN: W. Derrick		Tech. Information Service Ext.	
K. Wing	1	P.O. Box 62	
		Oak Ridge, Tennessee	